

SYNTHESIS OF CHARGED RECEPTORS WITH A BIS PHENOLIC ETHER SCAFFOLD,  
AND STUDIES OF THEIR BINDING TO PHOSPHATIDYLGLYCEROL, A BACTERIAL  
MEMBRANE COMPONENT

A Dissertation by

Wedhigangoda Arachchilage Pradeep Aruna Jayasinghe

Master of Science, Wichita State University, 2011

Master of Philosophy, University of Colombo, 2003

Bachelor of Science, The Open University of Sri Lanka, 2000

Submitted to the Department of Chemistry  
and the faculty of the Graduate School of  
Wichita State University  
in partial fulfillment of  
the requirements for the degree of  
Doctor of Philosophy

December 2013

© Copyright 2013 by Wedhigangoda Arachchilage Pradeep Aruna Jayasinghe

All Rights Reserved

SYNTHESIS OF CHARGED RECEPTORS WITH A BIS PHENOLIC ETHER SCAFFOLD,  
AND STUDIES OF THEIR BINDING TO PHOSPHATIDYLGLYCEROL, A BACTERIAL  
MEMBRANE COMPONENT

The following faculty members have examined the final copy of this dissertation for form and content, and recommend that it be accepted in partial fulfillment of the requirement for the degree of Doctor of Philosophy with a major in Chemistry.

---

Dennis H. Burns, Committee Chair

---

David M. Eichhorn, Committee Member

---

William Groutas, Committee member

---

Katie Mitchell-Koch, Committee Member

---

William Hendry, Committee member

Accepted for the Fairmount College of Liberal  
Arts and Sciences

---

Ron Matson, Interim Dean

Accepted for the Graduate School

---

Abu S. M. Masud, Interim Dean

## DEDICATION

To those who care for others.

## ACKNOWLEDGEMENTS

I'm grateful to my research supervisor Dr. D.H. Burns, whose encouragement, guidance and support enabled me to understand and develop the skills needed to perform my graduate studies. A word of thanks is herewith also conveyed to all my thesis committee members Dr. W.Groutas, Dr. D.Eichhorn, Dr. Katie Mitchell-Koch and Dr. W. Hendry for their guidance and support.

Dr. Erach R. Talaty ("Dr.T") is also lovingly remembered for his kind support and advice.

I would like to thank all the faculty members and the staff at the Chemistry Department, WSU. Many thanks go to all the past and present colleagues from our lab. The assistance given by Elaine Harvey, former librarian is greatly appreciated. Everybody who worked at the stock room, including Anne, Susan & Mary, thank you so much for your help and friendly cooperation.

I am grateful indebted to my family, parents, brother and all the relatives who encouraged, guided and supported me to complete this project.

## ABSTRACT

An ongoing project of our research group is to develop synthetic receptors for the head group of Phosphatidylglycerol, a bacterial membrane component. Previous studies with bis-phenolic oxygen linked scaffoldings with neutral binding sites showed relatively weak binding to the Phosphatidylglycerol (PG) anion. This study reports a fourteen step synthesis of a receptor molecule with a bis-phenolic oxygen ether linked scaffold, leading to an expansion of the binding pocket. The receptor is multifunctional with ammonia binding units for the phosphate anion portion of PG and two bis-hydroxyl groups to bind to the glycerol hydroxyls of PG head group. The receptor's initial characterization by means of  $^1\text{H}$  NMR binding studies with Phosphatidylglycerol anion has also been reported. It also describes the synthesis of a control receptor molecule, and its binding stoichiometry with Phosphatidylglycerol and phosphate anions.

## TABLE OF CONTENTS

Chapter		Page
1	INTRODUCTION	1
	1.1 Antimicrobial cationic peptides	1
	1.2 Phospholipids and membrane structure (target of AMPs)	7
2	INTRODUCTION TO PHOSPHATIDYLGLYCEROL RECEPTORS	14
3	SYNTHESIS OF RECEPTORS	21
4	ANION BINDING STUDIES	58
5	EXPERIMENTAL – MATERIALS & PROCEDURES	65
	REFERENCES	86
	APPENDIX	91

## LIST OF TABLES

Table		Page
1.	Results from $^1\text{H}$ NMR titration for receptors <b>1a</b> and <b>1c</b> and control receptor <b>2</b>	17
2.	Reaction conditions for demethylation of <b>30</b> with $\text{BCl}_3 \cdot \text{SMe}_2$	40
3.	Reaction conditions for phenolic oxygen bridging linkage of <b>32</b>	42
4.	$^1\text{H}$ NMR titration data for the receptor <b>5</b> with TBAPG	62
5.	Volumes and Equivalences of <b>5</b> and TBAPG for the $^1\text{H}$ NMR Titration	68

## LIST OF FIGURES

Figure		Page
1.	Core structure of penicillin	1
2.	Potential biological uses of host defence peptides	2
3.	The membrane target of antimicrobial peptides of multicellular organisms	4
4.	Carpet, Toroidal and Barrel-stave model of antimicrobial peptide induced killing	5
5.	Structure and assembly of phospholipids	8
6.	Phospholipids in water	8
7.	Eukaryotic cell membrane lipid components	9
8.	Eukaryotic cell membrane	9
9.	Common head groups of phospholipids indicated by X	10
10.	Prokaryotic cell membrane representation using bacteria	11
11.	1,2-dihexadecanoyl-sn-glycero-3-phospho-(1'-sn-glycerol) a phosphatidylglycerol	11
12.	1,3-bis (sn-3'-phosphatidyl)-sn-glycerol commonly known as cardiolipin	12
13.	The phosphatidylglycerol anion	13
14.	First generation of PG receptors	15
15.	Control receptor <b>2</b> .	16
16.	Initially proposed charged PG receptor	19
17.	Semi-empirical computer model showing the minimized energy structure of the unbound charged receptor <b>5</b>	20

LIST OF FIGURES (continued)

Figure	Page
18. TLC profile for reaction between Lithium diphenyl phosphine and <b>24</b>	36
19. TLC profile for the crude product <b>30</b> from dry box reaction	39
20. TLC profile for the dihydroxylation of <b>33</b>	44
21. ESI-MS values for different species found in crude <b>40</b>	50
22. <sup>1</sup> H NMR stack plot for the TFA reaction of <b>38a</b>	51
23. Charged receptor <b>5</b> and charged control receptor <b>46</b>	57
24. Charged receptors and the anions	58
25. The control receptors <b>2</b> and <b>46</b>	59
26. <sup>1</sup> H NMR Job plot of <b>46</b> - H <sub>2</sub> PO <sub>4</sub> <sup>-</sup> complex in 5 % CDCl <sub>3</sub> in DMF-d <sub>7</sub> at 30 °C	60
27. <sup>1</sup> H NMR Job plot of <b>46</b> - PG complex in 5 % CDCl <sub>3</sub> in DMF-d <sub>7</sub> at 30 °C	61
28. <sup>1</sup> H NMR Job plot of <b>5</b> -PG complex with with TBAPG in 5 % CDCl <sub>3</sub> in DMF-d <sub>7</sub> at 30 °C	62
29. <sup>1</sup> H NMR titration curves of of <b>5</b> with TBAPG in 5 % CDCl <sub>3</sub> in DMF-d <sub>7</sub> at 30 °C	62
30. Protons (chemical shift observed) for the <sup>1</sup> H NMR titration of <b>5</b> with TBAPG in 5 % CDCl <sub>3</sub> in DMF-d <sub>7</sub>	64
31. <sup>1</sup> H NMR (top) and <sup>13</sup> C NMR (bottom) data for compound <b>6</b>	93
32. <sup>1</sup> H NMR (top) and <sup>13</sup> C NMR (bottom) data for compound <b>7</b>	94
33. <sup>1</sup> H NMR (top) and <sup>13</sup> C NMR (bottom) data for compound <b>7</b>	94
34. <sup>1</sup> H NMR (top) and <sup>13</sup> C NMR (bottom) data for compound <b>7</b>	94
35. <sup>1</sup> H NMR data for compound <b>9</b>	95

## LIST OF FIGURES (continued)

Figure	Page
36. $^1\text{H}$ NMR (top) and $^{13}\text{C}$ NMR (bottom) data for compound <b>10</b>	96
35. $^1\text{H}$ NMR data for compound <b>12</b>	97
36. $^1\text{H}$ NMR (top) and $^{13}\text{C}$ NMR (bottom) data for compound <b>15</b>	98
37. $^1\text{H}$ NMR data for compound <b>16</b>	99
38. $^1\text{H}$ NMR (top) and $^{13}\text{C}$ NMR (bottom) data for compound <b>18</b>	100
39. $^1\text{H}$ NMR data for compounds <b>19a and 19b</b>	101
40. $^1\text{H}$ NMR data for 5-allyl-2-methoxybenzaldehyde	102
41. ESI-MS data for compound <b>20</b>	103
42. $^1\text{H}$ NMR (top) and $^{13}\text{C}$ NMR (bottom) for compound <b>21</b>	104
43. $^1\text{H}$ NMR data for compound <b>22</b>	105
44. $^1\text{H}$ NMR (top) and $^{13}\text{C}$ NMR (bottom) for compound <b>23</b>	106
45. $^1\text{H}$ NMR (top) and $^{13}\text{C}$ NMR (bottom) for compound <b>24</b>	107
46. $^1\text{H}$ NMR (top) HRMS data for compound <b>24</b>	108
47. $^1\text{H}$ NMR data for compound <b>26</b>	109
48. $^1\text{H}$ NMR (top) and $^{13}\text{C}$ NMR (bottom) data for compound <b>27</b>	110

LIST OF FIGURES (continued)

Figure		Page
49	HSMS data for compound <b>27</b>	111
50.	$^1\text{H}$ NMR (top) and $^{13}\text{C}$ NMR (bottom) data for compound <b>28</b>	112
51.	HSMS (top) and ESI-MS (bottom) data for compound <b>28</b>	113
52.	$^1\text{H}$ NMR (top) and $^{13}\text{C}$ NMR (bottom) for compound <b>29</b>	114
53.	HSMS data for compound <b>29</b>	115
54.	$^1\text{H}$ NMR (top) and $^{13}\text{C}$ NMR (bottom) for compound <b>30</b>	116
55.	HSMS data for compound <b>30</b>	117
56.	$^1\text{H}$ NMR (top) and $^{13}\text{C}$ NMR (bottom) data for compound <b>31</b>	118
57	HSMS (top) and ESI-MS (bottom) data for compound <b>31</b>	119
58.	FTIR data for compound <b>31</b>	120
59.	$^1\text{H}$ NMR (top) and $^{13}\text{C}$ NMR (bottom) for compound <b>32</b>	121
60.	HSMS (top) and ESI-MS (bottom) data for compound <b>32</b>	122
61.	$^1\text{H}$ NMR (top) and $^{13}\text{C}$ NMR (bottom) for compound <b>33</b>	123
62.	HSMS data for compound <b>33</b>	124
63.	$^1\text{H}$ NMR (top) and $^{13}\text{C}$ NMR (bottom) data for compound <b>34</b>	125

## LIST OF FIGURES (continued)

Figure		Page
64.	HSMS (top) and ESI-MS (bottom) data for compound <b>34</b>	126
65.	FTIR data for compound <b>34</b>	127
66.	$^1\text{H}$ NMR (top) and $^{13}\text{C}$ NMR (bottom) data for compound <b>35</b>	128
67.	HSMS (top) and ESI-MS (bottom) data for compound <b>35</b>	129
68.	$^1\text{H}$ NMR (top) and $^{13}\text{C}$ NMR (bottom) data for compound <b>36</b>	130
69.	$^1\text{H}$ HSMS (top) and ESI-MS (bottom) data for compound <b>36</b>	131
70.	FTIR data for compound <b>36</b>	132
71.	$^1\text{H}$ NMR (top) and $^{13}\text{C}$ NMR (bottom) for compound <b>38</b>	133
72.	HSMS (top) and ESI-MS (bottom) data for compound <b>38</b>	134
73.	$^1\text{H}$ FTIR data for compound <b>38</b>	135
74.	$^1\text{H}$ NMR (top) and $^{13}\text{C}$ NMR (bottom) for compound <b>39</b>	136
75.	$^{19}\text{F}$ NMR data for compound <b>39</b>	137
76.	$^1\text{H}$ HSMS (top) and ESI-MS (bottom) data for compound <b>39</b>	138
77.	$^1\text{H}$ NMR (top) and FTIR (bottom) data for compound <b>40</b>	139

LIST OF FIGURES (continued)

Figure		Page
78.	ESI-MS data for compound <b>40</b>	140
79.	<sup>1</sup> H NMR (top) and <sup>13</sup> C NMR (bottom) data for compound <b>5</b>	141
80.	<sup>19</sup> F NMR (top) and <sup>31</sup> P NMR (bottom) data for compound <b>5</b>	142
81	HSMS (top) and ESI-MS (bottom) data for compound <b>5</b>	143
82	<sup>1</sup> H NMR (top) and <sup>13</sup> C NMR (bottom) data for compound <b>41</b>	144
83	HSMS data for compound <b>42</b>	145
84	<sup>1</sup> H NMR (top) and <sup>13</sup> C NMR (bottom) data for compound <b>42</b>	146
85	HSMS data for compound <b>42</b>	147
86	<sup>1</sup> H NMR (top) and <sup>13</sup> C NMR (bottom) data for compound <b>43</b>	148
87	HSMS data for compound <b>43</b>	149
88	FTIR data for compound <b>43</b>	150
89	<sup>1</sup> H NMR (top) and <sup>13</sup> C NMR (bottom) data for compound <b>44</b>	151
90	HSMS data for compound <b>44</b>	152
91	FTIR data for compound <b>44</b>	153
92	<sup>1</sup> H NMR (top) and <sup>13</sup> C NMR (bottom) data for compound <b>45</b>	154
93	HSMS data for compound <b>45</b>	155
94	<sup>19</sup> F NMR data for compound <b>45</b>	156
95	<sup>1</sup> H NMR (top) and <sup>13</sup> C NMR (bottom) data for compound <b>46</b>	157
96	HSMS data for compound <b>46</b>	158
97	<sup>19</sup> F NMR (top) and <sup>31</sup> P NMR (bottom) data for compound <b>46</b>	159

LIST OF FIGURES (continued)

Figure		Page
98	$^1\text{H}$ NMR (top) and $^{31}\text{P}$ NMR (bottom) data for compound <b>PG neutral</b>	160
99	$^1\text{H}$ NMR (top) and $^{31}\text{P}$ NMR (bottom) data for compound <b>3</b>	161
100	$^1\text{H}$ NMR data for the unknown compound	162

## LIST OF SCHEMES

Scheme	Page
1. Synthesis of TBAPG <b>3</b>	16
2. Retrosynthetic scheme of the original planned synthesis of the charged receptor	22
3. Bis anisole scaffold formation via Grignard reaction and bromination of the scaffold	23
4. Introduction of masked propanols to the bis anisole scaffold using Grignard chemistry	24
5. Formylation of the hydrogenated bis anisole scaffold with Duff reaction	26
6. Formylation attempt of <b>10</b> using 4-formyl morpholine	26
7. Introduction of Dimethoxymethane protected propanol to the bis anisole scaffold	27
8. Formylation attempt on <b>16</b> .	27
9. D <sub>2</sub> O quenching of the <b>16</b> anion	28
10. Model study for the formylation of 1-Allyl-4-methoxy benzene	29
11. Introduction of allyl groups to the bisanisole scaffold	30
12. Formylation of <b>19</b>	31
13. Revised retrosynthetic pathway	32

LIST OF SCHEMES (continued)

Scheme	Page
14. Synthesis of compound <b>23</b>	33
15. Synthesis of compound <b>24</b> .	34
16. Demethylation attempts on <b>24</b>	35
17. Lithium diphenyl phosphine reaction with THF.	36
18. Synthesis of compound <b>28</b>	37
19. Bromination of <b>28</b>	38
20. Introduction of allyl groups to compound <b>29</b>	38
21. Demethylation of the dry box product using $\text{BCl}_3 \cdot \text{SMe}_2$ .	40
22. Bromination of <b>31a</b>	41
23. Ether linkage between the phenolic oxygens of <b>32</b>	41
24. Dihydroxylation of 1-Allyl-4-methoxybenzene	43
25. Dihydroxylation of compound <b>33</b>	44
26. Acetonide protection of compound <b>34</b> .	45
27. Cyanation of the compound <b>35</b>	46
28. Model studies for the nitrile reduction	47
29. Nitrile reduction of compound <b>36b</b>	48

LIST OF SCHEMES (continued)

Scheme	Page
30. Conversion of <b>39</b> to <b>40</b> .	49
31. Deprotection of amino and diol functionality in compound <b>38a</b>	50
32. Counter ion exchange of <b>39</b>	52
33. Hydrogenation of compound <b>32</b>	52
34. Preparation of <b>42</b> via an ether linkage	53
35. Bis cyanation of compound <b>43</b>	54
36. Nitrile reduction of compound <b>43b</b>	55
37. Boc cleavage of compound <b>44b</b>	56
38. Counter ion exchange of <b>45</b> .	56

## LIST OF ABBREVIATIONS

18-C-6	18-crown-6
Ac	acetyl
Ac <sub>2</sub> O	acetic anhydride
AMP	antimicrobial peptides
Br	bromine
BBr <sub>3</sub>	boron tribromide
BCl <sub>3</sub> .SMe <sub>2</sub>	boron trichloride dimethyl sulfide
Boc <sub>2</sub> O	Di- <i>tert</i> -butyl dicarbonate
C	carbon
<sup>0</sup> C	degree Celsius
cal.	calories
calc.	calculated
CD <sub>3</sub> OD	deuterated methanol
CDCl <sub>3</sub>	deuterated chloroform
CH <sub>2</sub> Cl <sub>2</sub>	dichloromethane
CHCl <sub>3</sub>	chloroform
CH <sub>2</sub> ClCH <sub>2</sub> Cl	1, 2-dichloroethane
CH <sub>2</sub> I <sub>2</sub>	diiodomethane
CuCN	Copper cyanide
d	doublet
D	deuterium
DBDMH	1,3-dibromo-5,5-dimethylhydantoin

## LIST OF ABBREVIATIONS (continued)

DMSO	dimethylsulfoxide
DMF	N, N-dimethylformamide
DPPF	Diphenylphosphinoferrocene
ESI	electrospray ionization
Et <sub>4</sub> N <sup>+</sup> CN <sup>-</sup>	Tetraethylammoniumcyanide
g	grams
H	enthalpy
h	hours
HRMS	high resolution mass spectrometry
Hz	hertz
ITC	isothermal titration calorimetry
J	coupling constant
K <sub>a</sub>	association constant
log	logarithmic
m	multiplet
M	molar
MeOH	methanol
MHz	megahertz
ml	milliliters
mol.	moles
mmol.	millimoles

## LIST OF ABBREVIATIONS (continued)

MS	mass spectrometry
PPG	Phosphatidylglycerol
PPh <sub>3</sub>	triphenyl phosphine
PTSA	<i>p</i> -toluene sulfonic acid
ppm	parts per million
Py	pyridine
q	quartet, quintuplet
rt.	room temperature
S	entropy
s	singlet
t	triplet
TBAPG	tetrabutylammoniumphosphatidylglycerol
t-BuLi	tetra butyllithium
temp.	temperature
TMED	tetramethylethylenediamine
THF	tetrahydrofuran
TLC	thin layer chromatography
TFA	trifluoroacetic acid

## LIST OF SYMBOLS

$\Delta$	delta, or change
$\delta$	chemical shift
$\mu$	micro, E-6
$\nu$	1/cm

# CHAPTER 1

## INTRODUCTION

### 1.1 Antimicrobial cationic peptides (CAMPs)

The day Alexander Fleming found a mold of *Penicillium notatum* on one of his laboratory glass plates, the discovery of antibiotics began by accident. In 1943 with the industrial scale fermentation of penicillin (Figure 1) the medicinal world began a new chapter with the dawn of the antibiotic age [1], [2].

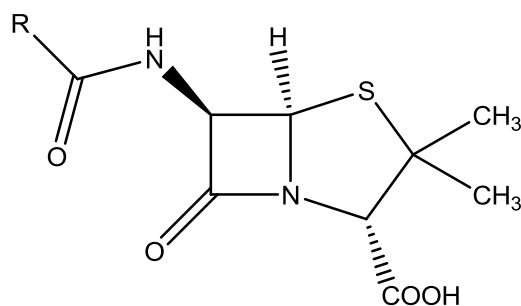


Figure 1. Core structure of penicillin

Since then many antibiotics have been developed, such as tetracycline, streptomycin and chloramphenicol. The successful treatment of many bacterial infections, during medical procedures, including surgeries and chemotherapies were aided by the vast growing number of antibiotics. The word antibiotic was introduced by Selman Waksman in 1941 as a noun to describe any small molecule made by a microbe that antagonizes the growth of other microbes [3]. However, throughout these years the emergence of many multi drug resistive bacterial strains is becoming a growing problem making many of the currently available antibiotics ineffective. It is known that more than 95% of strains of *Staphylococcus aureus* bacteria are

resistant to penicillin. The pervasive use of antibiotics in animal feeds to prevent infections and promote growth is considered as a main reason for this resistivity. Reduced drug uptake, enzymatic alteration of the antibiotic, modification of targets, overproduction of the target, active pumping of drugs out of the cell, drug sequestering by protein binding and metabolic bypass of the targeted pathway are among many mechanisms bacteria use to evade antibiotic activity [4].

These disturbing trends have prompted researchers to look upon the antimicrobial peptides known as cationic peptides (AMPs) or their mimics as potential antibiotics. Antimicrobial peptides are considered crucial components of the innate immune system of multicellular organisms. These host defense peptides exhibit a wide range of activity (Figure 2) against Gram-positive and Gram-negative bacteria [5].

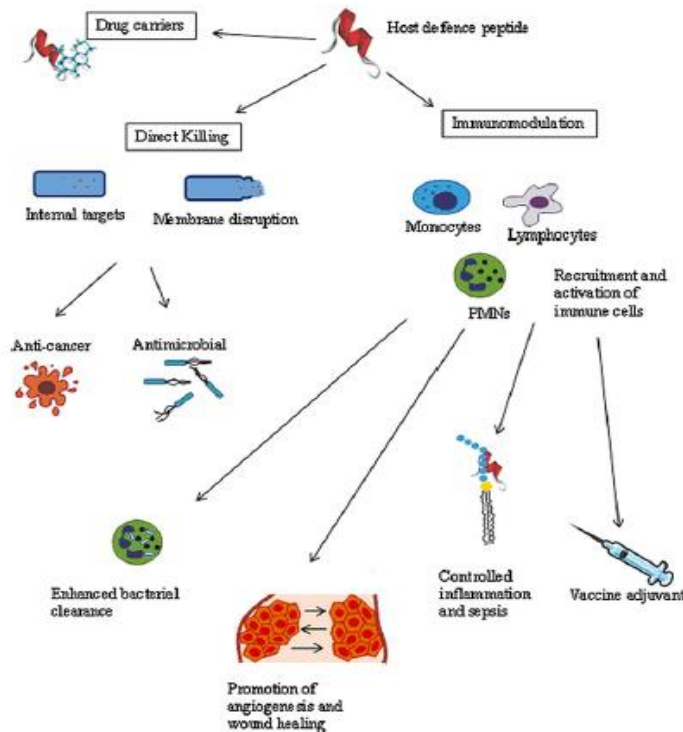


Figure 2. Potential biological uses of host defence peptides [6]

There are several subtypes of AMPs based in their amino acid composition & structure.

The anionic antimicrobial peptides are small (721.6-823.8 Da) and present in surfactant extracts, bronchoalveolar lavage fluid and airway epithelial cells. Produced in millimolar concentrations, they require zinc as a cofactor for antimicrobial activity. Linear cationic  $\alpha$ -helical peptides lack cysteine residues. This subgroup has about 290 different cationic peptides and in aqueous solutions, most of these peptides are disordered. When trifluoroethanol, sodium dodecyl sulphate micelles, phospholipid vesicles and liposomes are present, all or part of the molecule is converted to an  $\alpha$ -helix. The cationic antimicrobial peptides are mostly linear, but some may form extended coils. The bactenecins and PR-39 from this subgroup are rich in proline and arginine residues. Prophenin is rich in proline and phenylalanine residues. Indolicidin is rich in tryptophan residues. Another group of antimicrobial peptides contains 380 of both cationic and anionic peptides. They possess cysteine residues and form disulfide bonds and stable  $\beta$ -sheets [7].

Beside the structural classification, there are other classifications for AMPs. They are based on their origin, biosynthesis mechanism, localization, biological function, mechanism of action, activity and specificity. As a result AMP classification is considered dynamic [8]. Size, sequence, charge, conformation and structure, hydrophobicity and amphipathicity are considered as the characteristics that affect antimicrobial activity and specificity.

The size of antimicrobial peptides varies from 6 amino acid residues for anionic peptides to 42 amino acid residues for 90- $\beta$  defensins. Cationic AMPs contain the basic amino acid residues lysine or arginine, the hydrophobic residues alanine, phenylalanine, leucine or tryptophan and other residues such as valine, tyrosine and isoleucine. Charged AMPs, anionic peptides that

complex with zinc, or cationic peptides exhibit more activity than the neutral peptides. Cationic peptides are rich in arginine and lysine while anionic peptides are rich in glutamic and aspartic acids. A variety of secondary structures were recognized for AMPs such as  $\alpha$ -helices, relaxed coils, and anti-parallel  $\beta$ -sheet structures. When hydrophobic amino acid residues align along one side and the hydrophilic amino acid residues align along the opposite side of a helical molecule, it is called amphipathicity. Amphipathic  $\alpha$ -helical peptides are considered to be more active than peptides with less defined secondary structures. Hydrophobicity enables the water soluble antimicrobial peptides to partition into the membrane lipid bilayer. When they are hydrophobic, the  $\alpha$ -helical peptides exhibit amphipathicity [7].

H. G. Boman in 1995 reported that cell killing by some linear  $\alpha$ -helical peptides was rapid and technically challenging to characterize the steps preceding cell death. It is also reported that certain peptides such as Ceropin P1, PR-39 and Magainin-2 kill bacteria within 15-90 minutes [9].

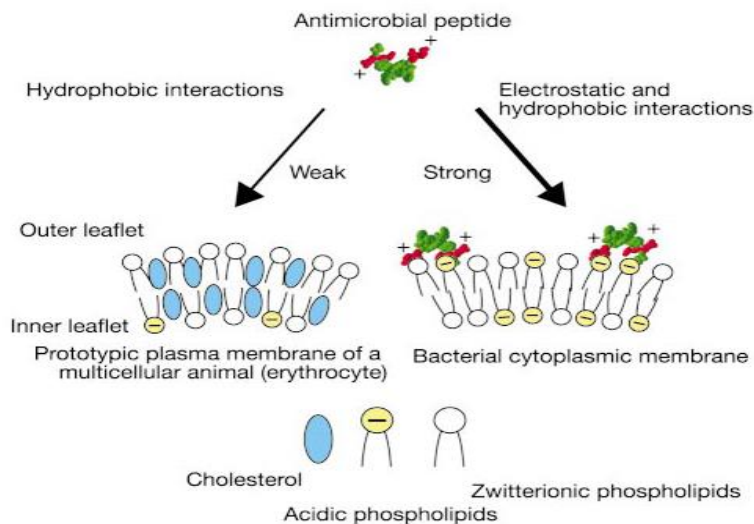


Figure 3. The membrane target of antimicrobial peptides of multicellular organisms [10].

Cationic antimicrobial peptides are first attracted to the net negative charge (anionic phospholipids and phosphate groups lipopolysaccharide) existing on the outer envelope of Gram-negative bacteria and to the teichoic acids on the surface of Gram positive bacteria.

Barrel-stave, carpet and toroidal pore are three proposed models used to describe the way cationic peptides disrupt the bacterial membrane. Later studies have shown that the activity of AMPs was not limited to perforation of bacterial membranes. They can also inhibit cellular processes such as DNA/RNA synthesis, protein synthesis, cell division, cell wall synthesis and protein folding, by translocating across the bacterial cytoplasmic membrane [6].

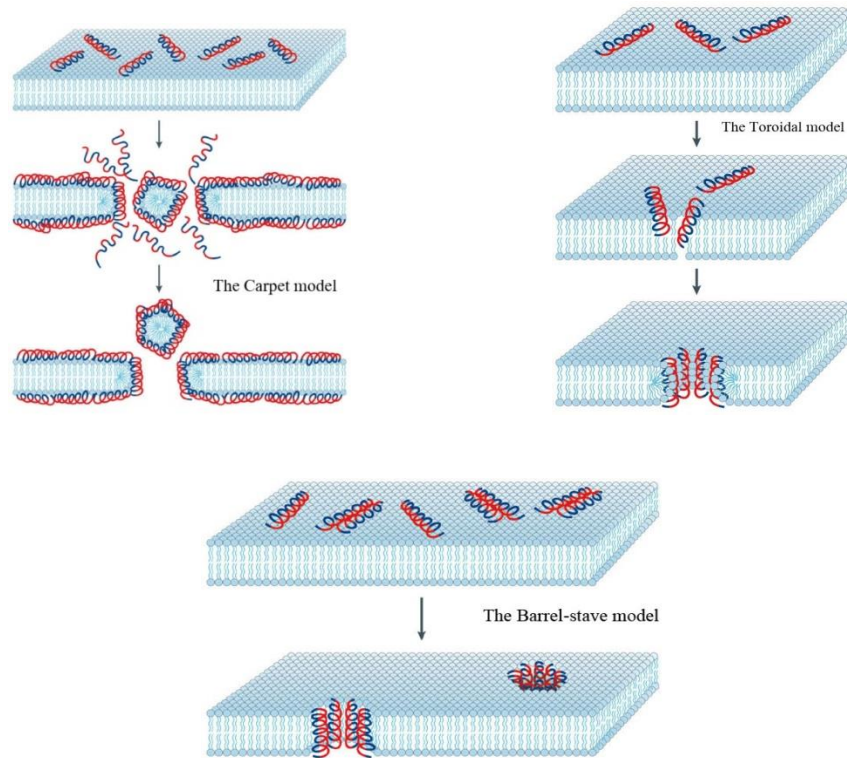


Figure 4. Carpet, Toroidal and Barrel-stave model of antimicrobial peptide induced killing [7]

The barrel-stave model describes the formation of anti-microbial peptide dimers and multimers after the binding of the peptides to the negatively charged bacterial membrane. This assembly of AMPs penetrates the membrane with their hydrophobic part facing the lipid bilayer and the hydrophilic components forming the internal lumen pores. The assembled peptide molecules inside the pore have a barrel like structure. In the carpet model, the peptides cover the surface of the outer membrane of the bilayer and destroy it with concomitant pore formation. The toroidal pore formation involves the fixation of the inner and outer lipid bilayer by the AMPs [8].

Currently more than 1000 natural cationic peptides with antimicrobial properties have been identified. One of the most important properties of AMPs is the lack of bacterial resistance. AMPs show activity against Gram-positive bacteria, Gram-negative bacteria and viruses. For example, nisin, which is produced by the bacterium *Lactococcus lactis* subsp. *lactis*, can inhibit bacterial growth through the formation of pores in the bacterial membrane. Dermaseptin makes a direct inactivation of HIV particle by destabilizing the viral membrane. Nisin has been also used as a food preservative. The cationic peptide polymixin B produced by the bacterium *Bacillus polymyxa* and gramicidin S, produced by *Bacillus brevis* were used as topical over-the-counter medicines. However, AMPs such as pexiganan from frog magainin, targeted the prevention of diabetic foot ulcers, and iseganan isolated from pig protegrin-1, targeted the prevention of oral mucositis in radiation therapy patients, have completed phase III clinical trials but failed to achieve New Drug Application (NDA) approval. This is mainly due to not having an advantage over the existing therapeutics [6]. Peptides are primarily produced using solid phase synthesis which is expensive. When using solution based synthesis, scaling up is considered relatively slow when large amounts of peptides are required for clinical trials. Usage of AMPs in repetitive doses and their application in higher concentrations would be different from the natural function

of AMPs within innate immunity. AMPs as therapeutics will not be deactivated by cell based mechanisms or will not be shielded in protective cellular compartments to minimize damage to the host. Routes of administration and stability in vivo are also challenging for AMPs as therapeutics. It is found that the half- life of AMPs in serum of mice is 30 minutes, although for efficient bacterial killing, they are required to be present at required concentrations for longer time periods [11]. Therefore the instability of antimicrobial peptides towards endogenous proteases, high cost to synthesize and substantial host effects such as toxicity are drawbacks for many CAMPs from being good therapeutic agents [4].

## **1.2 Phospholipids and membrane structure (target of AMPs)**

There are two classes of phospholipids present in the biological membranes. One class contains a glycerol backbone while the other has a sphingosine backbone. Of these two lipid classes, the glycerol containing phospholipids are the most common in nature, and are named as phosphoglycerides. They are glycerophosphoric acid derivatives that contain a minimum of one *O*-acyl, *O*-alkyl, or *O*-alk-i-enyl group linked covalently to the glycerol backbone. Phospholipid anions are similar to other alkyl phosphate anions such as nucleosides, where the phosphate oxygens are bound to alkyl groups. The glycerol oxygens of phospholipids are linked to long carbon chains (7-29 methylene units) via ester linkages, making them insoluble in water. The polar hydrophilic head group and the hydrophobic tail region are the two distinct structural regions found in these phosphoglycerides. Phospholipids exhibit a two layer structure (lipid bilayer) in an aqueous environment with the fat soluble hydrophobic tails sandwiched in the middle and the head groups outside (Figure 5). The exterior of these phospholipid aggregates

contains the polar phosphate groups while the hydrocarbon chains comprise the interior of the sphere (Figure 6). These aggregates are called micelles, and they form emulsions in water [12].

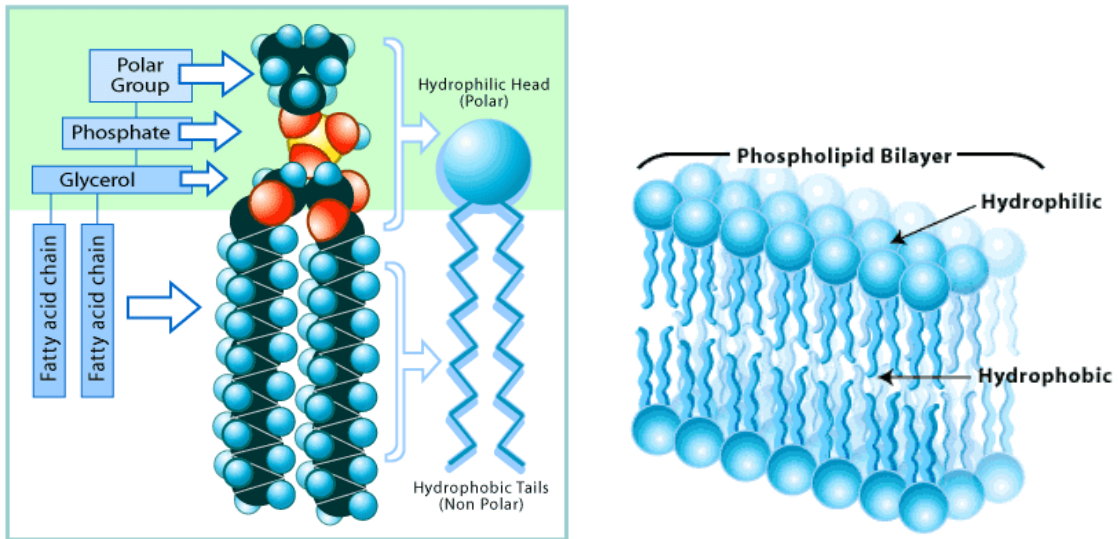


Figure 5. Structure and assembly of phospholipids [13]

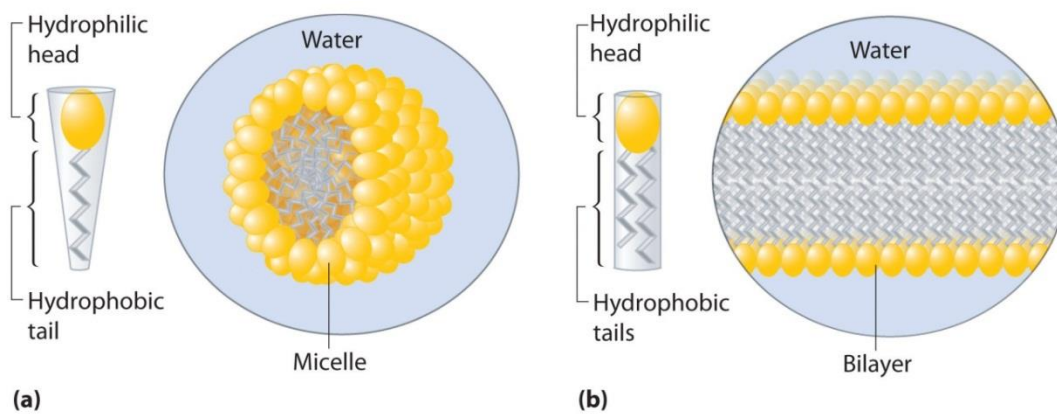


Figure 6. Phospholipids in water [14]

The cell membranes of both eukaryotes and prokaryotes have phospholipids and fatty acids along with varying amounts of proteins and sugars. The eukaryotic cell membrane is comprised five types of phospholipids. The outer leaflet of the cell membrane consists mostly of sphingomyelin and phosphatidylcholine. Phosphatidylethanolamine, phosphatidylserine and phosphatidylinositol are found in the inner leaflet of the eukaryotic cell membrane (Figure 7), while phosphatidylglycerol and cardiolipin are found in prokaryote membranes [15], [17].

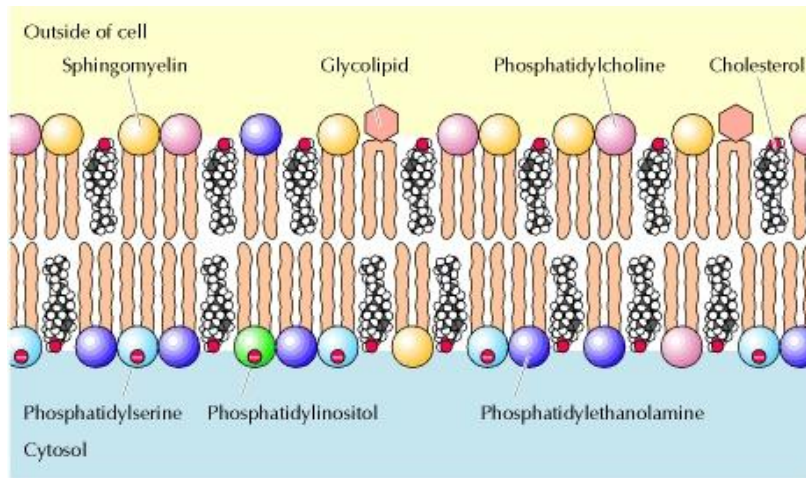


Figure 7. Eukaryotic cell membrane lipid components [15]

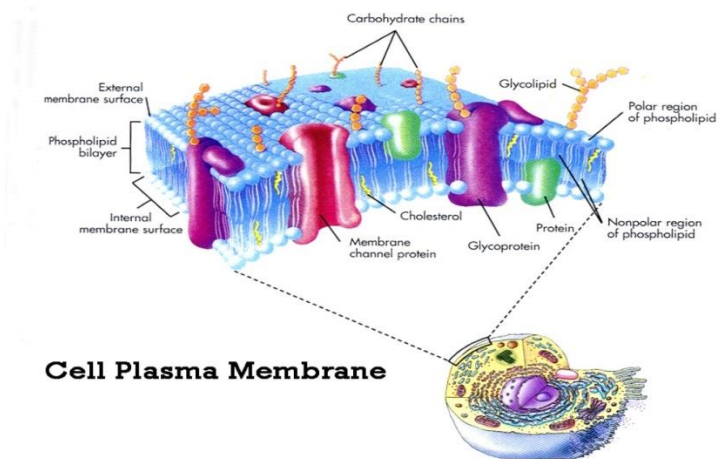
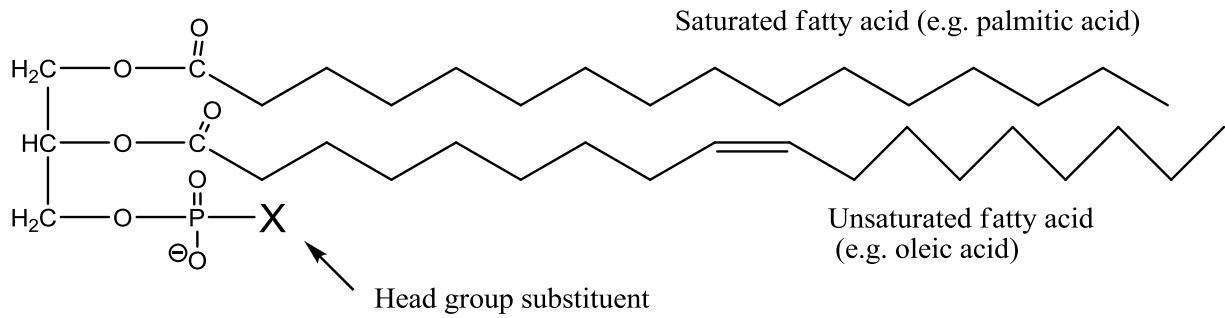


Figure 8. Eukaryotic cell membrane [16]

Glycerophospholipid  
(general structure)



Name of glycerophospholipid	Name of X	Formula of X	Net charge (at pH 7)
Phosphatidic acid	—	— H	- 1
Phosphatidylethanolamine	Ethanolamine	— CH <sub>2</sub> —CH <sub>2</sub> —NH <sub>3</sub> <sup>+</sup>	0
Phosphatidylcholine	Choline	— CH <sub>2</sub> —CH <sub>2</sub> —N(CH <sub>3</sub> ) <sub>3</sub> <sup>+</sup>	0
Phosphatidylserine	Serine	— CH <sub>2</sub> —CH—NH <sub>3</sub> <sup>+</sup>   COO <sup>-</sup>	- 1
Phosphatidylglycerol	Glycerol	— CH <sub>2</sub> —CH—CH <sub>2</sub> —OH   OH	- 1
Phosphatidylinositol 4,5-bisphosphate	<i>myo</i> -Inositol 4,5-bisphosphate		- 4
Cardiolipin	Phosphatidyl-glycerol	— CH <sub>2</sub>   CHOH   CH <sub>2</sub> —O—P(=O)(O <sup>-</sup> )—O—CH <sub>2</sub>   CH—O—C(=O)—R <sup>1</sup>   CH <sub>2</sub> —O—C(=O)—R <sup>2</sup>	- 2

Figure 9. Common head groups of phospholipids indicated by X [17]

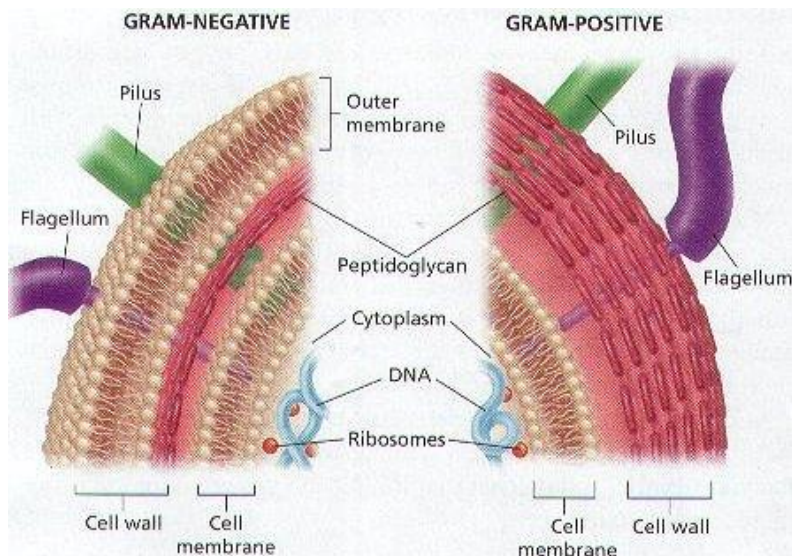


Figure 10. Prokaryotic cell membrane representation using bacteria [18]

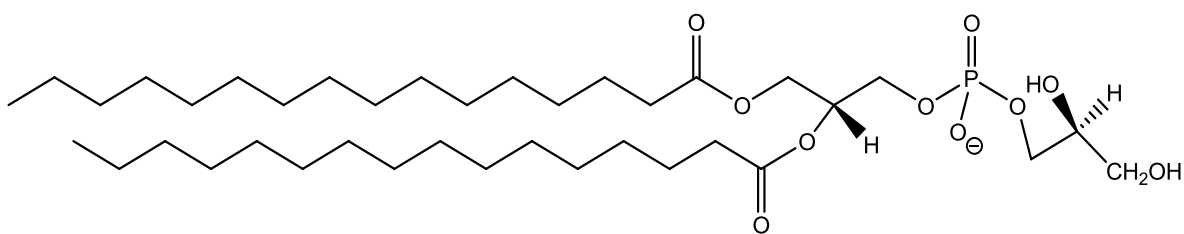


Figure 11. 1,2-dihexadecanoyl-sn-glycero-3-phospho-(1'-sn-glycerol) a phosphatidylglycerol

[19]

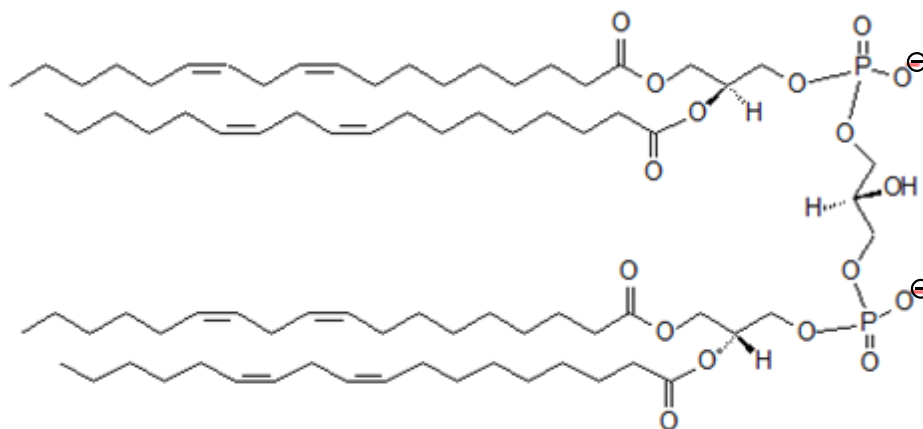


Figure 12. 1,3-bis (sn-3'-phosphatidyl)-sn-glycerol commonly known as cardiolipin [20]

The prokaryotic cell membranes outer leaflets contain anionic phospholipids such as phosphatidylglycerol, while the outer leaflet of eukaryotic cell membranes are composed of zwitterionic phospholipids [12]. Phosphatidylglycerol is the major anionic phospholipid found in bacterial membranes. An essential requirement for any antimicrobial peptide or synthetic mimic would be that it would selectively disrupt prokaryotic membranes and not eukaryotic membranes. Introduction of a recognition unit specific for bacterial membrane components would increase the high membrane selectivity of such synthetic mimic of CAMP.

Therefore our interest has been in the development of receptors that would bind to the bacterial membrane component anionic phosphatidylglycerol (Figure 13). Linking these receptors to membrane disruptors would pave the way for synthetic antibiotics that could mimic the action of CAMPs with lessened host toxicity.

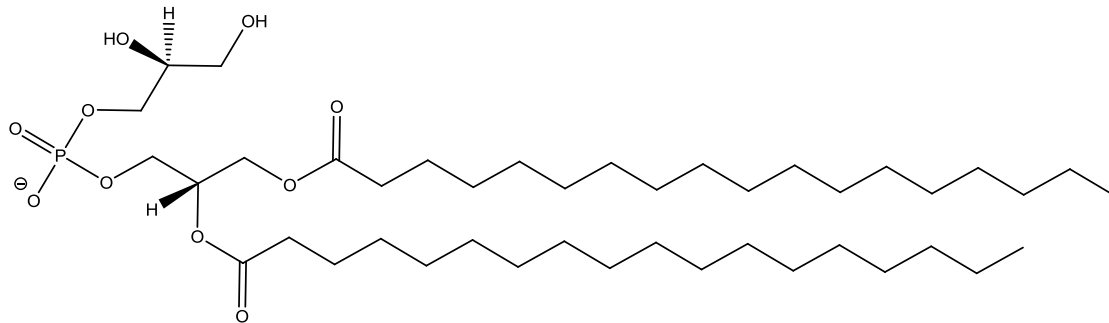


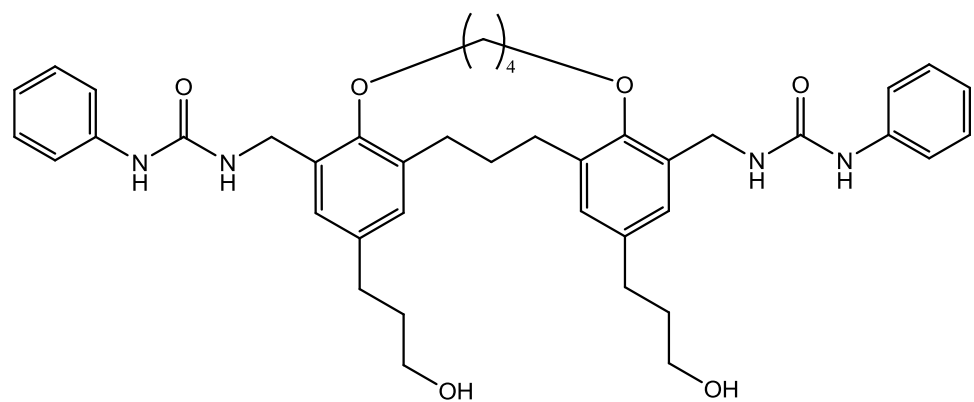
Figure 13. The phosphatidylglycerol anion (PG)

## CHAPTER 2

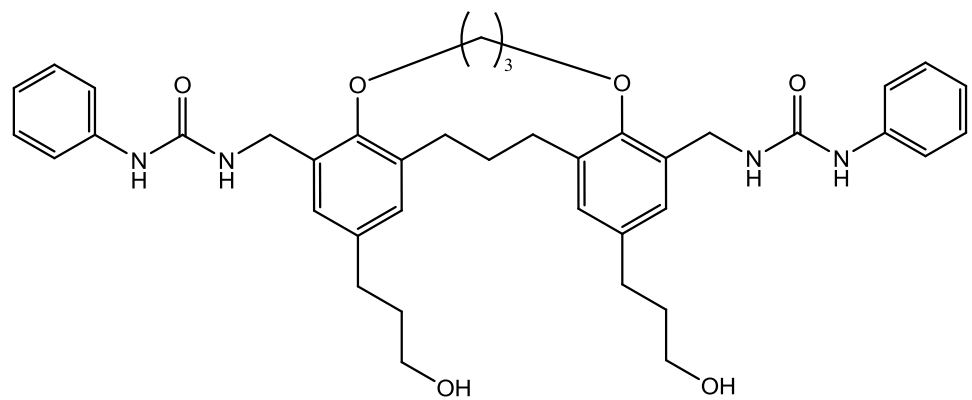
### INTRODUCTION TO PHOSPHATIDYLGLYCEROL RECEPTORS

The chemical and physicochemical properties of the substrate to be bound should be considered to a great extent when it comes to receptor designing. This is a challenging task for anions, since unlike cations, they are relatively large. Secondly, a large variety of shapes and geometries are exhibited. Most anions exist only in a relatively narrow pH window. They have high free energies of solvation, and as a result, the receptor has stiff competition from the surrounding medium. The choice of anion binding sites that occupy appropriate positions in the ligand is very important, because the size and shape of the receptor have to be complementary to the size and geometry of the anion. Anion receptors can be made as either neutral, electron deficient or positively charged. Many neutral receptors have incorporated urea, thiourea or amide groups to their binding sites since hydrogen bonding is the main force in their anion recognition, which mimics the interaction of amide NH groups along the protein backbone with the substrate in anion binding proteins [21].

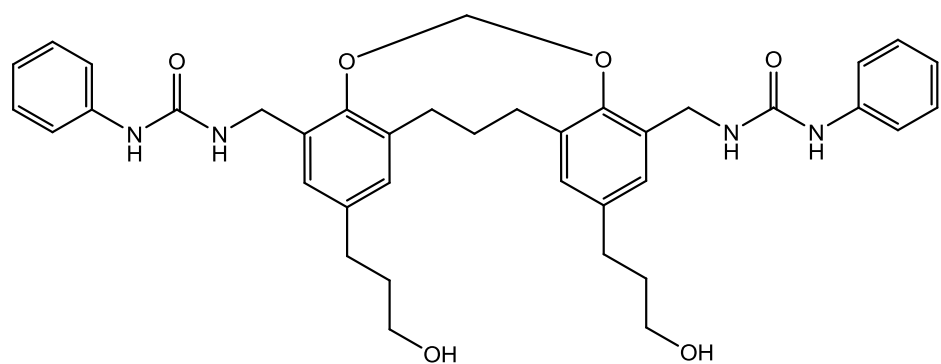
Our research group has previously developed a family of neutral receptors containing multi-functional binding sites designed to align with the phosphate anion and glycerol hydroxyl binding domains of the phosphatidylglycerol lipid (Figure 14) [22, 23].



**1a**



**1b**



**1c**

Figure 14. First generation of PG receptors [22,23].

Based on molecular modeling, the receptor scaffold was designed to contain urea functionality positioned to interact with the phosphate anion portion, and hydroxyl groups to interact with one or both of the glycerol hydroxyls on PG. The binding motifs were studied using solution NMR spectroscopy. Since only trace amounts of receptor **1b** were purified, it was not used for binding studies. Only receptors **1a** and **1c** were used in binding studies. A control receptor **2** was also synthesized, replacing the hydroxypropyl substituents with propyl groups (Figure 15).

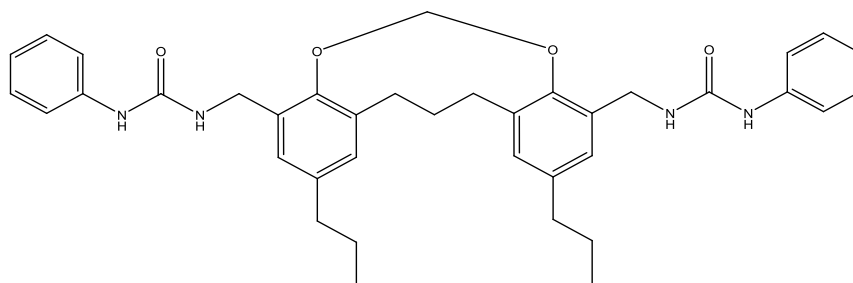
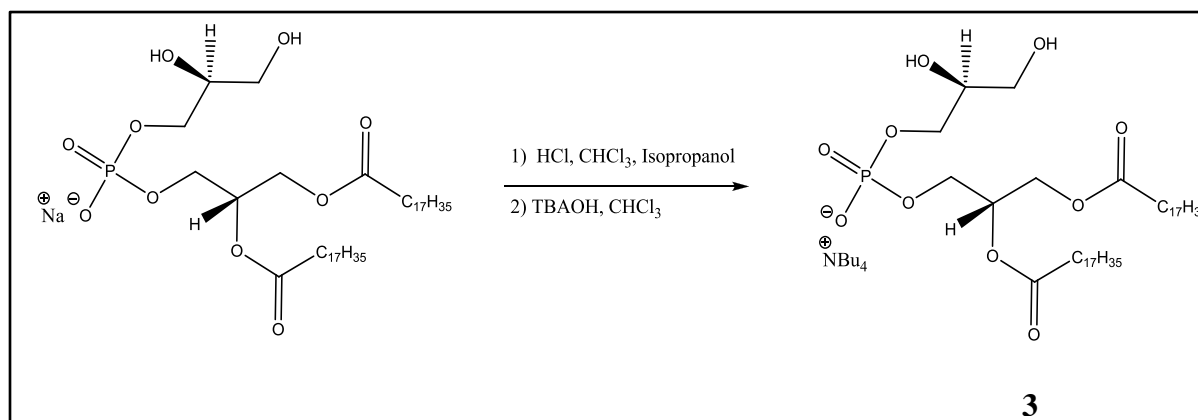


Figure 15. Control receptor **2**.

The tetrabutyl ammonium salt of the PG anion (TBAPG) was synthesized using the mono sodium salt of the lipid diastearoyl-phosphatidylglycerol (Scheme 1) [24].



Scheme 1. Synthesis of TBAPG **3** [24].

The stoichiometry for the binding of the two receptors (**1a**, and **1c**) and the control **2** with tetrabutyl ammonium phosphate monobasic (TBAH<sub>2</sub>PO<sub>4</sub>) or TBAPG were determined with Job plots, using <sup>1</sup>H NMR with DMF-d<sub>7</sub> as the solvent at 30 °C (Table 1) [25]. WinEQNMR for windows software was used to determine the binding constants by following titrations with the TBAPG in DMF-d<sub>7</sub> using <sup>1</sup>H NMR for compounds **1a** and **1c**, and TBAH<sub>2</sub>PO<sub>4</sub> for compound **2** [26].

TABLE 1

RESULTS FROM <sup>1</sup>H NMR TITRATIONS FOR RECEPTORS **1a**, **1c** AND CONTROL  
RECEPTOR **2**

Receptor	Binding Ratio	K (M <sup>-1</sup> ) [Error]	Anion salt
<b>1a</b>	Mixture		TBA H <sub>2</sub> PO <sub>4</sub>
<b>1a</b>	1 : 1	100 [± 15]	TBA PG
<b>1c</b>	Mixture		TBA H <sub>2</sub> PO <sub>4</sub>
<b>1c</b>	1 : 1	3.4 x 10 <sup>2</sup> [± 60]	TBA PG
<b>2</b>	1 : 1	1.2 x 10 <sup>3</sup> [±200]	TBA H <sub>2</sub> PO <sub>4</sub>
<b>2</b>	Mixture		TBA PG

A chemical shift of 2.3 ppm large down field movement with inorganic phosphate anion and 0.45 ppm movement with the TBAPG of urea protons resonance, upon addition of either salt to the receptor solution, has indicated the inorganic phosphate anion or the PG head group's phosphate anion portion formed strong hydrogen bonds with the receptor's urea groups. Since

receptors **1a** and **1c** contained multiple binding domains, none of them exhibit 1:1 binding stoichiometry with  $\text{TBAH}_2\text{PO}_4$ . Both receptors showed 1:1 binding stoichiometry with TBAPG, where both receptors and the anion contain multiple binding domains. The control receptor **2**, possessing only the urea binding unit, exhibited 1:1 binding with  $\text{TBAH}_2\text{PO}_4$ , but not with TBAPG. The control receptor **2** exhibited moderately strong binding with  $\text{TBAH}_2\text{PO}_4$ , and having very similar urea binding units as with **1a** and **1c**, it showed a complementary fit to the structure of the phosphate anion. Receptor **1c** showed 3-4 times stronger binding with TBAPG than receptor **1a**. Receptor **1c** had a shorter methylene bridge between the phenolic oxygens, while receptor **1a** had a longer four methylene unit bridge between them (Figure. 14). However, receptor **1c** did not interact with TBAPG as strongly as control receptor **2** did with  $\text{TBAH}_2\text{PO}_4$  (Table 1). Upon titration with TBAPG, the urea protons of receptor **1c** did not signal a far downfield movement as observed in the urea protons of control receptor **2**, titrated with  $\text{TBAH}_2\text{PO}_4$ . The above results indicated receptor **1c** did not form strong hydrogen bonding anion interactions with TBAPG. The phosphate anion portion of the bulky PG lipid (Figure 13) had poor interactions with the urea binding units of **1c** since it could not approach the urea moieties as closely as the  $\text{H}_2\text{PO}_4$  anion [22, 23].

Both receptors **1a** and **1c** contained hydroxyl groups in addition to the urea binding units and as a result they exhibited no distinct stoichiometry of binding with  $\text{TBAH}_2\text{PO}_4$ . The job plot for control receptor **2** possessing urea groups as the only binding motifs displayed no distinct stoichiometry of binding for the TBAPG, and instead was indicative of a mixture of 1:1 and 1:2 receptor to anion binding. Receptors **1a** and **1c**, having several potential anion binding units, exhibited a well behaved 1:1 binding stoichiometry with TBAPG. The binding moieties in **1a** and **1c** were aligned with those in PG in the receptor-anion complex (receptor urea groups were

bound to phosphate anion portion of the lipid while receptor hydroxyls were interacting with PG's glycerol hydroxyls). This complementary fit of PG to receptor would prevent the complex's functional groups from interacting with a second receptor or lipid molecule. The control receptor **2**, which lacks the terminal hydroxyls, may not have proper alignment for all binding groups of PG, and therefore any non-bound functional group from the complex would interact with either a receptor or a PG anion molecule, and would exhibit a complex binding stoichiometry (Table 1) [22, 23].

Since receptor **1c**, with neutral binding sites, exhibited only a moderate binding with TBAPG (Table 1), we modified the structure to impart more selectivity. We decided to increase binding affinity towards PG by introducing positive charges. Also, to better accommodate the PG head group, we deviated from the initially proposed structure **4** (Figure 16) by expanding the binding pocket, with increased number of methylene bridging units in the scaffolding. The number of terminal hydroxyl groups was also increased from 2 to 4 to increase possibilities for the glycerol hydroxyl and receptor interactions. (Figure 17, compound **5**). Studies of compound **5** are discussed in Chapter 4.

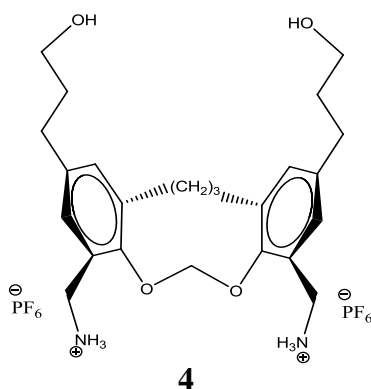
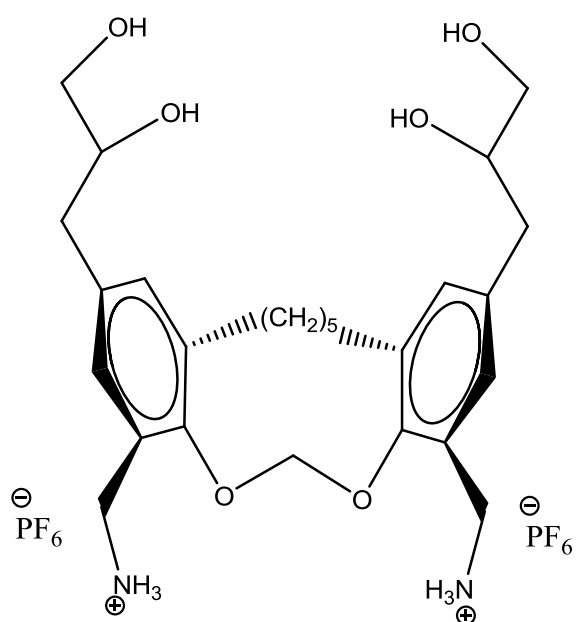
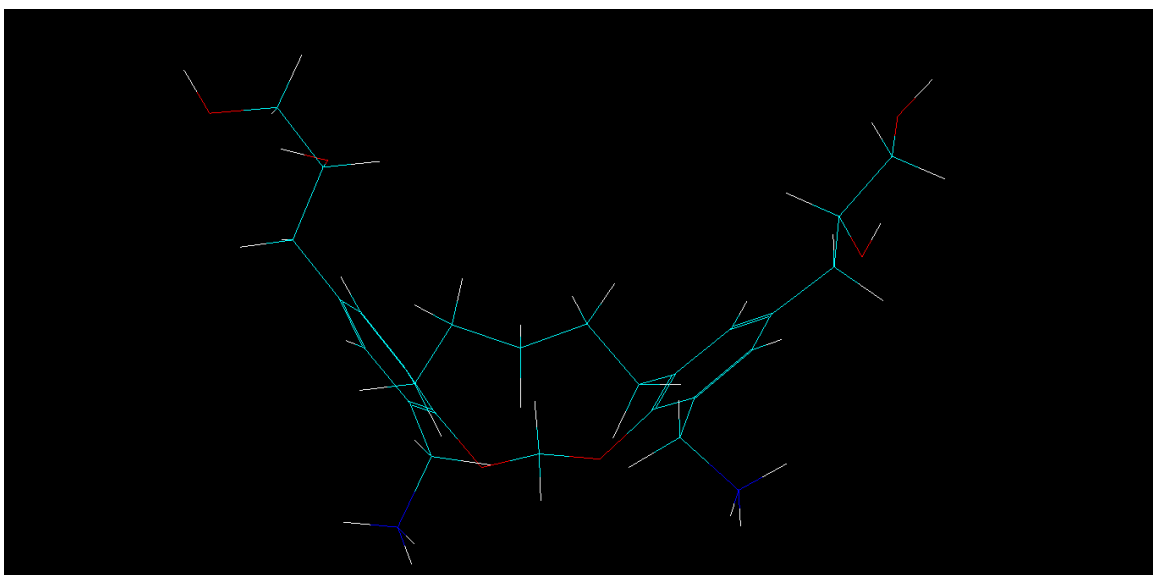


Figure 16. Initially proposed charged PG receptor



**5**

Figure 17. Semi-empirical computer model showing the minimized energy structure of the unbound charged receptor **5**

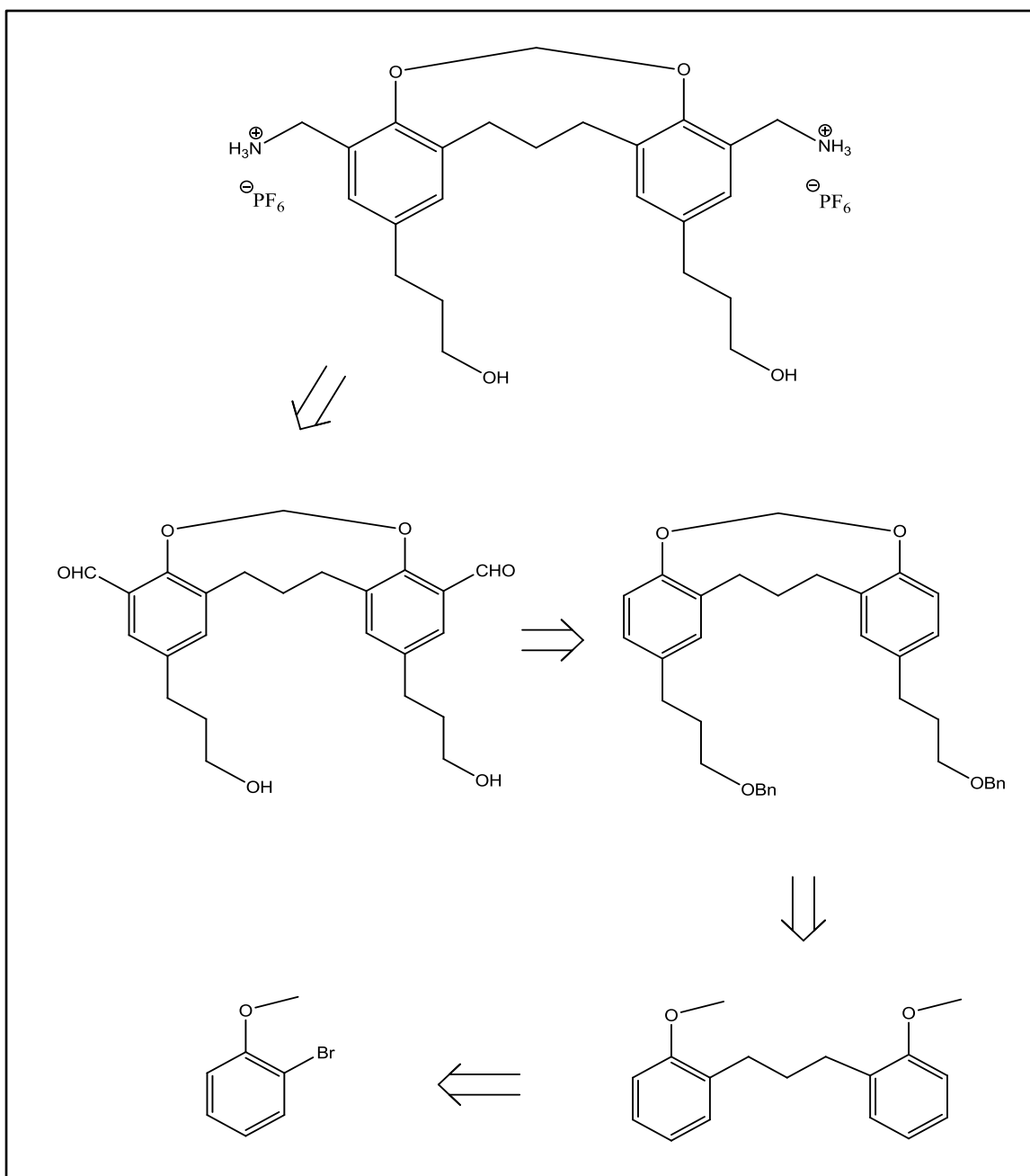
## CHAPTER 3

### SYNTHESIS OF RECEPTORS

An ether linkage via a methylene unit was used to connect the two phenols in the bis phenolic scaffold of the receptor. The initially proposed receptor had a propylene linker bridging the scaffold from its *ortho* positions. Extending outward from the scaffold are the functionalities responsible for binding to the head group of the PG anion. The positively charged amine groups were positioned to interact with the phosphate anion portion while the terminal hydroxyl groups were to interact with the glycerol hydroxyls on the PG anion.

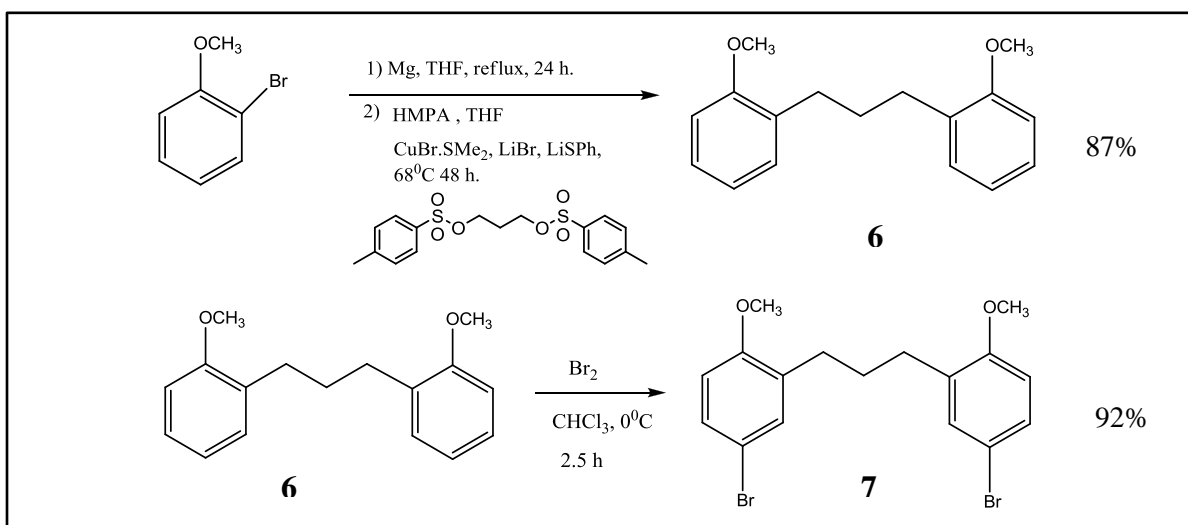
The synthesis was planned to involve four major steps, beginning with construction of the scaffold and attachment of primary alcohols to its *para* positions. Formylation of the scaffold, and its reductive amination were the key steps of the synthesis. The acidic protons of the phenols needed to be protected, since Grignard reactions would be used in the scaffold construction. Therefore 2-bromoanisole was chosen as the precursor and its retrosynthetic outline is given in Scheme 2.

A homogenous copper (I) catalyst developed in our lab was used for the Grignard reactions [27, 28]. Once the primary alcohols were introduced, *ortho* formylation of the scaffold was carried out. Reductive amination followed by introducing charges on the amine groups were planned as the last couple of synthesis steps for the receptor. The homogenous copper catalyst was used in the coupling reaction to introduce the propyl link between the two anisoles. Lithium thiophenolate, a component of the copper (I) catalyst was prepared in the lab using thiophenol and methyl lithium [27, 28]. Two molecules of 2-bromoanisole were reacted with one molecule



Scheme 2. Retrosynthetic scheme of the original planned synthesis of the charged receptor

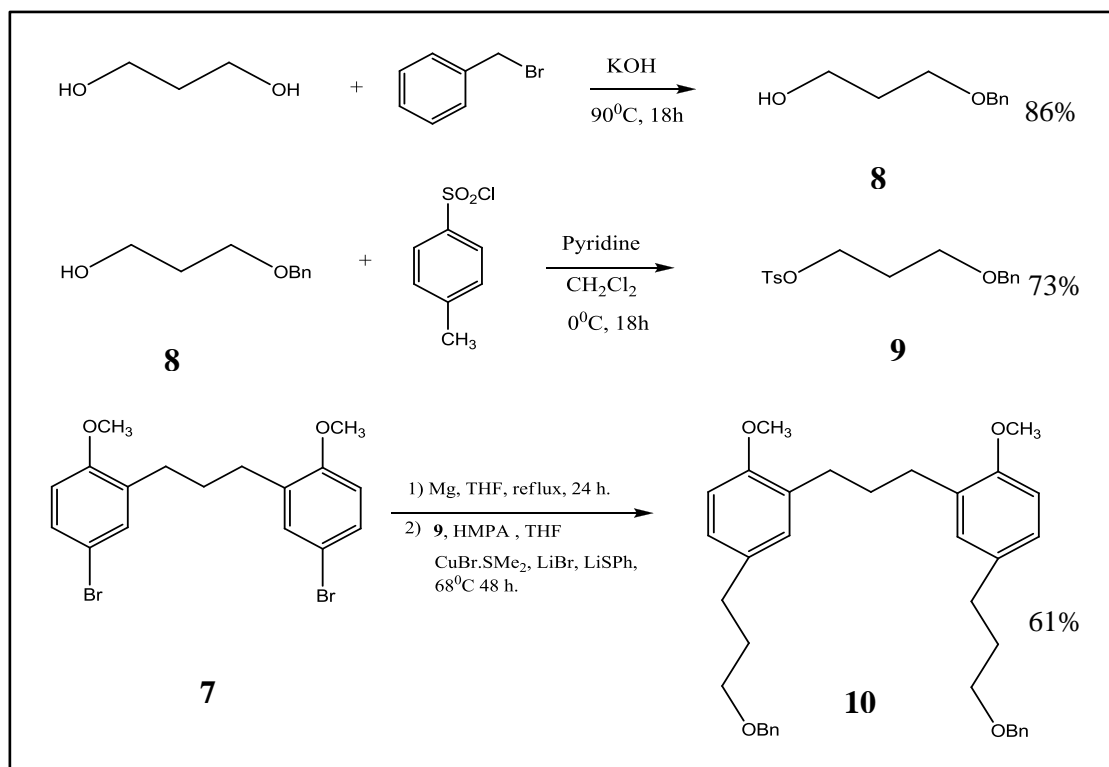
of 1,3-propanediol-bis-tosylate to produce the bis anisole **6** in 87% yield. Compound **7** was made in 92% yield by brominating **6** in the *para* positions using liquid bromine via electrophilic aromatic substitution (Scheme 3). The next step was to introduce masked propanolic functionality to the scaffold using copper (I) catalyzed Grignard coupling reaction chemistry (Scheme 4) [22, 27, 28].



Scheme 3. Bis anisole scaffold formation via Grignard reaction and bromination of the scaffold

In order to facilitate the Grignard coupling reaction, acidic alcohol protons were masked as benzyl ethers, which can be easily deprotected upon hydrogenation. The electrophile for the Grignard reaction was made using commercially available 1,3-propanediol. To one equivalent of 1,3-propanediol, 0.5 equivalents of base was added to form the potassium alkoxide which would then undergo nucleophilic substitution with benzyl bromide. The diol acted here as both the solvent and the reactant. The remaining alcohol group of the compound **8** was tosylated using

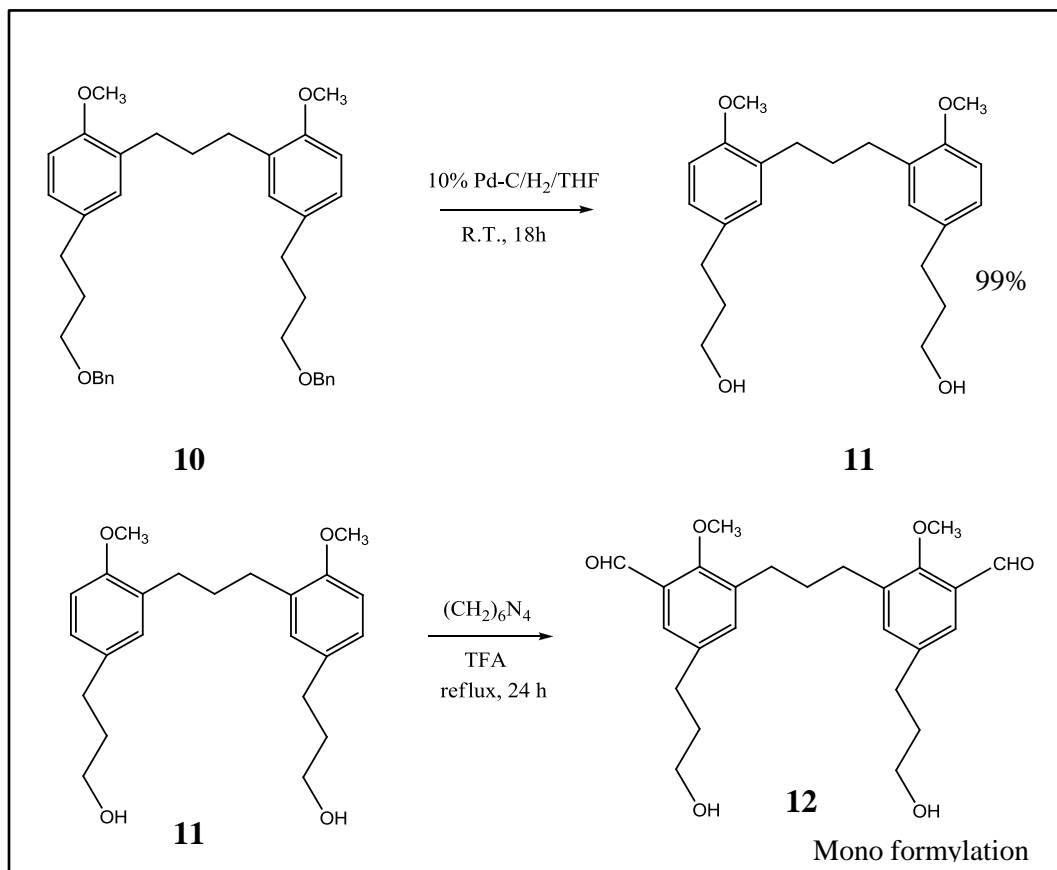
tosyl chloride, CH<sub>2</sub>Cl<sub>2</sub> and pyridine. The crystalline product **9** was prepared in large scale (fifty gram scale), since 5 equivalents of **9** were needed for the copper catalyzed Grignard coupling reaction with bis-bromo anisole **7**. The reaction to prepare the alkyl magnesium bromide of **7** was carried out for 24 h. It was then added to the electrophile **9** in the presence of the homogenous Cu (I) catalyst. To obtain the optimum yield of bis anisole scaffold **10**, the reaction was carried out in the glove box (Scheme 4) [22].



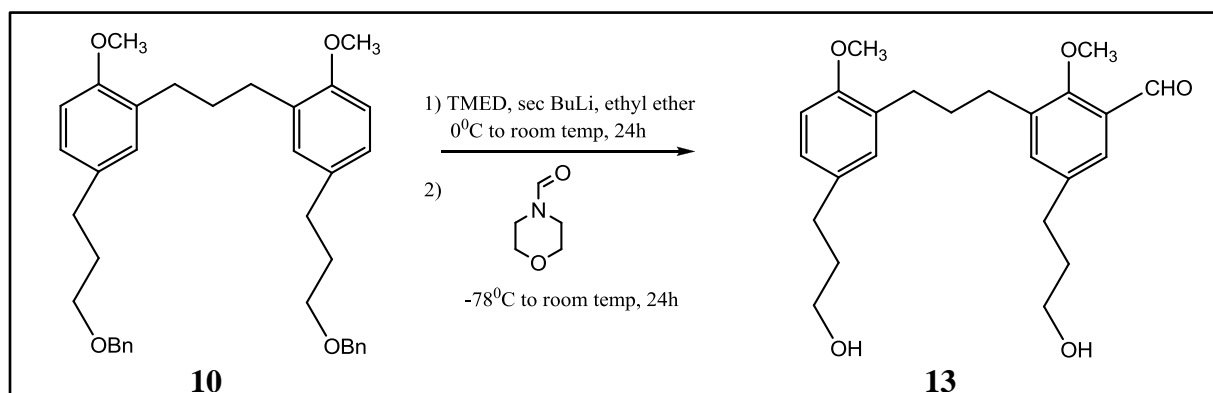
Scheme 4. Introduction of masked propanols to the bis anisole scaffold using Grignard chemistry

We attempted to formylate compound **10** using the Duff reaction. Based on the previous work done by a graduate student in our lab, prior to the Duff reaction, we deprotected the hydroxyl groups of **10** by hydrogenation to yield **11** in high yield [29]. It was then subjected to

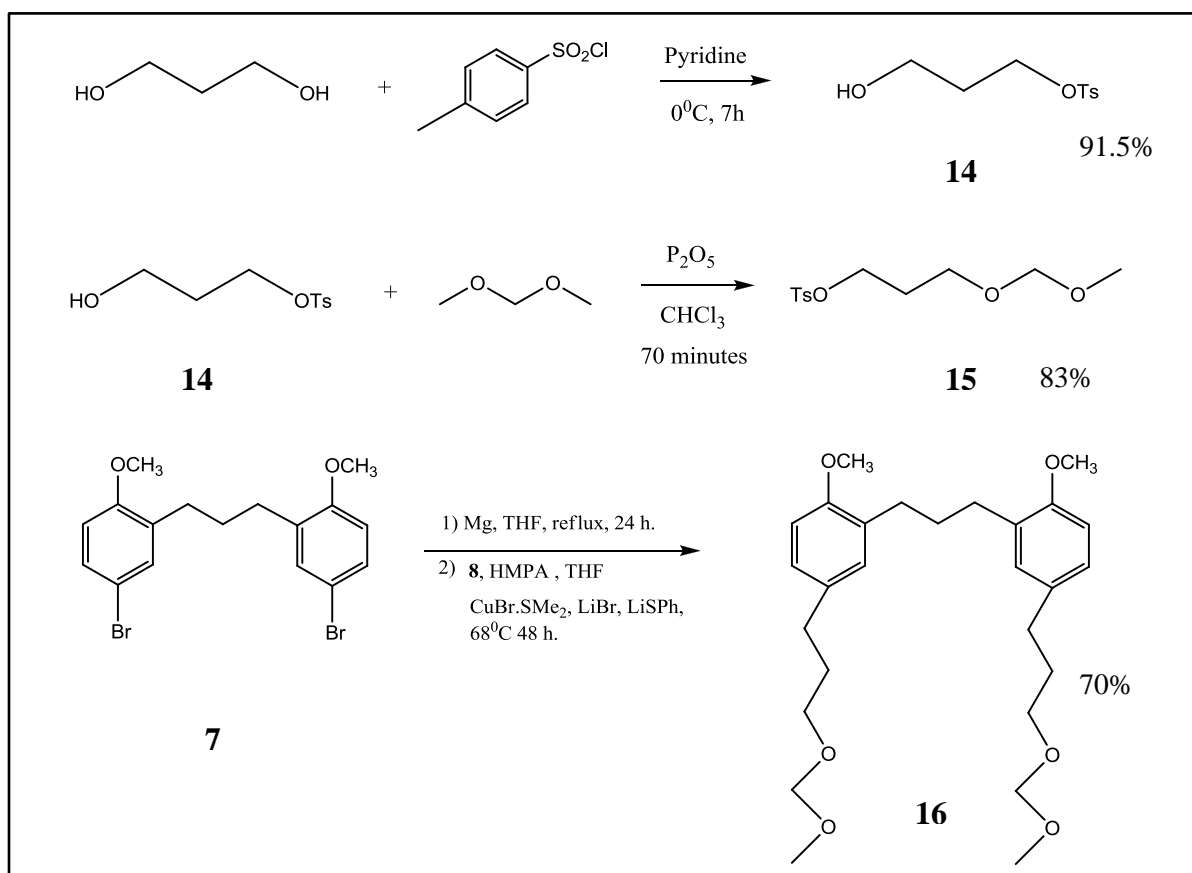
Duff reaction using hexamethylenetetramine and TFA under reflux conditions [30]. We were unable to get the desired product **12** but always ended up with the mono formylated compound with a small amount of **12** in the crude product (Scheme 5). We then decided to formylate compound **10** using N-formyl morpholine. First we made the dianion of **10** using sec-butyllithium in the presence of TMED and the reaction mixture was cooled to  $-78^{\circ}\text{C}$  before introducing 4-formyl morpholine (Scheme 6). We ended up having hydroxyl groups deprotected with a mixture of mono and di formylation. We then decided to change the hydroxyl protecting group from benzyl to methoxy methane. One equivalent of 1,3-propanediol was tosylated using 0.5 equivalents of tosyl chloride and 0.25 equivalents of pyridine to yield **14**. The remaining alcohol group was then protected as a MOM ether using dimethoxymethane in the presence of  $\text{P}_2\text{O}_5$  [30]. The resulting compound **15** was subjected to Grignard coupling reaction with **7** using the copper (I) catalyst to yield **16** (scheme 7). Introduction of formyl groups to **16** was attempted using 4-formyl morpholine but furnished a mixture of mono formylated product and starting material (Scheme 8).



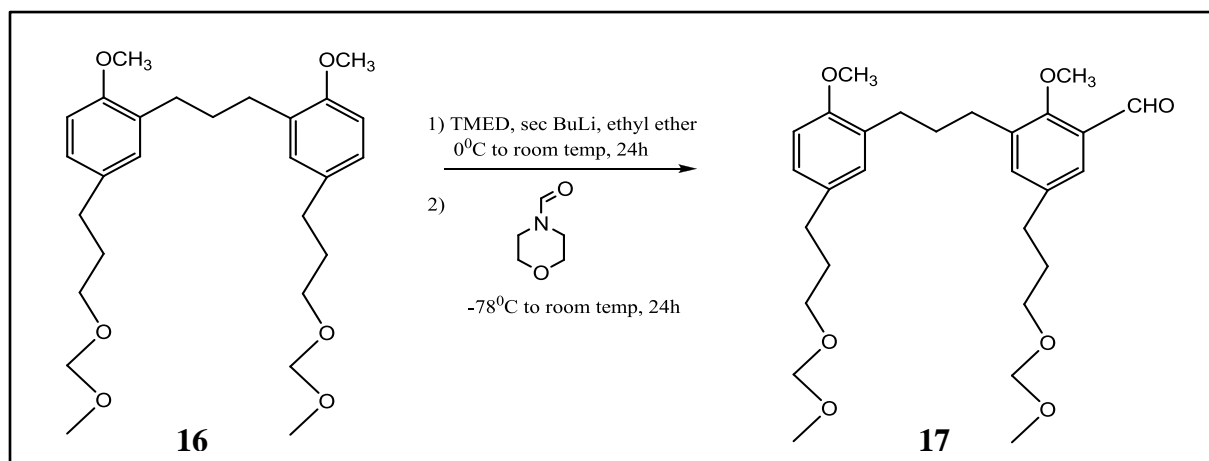
Scheme 5. Formylation of the hydrogenated bis anisole scaffold with Duff reaction



Scheme 6. Formylation attempt of **10** using 4-formyl morpholine

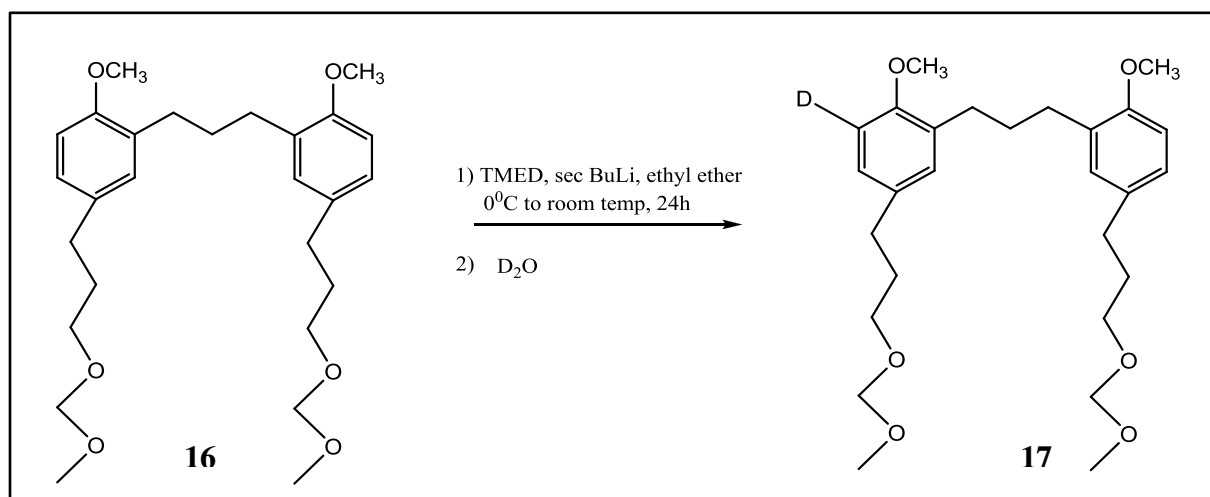


Scheme 7. Introduction of dimethoxymethane protected propanol to the bis anisole scaffold



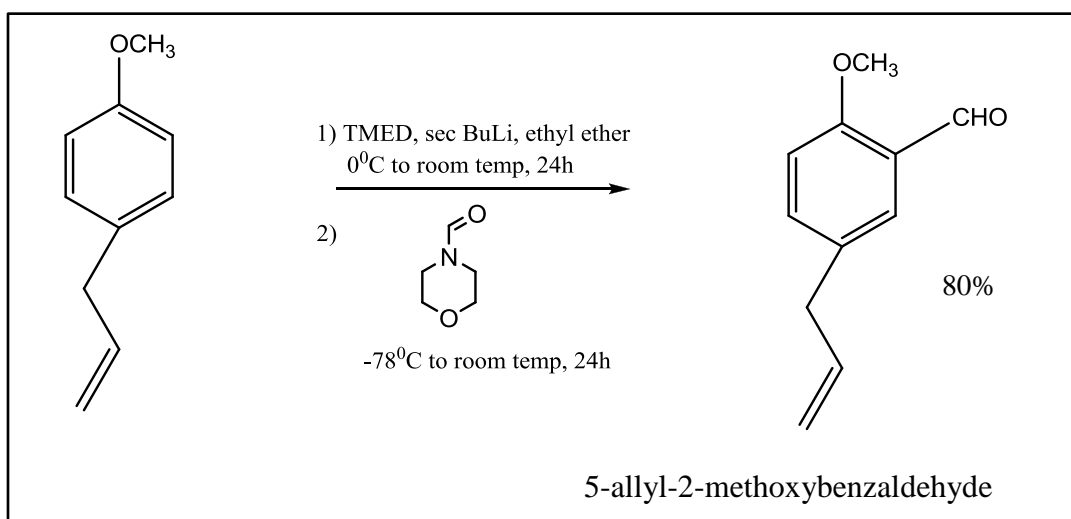
Scheme 8. Formylation attempt on **16**.

Hence we decided to find out whether the dianion of **16** was made upon reacting with sec. BuLi (Scheme 9). By quenching with D<sub>2</sub>O, we found that the mono anion was made after 24 h and no di anion was made even after carrying out the reaction for 36 h.



Scheme 9. D<sub>2</sub>O quenching of the **16** anion.

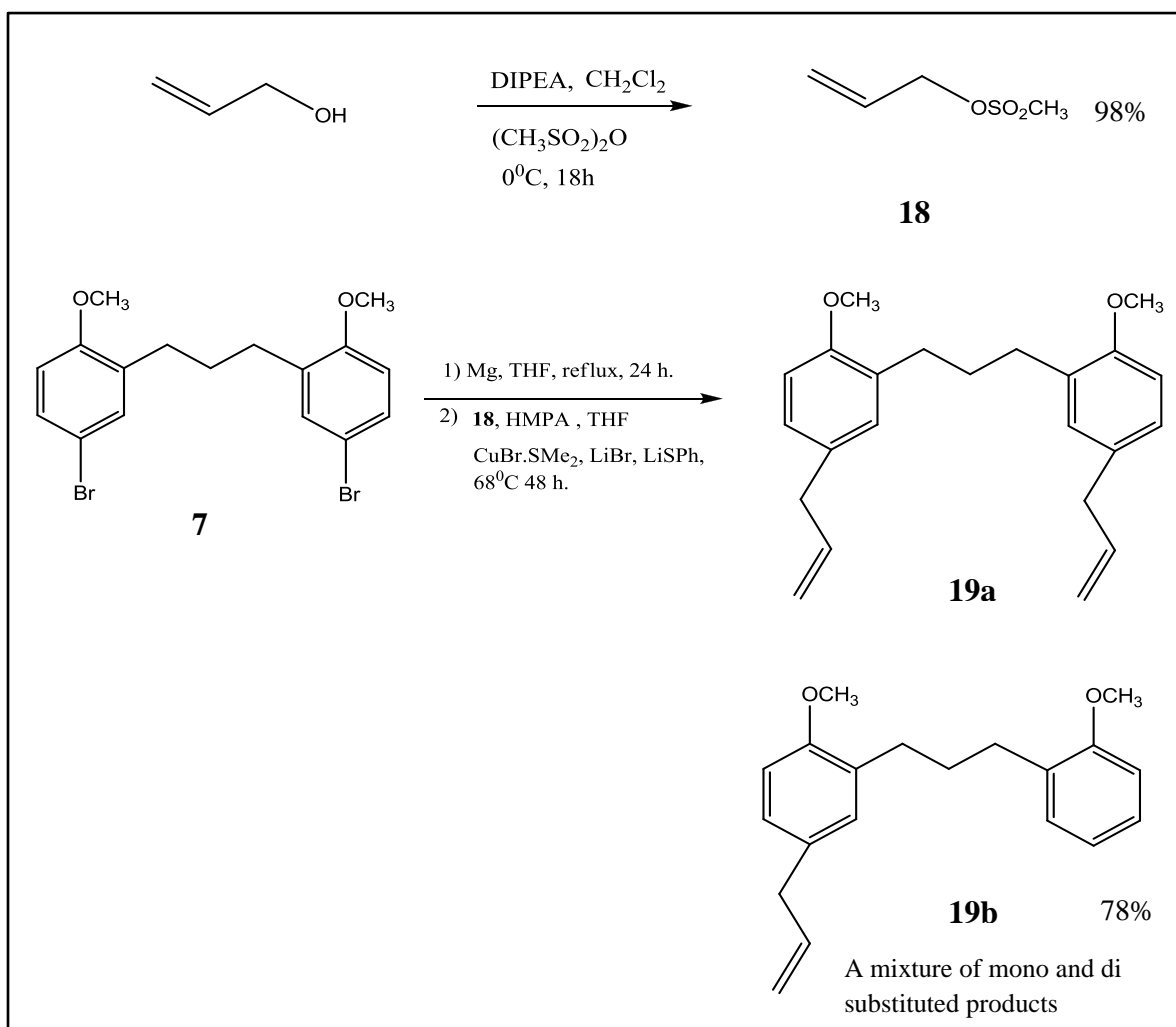
The failure to protect the benzylic groups of **10** or to form the dianion of compound **16** prompted us to change the structure of the *para* substituents. As a result we decided to introduce allyl functionality to the bis anisole scaffold, which could be converted to hydroxyl functionality later in the reaction pathway. Prior to the synthesis of **19** with the bis allyl functionality, we did model studies using 1-allyl-4-methoxy benzene, and the 4-formyl morpholine reaction yielded 80 % of 5-allyl-2-methoxybenzaldehyde as shown in Scheme 10.



Scheme 10. Model study for the formylation of 1-Allyl-4-methoxy benzene.

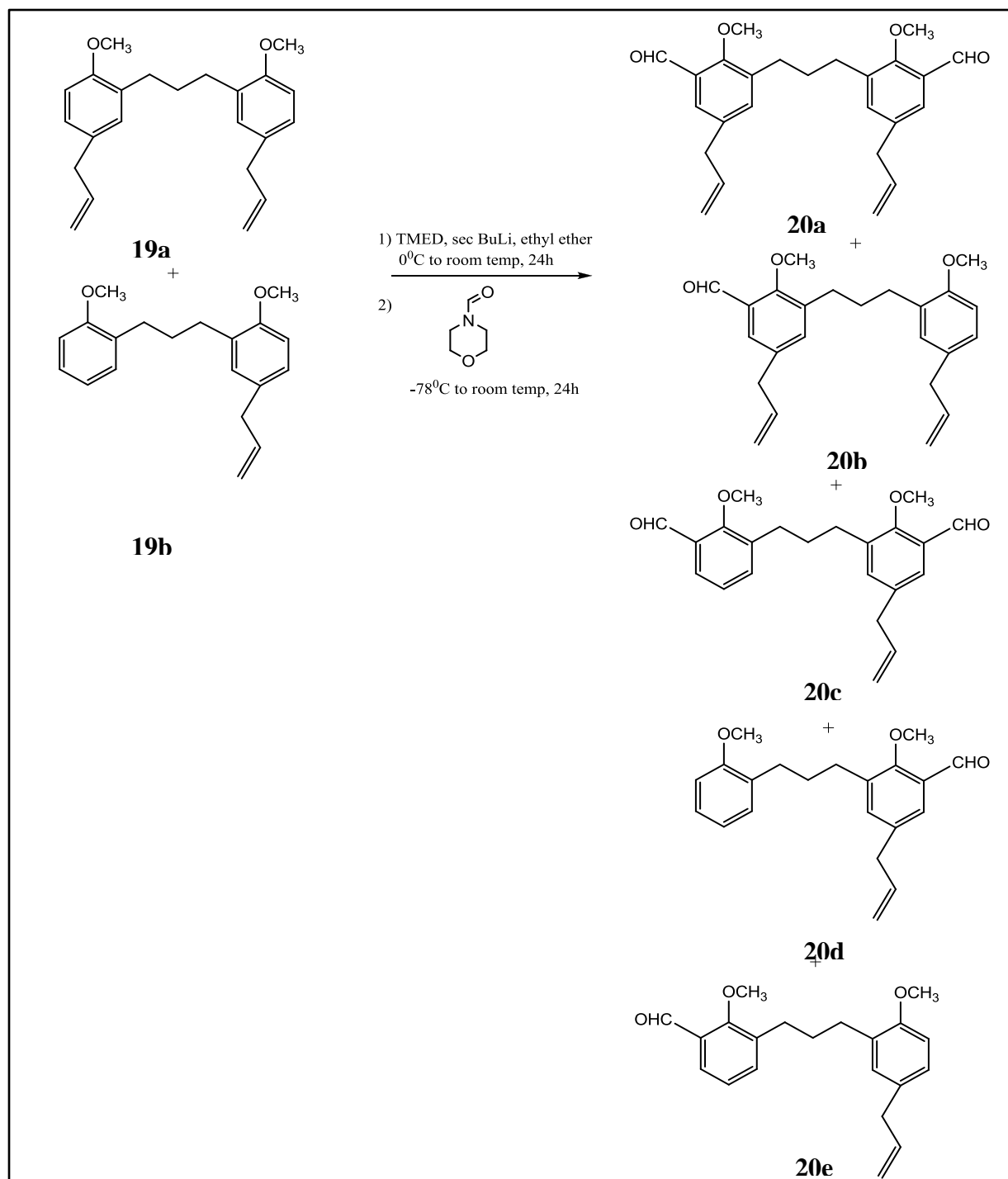
The electrophile allyl mesolate **18** was made from 2-Propen-1-ol, and was used without further purification for the coupling with the bis bromo compound **7** [31]. The Grignard coupling reaction for the synthesis of **19** always gave us a mixture of mono and di substituted products as shown in Scheme 11. Radial chromatography using 2% Isopropyl amine in Hexane eluted the mono and di substituted mixture as a single band (Figure 19). This mixture of products proved problematic in the next synthetic step due to the formation of several aldehydes (Scheme 12).

Therefore, we decided to alter our synthetic pathway and take a different route. Also, based on anion binding studies done by our group, in order to best accommodate the PG anion's head group, it was decided to increase the number of methylene linker units bridging the bis anisole scaffold from 3 to 5. The revised retrosynthetic outline is given in Scheme 13.

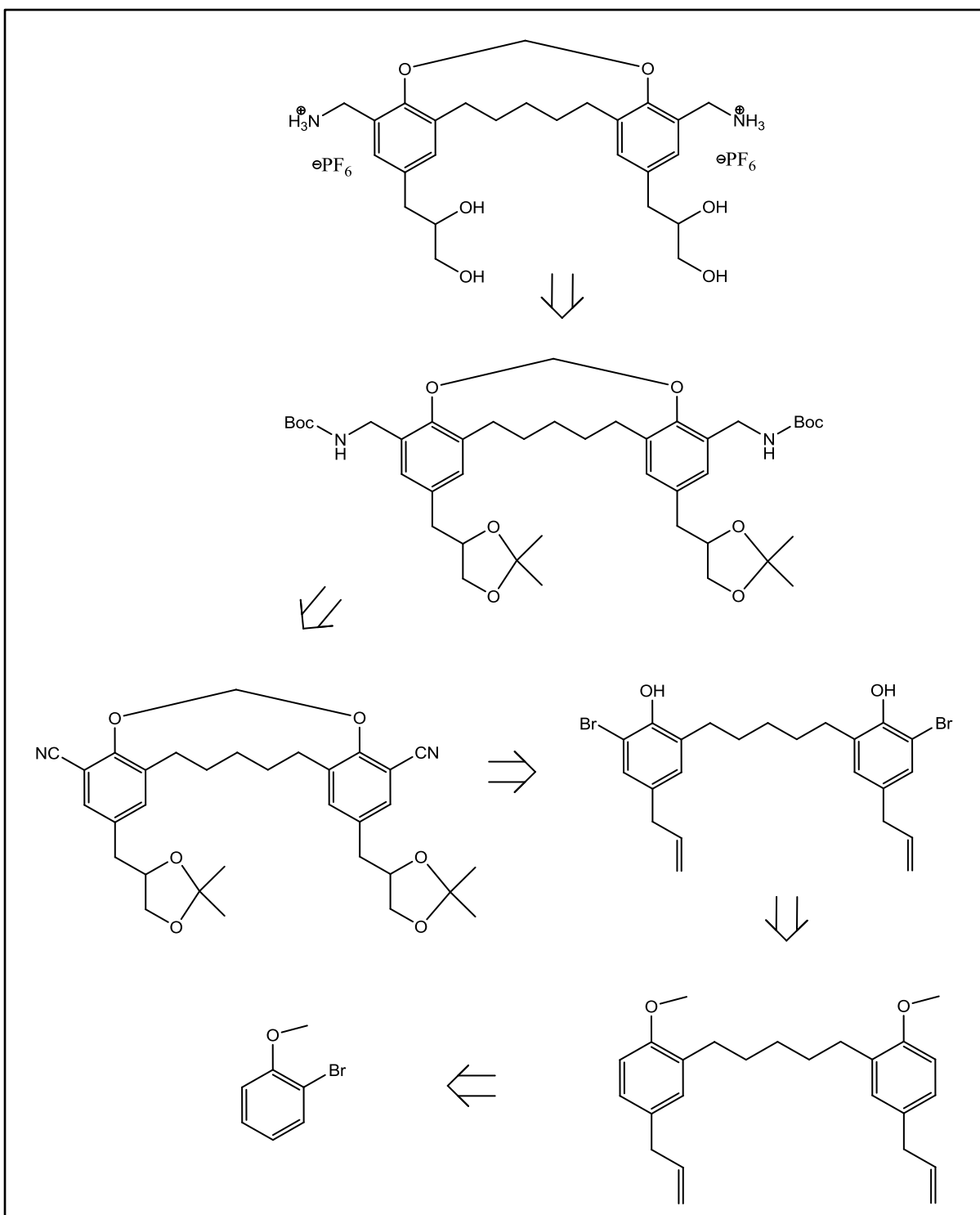


Scheme 11. Introduction of allyl groups to the bisanisole scaffold.

The revised synthetic pathway was started by converting the two hydroxyl groups of diethylene glycol into leaving groups. Diethylene glycol was chosen based on previous work done by a graduate student in our lab [27]. The resulting bis tosylate **21** was then used for the Grignard coupling reaction to yield **22** (Scheme 14).

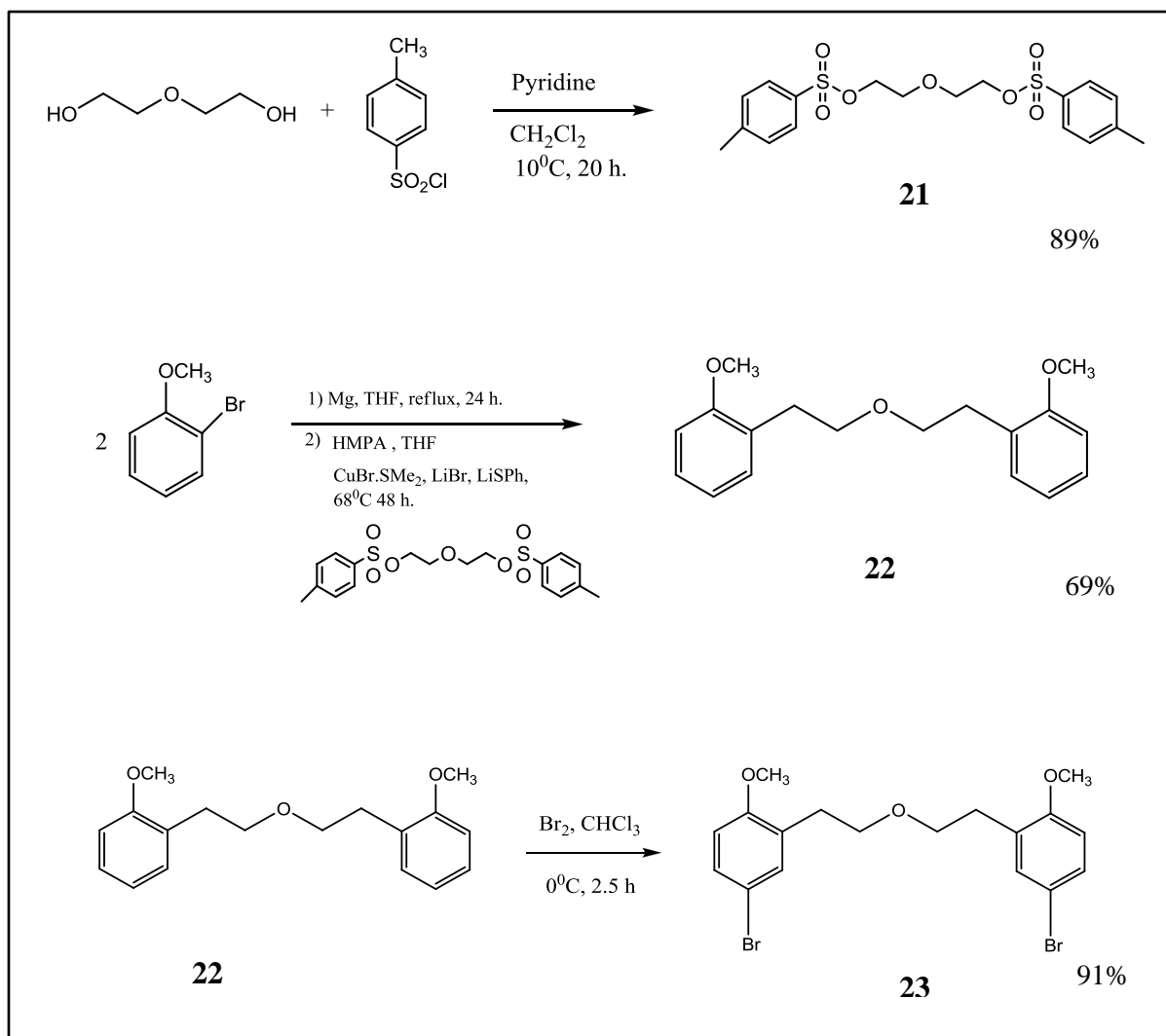


Scheme 12. Formylation of **19**

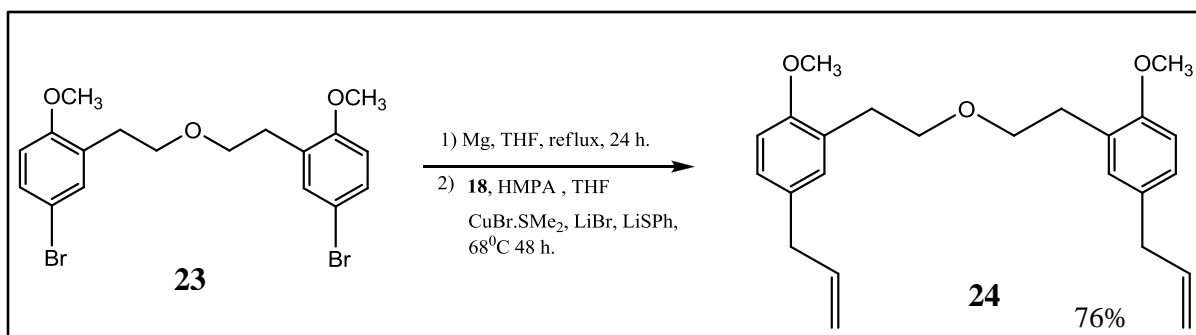


Scheme 13. Revised retrosynthetic pathway

Unlike compound **6**, where its crude form was a solid, **22** was an oily compound. Before further purifications, crude products of all Grignard coupling reactions were passed through a silica pad using 20% Ethyl acetate in Hexane as the eluent to remove toxic HMPA. A gravity column separation using 100% Hexane as the eluent yielded pure **22**. The crude **23** was also an oily compound and it was subjected to a column chromatographic separation using 75% CH<sub>2</sub>Cl<sub>2</sub> in Hexane as the eluent to obtain pure **23** in 91% yield (Scheme 14).

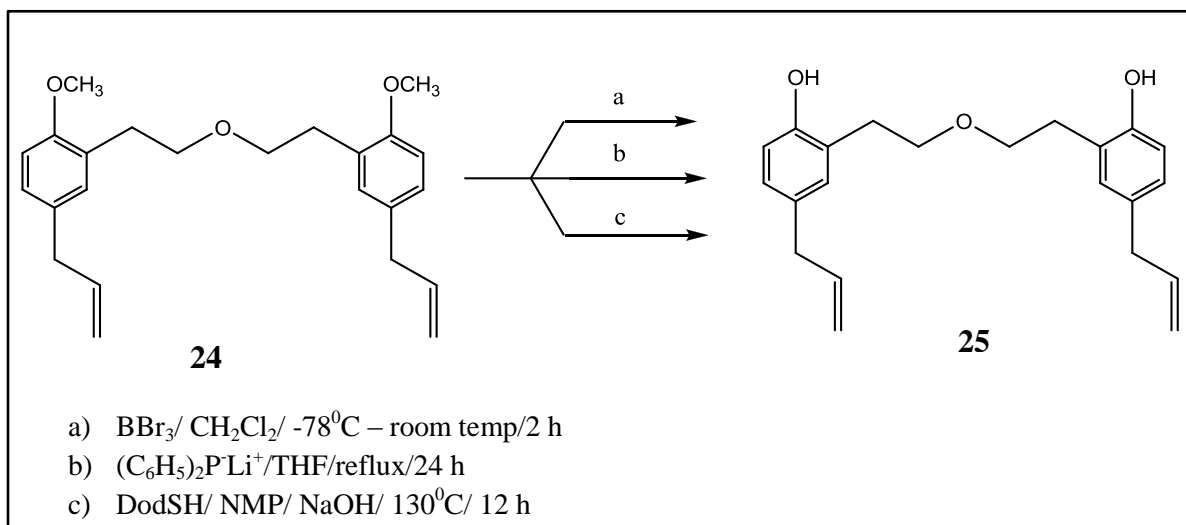


Scheme 14. Synthesis of compound **23**.



Scheme 15. Synthesis of compound **24**.

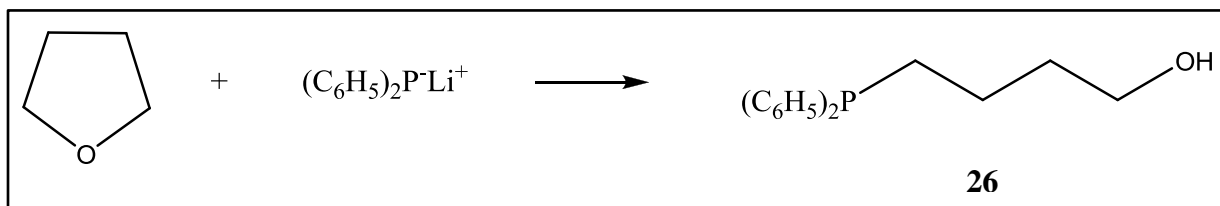
Compounds **23** and **18** were dried over benzene using a Dean-Stark apparatus, prior to the dry box reaction for the synthesis of **24**. After passing through a silica pad to remove HMPA, gravity column separation using 50% CH<sub>2</sub>Cl<sub>2</sub> in Hexane as the eluent yielded pure **24** (Scheme 15). It is noteworthy that this reaction did not furnish the mono substituted product. The demethylation of **24** was attempted using three different types of reactions, but little or no product was isolated [32-35]. The <sup>1</sup>H NMR spectra for reactions a and b, indicated that compound **24** was demethylated, but the purification was problematic. Reaction c did not demethylate the starting material (Scheme 16). For all three demethylation reactions, compound **24** was used after drying over benzene using a Dean-Stark apparatus.



Scheme 16. Demethylation attempts on **24**.

The demethylation reaction with  $\text{BBr}_3$  was carried out at  $-78^\circ\text{C}$  using  $\text{CH}_2\text{Cl}_2$  as the solvent, under an inert atmosphere [33]. Two equivalents of  $\text{BBr}_3$  were reacted with one equivalent of **24**. When  $\text{BBr}_3$  was syringed into the reaction flask, the solution changed from colorless to a yellow color. After 30 minutes, it was allowed to warm to room temperature and continued stirring for 2 hours. The reaction was quenched by the addition of methanol. The  $^1\text{H}$  NMR spectrum of the crude product indicated compound **24** was demethylated, but once isolated, it gave a very low yield of **25** (8-10%). As a result we decided to use a 0.5M solution of lithium diphenyl phosphine, another demethylating reagent, for the reaction [34]. The phosphine reagent was reacted with **24** under reflux conditions using dry THF for 24 h. (Scheme 16). The reaction was quenched with cold 1.5M HCl. The crude product's TLC profile indicated three distinct spots and, once subjected to radial chromatographic purification, unreacted starting material and a

small percentage of demethylated product (7%) were isolated. We also isolated another compound which was a product from the reaction between THF and lithium diphenyl phosphine (Scheme 17, Figure 18). We also used 1-dodacanethiol in the presence of NMO under basic conditions at 130<sup>0</sup>C for demethylation, also resulting in little or no product produced (Scheme 16) [35].



Scheme 17. Lithium diphenyl phosphine reaction with THF.

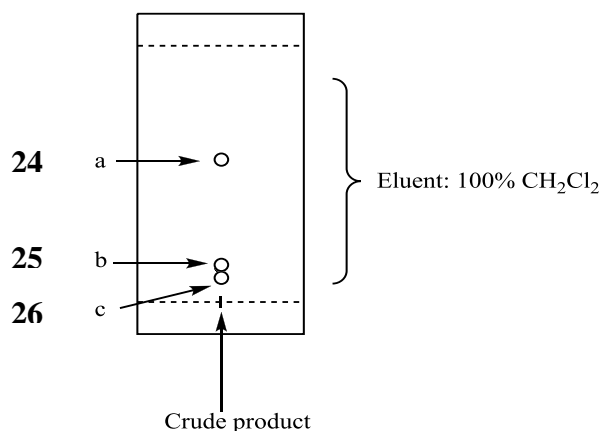
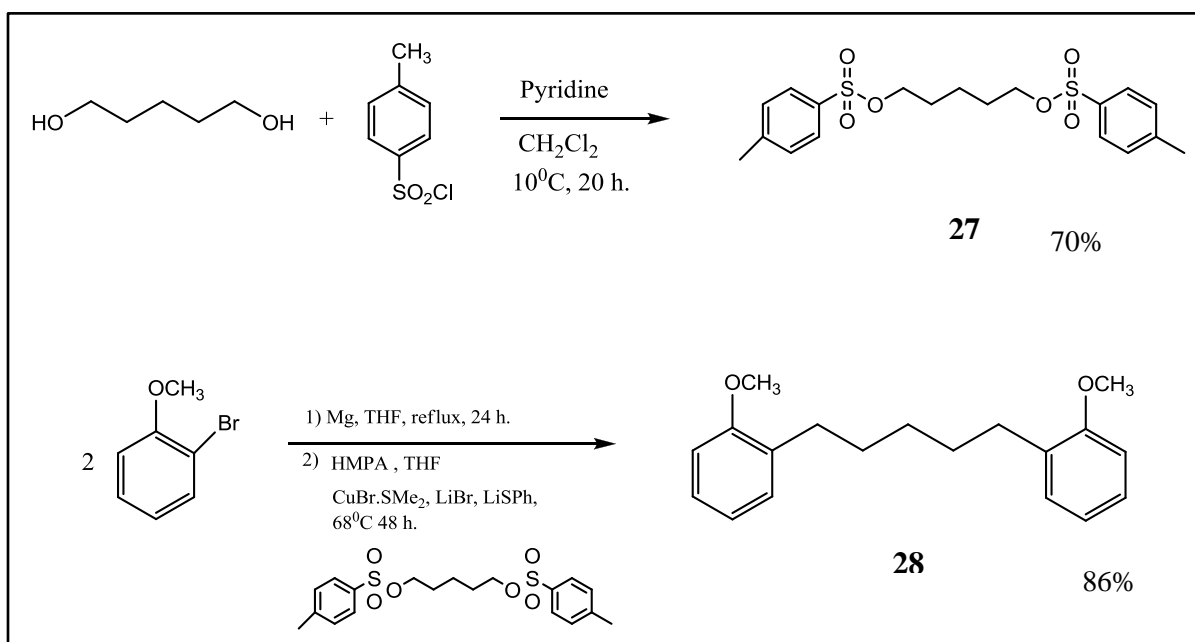


Figure 18. TLC profile for reaction between Lithium diphenyl phosphine and **24**.

Based on the by-products of the  $\text{BBr}_3$  reaction, we believe that boron was coordinating to the oxygen in the ethoxyethane linker without demethylating the bis phenolic ether. The failure to demethylate **24** prompted us to replace the ethoxyethane type bridging unit with a pentane

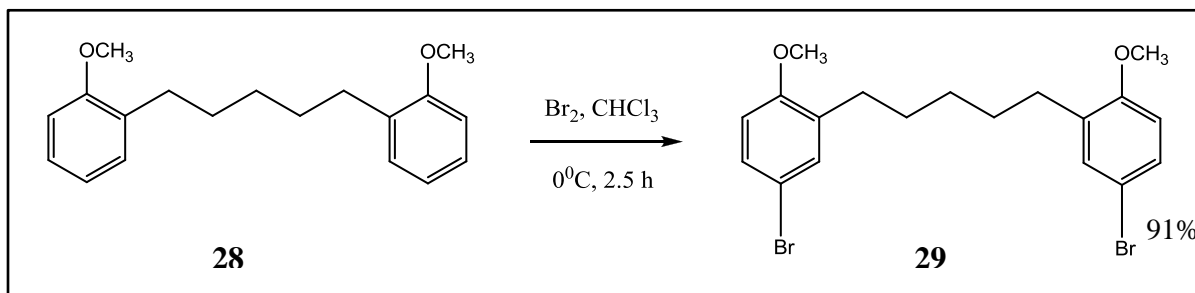
linkage. 1,5-Pentanediol was converted to its bis tosylate **27**. The crude product was recrystallized from ethanol to yield 70% of pure **27**. It was then used for the Cu (I) catalyzed Grignard coupling reaction with 2-Bromoanisole (Scheme 18).



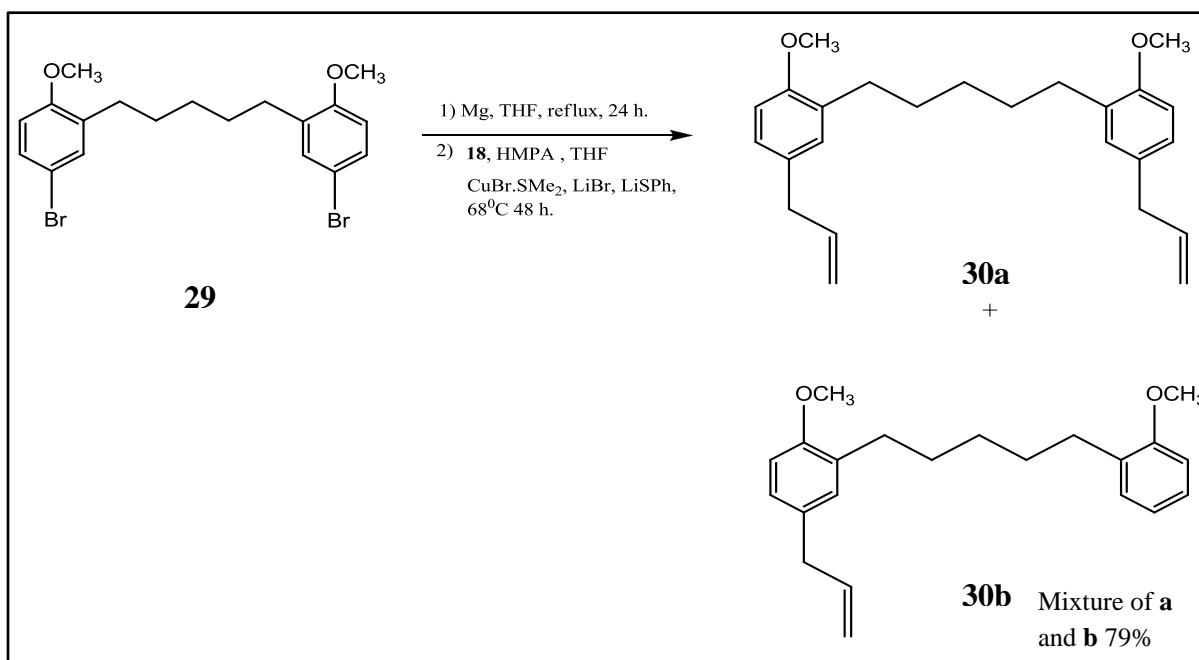
Scheme 18. Synthesis of compound **28**.

Compound **28** was then brominated in the *para* position using liquid  $\text{Br}_2$  in  $\text{CHCl}_3$  at  $0^\circ\text{C}$  (Scheme 19). The crude product of **29** was recrystallized from ethanol and used for the Grignard coupling reaction with allyl mesolate **18**. Similar to the results obtained in Scheme 11, the dry box reaction gave us the desired di-substituted product **30a**, along with the mono substituted **30b** (Scheme 20). It was eluted as a single band from a gravity column separation (90:10

Hexane/EtOAc), yielding a 79% combined yield of the mono and di substituted product (Figure 19).



Scheme 19. Bromination of **28**



Scheme 20. Introduction of allyl groups to compound **29**.

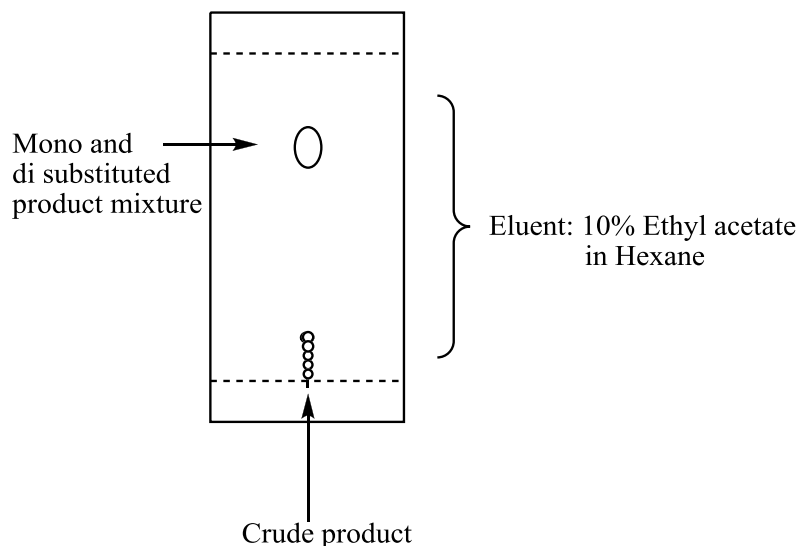


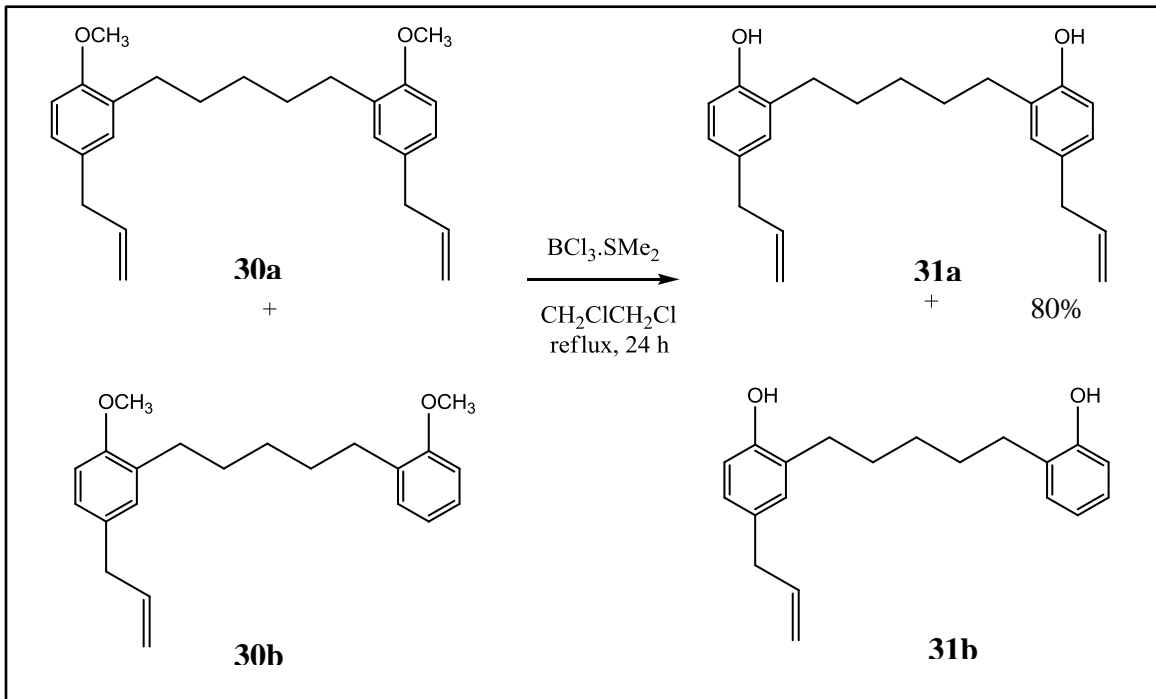
Figure 19. TLC profile for the crude product **30** from dry box reaction

The inseparable mixture of **30a** and **30b** was reacted with  $\text{BBr}_3$  to demethylate the bis anisole but the product was furnished in low yield (8%). Since the lithium diphenyl phosphine reaction and 1-dodecanethiol reaction also gave us very poor or no yield of the demethylated product, we decided to use a different method using boron trichloro [1,1'-thiobis(methane)] as the demethylating reagent [34]. Dry dichloroethane was used as the solvent. The reaction conditions were varied as shown in Table 2, to optimize the yield. Gravity column separation using the eluent of 15% ethyl acetate and 2% isopropyl amine in hexane allowed us to isolate the pure **31a** from each reaction. Allowing the reaction to run for 24 h using three equivalents of  $\text{BCl}_3\text{:SMe}_2$  furnished the highest yield.

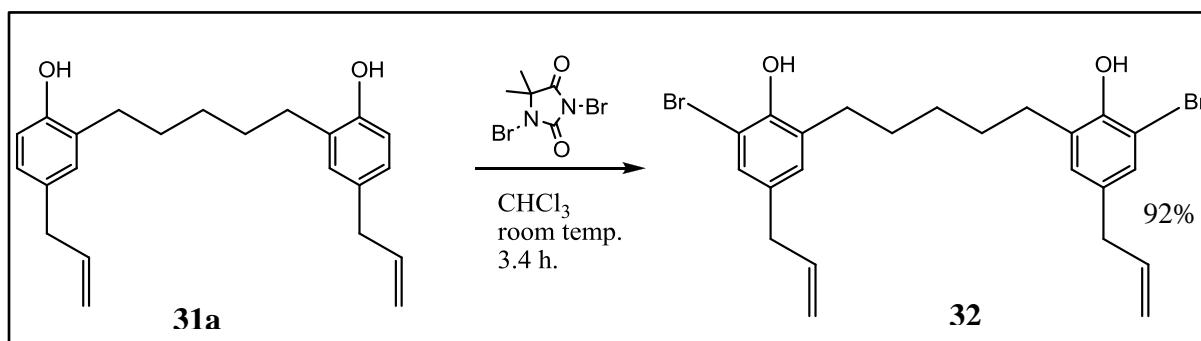
TABLE 2.

REACTION CONDITIONS FOR DEMETHYLATION OF **30** WITH  $\text{BCl}_3\cdot\text{SMe}_2$ 

Reaction	Equivalents of <b>30a</b> and <b>30b</b>	Equivalents of $\text{BCl}_3\cdot\text{SMe}_2$	Reaction Concentration	Solvent	Reaction Time	% Yield
1	1	2	0.25M	1,2-dichloroethane	24 h.	45
2	1	2	0.25M	1,2-dichloroethane	48 h.	45
3	1	3	0.25M	1,2-dichloroethane	24 h.	80

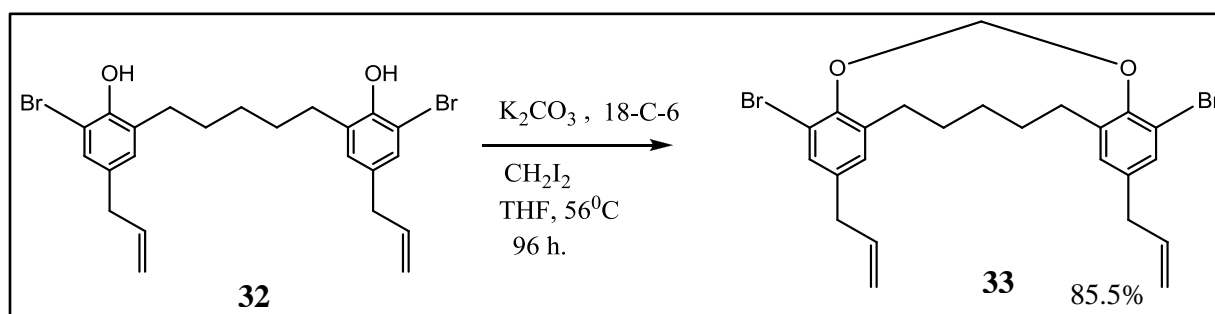
Scheme 21. Demethylation of the dry box product using  $\text{BCl}_3\cdot\text{SMe}_2$ .

After optimizing the demethylation reaction, our next step was to brominate the two *ortho* positions of the compound **31a**. One equivalent of **31a** was reacted with 1.16 equivalents of DBDMH at room temperature using  $\text{CHCl}_3$  as the solvent (Scheme 22) [35].



Scheme 22. Bromination of **31a**.

A gravity column separation of the crude product using 100%  $\text{CHCl}_3$  as the eluent gave pure **32** in 92% yield as the first band. 5,5-Dimethylhydantoin eluted as the polar second band from the column. Our next task was to introduce a methylene bridging link between the two phenolic oxygens of compound **32**.



Scheme 23. Ether linkage between the phenolic oxygens of **32**.

Compound **32** (1 equivalent) was reacted with  $K_2CO_3$  (3 equivalents) to produce the dianion in the presence of phase transfer catalyst 18-crown-6 (1.5 equivalents), along with one equivalent of diiodomethane. Another equivalent of  $CH_2I_2$  was added to the reaction mixture (only for reactions 2, 3 and 4) after 24 h. While keeping the reactant equivalents constant, the concentration of the reaction and reaction times were varied to optimize the yield percentages. The yield was almost doubled when we changed the reaction concentration from  $5 \times 10^{-2}$  M to  $5 \times 10^{-3}$  M. It was further improved when the reaction time was increased to 96 h, where the greenish yellow color of the reaction mixture changed to colorless, which seems to be indicative that the reaction was complete (Scheme 23, Table 3).

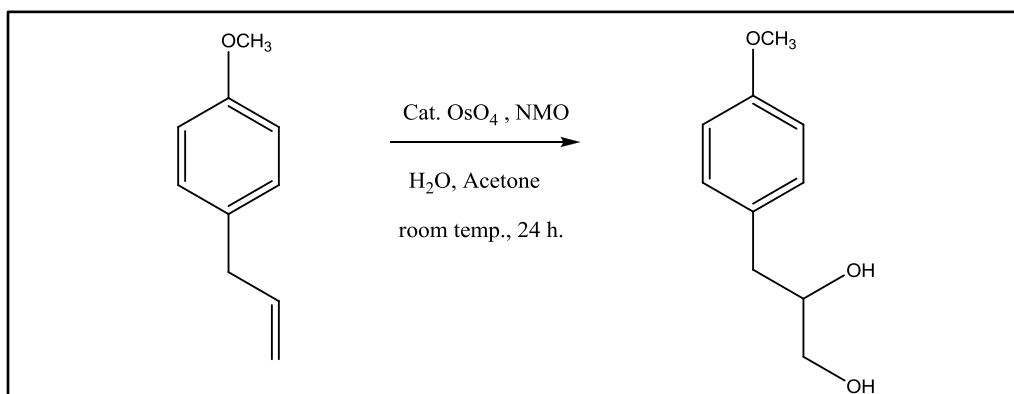
TABLE 3.

REACTION CONDITIONS FOR PHENOLIC OXYGEN BRIDGING LINKAGE OF **32**

Reaction	Reaction Concentration	Reaction time	Color	% Yield
1	$5 \times 10^{-2}$ M	24h	Green/Yellow (no color change)	28.3
2	$5 \times 10^{-2}$ M	36h	Green/Yellow (no color change)	30
3	$5 \times 10^{-3}$ M	36h	Green/Yellow (no color change)	59.2
4	$5 \times 10^{-3}$ M	96h	Green/Yellow to colorless	85.5

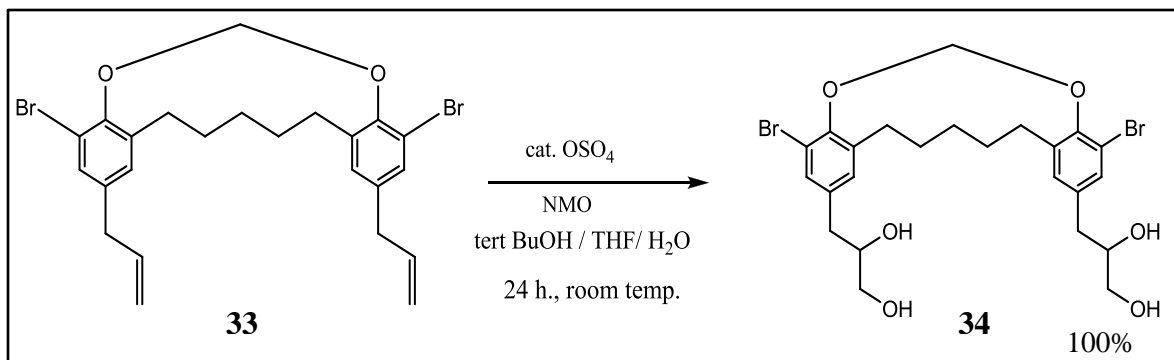
The next step of the reaction scheme was to convert the bromines in the *ortho* position to nitrile functionality. The authors of the paper to which we referred used a palladium species as the reaction catalyst [36]. Therefore to prevent coordination with  $\text{Pd}_2(\text{dba})_3$ , we decided to dihydroxylate the allyl groups in the *para* positions of the receptor scaffold **33**, and protect them as acetonides, prior to the conversion of bromines to nitriles [37].

Our model studies with 1-Allyl-4-methoxybenzene, indicated dihydroxylation using a catalytic amount of  $\text{OsO}_4$  in the presence of NMO leaves no starting material after a 24 h reaction period (Scheme 24) [38]. When we applied the same solvent system (1:1.5 Acetone /  $\text{H}_2\text{O}$ ) for the osmylation of compound **33**, it did not produce **34**.



Scheme 24. Dihydroxylation of 1-Allyl-4-methoxybenzene.

When the solvent system was changed to (10:3:1 tert.BuOH/THF/ $\text{H}_2\text{O}$ ), the TLC profile did not show any **33** after a 24 h. reaction time (Scheme 25, Figure 20) [39]. The resulting dihydroxylated compound was used for the next synthetic step without further purification.



Scheme 25. Dihydroxylation of compound **33**.

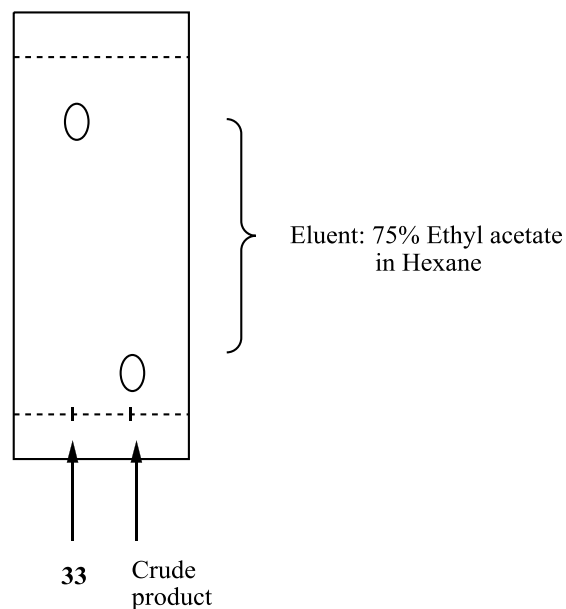
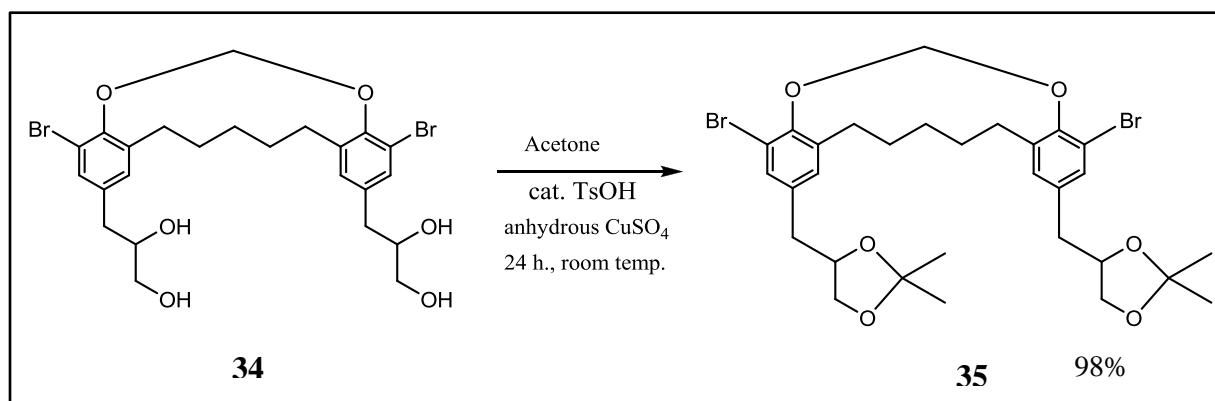


Figure 20. TLC profile for the dihydroxylation of **33**.

The two 1,2-diol groups of the compound **34** were then protected as ketals using TsOH and acetone in the presence of anhydrous  $\text{CuSO}_4$  (Scheme 26) [40].  $\text{CuSO}_4$  was used to remove water produced in the acetonide protection. During the workup of the reaction, the crude product was

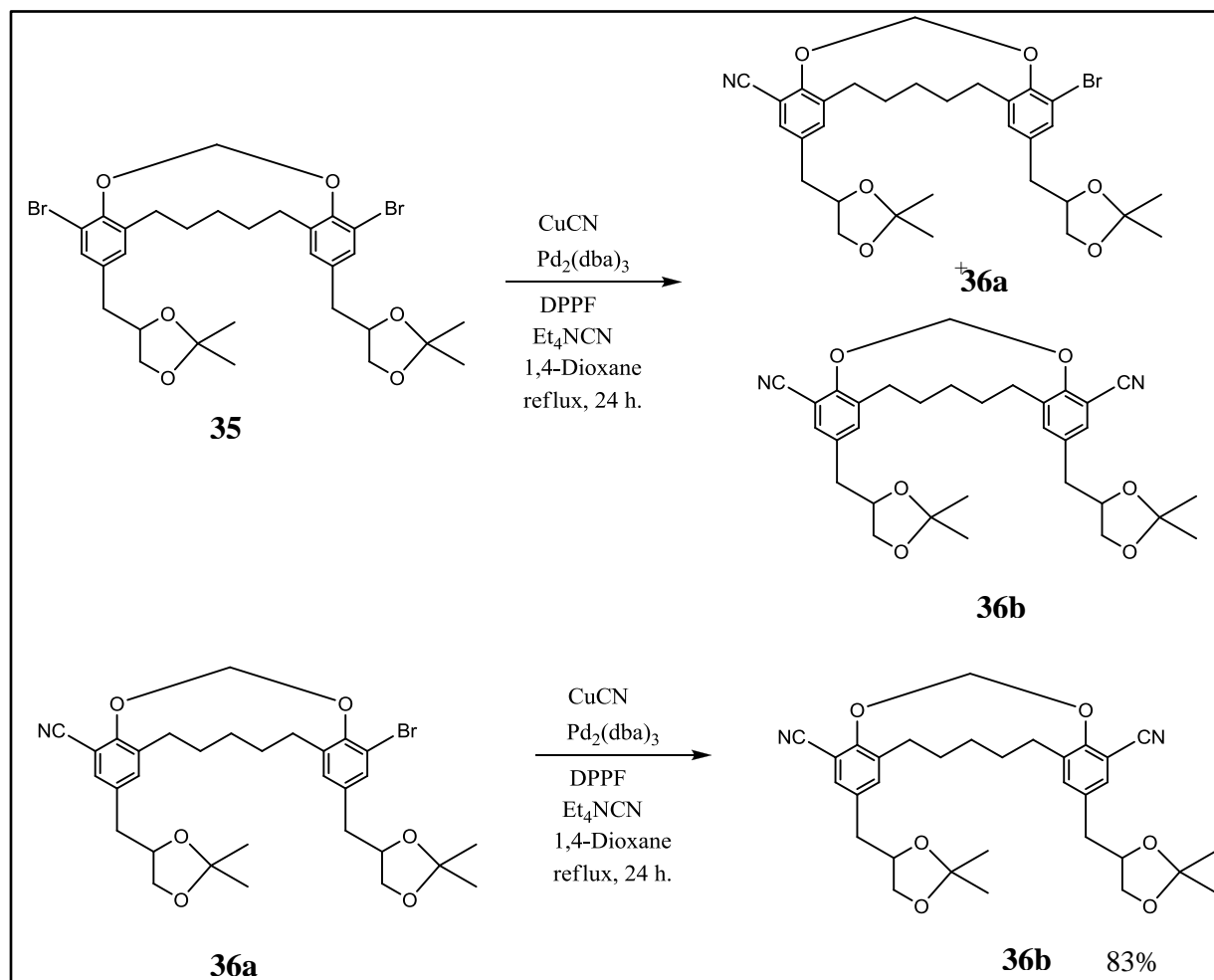
dissolved in EtOAc and washed with a saturated aqueous solution of  $\text{NaHCO}_3$  to remove the TsOH. The resulting product was passed through a silica pad (98:2 EtOAc/Isopropylamine). It was then used for the palladium catalyzed cyanation without further purification [36].



Scheme 26. Acetonide protection of compound **34**.

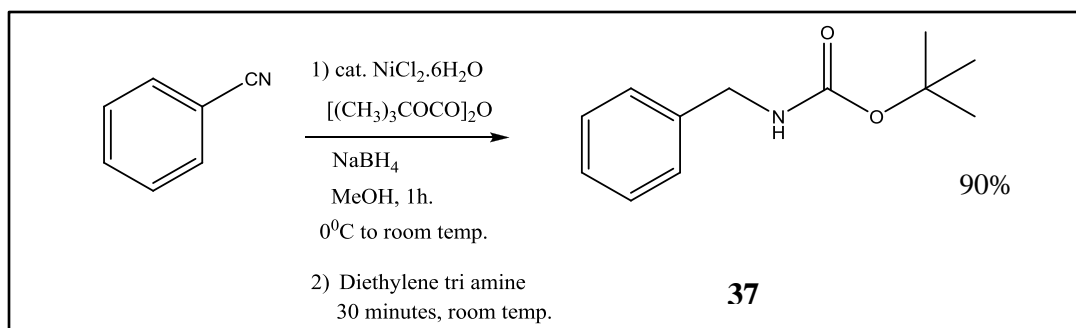
The dry bis acetonide **35** (1 equivalent) was reacted with  $\text{CuCN}$  (8 equivalents), in the presence of catalytic amounts of  $\text{Pd}_2(\text{dba})_3$  (0.08 equivalents) and DPPF (0.2 equivalents). Two equivalents of  $\text{Et}_4\text{NCN}$  have been used as an additive for the reaction [36]. It was refluxed for 24 h in 1,4-Dioxane and the crude product was passed through a Celite pad to remove all the inorganic species. The  $^1\text{H}$  NMR spectral data of the crude product indicated that the palladium catalyzed cyanation furnished a mixture of the mono cyanated and the bis cyanated products. Without further purification, we repeated the reaction on the dried crude product, with an alteration in the reactant equivalences. Only 4 equivalents of  $\text{CuCN}$  were used with one equivalent of  $\text{Et}_4\text{NCN}$ . No changes were done for Pd (0) catalyst and DPPF equivalents. The reaction was carried out again for 24h in 1,4-dioxane. After the work up, we found there was no

mono cyanated compound in the crude product. Radial chromatographic separation (98:2 Hexane/Isopropyl amine) gave us the pure **36b** in 83% yield (Scheme 27).



Scheme 27. Cyanation of the compound **35**.

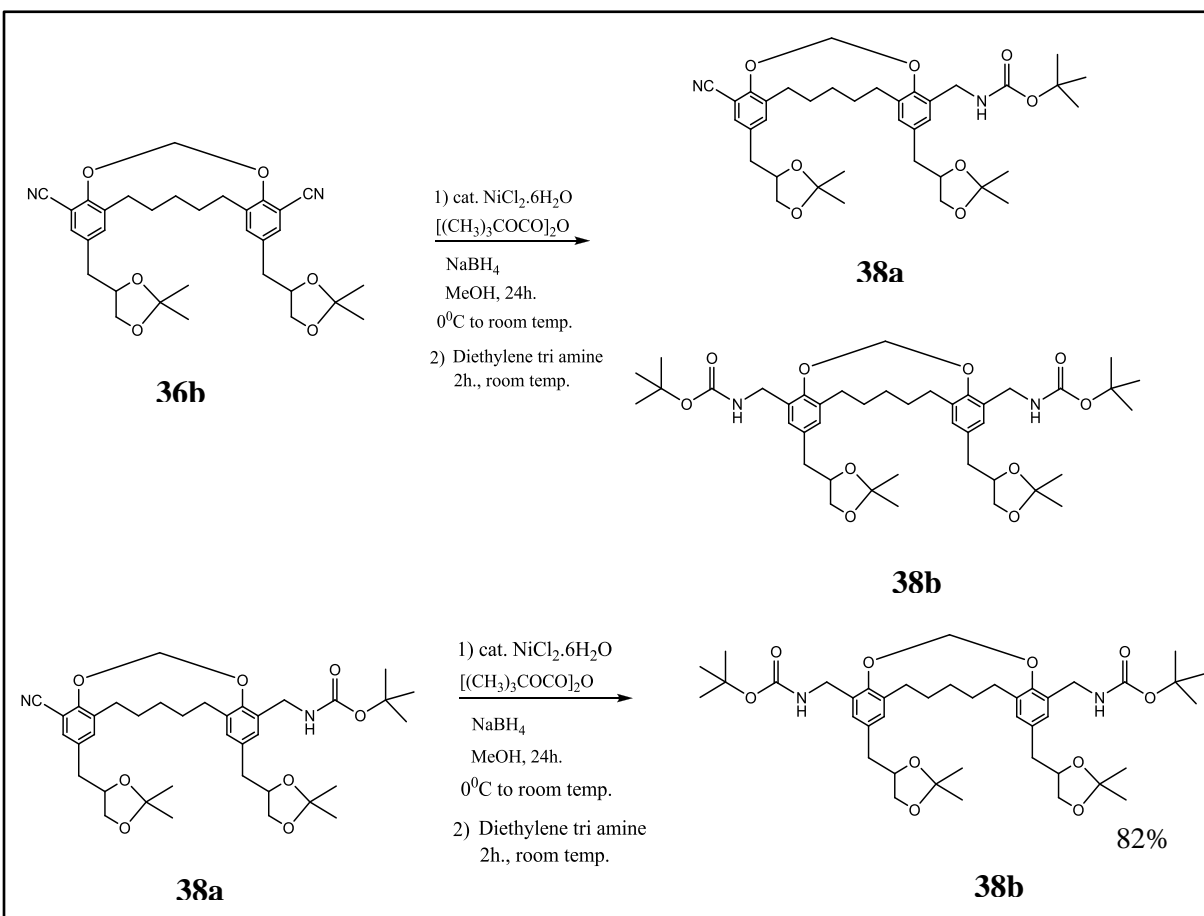
Our next reaction was to reduce the nitrile groups of **36b** to amine groups. We used benzonitrile in a model study to perform the reduction to produce Boc protected amine. The reaction gave us *tert*-butyl benzylcarbamate, **37** in high yield (Scheme 28) [41, 42].



Scheme 28. Model studies for the nitrile reduction.

The nickel boride catalyzed reduction was then carried out using compound **36b**. A catalytic amount of nickel (II) chloride in combination with excess  $\text{NaBH}_4$ , in the presence of  $\text{Boc}_2\text{O}$  was used in the reaction mixture. Dry methanol was used as the solvent. To a stirred solution of compound **36b** in methanol at  $0^\circ\text{C}$ ,  $\text{Boc}_2\text{O}$  (4 equivalents) was added. Using a Schlenk tube, 14 equivalents of  $\text{NaBH}_4$  were added in small portions over 30 minutes. The exothermic effervescent reaction was carried out for 24 h. The reaction mechanism is believed to be initiated by the formation of nickel boride through the reaction of  $\text{NiCl}_2$  and  $\text{NaBH}_4$ . The nitrile group is then coordinated to the boride surface and is exposed to hydride attack from excess  $\text{NaBH}_4$  [41,42]. To avoid dimerization, which is a common side product in the hydrogenation of nitriles, the primary amines once formed were protected in situ using  $\text{Boc}_2\text{O}$ . During the reaction workup, diethylene triamine, a stronger coordinating ligand for the nickel species than the Boc protected amines, was added to the solution and stirred for 2 h. Mass spectral data and  $^1\text{H}$  NMR indicated the crude product was a mixture of **38a** and **38b**. The dry crude product was again subjected to nitrile reduction using the same reaction conditions, using  $\text{Boc}_2\text{O}$  (2 equivalents),  $\text{NaBH}_4$  (7 equivalents) and 2 equivalents of diethylene triamine (Scheme 29). The repeated 24 h

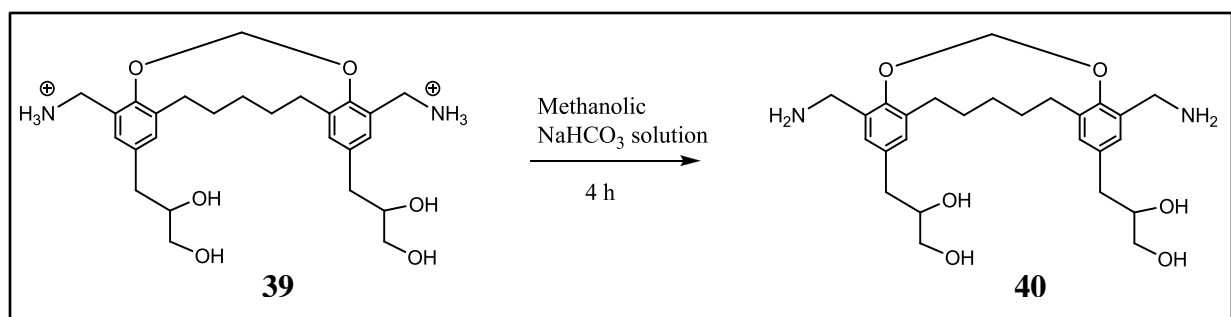
reaction gave us pure **38b** in 82% yield after the crude product was recrystallized using EtOAc and hexane.



Scheme 29. Nitrile reduction of compound **36b**.

To deprotect amino and diol functionality, TFA was used [43]. Although compound **38b** was readily soluble in pure ethyl acetate, the resulting polar **39** product was insoluble in ethyl acetate. On the other hand, **39** was soluble in methanol, but **38b** was only partially soluble in methanol. Since acetonide cleavage was aided by water, a mixture of solvents (80:18:2

methanol/ethyl acetate/water) were used as the reaction medium. To determine the optimum reaction time, we used deuterated TFA, CD<sub>3</sub>OD and D<sub>2</sub>O and the reaction progress was monitored using <sup>1</sup>H NMR. We found that the reaction would make no progress after 30 minutes time. It yielded a mixture of products. Since charged compounds were problematic to purify, we decided to convert the charged ammonia groups to their neutral amine counterparts by reacting crude **39** with saturated methanolic solution of NaHCO<sub>3</sub> (Scheme 30).



Scheme 30. Conversion of **39** to **40**.

<sup>1</sup>H NMR spectrum of **40** indicated a mixture of products (Figure 77) and the ESI-MS spectrum indicated m/z peaks at 555.0, 571.0, 593.0 and 611.0 (Figure 21, Figure 78). These data confirmed although the optimum reaction time was 30 minutes, the TFA deprotection of diol groups was not completed after 30 minutes. Therefore, to fully deprotect the 1,2-diol groups, the reaction was carried out for 30 minutes, solvent and excess TFA were removed under high vacuum at room temperature, and the crude product was subjected to same reaction conditions for another 30 minutes. The deprotection reaction was carried out like wise for a total of 120 minutes (4 x 30 minutes) (Scheme 31, Figure 22).

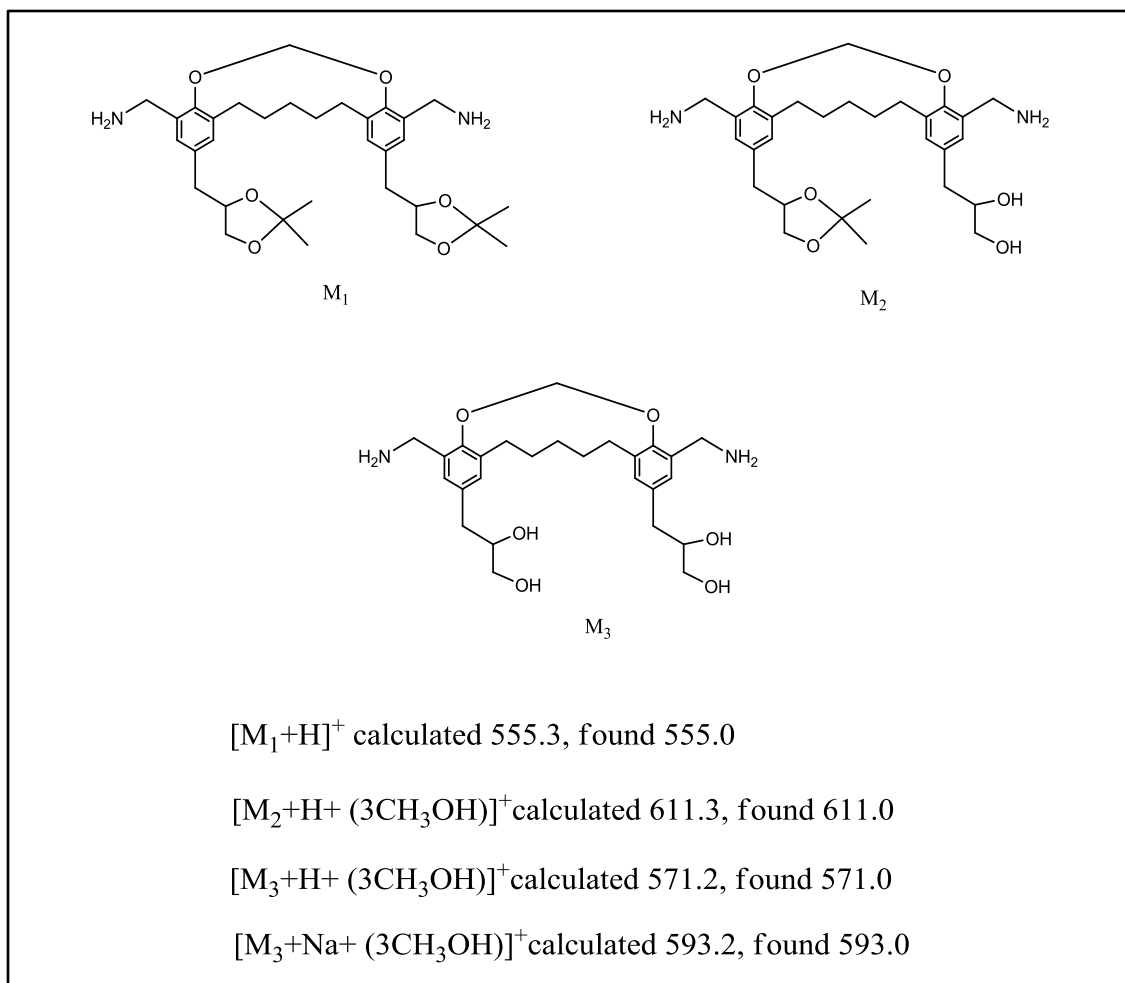
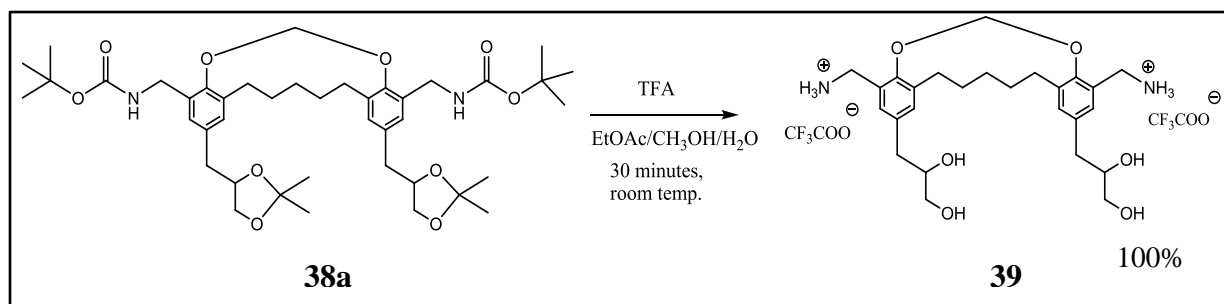


Figure 21. ESI-MS values for different species found in crude **40**.



Scheme 31. Deprotection of amino and diol functionality in compound **38a**.

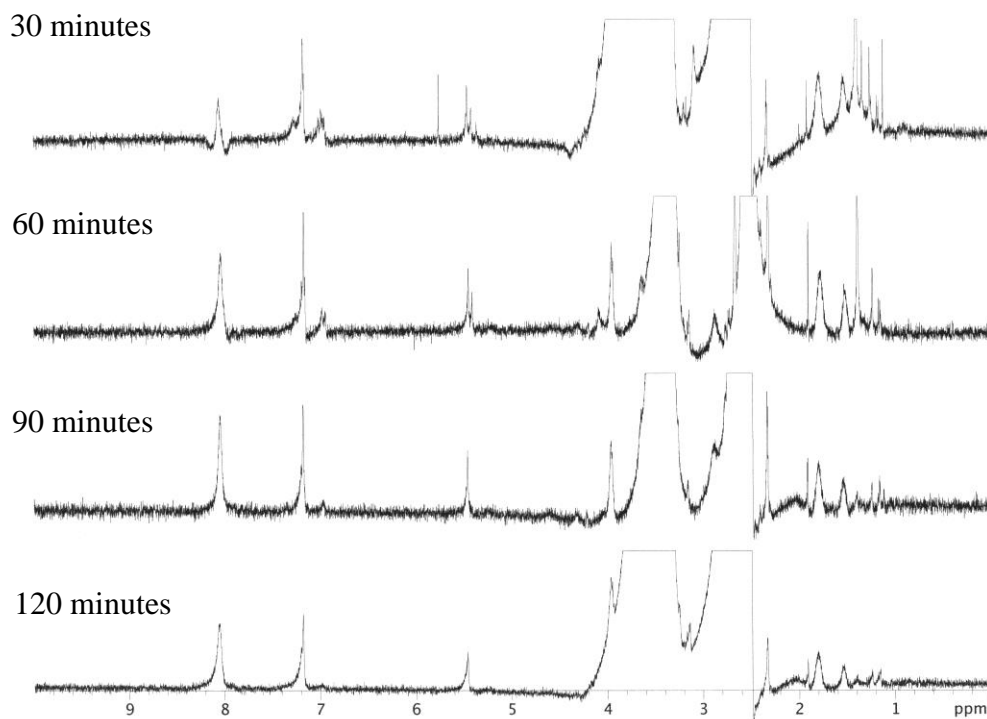
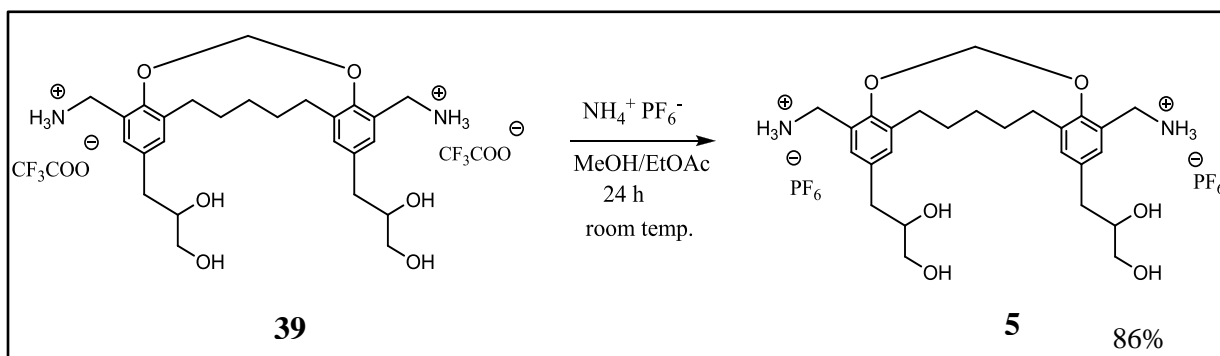


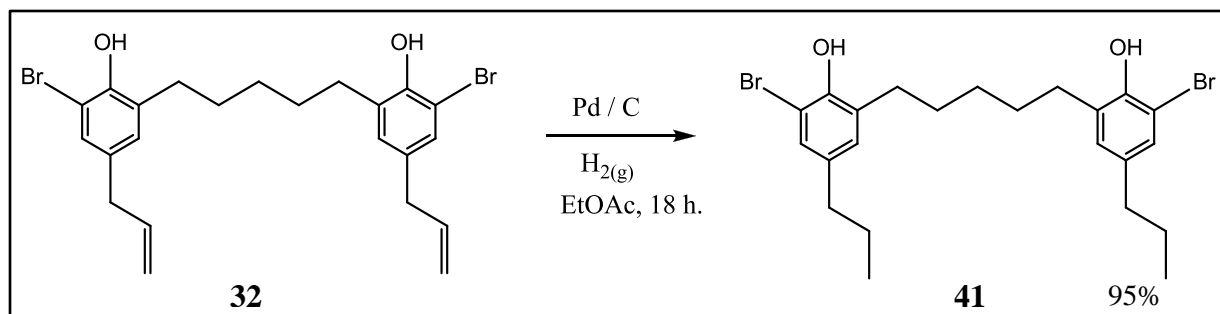
Figure 22.  $^1\text{H}$  NMR stack plot for the TFA reaction of **38a**.

The charged compound **39** was then subjected to a counter anion exchange using ammonium hexafluorophosphate. The  $\text{PF}_6^-$  ion was chosen as the counter ion since it makes charged receptors more soluble in organic solvents. It is also known to facilitate crystallization of charged organic complexes. Ten equivalents of  $\text{NH}_4^+\text{PF}_6^-$  were reacted with crude **39** and after 24 h, the organic layer was removed under vacuum. The crude solid was dissolved in ethyl acetate and was washed with  $\text{H}_2\text{O}$  to remove excess  $\text{NH}_4^+\text{PF}_6^-$  (Scheme 32). Assuming that some amount of **5** may also be in the water layer, we backwashed the aqueous layer with n-Butanol and once the solvent was removed under vacuum we found an unknown compound (Figure 100).



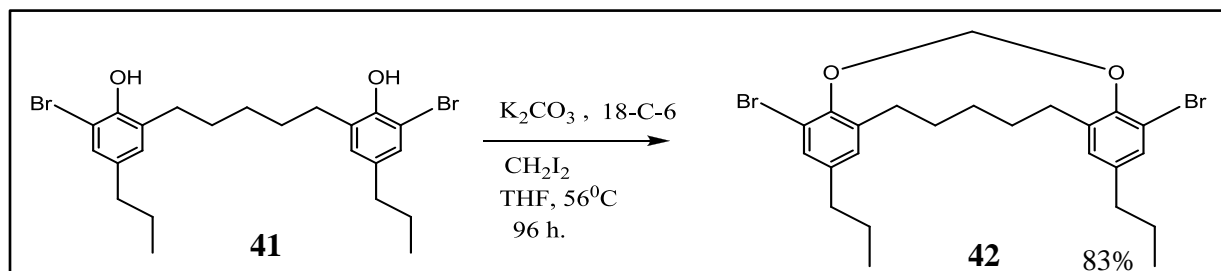
Scheme 32. Counter ion exchange of **39**.

A control receptor **46** was also synthesized replacing the 2,3-dihydroxy propyl substituents with propyl groups. It was considered as a control since there were no appendages to interact with the glycerol hydroxyls of the PG head group, although there were charged ammonium groups to interact with the anion portion of the head group. The bis *ortho* bromo phenolic compound **32** was hydrogenated using Pd/C as the catalyst (Scheme 33). After 18h, the TLC profile indicated no starting material and the crude product was purified by column chromatography (84:14:2 hexane/EtOAc/isopropyl amine).



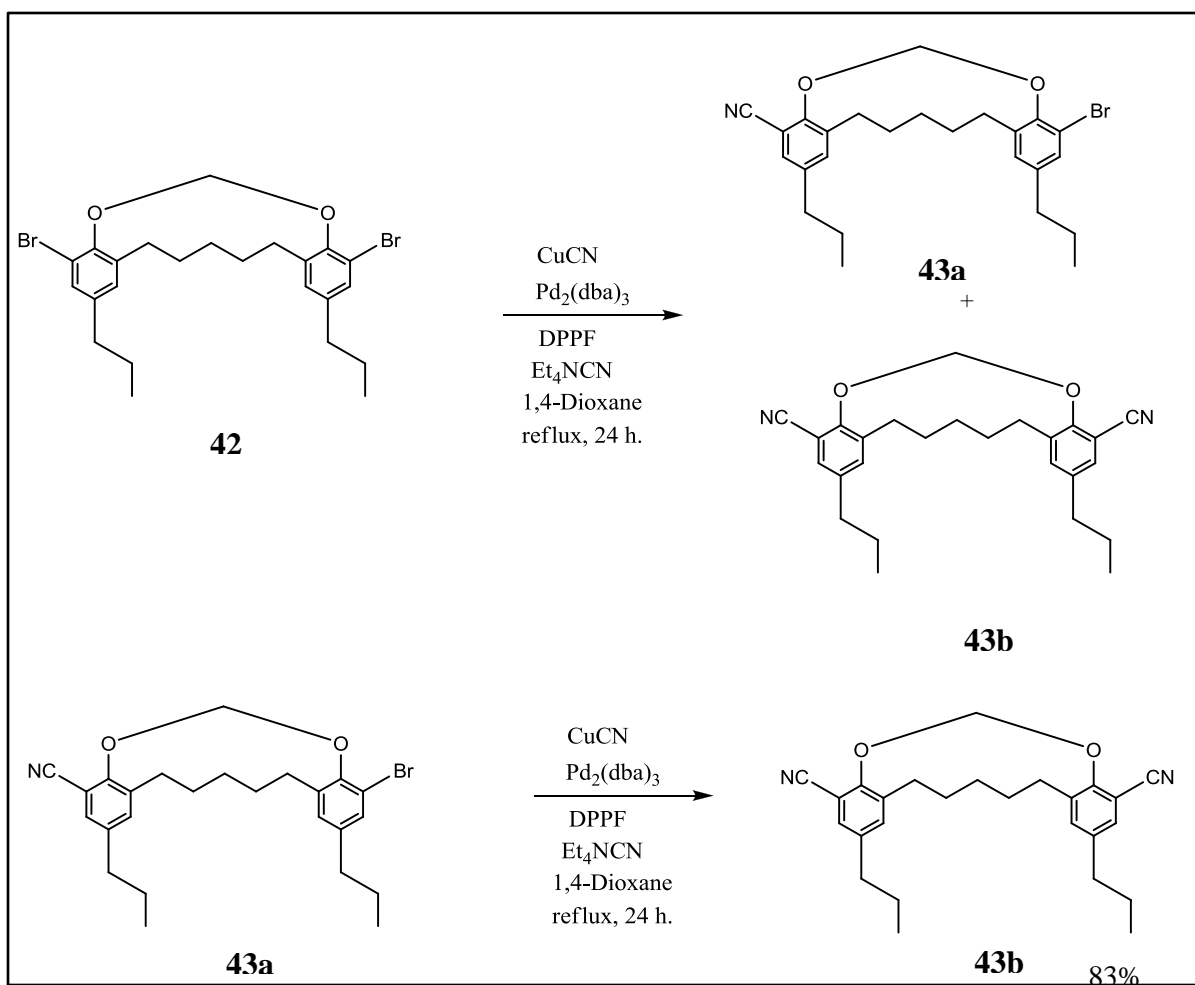
Scheme 33. Hydrogenation of compound **32**.

The phenolic oxygens of the resulting **41** were bridged via a methylene unit using diiodomethane, in the presence of  $K_2CO_3$  and 18-C-6 (Scheme 34). The product was purified using radial chromatography (98:2 hexane/isopropylamine).



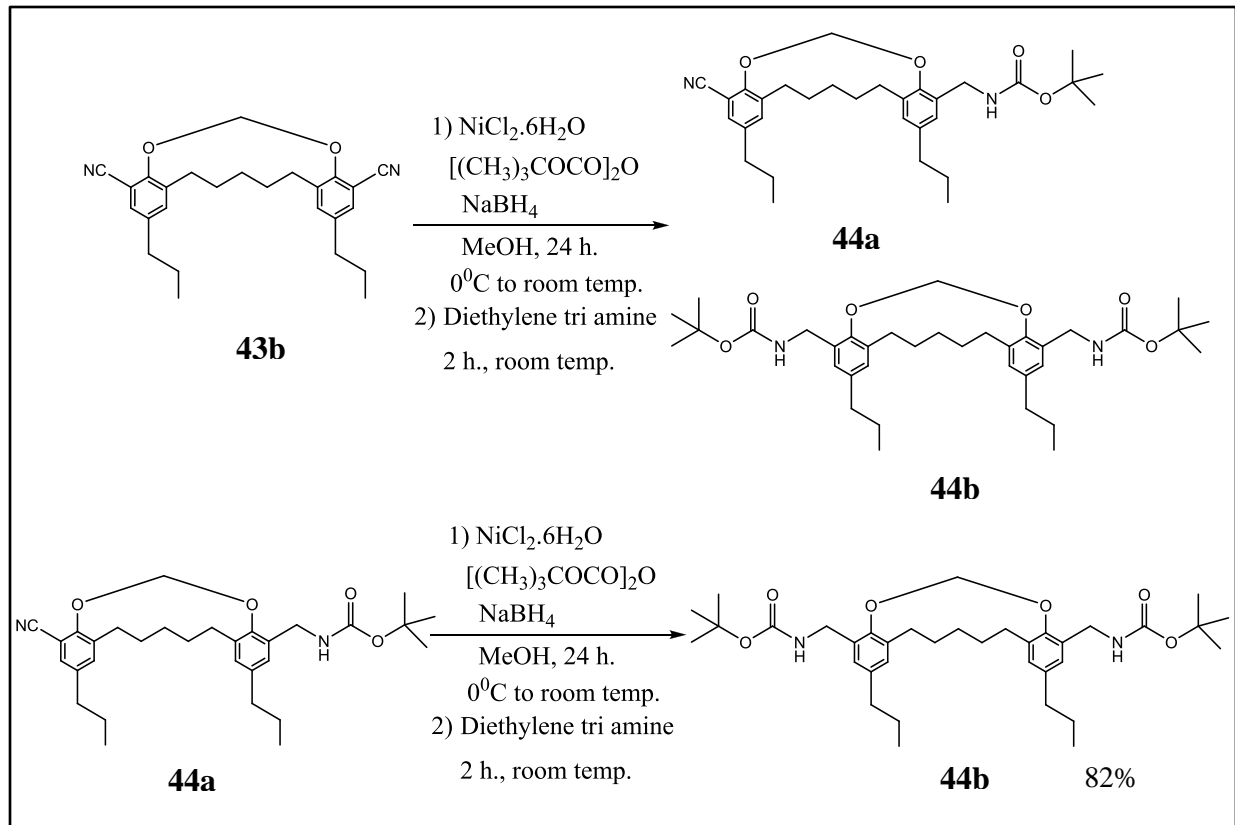
Scheme 34. Preparation of **42** via an ether linkage.

The ether linked **42** compound's bromines in the *ortho* positions were then converted to nitriles, similar to the reaction conditions given in Scheme 26. Radial chromatographic purification (98:2 Hexane/Isopropylamine) resulted in 83% yield for **43** (Scheme 35).



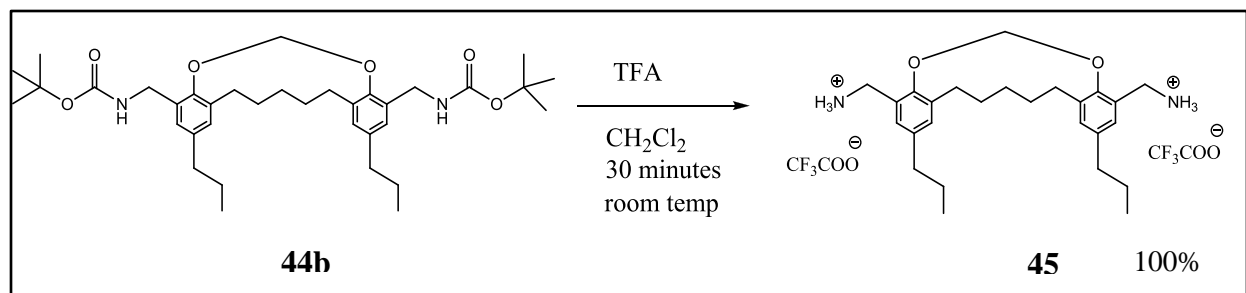
Scheme 35. Bis cyanation of compound **43**.

Pure **43b** was then subjected to nitrile reduction using similar reaction conditions given in Scheme 28. After 48 h reaction, the crude product was passed through a Celite pad using ethyl acetate and was purified using radial chromatography (95:5 hexane/isopropylamine) (Scheme 36).



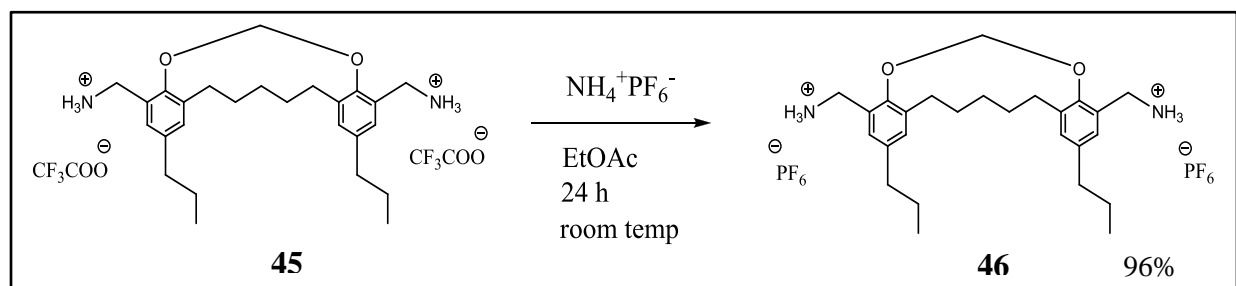
Scheme 36. Nitrile reduction of compound **43b**.

The Boc protected control receptor **44b** was then reacted with TFA, using  $\text{CH}_2\text{Cl}_2$  as the solvent (Scheme 37). After 30 minutes, solvent was removed under vacuum and the crude product was used for the anion exchange reaction without any purification.



Scheme 37. Boc cleavage of compound **44b**.

Compound **39**, possessing four hydroxyl groups and trifluoroacetate counter ions, was not soluble in ethyl acetate. As a result, a mixture of methanol and ethyl acetate were used for its counter ion exchange reaction (Scheme 30). On the other hand, the control receptor compound **45**, which lacks hydroxyl groups in the terminal propyl groups, was readily soluble in ethyl acetate but showed partial solubility in methanol. Therefore it was decided to use ethyl acetate as the solvent for the counter ion exchange reaction of **45** (Scheme 38).



Scheme 38. Counter ion exchange of **45**.

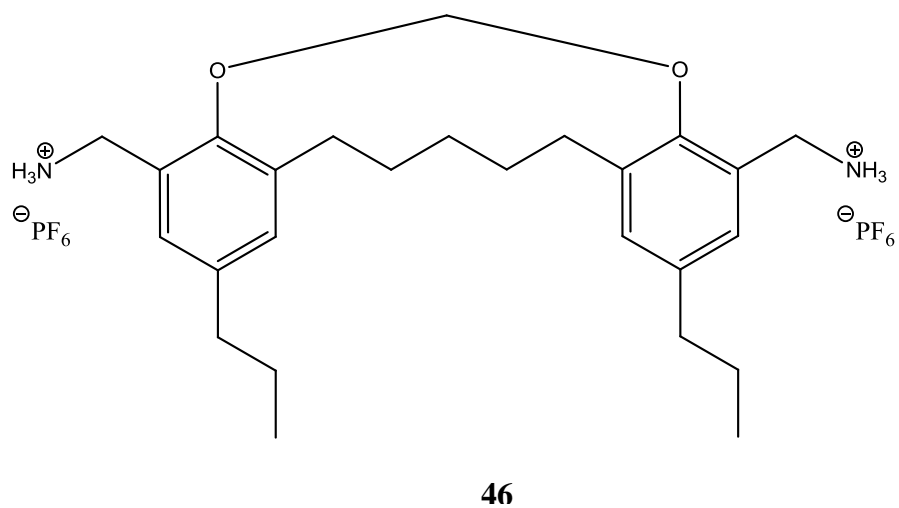
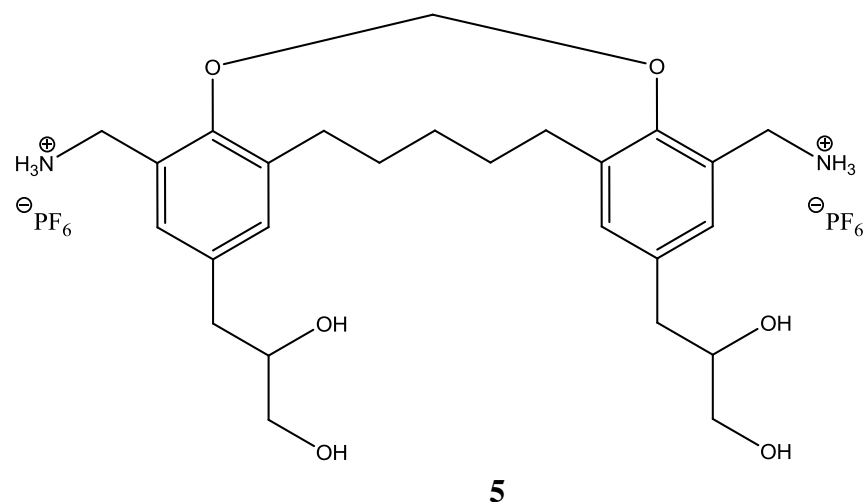


Figure 23. Charged receptor **5** and charged control receptor **46**.

The overall yield for **5** after 14 synthetic steps was 15.3%, while for the control receptor **46** it was 16.08% with 13 steps.

## CHAPTER 4

### ANION BINDING STUDIES

Compound **46** was considered as a control receptor when compared to compound **5**, since it has the charged ammonium binding moieties so as only to bind the phosphate anion head group of the PG anion. In addition to the ammonium groups, compound **5** also possesses binding units for the glycerol hydroxyls of PG (Figure 24). The binding stoichiometry of the two receptors for anions were determined by Job plots constructed from  $^1\text{H}$  NMR titration studies. All  $^1\text{H}$  NMR titration studies were carried out using 5 %  $\text{CDCl}_3$  in  $\text{DMF-d}_7$  at  $30^\circ\text{C}$ .

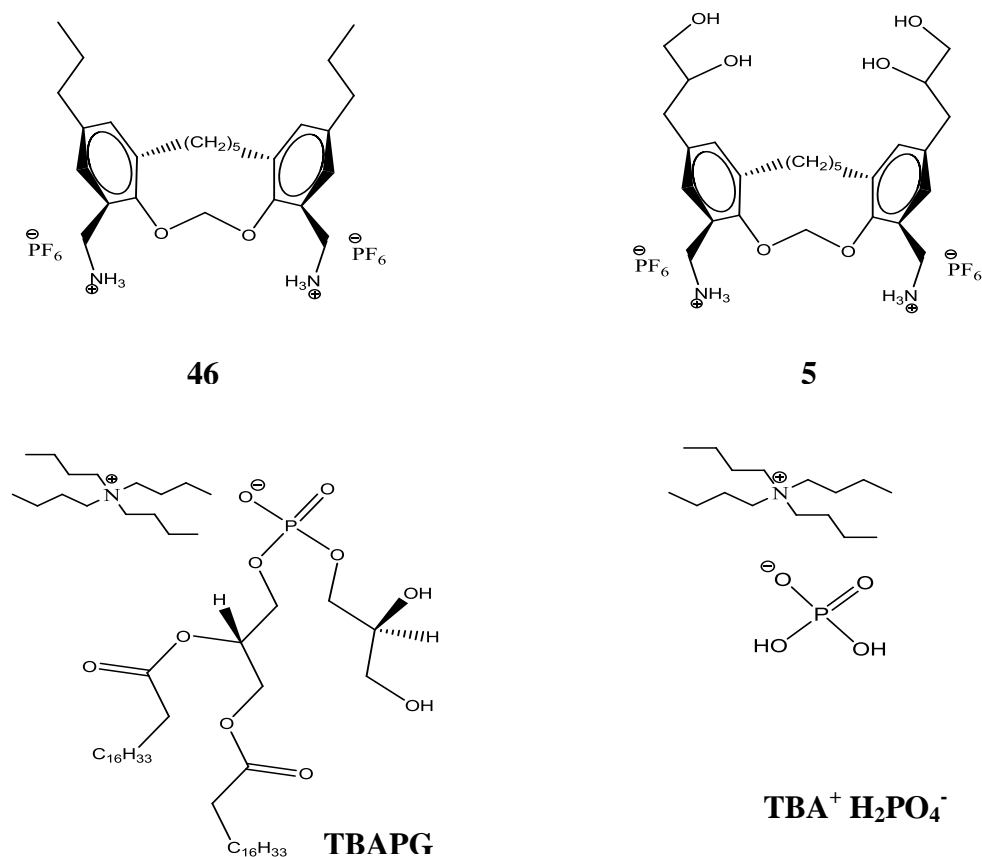


Figure 24. Charged receptors and the anions used in binding studies

We began the binding studies by performing a  $^1\text{H}$  NMR Job plot for the control receptor **46** with inorganic dihydrogen phosphate anion. The  $^1\text{H}$  NMR Job plot indicated the binding stoichiometry of **46** to inorganic dihydrogen phosphate anion was 1: 2 (Figure 25). This result deviated from the results of previous work done in our lab, where compound **2**, a control urea receptor exhibited a 1:1 binding stoichiometry with the same anion (Table 1).

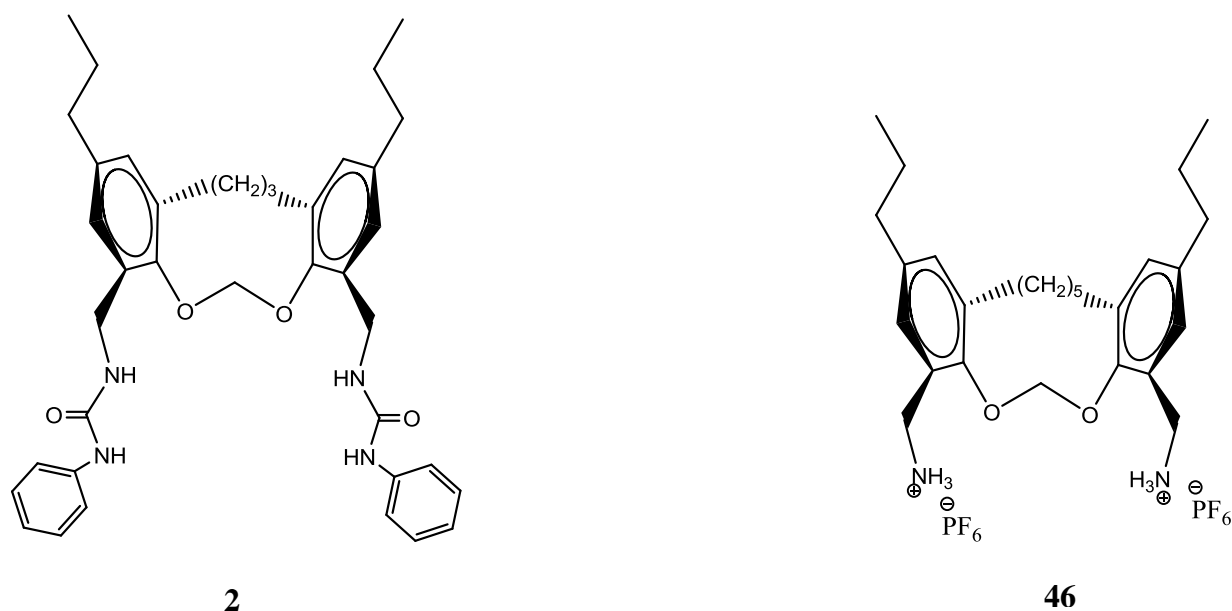


Figure 25. The control receptors **2** and **46**.

The control receptor **2** had urea binding units as opposed to **46** which had charged ammonium moieties to interact with the dihydrogen phosphate anion. Although charged ammonium groups were expected to have stronger interactions with the dihydrogen phosphate anion than the urea groups, the 1:1 binding stoichiometry of compound **2** with the dihydrogen phosphate anion was indicative that the binding cavity of **2** comprising three methylene units (between the phenyl rings) as compared to five methylene units of **46** was having a better fit to the phosphate anion.

On the other hand the two methylene unit extended binding cavity of compound **46** had more space to accommodate two such phosphate anions, as indicated by the  $^1\text{H}$  NMR Job plot titrations. Greater chelation properties of charged ammonium groups compared to that of urea groups may also have had influenced the 1:2 stoichiometric interactions between **46** and the dihydrogen phosphate ion.

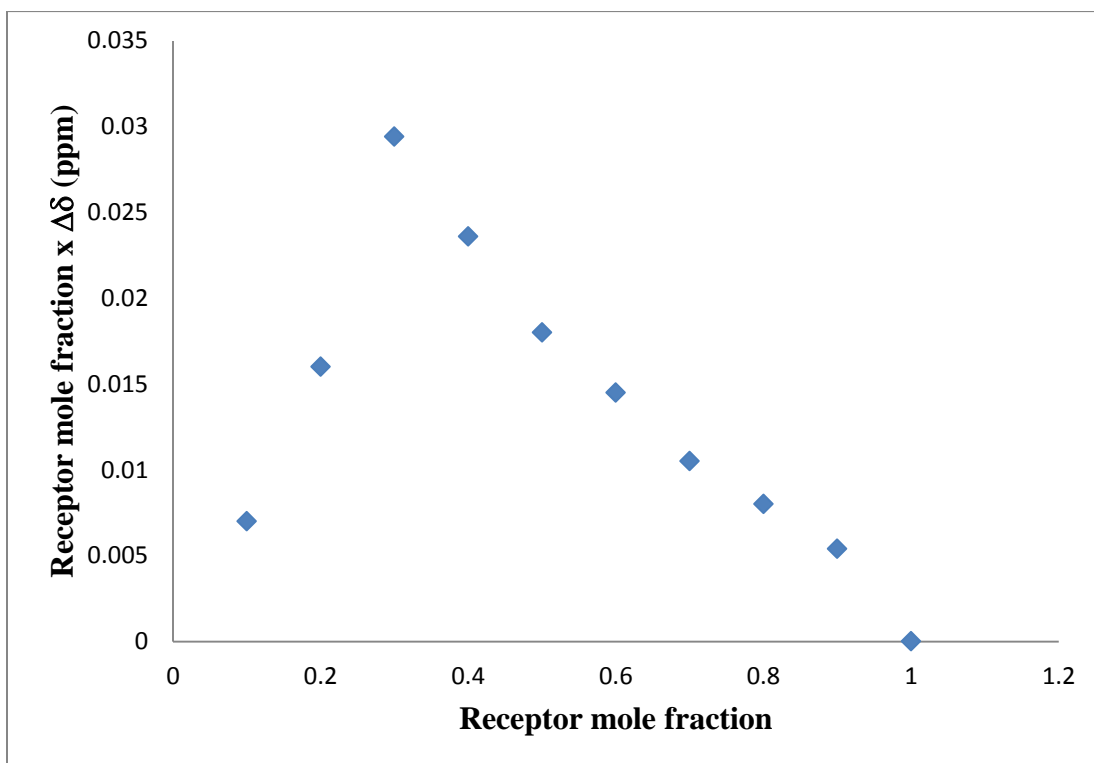


Figure 26.  $^1\text{H}$  NMR Job plot of **46** -  $\text{H}_2\text{PO}_4^-$  complex in 5 %  $\text{CDCl}_3$  in  $\text{DMF-d}_7$  at  $30^\circ\text{C}$

We then performed a  $^1\text{H}$  NMR Job plot to determine the binding stoichiometry of compound **46** with the PG anion and the Job plot indicated a 1:1 and 1:2 mixed binding stoichiometry for the control receptor and the anion (Figure 27). The  $^1\text{H}$  NMR binding studies were not carried out for the control system **46**, since it showed no 1:1 binding stoichiometry with PG anion.

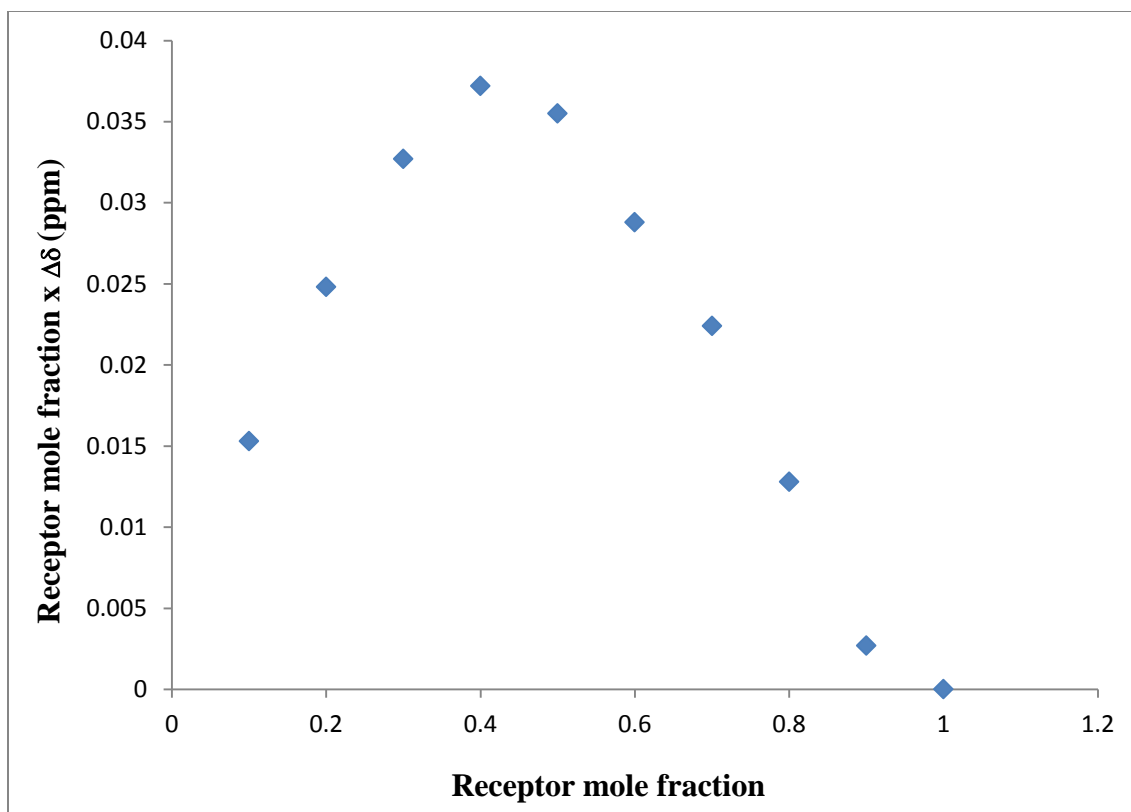


Figure 27.  $^1\text{H}$  NMR Job plot of **46** - PG complex in 5 %  $\text{CDCl}_3$  in  $\text{DMF-d}_7$  at  $30^\circ\text{C}$

Since the Job plot titration studies of **46** with inorganic phosphate exhibited a 1:2 binding stoichiometry and both compound **46** and compound **5** had five methylene unit binding cavities, it was decided not to perform the  $^1\text{H}$  NMR Job plot titrations for compound **5** with inorganic phosphate anion.

The  $^1\text{H}$  NMR Job plot for the receptor compound **5** exhibited a 1:1 binding stoichiometry with TBAPG (Figure 28) and therefore  $^1\text{H}$  NMR titration studies were carried out for TBAPG and compound **5**.

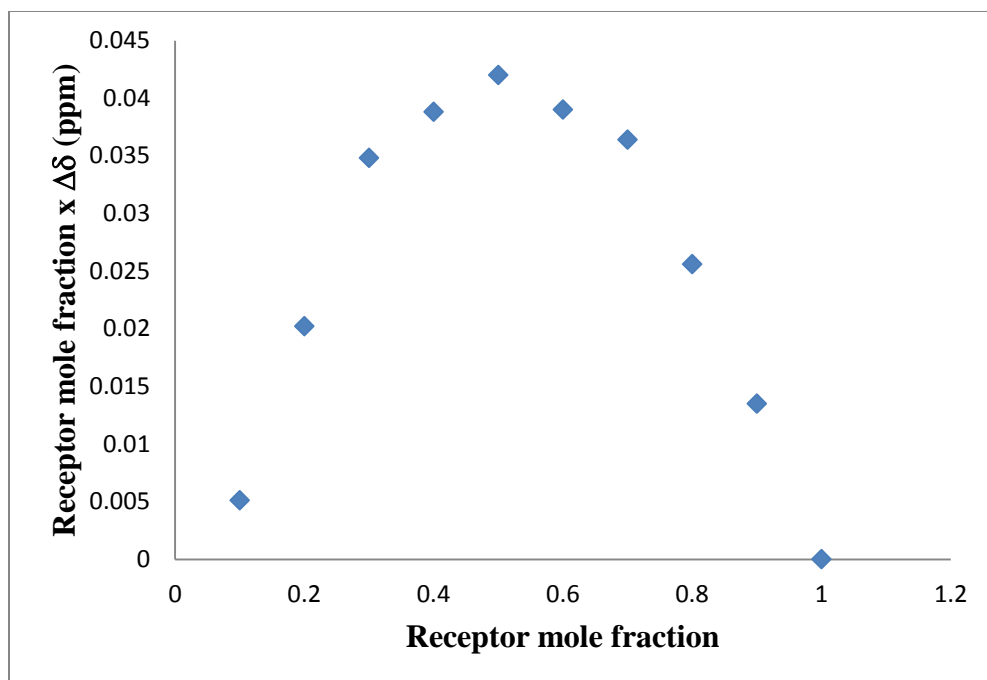


Figure 28.  $^1\text{H}$  NMR Job plot of **5** - PG complex in 5 %  $\text{CDCl}_3$  in  $\text{DMF-d}_7$  at  $30^\circ\text{C}$

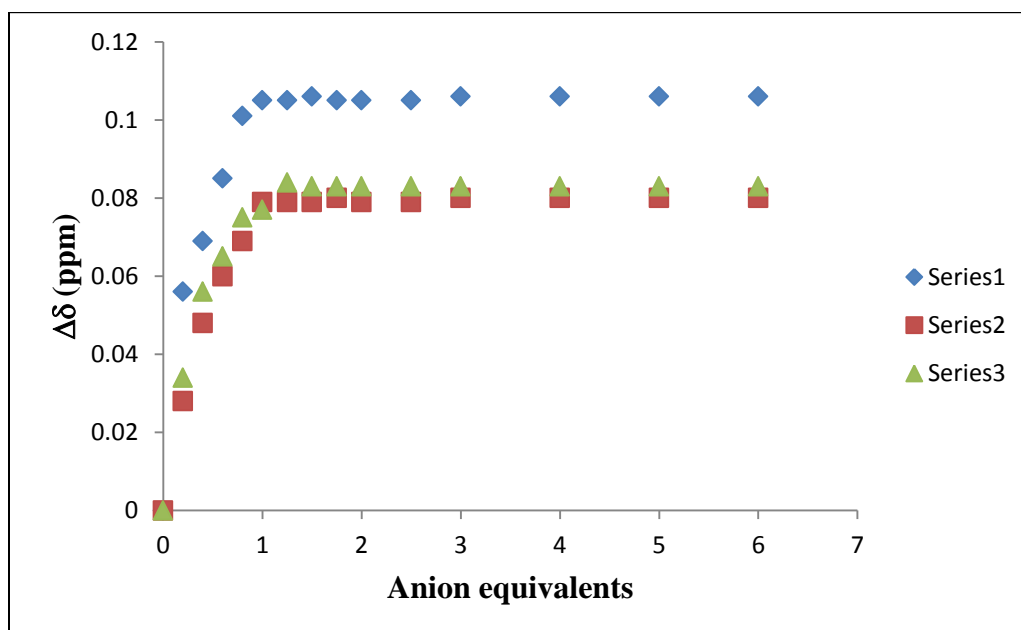


Figure 29.  $^1\text{H}$  NMR titration curve of **5** with TBAPG in 5 %  $\text{CDCl}_3$  in  $\text{DMF-d}_7$  at  $30^\circ\text{C}$

TABLE 4

<sup>1</sup>H NMR Titration Data for the Receptor **5** with TBAPG

<b>Proton</b>	<b>K</b>	<b>% Error</b>
1	17445	8.08
2	17445	8.08
3	17445	8.08

We observed three protons change their chemical shifts for receptor **5** upon the addition of the TBAPG salt solution during the <sup>1</sup>H NMR titration. The ammonium proton downfield chemical shift was seen only up to the addition of 0.6 equivalents of TBAPG, since they were not visible after 0.6 equivalents titration of the TBAPG salt solution. The benzyl protons a, displayed an upfield chemical shift, while the aromatic protons b and the bisphenolic ether linking methylene protons c displayed a downfield chemical shift (Figure 30). The non-linear regression analysis of the binding isotherms using WinEQNMR software indicated all three protons had similar binding constants and the same % errors. Since these data were for a single titration, more titrations should be carried out to obtain an average binding constant. Also, isothermal titration calorimetry (ITC) needs to be carried out to compare the  $K_{eq}$  results from <sup>1</sup>H NMR spectroscopic studies, as well as to determine  $\Delta G$ ,  $\Delta H$  and  $\Delta S$  of binding for **5** and TBAPG.

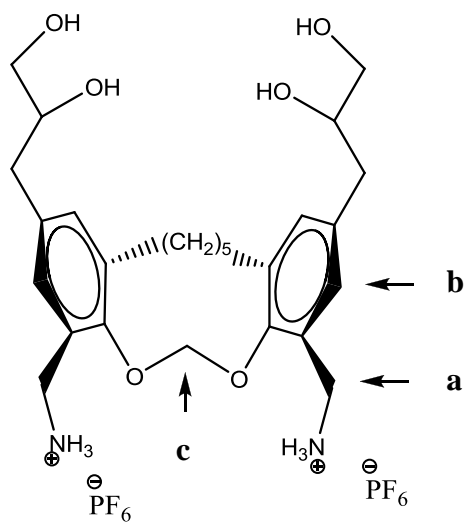


Figure 30. Protons (chemical shift observed) for the <sup>1</sup>H NMR titration of **5** with TBAPG in 5 % CDCl<sub>3</sub> in DMF-d<sub>7</sub> at 30 °C

## CHAPTER 5

### EXPERIMENTAL-MATERIALS AND PROCEDURES

All the solvents and reagents used in reactions were dried and purified by literature methods and these procedures are described as a part of each experiment when appropriate [44]. THF and 1,4-dioxane were freshly distilled from Na in the presence of benzophenone. 1,2-dichloroethane was freshly distilled from CaH<sub>2</sub>. Acetone was distilled from Boron oxide. All reactions described were performed under a nitrogen atmosphere. All reaction intermediate products were dried with a Dean-Stark apparatus using benzene, and further dried under vacuum prior to use. All melting points (Mel-Temp) are uncorrected. IR spectra were recorded on a Thermo Fisher Avatar 360 FT-IR ATR instrument. The <sup>1</sup>H NMR spectra were recorded at Mercury 300 or INOVA 400 spectrometers in 300 or 400 MHz in CDCl<sub>3</sub> using the chloroform peak as the reference; DMSO-d<sub>6</sub> using DMSO as the reference; DMF-d<sub>7</sub> using DMF as the reference; or in CD<sub>3</sub>OD using methanol as the reference peak. ESI-MS were obtained with a Varian 1200L quadrupole MS. Purity affirmation was accomplished by HRMS of analytical samples by the Mass Spectrometry Lab at the University of Kansas. Parr 3911 Hydrogenation Apparatus with a 66CA2 250 mL borosilicate glass reaction bottle was used for hydrogenation reactions. Analytical samples (receptors) were dried under vacuum in a desiccator with P<sub>2</sub>O<sub>5</sub> for a minimum of three days or dried under vacuum in a drying pistol at 112 °C for a minimum of two days. Anions were dried under vacuum in a desiccator with Drierite for a minimum of three days. Column chromatography was carried out on silica gel (Davisil 633). Prep thin-layer chromatography was performed on pre-coated 1500 mm plates from Analtech (silica gel F).

Radial chromatography when performed was accomplished using a Chromatotron (Harrison Research, Palo Alto, California).

### Job Plot

The  $^1\text{H}$  NMR Job plot of compound **5** with TBAPG is given as an example. Dry **5** (1.3 mg) was weighed on a six-point microbalance and placed into a 1 mL volumetric flask. TBAPG (1.7 mg) was weighed out in a glove bag (nitrogen atmosphere) into a tared (using a 4-point balance) separate 1mL volumetric flask. This amount was chosen so that when the solids were dissolved, their molar concentrations would be identical (0.0017M). The solids were then dissolved to the mark with dry (95: 5 DMF- $d_7$ /CDCl $_3$ ) solution. Aliquots of receptor solution and the anion solution were placed into separate NMR tubes as follows:

tube 1	0.15 mL receptor solution	0 mL anion solution	0.15 mL pure solvent
tube 2	0.135 mL receptor solution	0.0145 mL anion solution	0.1505 mL pure solvent
tube 3	0.12 mL receptor solution	0.0289 mL anion solution	0.1511 mL pure solvent
tube 4	0.105 mL receptor solution	0.0434 mL anion solution	0.1516 mL pure solvent
tube 5	0.09 mL receptor solution	0.0578 mL anion solution	0.1522 mL pure solvent
tube 6	0.075 mL receptor solution	0.0723 mL anion solution	0.1527 mL pure solvent
tube 7	0.06 mL receptor solution	0.0868 mL anion solution	0.1532 mL pure solvent
tube 8	0.045 mL receptor solution	0.1012 mL anion solution	0.1538 mL pure solvent
tube 9	0.03 mL receptor solution	0.1157 mL anion solution	0.1543 mL pure solvent
tube 10	0.015 mL receptor solution	0.1302 mL anion solution	0.1548 mL pure solvent

Total volume for each NMR tube was 0.3 mL. For each NMR tube, the sum of the molar equivalents of both anion and the receptor was same. Tubes 1 through 10, equivalents of receptor

were descending as 1, 0.9, 0.8, 0.7, 0.6, 0.5, 0.4, 0.3, 0.2, and 0.1, while anion equivalents were ascending as 0, 0.1, 0.2, 0.3, 0.4, 0.5, 0.6, 0.7, 0.8 and 0.9. Each NMR tube was turned upside down and back many times to thoroughly mix the solution. After obtaining the  $^1\text{H}$  NMR spectrum for each tube at  $30\text{ }^\circ\text{C}$ , the change in chemical shift of the benzyl protons next to the charged ammonia groups, relative to its shift recorded from tube 1, ( $\Delta$  chemical shift x mole fraction) was plotted vs. mole fraction of receptor in each tube.

### **NMR Titration**

Dry compound **5** (0.002 g) was weighed on a 6-point micro balance and placed into a 1 mL volumetric flask. Dry TBAPG (0.0294 g) was weighed in a glove bag placed into a tared (using a 4-point balance) separate 1 mL volumetric flask. A solution of (95:5  $\text{DMF-d}_7/\text{CDCl}_3$ ) was added to the mark to dissolve each solid. Concentration of receptor was  $2.6 \times 10^{-3}$  M while for TBAPG it was  $2.88 \times 10^{-2}$  M. These concentrations were chosen to accurately measure the small volume of added increments of the anion solution to the 0.5 mL of receptor solution in the NMR tube without exceeding the total volume of 0.8 mL (once all the anion equivalents had been added).  $^1\text{H}$  NMR titrations were started by placing 0.5 mL of the receptor from the volumetric flask (in a glove bag) and obtaining a spectrum from a 400 MHz NMR at  $30\text{ }^\circ\text{C}$ . Proton NMR spectra were obtained after each addition of the anion equivalence into the NMR tube. The contents in the NMR tube were thoroughly mixed upon the addition of each anion equivalent by turning the NMR tube upside down and back again. The equivalents of the receptor and the anion, and the added volumes are given in Table 5. The resultant concentrations of TBAPG, **5**, and proton shift of three different protons (benzyl proton, aromatic proton and the methylene

protons that bridged the bis phenols), from each added increment were then used as inputs for non-linear regression analysis using the WinEQNMR software to obtain a binding constant.

TABLE 5

Volumes and Equivalences of **5** and TBAPG for the  $^1\text{H}$  NMR Titration

Receptor Equivalence	Anion Equivalence	Volume of Anion Solution (mL)	Total Volume in the NMR Tube (mL)
1	0	0	$5 \times 10^{-1}$
1	0.2	$9.1 \times 10^{-3}$	$5.09 \times 10^{-1}$
1	0.4	$9.1 \times 10^{-3}$	$5.18 \times 10^{-1}$
1	0.6	$9.1 \times 10^{-3}$	$5.27 \times 10^{-1}$
1	0.8	$9.1 \times 10^{-3}$	$5.36 \times 10^{-1}$
1	1	$9.1 \times 10^{-3}$	$5.45 \times 10^{-1}$
1	1.25	$1.13 \times 10^{-2}$	$5.56 \times 10^{-1}$
1	1.5	$1.13 \times 10^{-2}$	$5.67 \times 10^{-1}$
1	1.75	$1.13 \times 10^{-2}$	$5.79 \times 10^{-1}$
1	2	$1.13 \times 10^{-2}$	$5.90 \times 10^{-1}$
1	2.5	$2.26 \times 10^{-2}$	$6.13 \times 10^{-1}$
1	3	$2.26 \times 10^{-2}$	$6.35 \times 10^{-1}$
1	4	$4.53 \times 10^{-2}$	$6.81 \times 10^{-1}$
1	5	$4.53 \times 10^{-2}$	$7.26 \times 10^{-1}$
1	6	$4.53 \times 10^{-2}$	$7.71 \times 10^{-1}$

### **prop-2-enyl methanesulfonate (18)**

Freshly distilled dry 2-propen-1-ol (5 mL, 73.1 mmol) was taken to a flame dried 500 mL round bottom flask, equipped with a stir bar. Dry CH<sub>2</sub>Cl<sub>2</sub> (200 mL) was introduced to the flask followed by N,N-diisopropyl ethyl amine (25.5 mL, 146.3 mmol). The mixture was stirred for 15 minutes under nitrogen at 0<sup>0</sup>C. A second solution of methane sulfonic anhydride (14.02 g, 80.5 mmol) in dry CH<sub>2</sub>Cl<sub>2</sub> (117.5 mL) was syringed into the reaction mixture dropwise over 25 minutes. The reaction mixture was stirred at 0<sup>0</sup>C under nitrogen atmosphere for 18 h. After quenching with 1.5 M HCl (200 mL), the layers were separated. Aqueous layer was extracted with CH<sub>2</sub>Cl<sub>2</sub> (3 x 75 mL). The combined organic layers were washed with saturated NaHCO<sub>3</sub> (2 x 100 mL) followed by brine (2 x 100 mL) and dried with anhydrous Na<sub>2</sub>SO<sub>4</sub>. The solvent was removed under vacuum to yield **18** as an oil (9.75 g, 71.64 mmol, 98%). <sup>1</sup>H NMR (400 MHz, CDCl<sub>3</sub>) δ 2.88 (s, 3H), 4.57 (d, 2H, J=7.6 Hz), 5.23-5.34 (m, 2H), 5.77-5.85 (m, 1H); <sup>13</sup>C NMR (100.5 MHz, CDCl<sub>3</sub>) δ 37.6, 70.4, 120.4, 130.4

### **pentane-1,5-diyl bis (4-methylbenzenesulfonate) (27)**

1,5-Pentanediol (6.77 g, 65 mmol) and dry pyridine (41.19 g, 520.8 mmol) were cooled to 10<sup>0</sup>C in an ice-water bath. Solid tosyl chloride (16.4 g, 86 mmol) was slowly added to the reaction mixture (25 minutes). The reaction mixture was stirred at 10<sup>0</sup>C for 2h. A second portion of tosyl chloride (10.9 g, 57.1 mmol) dissolved in dry CH<sub>2</sub>Cl<sub>2</sub> (40 mL) was added dropwise to the reaction mixture using an addition funnel. The reaction mixture was stirred overnight, gradually warming to room temperature. After 20 h, CH<sub>2</sub>Cl<sub>2</sub> (80 mL) and H<sub>2</sub>O (100 mL) were added to the solution. It was transferred to a separatory funnel and the organic layer was separated. The

aqueous layer was extracted with CH<sub>2</sub>Cl<sub>2</sub> (3 x 50 mL), and the combined organic layers were washed with 3M HCl (3 x 60 mL) and saturated NaHCO<sub>3</sub> (80 mL). The organic layer was dried over anhydrous Na<sub>2</sub>SO<sub>4</sub> and concentrated under vacuum. The crude solid was recrystallized from ethanol to yield **27** as white crystals (18.77 g, 45.5 mmol, 70%). mp: 79-80.5 °C; <sup>1</sup>H NMR (400 MHz, CDCl<sub>3</sub>) δ 1.31-1.36 (m, 2H), 1.54-1.61 (m, 4H), 2.43 (s, 6H), 3.95 (t, 4H, J=6.4 Hz), 7.32 (d, 4H, J=7.6 Hz), 7.72 (d, 4H, J=7.2 Hz); <sup>13</sup>C NMR (100.5 MHz, CDCl<sub>3</sub>) δ 21.7, 21.8, 28.3, 70.2, 128.0, 130.10, 130.14, 133.0, 145.1; HRMS (ESI) calcd for C<sub>19</sub>H<sub>24</sub>O<sub>6</sub>S<sub>2</sub>Na (M+Na)<sup>+</sup> 435.0912, found 435.0913.

### **1,1'-(1,5-pentanediy)bis[2-methoxybenzene] (28)**

THF (223.69 mL) was added to magnesium turnings (34.52 g, 1440 mol), and the reaction mixture was heated to reflux under a nitrogen atmosphere. A solution of 2-bromoanisole (18.1 mL, 140 mmol) in THF (55.9 mL) was added via a syringe at a rate of 0.6 mL/min to the reaction mixture. The resulting Grignard reaction was allowed to stir at reflux for 24 h and then cooled to room temperature. A second solution consisting of 1,5-pentanediol, bis(4-methylbenzenesulfonate) **27** (30 g, 70 mmol) in THF (53.1 mL), 41.4 mL (6 mol %) of 0.1 M (LiBr/CuBr·SMe<sub>2</sub>/LiSPh/THF) copper catalyst solution, and HMPA (16.7 mL; 6% v/v based on the volume of the Grignard reaction) was heated to reflux. The cooled Grignard solution, decanted from excess magnesium, was then added dropwise to the refluxing reaction mixture with a cannulating needle. After 2.5h, an additional 20.7 mL (3 mol %) of 0.1 M (LiBr/CuBr·SMe<sub>2</sub>/LiSPh/THF) copper catalyst solution was added, and the reaction mixture was stirred at reflux for additional 48h. The reaction was then cooled to room temperature, quenched with 1.5 M HCl (235 mL), and extracted with CH<sub>2</sub>Cl<sub>2</sub> (4 x 80 mL). The combined organic layers

were washed with another portion of 1.5M HCl (235 mL), followed by Brine (235 mL), dried over Na<sub>2</sub>SO<sub>4</sub>, and concentrated under vacuum, passed through a silica pad using EtOAc to remove HMPA. The solvent was removed under reduced pressure leaving 18.8 g of crude material. It was subjected to column chromatography (90:10 Hexane/EtOAc) to yield the product as a colorless oil (17.7 g, 62.53 mmol, 86%). <sup>1</sup>H NMR (400 MHz, CDCl<sub>3</sub>) δ 1.42-1.47 (m, 2H), 1.60-1.68 (m, 4H), 2.63 (t, 4H, J=7.6 Hz), 3.83 (s, 6H), 6.85-6.92 (m, 4H), 7.14-7.19 (m, 4H); <sup>13</sup>C NMR (100.5 MHz, CDCl<sub>3</sub>) δ 29.7, 29.9, 30.3, 55.4, 110.3, 120.4, 126.9, 129.9, 131.4, 157.6; HRMS (ESI) calcd for C<sub>19</sub>H<sub>24</sub>O<sub>2</sub> (M)<sup>+</sup> 284.1776, found 284.1772.

### **1, 1' – (1, 5-pentanediy)bis[5-bromo-2-methoxybenzene] (29)**

Bis-anisole **28** (3.33 g, 12.0 mmol) was dissolved in CHCl<sub>3</sub> (13.4 mL). The solution was cooled to 0°C on an ice-water bath, and bromine (3.73 g, 23.4 mmol) was added drop wise (CHCl<sub>3</sub> with ethanol inhibitor was used directly from the bottle; HBr gas produced in the reaction was collected in two KOH traps cooled on dry ice/acetone baths). The reaction was stirred an additional 2.5 h, quenched with 1.5 M HCl (100 mL), extracted with Et<sub>2</sub>O (3 x 50 mL), washed with brine (100 mL), and concentrated under vacuum. The crude product was recrystallized by ethanol to yield a white solid (4.72 g, 10.67 mmol, 91%). mp 49-50 °C; <sup>1</sup>H NMR (400 MHz, CDCl<sub>3</sub>) δ 1.36-1.42 (m, 2H), 1.55-1.62 (m, 4H), 2.56 (t, 4H, J=7.6 Hz), 3.79 (s, 6H), 6.70 (d, 2H, J=8.4 Hz), 7.23-7.26 (m, 4H); <sup>13</sup>C NMR (100.5 MHz, CDCl<sub>3</sub>) δ 29.4, 29.6, 30.0, 55.6, 112.1, 112.7, 129.5, 132.5, 133.8, 156.7; HRMS (ESI) calcd for C<sub>19</sub>H<sub>22</sub>O<sub>2</sub>Br<sub>2</sub> (M)<sup>+</sup> 439.9987, found 439.9961.

### **1,1'-(1,5-pentanediy)bis[5-(2-propenyl)-2-methoxybenzene] (30)**

The reaction was carried out in a glove box. THF (8.6 mL) was added to magnesium turnings (2.17 g, 90.4 mmol), and the reaction mixture was heated to reflux. The bis-anisole **29** (4.00 g, 9.04 mmol) was dissolved in THF (10.1 mL) and transferred into the refluxing reaction mixture via syringe at a rate of 0.12 mL/min. The resulting Grignard solution was stirred at reflux for 24 h and then cooled to ambient temperature. A second solution consisting of mesolate **18** (6.15 g, 45.2 mmol) dissolved in THF (7.9 mL), 6.4 mL (12 mol %) of 0.1M (LiBr/CuBrSMe<sub>2</sub>/LiSPh/THF) copper catalyst solution, and HMPA (1.2 mL; 6% v/v based on the volume of the Grignard reaction) was heated to reflux. The cooled Grignard solution, decanted from excess magnesium, was then added to the refluxing reaction mixture using a syringe. After 2.5h, an additional 3.0 mL (6 mol %) of 0.1 M (LiBr/CuBrSMe<sub>2</sub>/LiSPh/THF) copper catalyst solution was added, and the reaction mixture was stirred at reflux for additional 48h. The reaction was then cooled to ambient temperature, taken out of the glove box and quenched with 1.5 M HCl (50 mL), and extracted with CH<sub>2</sub>Cl<sub>2</sub> (4 x 40 mL). The combined organic layers were washed with another portion of 1.5M HCl (50 mL), followed by Brine (100 mL), dried over Na<sub>2</sub>SO<sub>4</sub>, and concentrated under vacuum to yield a yellow oil. After passing through a silica pad using EtOAc to remove HMPA, the resulting oil was subjected to a gravity column separation (90:10 Hexane/EtOAc), yielding a yellow oil of a mixture of **30a** and **30b** (2.6 g, 7.14 mmol, 79%). <sup>1</sup>H NMR (400 MHz, CDCl<sub>3</sub>) δ 1.45-1.51 (m, 2H), 1.63-1.70 (m, 4H), 2.64 (t, 4H, J=7.6 Hz), 3.36 (d, 4H, J=6.8 Hz), 3.85 (s, 6H), 5.07-5.14 (m, 4H), 5.97-6.04 (m, 2H), 6.81 (d, 2H, J=8 Hz), 7.01-7.03 (m, 4H); <sup>13</sup>C NMR (100.5 MHz, CDCl<sub>3</sub>) δ 29.8, 30.0, 30.2, 39.6, 55.5, 110.3, 115.4, 126.6, 130.2, 131.4, 131.7, 138.2, 155.9; HRMS (ESI) calcd for C<sub>25</sub>H<sub>32</sub>O<sub>2</sub> (M)<sup>+</sup> 364.2402, found 364.2376.

### **1,1'-(1,5-pentanediy)bis[5-(2-propenyl)-2-hydroxybenzene] (31a)**

Dry mixture of **30a** and **30b** (0.62 g, 1.7 mmol) was dissolved in dry 1, 2-dichloroethane (6.75 mL).  $\text{BCl}_3 \cdot \text{SMe}_2$  (0.91 g, 5 mmol) was added to the solution and the reaction mixture refluxed for 24 h under  $\text{N}_2$  atmosphere. The mixture was cooled to  $0^\circ\text{C}$  and quenched with a saturated methanolic solution of  $\text{NaHCO}_3$  (4 mL). The solution was diluted with EtOAc (15 mL), washed with brine (2 x 20 mL), and dried over anhydrous  $\text{Na}_2\text{SO}_4$ . The crude product was purified by silica gel column chromatography (83: 15: 2 Hexane / Ethyl acetate/ Isopropylamine) to yield **31a** as a white solid (0.45 g, 1.35 mmol, 80%). mp  $90\text{-}91^\circ\text{C}$ ;  $^1\text{H}$  NMR (400 MHz,  $\text{DMSO-d}_6$ )  $\delta$  1.28-1.32 (m, 2H), 1.49-1.53 (m, 4H), 2.45 (t, 4H,  $J=7.6$  Hz), 3.20 (d, 4H,  $J=6.8$  Hz), 5.07-5.14 (m, 4H), 5.86-5.90 (m, 2H), 6.67 (d, 2H,  $J=8.4$  Hz), 6.76 (d, 2H,  $J=8$  Hz), 6.82 (s, 2H), 8.97 (s, 2H);  $^{13}\text{C}$  NMR (100.5 MHz,  $\text{DMSO-d}_6$ )  $\delta$  29.0, 29.3, 29.7, 38.9, 115.0, 115.4, 126.5, 128.3, 129.2, 129.8, 138.4, 150.6; FTIR (ATR)  $\nu$   $3267\text{ cm}^{-1}$ ; HRMS (ESI) calcd for  $\text{C}_{23}\text{H}_{27}\text{O}_2$  (M-H) $^-$  335.2011, found 335.1989.

### **1,1'-(1,5-pentanediy)bis[3-bromo-5-(2-propenyl)-2-hydroxybenzene] (32)**

Dry bis phenol **31a** (0.36 g, 1.1 mmol) was dissolved in freshly distilled  $\text{CHCl}_3$  (6.9 mL). 1,3-dibromo-5,5-dimethylhydantoin (0.19 g, 0.65 mmol) was added to the reaction mixture under  $\text{N}_2$  atmosphere. The reaction flask was covered with aluminum foil, and the reaction mixture was stirred at room temperature. After 0.5 h, another 0.65 mmol of 1,3-dibromo-5,5-dimethylhydantoin was added and continued to stir for 3.4 h. The solvent was removed under reduced pressure and the resulting crude solid was purified by silica gel column chromatography (100 %  $\text{CHCl}_3$ ), to yield an orange color solid (0.50 g, 1.01 mmol, 92%). mp  $65\text{-}66^\circ\text{C}$ ;  $^1\text{H}$  NMR

(400 MHz, DMSO- $d_6$ )  $\delta$  1.21-1.25 (m, 2H), 1.40-1.51 (m, 4H), 2.48 (t, 4H,  $J=7.6$  Hz), 3.16 (d, 4H,  $J=6.8$  Hz), 4.92-5.14 (m, 4H), 4.97-5.04 (m, 2H), 5.79-5.90 (m, 2H), 6.81 (s, 2H), 7.05 (s, 2H), 8.69 (s, 2H);  $^{13}\text{C}$  NMR (100.5 MHz, DMSO- $d_6$ )  $\delta$  28.7, 29.3, 30.4, 38.3, 111.2, 115.8, 129.3, 129.4, 131.7, 132.4, 137.7, 149.5; HRMS (ESI) calcd for  $\text{C}_{23}\text{H}_{26}\text{O}_2\text{Br}_2$  (M) $^+$  492.0300, found 492.0326.

### **3,11-diallyl-1,13-dibromo-6,7,8,9-tetrahydro-5H-dibenzo[d,k][1,3]dioxacyclododecine (33)**

Dry **32** (0.4 g, 0.81 mmol) was added to a 500 mL round bottom flask followed by  $\text{K}_2\text{CO}_3$  (0.34 g, 2.43 mmol) and 18-Crown-6 (0.32 g, 1.21 mmol) in a glove bag. The reaction flask was fitted with a condenser, and removed from the glove bag. Dry THF (300 mL) was added to the flask under  $\text{N}_2$  atmosphere. It was warmed to  $54^\circ\text{C}$  and stirred for 0.5 h.  $\text{CH}_2\text{I}_2$  (64  $\mu\text{L}$ , 0.81 mmol) was syringed into the reaction mixture and the reaction was stirred at  $54^\circ\text{C}$  for 24 h. After 24 h,  $\text{CH}_2\text{I}_2$  (64  $\mu\text{L}$ , 0.81 mmol) again was added to the pale green reaction mixture and the reaction temperature was raised to  $71^\circ\text{C}$  and the mixture was stirred under reflux for a further 72 h. The colorless solution was quenched by pouring onto 0.1 M HCl (200 mL). Then the organic layer was separated and the aqueous layer was extracted with  $\text{CH}_2\text{Cl}_2$  (2 x 100 mL). The combined organic layers was washed with saturated  $\text{NaHCO}_3$  (3 x 100 mL) followed by saturated brine solution (150 mL). It was dried over anhydrous  $\text{Na}_2\text{SO}_4$  and solvent was removed under reduced pressure. Radial chromatography (98 : 2 Hexane / Isopropylamine) yielded pure product as a white solid (0.35 g, 0.69 mmol, 85.5%). mp  $85\text{-}87^\circ\text{C}$ ;  $^1\text{H}$  NMR (400 MHz,  $\text{CDCl}_3$ )  $\delta$  1.46-1.47 (m, 2H), 1.74-1.78 (m, 4H), 2.82 (t, 4H,  $J=7.4$  Hz), 3.23 (d, 4H,  $J=6.8$  Hz), 4.99-5.05 (m, 4H), 5.46 (s, 2H), 5.80-5.90 (m, 2H), 6.90 (d, 2H,  $J=1.6$  Hz), 7.16 (d, 2H,  $J=2$  Hz);  $^{13}\text{C}$  NMR (100.5

MHz, CDCl<sub>3</sub>)  $\delta$  25.4, 26.7, 29.1, 39.4, 103.0, 116.6, 117.9, 130.3, 130.7, 136.9, 138.3, 139.3, 153.7; HRMS (ESI) calcd for C<sub>24</sub>H<sub>26</sub>O<sub>2</sub>Br<sub>2</sub> (M)<sup>+</sup> 504.0300, found 504.0284.

**3,3'-(1,13-dibromo-6,7,8,9-tetrahydro-5H-dibenzo[d,k][1,3]dioxacyclododecine-3,11-diyl)dipropene-1,2-diol (34)**

To a 5 mL round bottom flask containing compound **33** (0.04 g, 0.08 mmol), the solvent mixture (10: 3: 1 *tert* BuOH\ THF\ H<sub>2</sub>O) (1 mL) was added. Fitted with a flow adapter, the reaction mixture was warmed to 40 °C to dissolve the solid compound. The solution was cooled to room temperature and N-methylmorpholine-N-oxide (0.02 g, 0.18 mmol) was added to the flask. A catalytic amount of OsO<sub>4</sub> was introduced to the flask by quickly opening the flow adapter and once the adapter was fitted back, the reaction mixture was stirred under nitrogen environment for 24 h. at 25 °C. A saturated aqueous solution of Na<sub>2</sub>S<sub>2</sub>O<sub>4</sub> (4 mL) was added to the solution and the solution mixture was stirred for 10 minutes. The solution was then extracted with n-BuOH (3 x 2.5 mL). The combined n-BuOH layers were washed with brine (2 x 2 mL). The combined brine layers were washed with n-BuOH (2 mL) and the organic layers were combined. Solvent was removed under vacuum and the resulting white solid was used for the next synthetic step without further purification (0.05 g, 0.08 mmol, 100 %). mp 148-152 °C; <sup>1</sup>H NMR (400 MHz, CDCl<sub>3</sub>)  $\delta$  1.46-1.47 (m, 2H), 1.74-1.78 (m, 4H), 2.82 (t, 4H, J=7.4 Hz), 3.23 (d, 4H, J=6.8 Hz), 4.99-5.05 (m, 4H), 5.46 (s, 2H), 5.80-5.90 (m, 2H), 6.90 (s, 2H), 7.16 (s, 2H); <sup>13</sup>C NMR (100.5 MHz, CDCl<sub>3</sub>)  $\delta$  26.5, 27.8, 29.9, 40.0, 66.7, 74.2, 104.2, 118.5, 132.4, 132.8, 139.0, 140.1, 154.8; FTIR (ATR)  $\nu$  3338 cm<sup>-1</sup>; HRMS (ESI) calcd for C<sub>24</sub>H<sub>31</sub>O<sub>6</sub>Br<sub>2</sub> (M+Na)<sup>+</sup> 595.0307, found 595.0306.

**1,13-dibromo-3,11-bis((2,2-dimethyl-1,3-dioxolan-4-yl)methyl)-6,7,8,9-tetrahydro-5H-dibenzo[d,k][1,3]dioxacyclododecine (35)**

To a stirred solution of dry **34** (1.2 g, 2 mmol) in dry acetone (37 mL) anhydrous CuSO<sub>4</sub> (1.4 g, 8.5 mmol) and a catalytic amount of anhydrous *para*-toluenesulfonic acid were added. The reaction was stirred for 24 h at room temperature. The solvent was removed under vacuum and the resulting solid was dissolved in (90: 10 EtOAc\ MeOH) (100 mL). It was washed with saturated aqueous solution of NaHCO<sub>3</sub> (3 x 40 mL). The organic layer was dried over anhydrous Na<sub>2</sub>SO<sub>4</sub> and the solvent was removed under vacuum. The resulting yellow solid was passed through a silica pad (98:2 EtOAc/isopropylamine), yielding **35** as a white solid (1.3 g, 1.96 mmol, 98%). mp 118-120 °C; <sup>1</sup>H NMR (400 MHz, CDCl<sub>3</sub>) δ 1.35 (s, 6H), 1.42 (s, 6H), 1.51-1.57 (m, 2H), 1.80-1.86 (m, 4H), 2.70 (dd, 2H, J=14 Hz; J=6.4 Hz), 2.85-2.90 (m, 6H), 3.61 (dd, 2H, J=8.2 Hz; J=7 Hz), 3.99 (dd, 2H, J=8.4 Hz; J=6 Hz), 4.26-4.32 (m, 2H), 5.51 (s, 2H), 7.01 (s, 2H), 7.27 (s, 2H); <sup>13</sup>C NMR (100.5 MHz, CDCl<sub>3</sub>) δ 25.3, 25.8, 26.6, 27.1, 29.0, 39.2, 68.9, 76.4, 102.8, 109.4, 117.9, 130.9, 131.3, 135.8, 139.3, 153.9; HRMS (ESI) calcd for C<sub>30</sub>H<sub>38</sub>O<sub>6</sub>Br<sub>2</sub> (M)<sup>+</sup> 652.1035, found 652.1010.

**3,11-bis((2,2-dimethyl-1,3-dioxolan-4-yl)methyl)-6,7,8,9-tetrahydro-5H-dibenzo[d,k][1,3]dioxacyclododecine-1,13-dicarbonitrile (36b)**

A mixture of dry **35** (0.97 g, 1.48 mmol), CuCN (1.1 g, 11.9 mmol), Pd<sub>2</sub>(dba)<sub>3</sub> (0.08 g, 0.09 mmol), DPPF (0.26 g, 0.47 mmol) and anhydrous 1,4-dioxane (7.4 mL) in the presence of Et<sub>4</sub>NCN (0.4 g, 2.96 mmol) was refluxed for 24 h. The reaction mixture was diluted with EtAOC (30 mL) and filtered through a Celite pad. The filtrate was washed with saturated NaHCO<sub>3</sub> (3 x

15 mL), dried over anhydrous Na<sub>2</sub>SO<sub>4</sub>, and the solvent was evaporated under reduced pressure. The residue was dried and once again reacted with CuCN (0.6 g, 5.95 mmol), Pd<sub>2</sub>(dba)<sub>3</sub> (0.04 g, 0.04 mmol), DPPF (0.13 g, 0.23 mmol) and anhydrous 1,4-dioxane (7.4 mL) in the presence of Et<sub>4</sub>NCN (1.5 mmol) under reflux conditions for 24 h. The reaction mixture was diluted with EtAOc (30 mL) and filtered through a Celite pad. The filtrate was washed with saturated NaHCO<sub>3</sub> (3 x 15 mL), dried over anhydrous Na<sub>2</sub>SO<sub>4</sub>, and the solvent was evaporated under reduced pressure. After passing through a silica pad using 100 % EtOAc, the residue was purified by radial chromatography (98:2 hexane/isopropylamine), to yield **36b** as a white solid (0.70 g, 1.23 mmol, 83 %). mp 143-144 °C; <sup>1</sup>H NMR (400 MHz, CDCl<sub>3</sub>) δ 1.33 (s, 6H), 1.40 (s, 6H), 1.50-1.56 (m, 2H), 1.78-1.85 (m, 4H), 2.74-2.92 (m, 8H), 2.82-2.92 (m, 6H), 3.59 (dd, 2H, J=8.2 Hz; J=7 Hz), 4.01 (dd, 2H, J=8.4 Hz; J=6 Hz), 4.24-4.30 (m, 2H), 5.76 (s, 2H), 7.29 (s, 2H), 7.32 (s, 2H); <sup>13</sup>C NMR (100.5 MHz, CDCl<sub>3</sub>) δ 25.3, 25.7, 26.5, 27.1, 28.2, 39.1, 68.8, 76.0, 102.2, 107.5, 109.6, 116.6, 131.6, 135.5, 136.8, 138.4 158.3; FTIR (ATR) ν 2233 cm<sup>-1</sup>; HRMS (ESI) calcd for C<sub>32</sub>H<sub>38</sub>N<sub>2</sub>O<sub>6</sub> (M+Na)<sup>+</sup> 569.2628, found 569.2624.

**tert-butyl(3,11-bis((2,2-dimethyl-1,3-dioxolan-4-yl)methyl)-6,7,8,9-tetrahydro-5H-dibenzo[d,k][1,3]dioxacyclododecine-1,13-diyl)bis(methylene)dicarbamate (38)**

To a stirred solution of dry bisnitrile **36b** (0.18 g, 0.33 mmol) in dry methanol (7 mL) that was cooled to 0 °C was added Boc<sub>2</sub>O (0.29 g, 1.34 mmol) and NiCl<sub>2</sub>·6H<sub>2</sub>O (0.02 g, 0.07 mmol) as solids. NaBH<sub>4</sub> (0.18 g, 4.68 mmol) was then added in small portions over 30 minutes via a Schlenk tube. The reaction was exothermic and effervescent. The resulting reaction mixture, containing a finely divided black precipitate, was allowed to warm to room temperature and left to stir for 24 h. Diethylenetriamine (143 μL, 0.67 mmol) was added and the mixture was allowed

to stir for 1 h before the removal of the solvent under vacuum. The purple residue was dissolved in EtOAc (50 mL) and extracted with saturated NaHCO<sub>3</sub> (2 x 25 mL). The organic layer was dried over anhydrous Na<sub>2</sub>SO<sub>4</sub> and the solvent removed in vacuum to yield a crude yellow solid. The dry crude solid was again dissolved in dry methanol (7 mL) and cooled to 0<sup>0</sup>C. Boc<sub>2</sub>O (0.14 g, 0.67 mmol) and NiCl<sub>2</sub>·6H<sub>2</sub>O (0.016 g, 0.07 mmol) were added to the reaction mixture and NaBH<sub>4</sub> (0.09 g, 2.34 mmol) was added in small portions over 30 minutes via a Schlenk tube. The reaction was allowed to warm to room temperature and stirred for 24 h. Diethylenetriamine (143 μL, 0.67 mmol) was added, and the mixture was allowed to stir for 1 h before the removal of solvent under vacuum. The purple residue was dissolved in EtOAc (50 mL) and extracted with saturated NaHCO<sub>3</sub> (2 x 25 mL). The organic layer was dried over anhydrous Na<sub>2</sub>SO<sub>4</sub> and the solvent removed in vacuum to yield a crude yellow solid. It was recrystallized using EtOAc and Hexane (0.2 g, 0.27 mmol, 82%). mp 149-150 °C; <sup>1</sup>H NMR (400 MHz, CDCl<sub>3</sub>) δ 1.33 (s, 6H), 1.41 (s, 6H), 1.42 (s, 18H), 1.48-1.58 (m, 2H), 1.76-1.85 (m, 4H), 2.69 (dd, 2H, J=13.4; J=7 Hz), 2.78-2.93 (m, 6H), 3.60 (dd, 2H, J=8.2 Hz; J=1.4 Hz), 3.95 (dd, 2H, J=5.8 Hz; J=1.4 Hz), 4.20 (d, 4H, J=5.6 Hz), 4.25-4.31 (m, 2H), 4.90 (br s, 2H), 5.38 (s, 2H), 6.97 (s, 4H); <sup>13</sup>C NMR (100.5 MHz, CDCl<sub>3</sub>) δ 25.5, 25.9, 27.2, 28.4, 28.5, 39.6, 40.3, 69.1, 76.7, 79.7, 102.4, 109.3, 127.8, 131.0, 132.1, 134.5, 137.8, 154.7, 155.9; FTIR (ATR) ν 3349 cm<sup>-1</sup>; HRMS (ESI) calcd for C<sub>42</sub>H<sub>62</sub>N<sub>2</sub>O<sub>10</sub>Na (M+Na)<sup>+</sup> 777.4302, found 777.4317

**(3,11-bis(2,3-dihydroxypropyl)-6,7,8,9-tetrahydro-5H-dibenzo[d,k][1,3]dioxacyclododecine-1,13-diyl)dimethanaminium 2,2,2-trifluoroacetate (39)**

Pure **38a** (0.06 g, 0.08 mmol) was dissolved in (80:18:2 methanol/ethyl acetate/water) (5 mL) and stirred at room temperature for 5 minutes. TFA (2 mL) was added and the reaction stirred for 0.5 h at room temperature. Then the excess reagent & solvents were removed under vacuum at room temperature. The crude oily residue was again dissolved in (80:18:2 methanol/ethyl acetate/water) (5 mL) and stirred at room temperature for 5 minutes. TFA (2 mL) was added and the reaction stirred for 0.5 h at room temperature. The excess reagent & solvents were removed under vacuum at room temperature. The reaction was repeated twice more and each time the progress was monitored using  $^1\text{H}$  NMR. Solvents and excess TFA were removed under vacuum at room temperature and the resulting crude semisolid was taken to the next step without further purification. (0.2 g, 0.27 mmol, 82%).  $^1\text{H}$  NMR (400 MHz, DMSO- $d_6$ )  $\delta$  1.52-1.53 (m, 2H), 1.77-1.78 (m, 4H), 2.75 (dd, 4H,  $J=14$  Hz;  $J=4.4$  Hz), 2.80-2.89 (m, 4H), 3.27-3.34 (m, 4H), 3.63-3.66 (m, 2H), 3.95 (d, 4H,  $J=5.6$  Hz), 4.27 (broad s 4H), 5.46 (s, 2H), 7.16 (d, 4H,  $J=4.8$  Hz), 8.12 (s, 6H);  $^{13}\text{C}$  NMR (100.5 MHz,  $\text{CD}_3\text{OD}$ )  $\delta$  14.6, 22.8, 26.4, 28.4, 29.2, 40.1, 66.6, 74.3, 93.7, 104.2, 111.5, 127.9, 130.2, 134.4, 138.2, 139.4, 156.2, 161.0; MS(ESI)  $m/z$  475.3 ( $\text{M}^+$ ), 238.1 ( $\text{M}^{2+}/2$ ) $^+$ ; HRMS (ESI) calcd for ( $\text{M}+\text{H}$ ) $^+$   $\text{C}_{26}\text{H}_{39}\text{N}_2\text{O}_6$  475.2808, found 475.2799

**(3,11-bis(2,3-dihydroxypropyl)-6,7,8,9-tetrahydro-5H-dibenzo[d,k][1,3]dioxacyclododecine-1,13-diyl)dimethanaminium hexafluorophosphate (V) (5)**

Compound **39** (0.02 g, 0.034 mmol) was dissolved in (60:40 methanol/ ethylacetate) (3 mL) and ammonium hexafluorophosphate (0.05 g, 0.34 mmol) was added to the solution. It was stirred

overnight at room temperature. Solvent was removed under vacuum and the crude residue was dissolved in ethylacetate (10 mL). It was washed with H<sub>2</sub>O (2 mL) and the organic layer was separated and the solvent was removed under vacuum to yield a white solid of **5** (0.02 g, 0.029 mmol, 86%). mp 129-131 °C; <sup>1</sup>H NMR (400 MHz, CD<sub>3</sub>OD) δ 1.55-1.63 (m 2H), 1.81-1.98 (m 4H), 2.65-2.70 (m, 4H), 2.85 (dd, 4H, J= 13.8 Hz, J= 5 Hz), 3.45- 3.54 (m 4H), 3.82-3.85 (m, 2H), 4.11 (s, 4H), 5.55 (s, 2H), 7.16 (s, 2H), 7.25 (s, 2H) ; <sup>13</sup>C NMR (100.5 MHz, CD<sub>3</sub>OD) δ 26.4, 28.4, 29.2, 40.1, 40.4, 66.7, 74.3, 104.3, 127.9, 130.1, 134.3, 138.1, 139.4, 156.2; MS(ESI) m/z 475.3 (M)<sup>+</sup>, 238.1 (M<sup>2+</sup>/2)<sup>+</sup>; HRMS (ESI) calcd for (M+H)<sup>+</sup> C<sub>26</sub>H<sub>39</sub>N<sub>2</sub>O<sub>6</sub> 475.2808, found 475.2807

#### **1,1'-(1,5-pentanediy)bis[3-bromo-5-propyl-2-hydroxybenzene] (41)**

Dry compound **32** (0.43g, 0.87 mmol) was placed into a Parr<sup>TM</sup> hydrogenation reaction bottle. **32** was dissolved in ethylacetate (15 mL). The bottle was flushed with a nitrogen atmosphere and a catalytic amount of 10 % Pd/C was introduced to the bottle. It was charged with H<sub>2</sub> gas in the high pressure Parr<sup>TM</sup> shaker hydrogen apparatus. The contents of the reaction bottle were flushed twice with hydrogen and then placed under hydrogen (35 atm) for 18 h. The progress of the reaction was followed by monitoring the change in the H<sub>2</sub> gas pressure and TLC at different times. The crude reaction mixture was passed through a Celite pad and subjected to a gravity column separation (80:20 EtOAc/Hexane) to yield a white solid (0.41 g, 0.83 mmol, 95%). mp 63-64 °C; <sup>1</sup>H NMR (400 MHz, DMSO-d<sub>6</sub>) δ 0.85 (t, 6H, J=7.2 Hz), 1.32-1.39 (m, 2H), 1.48-1.53 (m, 8H ), 2.41 (t, 4H, J=7.4 Hz), 2.55 (t, 4H, J=7.6 Hz), 6.85 (d, 2H, J=1.6 Hz), 7.11 (d, 2H, J=2 Hz), 8.61 (s, 2H); <sup>13</sup>C NMR (100 MHz, DMSO-d<sub>6</sub>) δ 13.7, 24.1, 29.3, 30.3, 37.5, 113.2, 128.7,

129.5, 131.5, 132.6, 149.3; HRMS (ESI) calcd for  $C_{23}H_{29}Br_2O_2$  (M-H)<sup>-</sup> 495.0534, found 495.0542.

**1,13-dibromo-3,11-dipropyl-6,7,8,9-tetrahydro-5H-dibenzo[d,k][1,3]dioxacyclododecine**

**(42)**

Dry **41** (0.41 g, 0.83 mmol) was placed in a 500 mL round bottom flask followed by  $K_2CO_3$  (0.34 g, 2.43 mmol) and 18-Crown-6 (0.32 g, 1.21 mmol) in a glove bag. Fitted with a condenser, the flask was removed from the glove bag and dry THF (300 mL) was added to the flask under  $N_2$  atmosphere. It was warmed to 54 °C and stirred for 0.5 h.  $CH_2I_2$  (65.5  $\mu$ L, 0.83 mmol) was syringed into the reaction mixture and stirred at 54 °C for 24 h. After 24 h,  $CH_2I_2$  (65.5  $\mu$ L, 0.83 mmol) again was added to the pale green reaction mixture and its temperature raised to 71 °C and stirred under reflux for a further 72 h. The colorless solution was quenched by pouring onto 0.1 M HCl (200 mL). The organic layer was separated and the acid layer was extracted with  $CH_2Cl_2$  (2 x 100 mL). The combined organic layers was washed with saturated  $NaHCO_3$  (3 x 100 mL) followed by saturated brine solution (150 mL). It was dried over anhydrous  $Na_2SO_4$  and solvent was removed under reduced pressure. Radial chromatography (98:2 Hexane/Isopropylamine) yielded the pure product as a white solid (0.35 g, 0.69 mmol, 83%) mp 82-83 °C;  $^1H$  NMR (400 MHz,  $CDCl_3$ )  $\delta$  0.92 (t, 6H, J=7.4 Hz), 1.53-1.63 (m, 6H), 1.82-1.86 (m, 4H), 2.48 (t, 4H, J= 7.6 Hz), 2.88-2.89 (m, 4H), 5.51 (s, 2H), 6.94 (d, 2H, J= 2 Hz), 7.20 (d, 2H, J= 2 Hz);  $^{13}C$  NMR (100 MHz,  $CDCl_3$ )  $\delta$  13.7, 24.4, 25.3, 26.5, 28.9, 37.2, 102.9, 117.5, 130.2, 130.4, 138.8, 140.7, 153.1; HRMS (ESI) calcd for  $C_{24}H_{30}Br_2O_2$  (M)<sup>+</sup> 508.0613, found 508.0622.

**3,11-dipropyl-6,7,8,9-tetrahydro-5H-dibenzo[d,k][1,3]dioxacyclododecine-1,13-dicarbonitrile (43a)**

A mixture of dry **42** (0.35 g, 0.68 mmol), CuCN (0.48 g, 5.4 mmol), Pd<sub>2</sub>(dba)<sub>3</sub> (0.04 g, 0.04 mmol), DPPF (0.12 g, 0.22 mmol) and anhydrous 1,4-dioxane (3.5 mL) in the presence of Et<sub>4</sub>NCN (0.18 g, 1.36 mmol) was refluxed for 24 h. The reaction mixture was diluted with EtAOc (10 mL) and filtered through a Celite pad. The filtrate was washed with saturated NaHCO<sub>3</sub> (3 x 5 mL), dried over anhydrous Na<sub>2</sub>SO<sub>4</sub>, and the solvent was evaporated under reduced pressure. The residue was dried and reacted once again with CuCN (0.24 g, 2.7 mmol), Pd<sub>2</sub>(dba)<sub>3</sub> (0.02 g, 0.02 mmol), DPPF (0.06 g, 0.11 mmol) and anhydrous 1,4-dioxane (3.5 mL) in the presence of Et<sub>4</sub>NCN (0.09 g, 0.68 mmol), with the reaction mixture under reflux for 24 h. The reaction mixture was diluted with EtAOc (10 mL) and filtered through a Celite pad. The filtrate was washed with saturated NaHCO<sub>3</sub> (3 x 5 mL), dried over anhydrous Na<sub>2</sub>SO<sub>4</sub>, and the solvent was evaporated under reduced pressure. After passing through a silica pad using 100 % EtOAc, the residue was purified by radial chromatography (98:2 Hexane/Isopropylamine), to yield **43a** as a white solid (0.29 g, 0.56 mmol, 83 %). mp 82-83 °C; <sup>1</sup>H NMR (400 MHz, CDCl<sub>3</sub>) δ 0.93 (t, 6H, J= 7.4 Hz), 1.53-1.54 (m, 2H), 1.58-1.64 (m, 4H), 1.79-1.88 (m, 4H), 2.54 (t, 4H, J= 7.6 Hz), 2.84 (t, 4H, J= 8.2 Hz), 5.75 (s, 2H), 7.24 (s, 2H), 7.25 (s, 2H); <sup>13</sup>C NMR (100 MHz, CDCl<sub>3</sub>) δ 13.5, 24.2, 25.1, 26.4, 28.0, 37.0, 102.3, 107.1, 116.7, 130.3, 135.7, 138.0, 140.0, 157.0; FTIR (ATR) ν 2225 cm<sup>-1</sup>; HRMS (ESI) calcd for C<sub>26</sub>H<sub>30</sub>N<sub>2</sub>O<sub>2</sub> (M+Na)<sup>+</sup> 425.2205, found 425.2181.

**tert-butyl (3,11-dipropyl-6,7,8,9-tetrahydro-5H-dibenzo[d,k][1,3]dioxacyclododecine-1,13-diyl)bis(methylene)dicarbamate (44b)**

In a two neck flask fitted with a Schlenk tube and a septum, a stirred solution of dry **43a** (0.29 g, 0.56 mmol) in dry methanol (11.8 mL) was cooled to 0 °C. Boc<sub>2</sub>O (0.48 g, 2.24 mmol) and NiCl<sub>2</sub>·6H<sub>2</sub>O (0.03 g, 0.11 mmol) were added to the mixture by opening the septum and quickly closing it. NaBH<sub>4</sub> (0.29 g, 7.84 mmol) was then added in small portions over 30 minutes via the Schlenk tube. The reaction was exothermic and effervescent. The resulting reaction mixture containing a finely divided black precipitate was allowed to warm to room temperature and left to stir for 24 h and then diethylenetriamine (240 µL, 1.12 mmol) was added. The mixture was allowed to stir for 1 h before the removal of the solvent under vacuum. The purple residue was dissolved in EtOAc (50 mL) and extracted with saturated NaHCO<sub>3</sub> (2 x 25 mL). The organic layer was dried over anhydrous Na<sub>2</sub>SO<sub>4</sub> and the solvent removed in vacuum to yield a crude yellow solid. The dry crude solid was again dissolved in dry methanol (11.8 mL) and the mixture cooled to 0 °C. Boc<sub>2</sub>O (0.24 g, 1.12 mmol) and NiCl<sub>2</sub>·6H<sub>2</sub>O (0.03 g, 0.11 mmol) were added to the reaction mixture and NaBH<sub>4</sub> (0.15 g, 3.92 mmol) was added in small portions over 30 minutes via a Schlenk tube. The reaction was allowed to warm to room temperature and stirred for 24 h. Diethylenetriamine (240 µL, 1.12 mmol) was then added. The mixture was allowed to stir for 1 h before the removal of the solvent under vacuum. The purple residue was dissolved in EtOAc (50 mL) and extracted with saturated NaHCO<sub>3</sub> (2 x 25 mL). The organic layer was dried over anhydrous Na<sub>2</sub>SO<sub>4</sub> and the solvent removed in vacuum to yield a crude yellow solid. It was recrystallized using EtOAc and Hexane (0.18 g, 0.46 mmol, 82%). mp 134-135 °C; <sup>1</sup>H NMR (400 MHz, CDCl<sub>3</sub>) δ 0.91 (t, 6H, J=7.4 Hz), 1.40 (s, 18H), 1.52-1.68 (m, 4H), 1.78-1.85 (m, 4H), 2.49 (t, 4H, J=7.8 Hz), 2.84-2.87 (m, 4H), 4.18 (d, 4H, J= 5.2 Hz), 4.83 (s, 2H), 5.36 (s, 2H),

6.928 (s, 4H);  $^{13}\text{C}$  NMR (100 MHz,  $\text{CDCl}_3$ )  $\delta$  14.1, 24.7, 25.6, 27.3, 28.4, 28.6, 37.6, 40.5, 79.5, 102.5, 127.2, 130.3, 131.7, 137.5, 139.6, 154.1, 155.9; FTIR (ATR)  $\nu$  3338  $\text{cm}^{-1}$ ; HRMS (ESI) calcd for  $\text{C}_{36}\text{H}_{55}\text{N}_2\text{O}_6\text{Na}$  ( $\text{M}+\text{H}$ ) $^+$  611.4060, found 611.4069, calcd for  $\text{C}_{36}\text{H}_{55}\text{N}_2\text{O}_6\text{Na}$  ( $\text{M}+\text{Na}$ ) $^+$  633.3880, found 633.3880.

**(3,11-dipropyl-6,7,8,9-tetrahydro-5H-dibenzo[d,k][1,3]dioxacyclododecine-1,13-diyl)dimethanaminium 2,2,2-trifluoroacetate (45)**

To a solution of Boc protected amine **44b** (0.047 g, 0.08 mmol) in anhydrous  $\text{CH}_2\text{Cl}_2$  (1 mL) was added TFA (1 mL) and the reaction mixture stirred for 0.5 h at room temperature. The excess reagent & solvent were removed under vacuum. The resulting crude oil like product was taken for the next reaction without further purification (0.05 g, 0.08 mmol, 100 %).  $^1\text{H}$  NMR (400 MHz,  $\text{CDCl}_3$ )  $\delta$  0.86 (t, 6H,  $J=7.4$  Hz), 1.50-1.56 (m, 6H), 1.72-1.76 (m, 4H), 2.43 (t, 4H,  $J=7.6$  Hz), 2.67-2.73 (m, 4H), 3.99 (s, 4H), 5.47 (s, 2H), 6.96 (s, 2H), 6.99 (s, 2H), 8.08 (s, 6H);  $^{13}\text{C}$  NMR (100 MHz,  $\text{CDCl}_3$ )  $\delta$  13.6, 24.3, 25.3, 25.6, 27.5, 37.2, 41.0, 99.7, 121.4, 125.0, 128.7, 133.2, 137.0, 141.1, 151.7, 161.5; HRMS (ESI) calcd for  $\text{C}_{26}\text{H}_{39}\text{N}_2\text{O}_2$  ( $\text{M}+\text{H}$ ) $^+$  411.3012, found 411.2997; calcd for  $\text{C}_{26}\text{H}_{38}\text{N}_2\text{O}_2\text{Na}$  ( $\text{M}+\text{Na}$ ) $^+$  433.2831, found 433.2826

**(3,11-dipropyl-6,7,8,9-tetrahydro-5H-dibenzo[d,k][1,3]dioxacyclododecine-1,13-diyl)dimethanaminium hexafluorophosphate(V) (46)**

The crude **45** (0.05 g, 0.08 mmol) was dissolved in ethyl acetate (2 mL) and a solution of  $\text{NH}_4\text{PF}_6$  (0.13 g, 0.8 mmol) dissolved in ethyl acetate (2 mL) was added. The resulting mixture was stirred for 24 h under a nitrogen atmosphere at room temperature. The solution was diluted

with ethyl acetate (10 mL) and washed with H<sub>2</sub>O (3 x 8 mL). Solvent was removed under vacuum to yield a white solid (0.05 g, 0.07 mmol, 96 %). mp 115-117 °C; <sup>1</sup>H NMR (400 MHz, DMSO) δ 0.85 (t, 6H, J= 7.2 Hz), 1.19-1.22 (m, 2H), 1.42-1.59 (m, 4H) 1.74-1.80 (m, 4H), 2.80-2.85 (m, 4H), 3.92 (s, 4H), 5.45 (s, 2H), 6.96 (s, 2H), 7.00 (s, 2H) 8.16 (s, 6H); <sup>13</sup>C NMR (100 MHz, CDCl<sub>3</sub>) δ 13.8, 24.4, 27.1, 27.6, 29.9, 37.2, 42.1, 98.9, 124.8, 128.7, 133.1, 136.6, 140.8, 151.4; HRMS (ESI) calcd for C<sub>26</sub>H<sub>39</sub>N<sub>2</sub>O<sub>2</sub> (M+H)<sup>+</sup> 411.3012, found 411.2997; calcd for C<sub>26</sub>H<sub>38</sub>N<sub>2</sub>O<sub>2</sub>Na (M+Na)<sup>+</sup> 433.2831, found 433.2816

## REFERENCES

## REFERENCES

1. [http://portal.acs.org/portal/PublicWebSite/education/whatischemistry/landmarks/fleming-penicillin/CNBP\\_028377](http://portal.acs.org/portal/PublicWebSite/education/whatischemistry/landmarks/fleming-penicillin/CNBP_028377) [05/02/2013]
2. <http://acswebcontent.acs.org/landmarks/landmarks/penicillin/discover.html> [05/04/2013]
3. Clardy, J., Fischbach, M., Currie, C., *The natural history of antibiotics*. *Curr Biol.*, 2009. June 9; 19(11): p. 437-441.
4. Wilcox, S., *The New Antimicrobials: Cationic Peptides*. *BioTeach Journal*, Fall 2004. Vol. 2: p. 88-91.
5. Oysten, P., Fox, M.A., Richards, J., Clark, G., *Novel peptide therapeutics for treatment of infections*. *Journal of Medicinal Microbiology*, 2009. 58: p 977-987.
6. Yeung, A., Gellatly, S., Hancock, R. E., *Multifunctional cationic host defence peptides and their clinical applications*. *Cell. Mol. Life Sci.* 2011. 68: p 2161-2176.
7. Brogden, K. A., *Antimicrobial Peptides: Pore formers or metabolic inhibitors in bacteria?*. *Nat. Rev. Microbiol.*, 2005. Vol. 3: p. 238-250.
8. Lazarev, V.N., Govorun, V.M., *Antimicrobial peptides and their use in medicine*. *Applied Biochemistry and Microbiology*, 2010. Vol. 46 (9): 803-814.
9. Boman, H. G., *Peptide antibiotics and their role in innate immunity*. *Annu. Rev. Immunol.*, 1995 13: p. 61-92.
10. Zasloff, M., *Antimicrobial peptides of multicellular organisms*. *Nat. Rev. Microbiol.*, 2002. Vol. 415: p. 389-395.
11. Bommarius, B., Kalman, D., *Antimicrobial and host defense peptides for therapeutic use against multidrug-resistant pathogens*. *IDrugs*, 2009. 12 (6): p.376-380.
12. Donald J. Hanahan, *A Guide to Phospholipid Chemistry*. 1997, Oxford University Press.
13. <http://www.alevelnotes.com/Biological-Membranes/128> [06/03/2013]
14. Averill, B., Eldredge, P., *General Chemistry: Principles, Patterns and Applications*. 2011, Prentice Hall.
15. Cooper, G. M., *The Cell, a molecular approach*. 2000, Sinauer Associates Inc.
16. <http://ccaoscience.wordpress.com/notes/the-plasma-membrane/> [06/18/2013]

17. Nelson, D. L., Cox, M. M., *Lehninger. Principles of Biochemistry*. 2005, W. H. Freeman
18. [http://microbewiki.kenyon.edu/index.php/Bacterial\\_Derived\\_Plastics](http://microbewiki.kenyon.edu/index.php/Bacterial_Derived_Plastics) [06/19/2013]
19. <http://lipidlibrary.aocs.org/Lipids/pg/file.pdf> [06/23/2013]
20. <http://lipidlibrary.aocs.org/lipids/dpg/index.htm> [06/23/2013]
21. Bowman-James, K., Bianchi, A., Garcia-Espana, E., *Anion Coordination Chemistry*. 2011, Wiley-VCH
22. Meece, F.A., *Studies towards Small-Molecule-Receptors Selective for Phospholipid Anionic Head Groups in Bacterial Membranes, Ph.D. Dissertation*. 2009, Wichita State University: Wichita.
23. Jayasinghe, C. P., *Synthesis and Characterization of Receptors to Bind Anionic Components of Bacterial Membranes, Ph.D. Dissertation*. 2011, Wichita State University: Wichita.
24. Alliband, A., Meece, F. A., Jayasinghe, C., Burns, D. H., *Synthesis and characterization of picket porphyrin receptors that bind phosphatidylglycerol, an anionic phospholipid found in bacterial membranes*. J. Org. Chem., 2013. 78: p. 356-362.
25. Burns, D.H., Calderon-Kawasaki, K., Kularatne, S., J. Org. Chem. 2005. 70: p. 2803-2807.
26. Hynes, M.J., *WinEQNMR. A Program for the calculation of equilibrium constants from NMR chemical shift data* J. Chem.Soc.Dalton Transactions, 1993: p. 311-312.
27. Chan, Ho-Kit, *An Improved Synthesis of exo-[N.M.N.M] Metacyclophanes Using a Novel Copper Catalyst in Chemistry Department*. 2000, Wichita State University: Wichita.
28. Burns, D. H., Miller, J. D., Chan, Ho-Kit, Michael O. Delaney, M. O., *Scope and Utility of a New Soluble Copper Catalyst [CuBr-LiPh-LiBr-THF]: A Comparison with Other Copper Catalysts in Their Ability to Couple One Equivalent of a Grignard Reagent with an Alkyl Sulfonate*. Journal of the American Chemical Society,. 1997. 119: p. 2125-2133.
29. Koralegedara, Manjula, *Synthesis of Charged Receptors Selective for Anionic Components of Bacterial Membranes Ph.D. Dissertation*, 2010, Wichita State University: Wichita.
30. Lindoy, L.F., Meehan, G. V., Svenstrup, N., *Mono- and Diformylation of 4-Substituted Phenols: A New Application of the Duff reaction*. Synthesis, 1998. 7: p. 1029-1032.

- 31 Hudson, R. F., Withey, R. J., *Nucleophilic reactivity. Part VII. The mechanism of hydrolysis of some unsaturated esters of methanesulphonic acid* Journal of the Chemical Society B: Physical Organic 1966, p. 237-240.
32. Wuts, P. G. M., Greene, T. W., *Greene's Protective Groups In Organic Synthesis*, 2007, 4<sup>th</sup> edition, Wiley, New York.
33. Kwak, Jae-Hwan, In, Jin-Kyung, Lee, M., Choi, E., Lee, H., Hong, J. T., Yun, Y., Lee, S. J., Seo, S., Suh, Y., Jung, Jae-Kyung, *Concise Synthesis of Obovatol: Chemoselective ortho-Bromination of Phenol and Survey of Cu-Catalyzed Diaryl Ether Couplings*. Arch Pharm Res., 2008. 31: No 12, p. 1559-1563.
34. Canceill, J., Collet, A., Gabard, J., Gottarelli, G., Spada, G. P. *C3-Cyclotrimeratrylene Derivatives*. Journal of the American Chemical Society, 1985. P. 1299-1308.
35. Chae, J., *Practical Demethylation of ArylMethyl Ethers using an Odorless Thiol Reagent*. Arch. Pharm. Res. 2008. 31: No 3, p. 305-309.
34. Denton, R. M., Scragg, J. T., *A Concise Synthesis of Dunnianol*. Synlett. 2010. No. 4, p. 633-635.
35. Alam, A., *1,3-Dibromo-5,5-dimethylhydantoin*. SynLett, 2005. 15: p. 2403-2403
36. Sakamoto, T., Obsawa, K., *Palladium-catalyzed cyanation of aryl and heteroaryl iodides with copper (I) cyanide*. J. Chem. Soc., Perkin Trans. 1. 1999. P. 2323-2326.
37. Grundl, M. A., Kennedy-Smith, J., Trauner, D., *Rational Design of a Chiral Palladium (0) Olefin Complex of Unprecedented Stability*. Organometallics. 2005. 24: p. 2831-2833.
38. VanRheenen, V., Kelly, R. C., Cha, D. Y., *An improved catalytic OsO<sub>4</sub> oxidation of olefins to cis-1,2-glycols using tertiary amine oxides as the oxidant*. Tetrahedron Letters. 1976, 17: No 23, p. 1973-1976.
39. G. A. Molander, R. Figueroa, *cis-Dihydroxylation of Unsaturated Potassium Alkyl- and Aryltrifluoroborates*. Org. Lett. 2006. 8: p. 75-78
40. Grieco, P. A., Yokoyama, Y., Withers, G. P., Okuniewicz, F. J., Wang, C. L. J., *C-12 substituted prostaglandins: synthesis and biological evaluation of (+-)-12-hydroxyprostaglandin F<sub>2</sub>.alpha. methyl ester*. J. Org. Chem. 1978. 43: No. 21, p. 4178-4182.
41. Caddick, S., Judd, D. B., Lewis, A. K., Reich, M. T., Williams, M. R. V., *A generic approach for the catalytic reduction of nitriles*. Tetrahedron. 2003. 59: p. 5417-5423.
42. Caddick, S., Haynes, A. K., Judd, D. B., Williams, M. R., *Convenient synthesis of protected primary amines from nitriles*. Tetrahedron Letters. 2000. 41: 3513-3516.

43. Shendage, D. M., Frohlich, R., Haufe, G., *Highly Efficient Stereoconservative Amidation and Deamidation of  $\alpha$ -Amino acids*. *Org. Lett.* 2004. 6: No. 21, p. 3675-3678.
44. Armarego, W. L. F., Perrin, D., *Purification of Laboratory Chemicals*. 1996, Butterworth Heinemann.

## APPENDIX

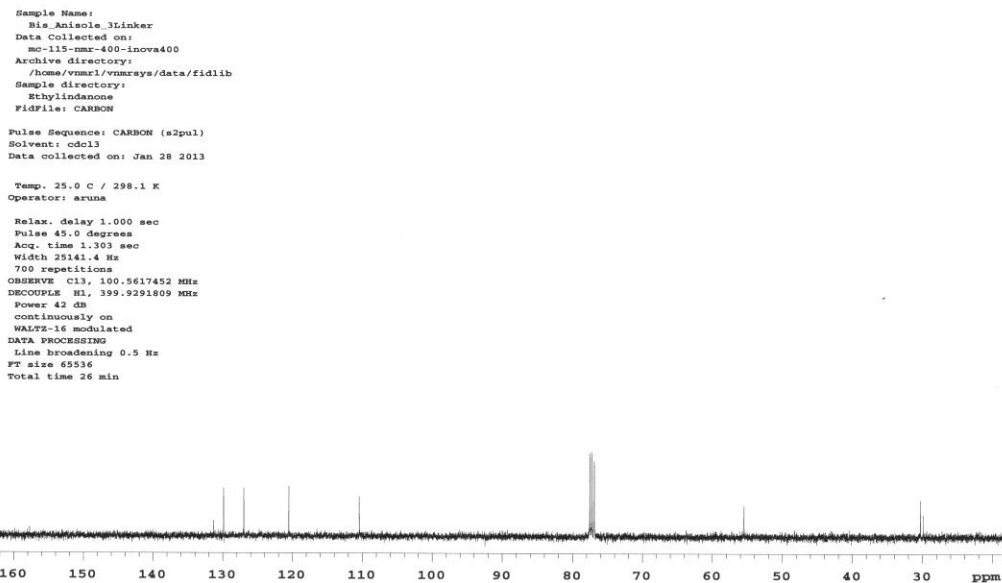
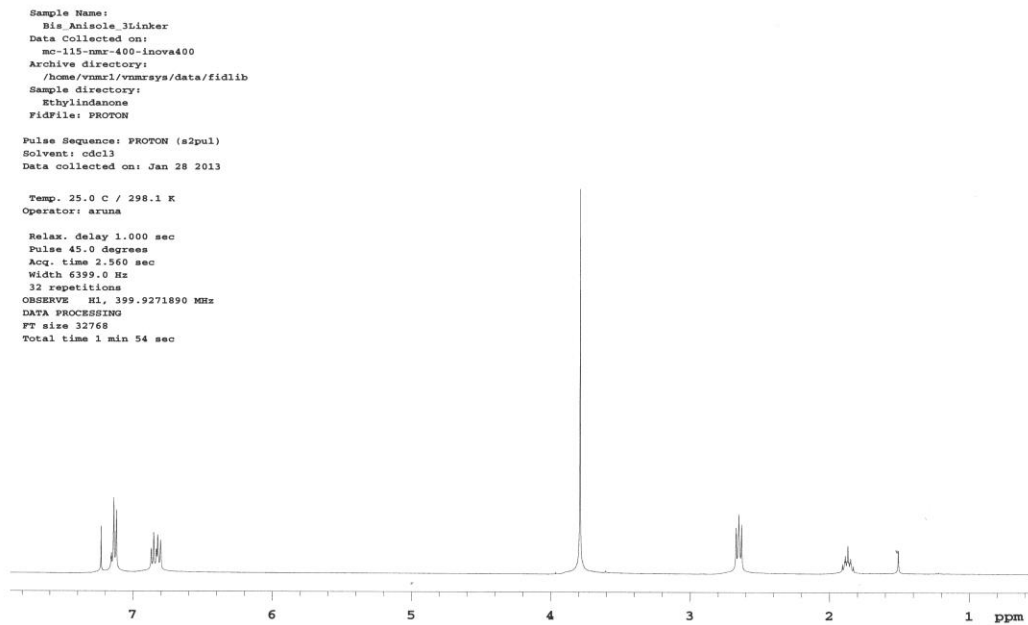
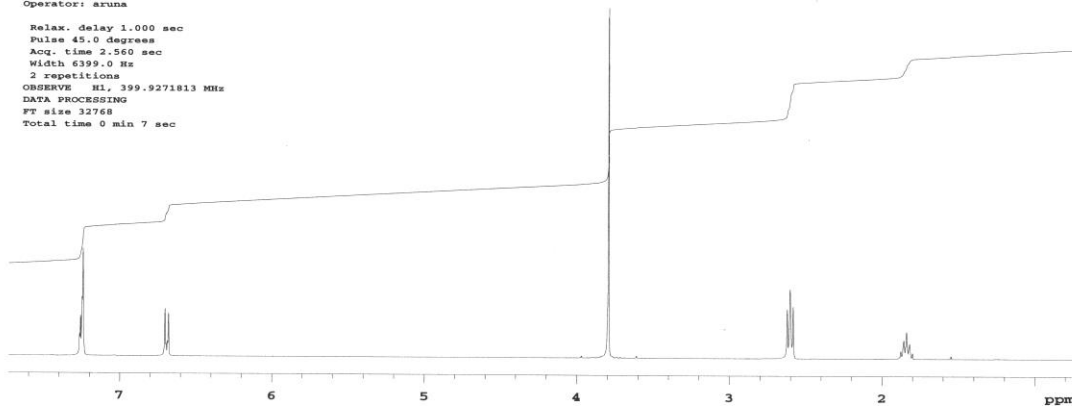


Figure 31.  $^1\text{H}$  NMR (top) and  $^{13}\text{C}$  NMR (bottom) data for compound **6**

Sample Name:  
Bisbromide\_3Linker  
Data Collected on:  
mc-115-nmr-400-inova400  
Archive directory:  
/home/vmrsl/vmrsls/data/fidlib  
Sample directory:  
Ethylindanone  
Fidfile: PROTON  
Pulse Sequence: PROTON (s2pul)  
Solvent: cdcl3  
Data collected on: Feb 11 2013

Operator: aruna

Relax. delay 1.000 sec  
Pulse 45.0 degrees  
Acq. time 2.560 sec  
Width 6399.0 Hz  
2 repetitions  
OBSERVE H1, 399.9271813 MHz  
DATA PROCESSING  
FT size 32768  
Total time 0 min 7 sec



Sample Name:  
Bisbromide\_3Linker  
Data Collected on:  
mc-115-nmr-400-inova400  
Archive directory:  
/home/vmrsl/vmrsls/data/fidlib  
Sample directory:  
Ethylindanone  
Fidfile: CARBON  
Pulse Sequence: CARBON (s2pul)  
Solvent: cdcl3  
Data collected on: Feb 11 2013

Temp. 19.1 C / 292.2 K  
Operator: aruna

Relax. delay 1.000 sec  
Pulse 45.0 degrees  
Acq. time 1.303 sec  
Width 25141.4 Hz  
130 repetitions  
OBSERVE C13, 100.5617498 MHz  
DECOUPLE H1, 399.9291809 MHz  
Power 42 dB  
continuously on  
WALTZ-16 modulated  
DATA PROCESSING  
Line broadening 0.5 Hz  
FT size 65536  
Total time 642 hr, 16 min

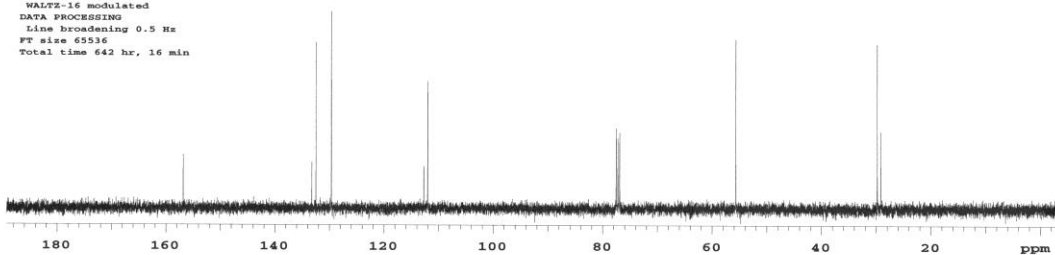


Figure 32.  $^1\text{H}$  NMR (top) and  $^{13}\text{C}$  NMR (bottom) data for compound 7

STANDARD 1H OBSERVE

Pulse Sequence: s2pu1  
Solvent: CDCl3  
Ambient temperature  
Mercury-300BS "nu300"

Relax. delay 1.000 sec  
Pulse 75.7 degree  
Acq. time 1.995 sec  
Width 4596.5 Hz  
16 repetitions  
OBSERVE H1, 300.1452509 MHz  
DATA PROCESSING  
FT size 32768  
Total time 0 min, 49 sec

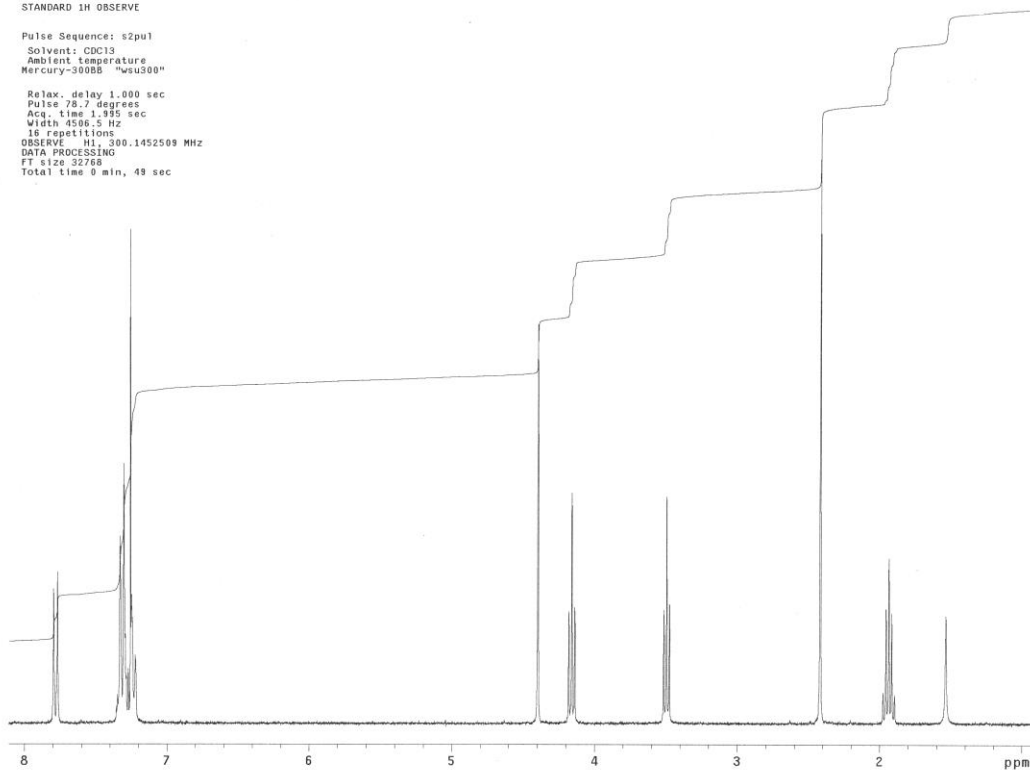


Figure 33. <sup>1</sup>H NMR data for compound 9

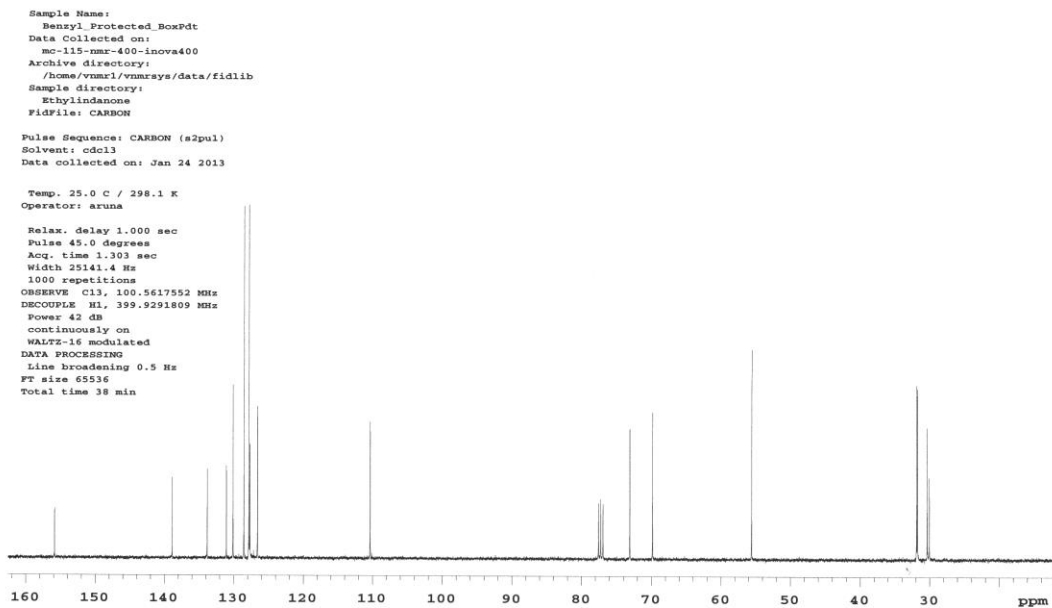
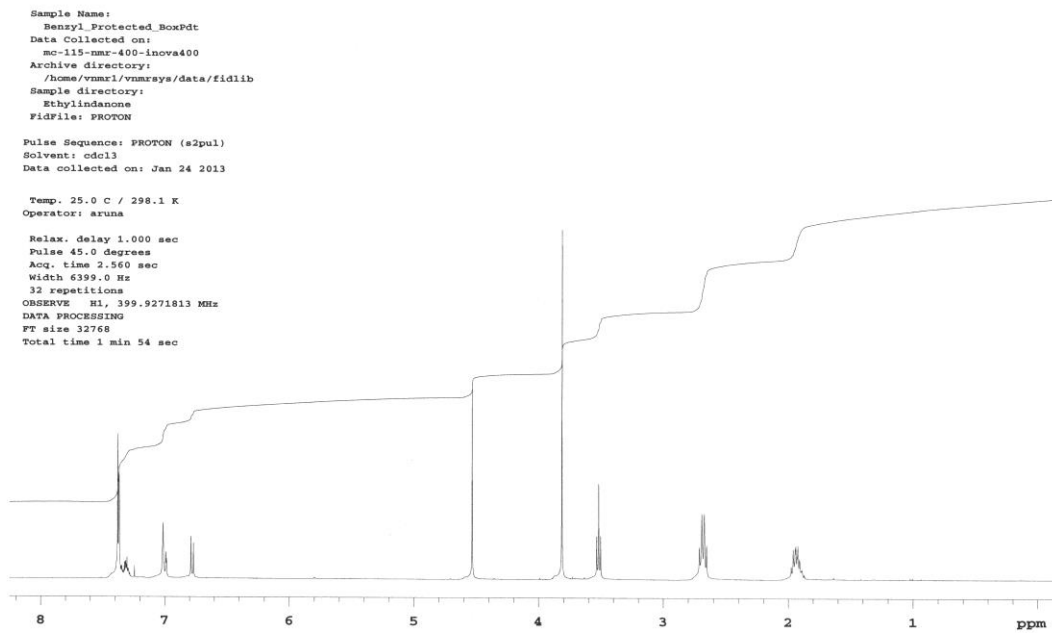


Figure 34.  $^1\text{H}$  NMR (top) and  $^{13}\text{C}$  NMR (bottom) data for compound **10**

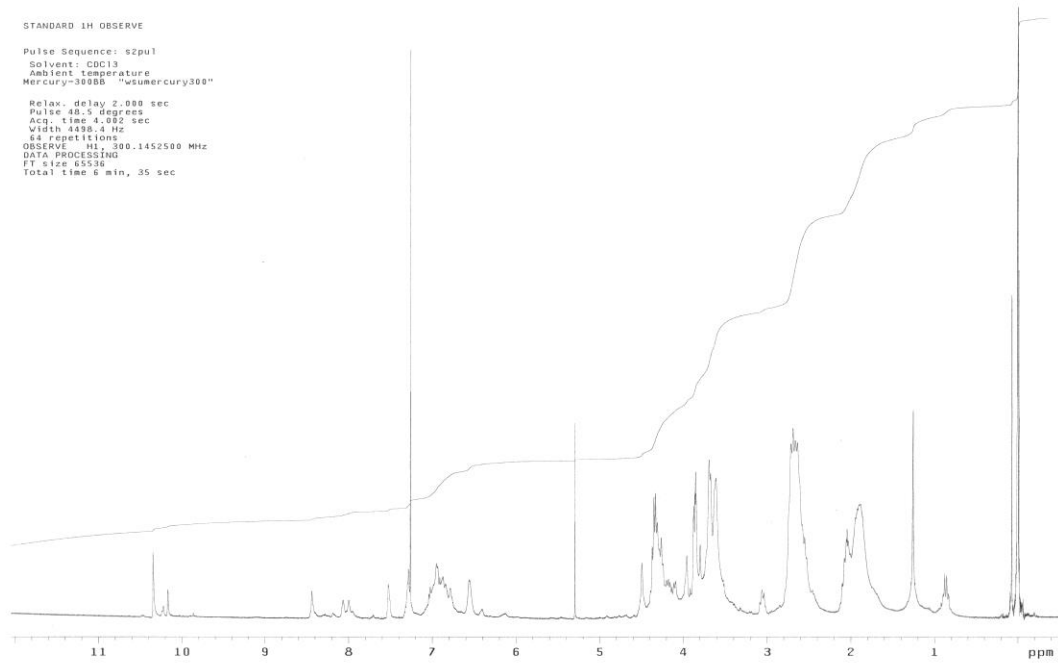


Figure 35.  $^1\text{H}$  NMR data for compound **12**

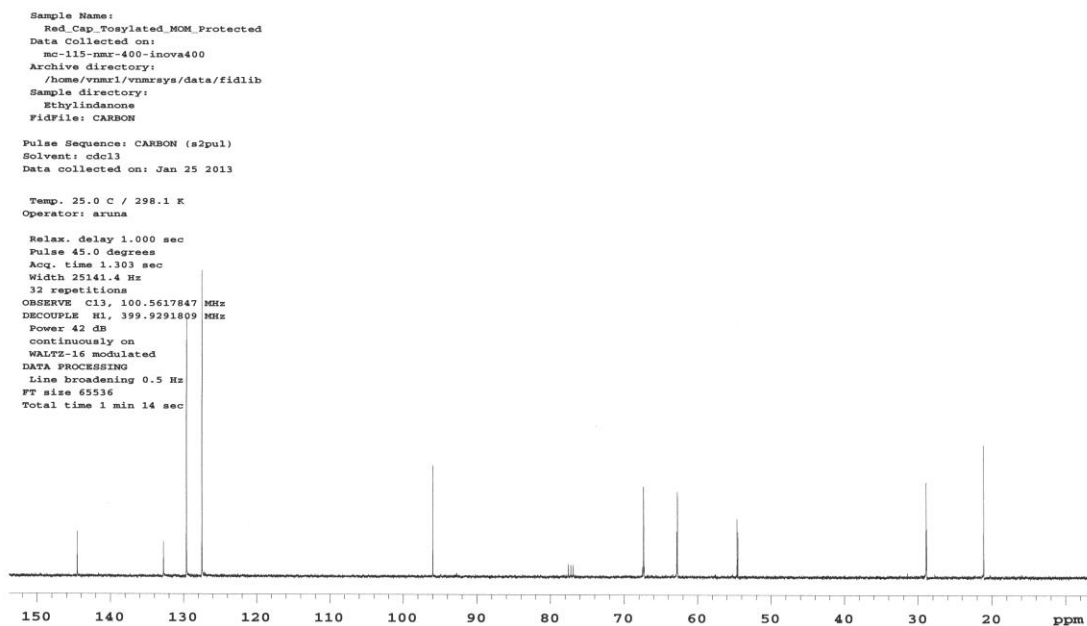
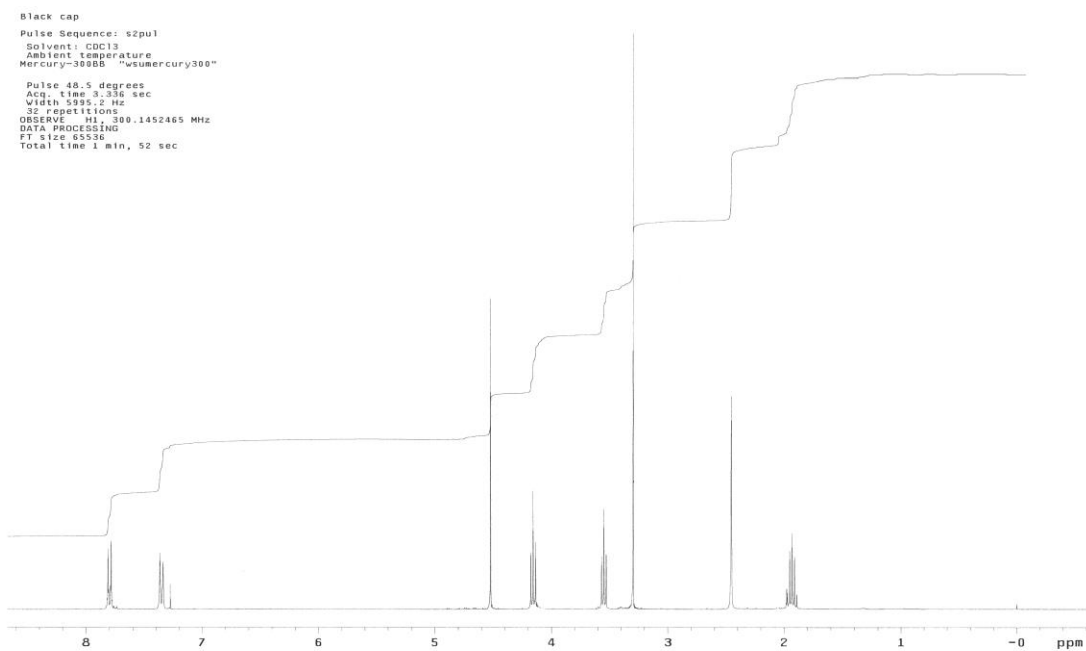


Figure 36.  $^1\text{H}$  NMR (top) and  $^{13}\text{C}$  NMR (bottom) data for compound **15**

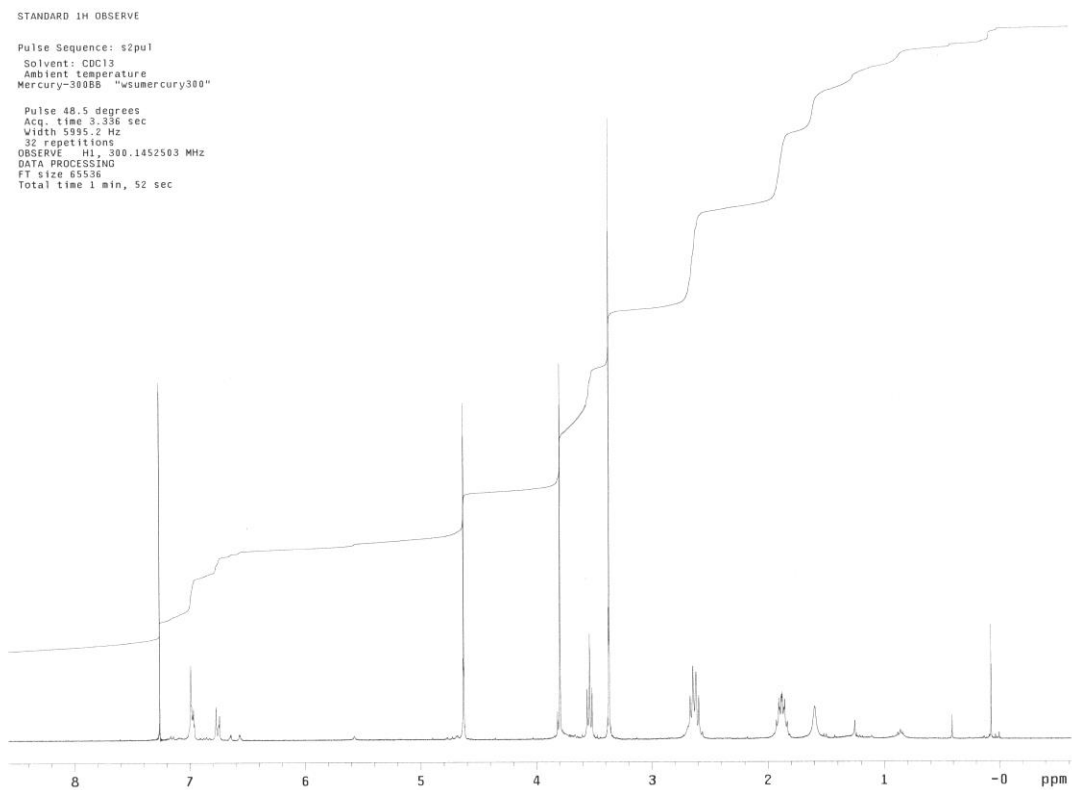


Figure 37. <sup>1</sup>H NMR data for compound **16**

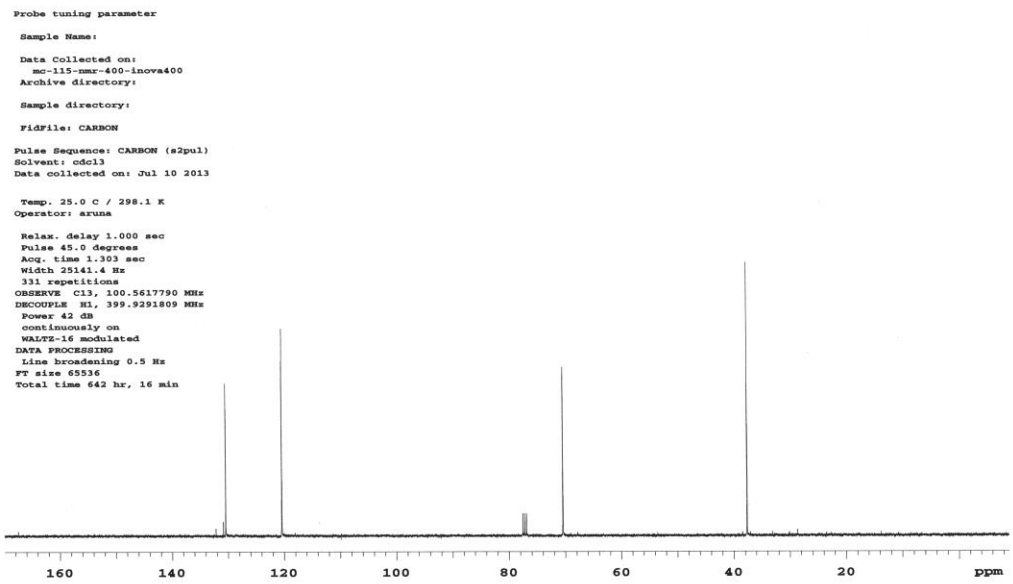
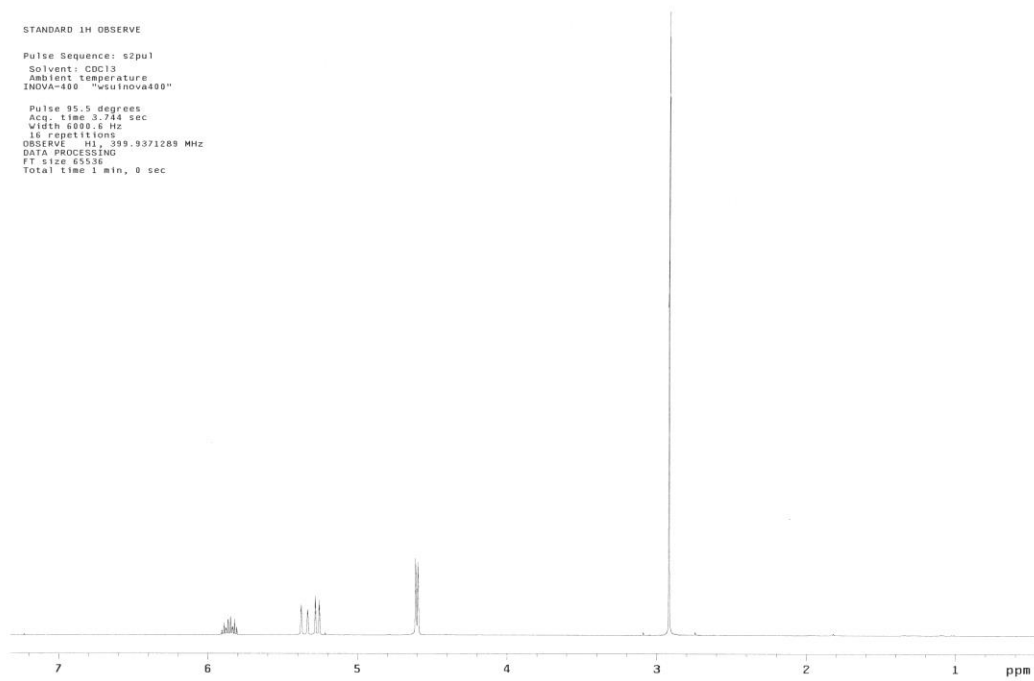


Figure 38.  $^1\text{H}$  NMR (top) and  $^{13}\text{C}$  NMR (bottom) data for compound **18**

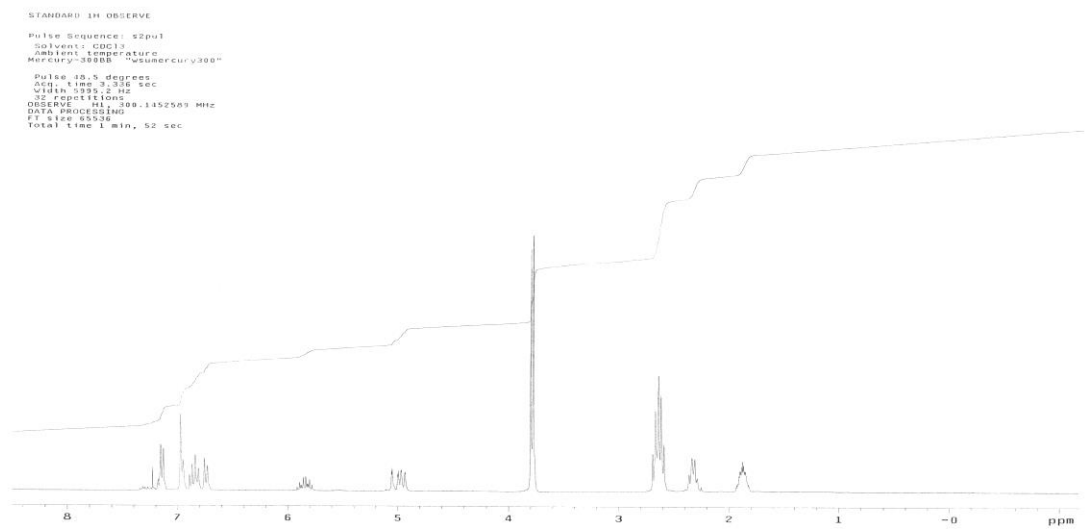


Figure 39. <sup>1</sup>H NMR data for compounds **19a** and **19b**

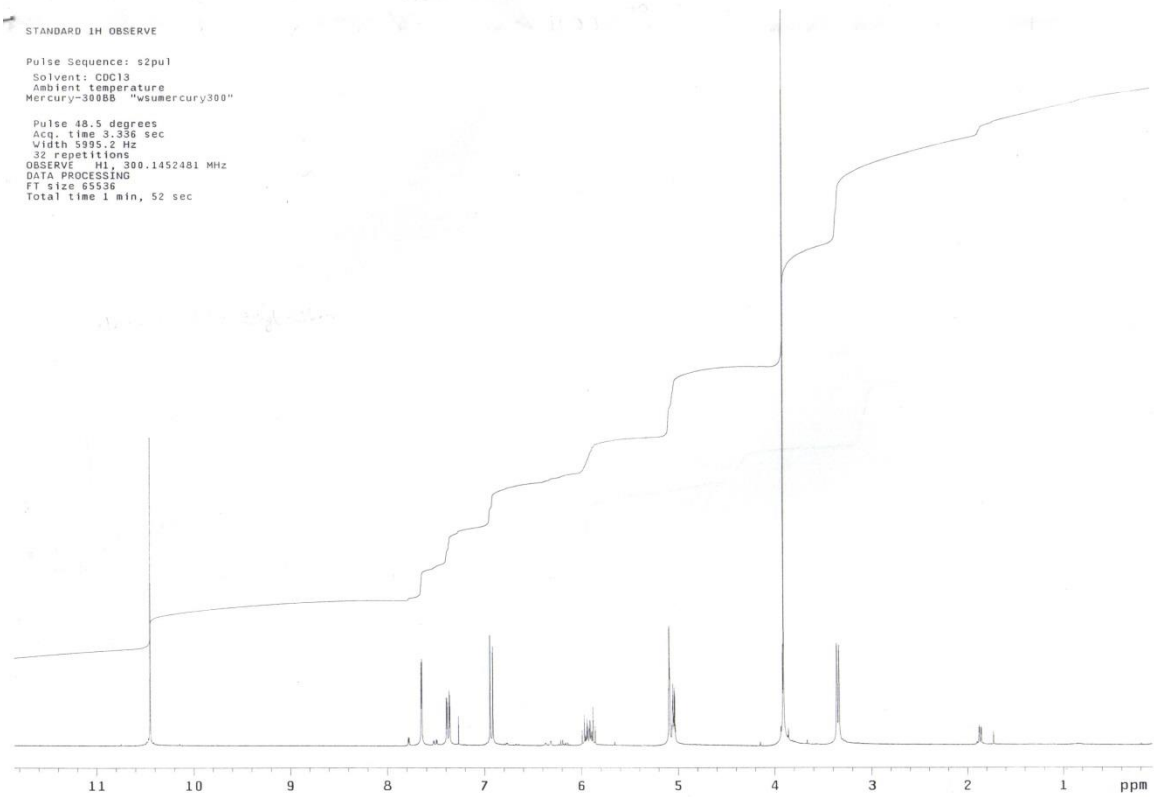


Figure 40.  $^1\text{H}$  NMR data for 5-allyl-2-methoxybenzaldehyde

Spectrum Plot - 5/2/2008 12:44 PM

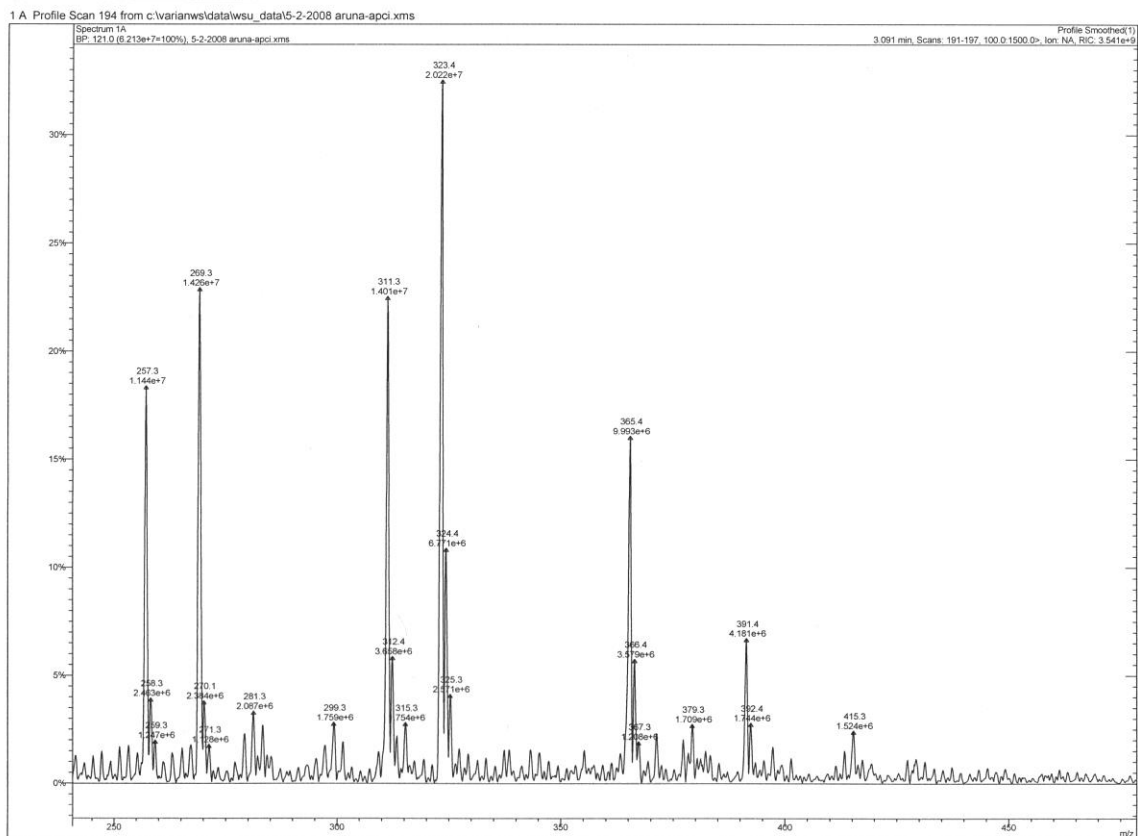


Figure 41. ESI-MS data for compound 20

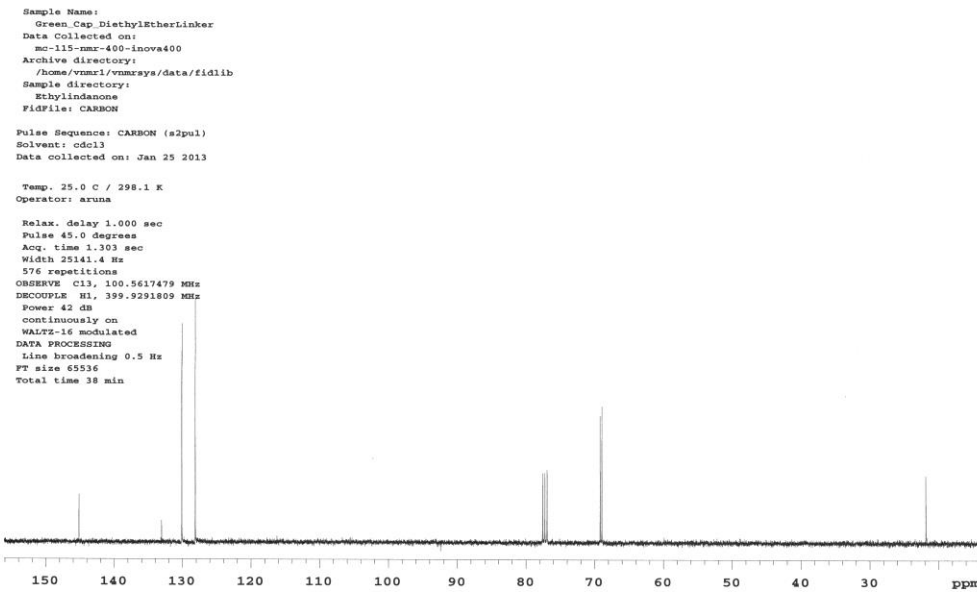
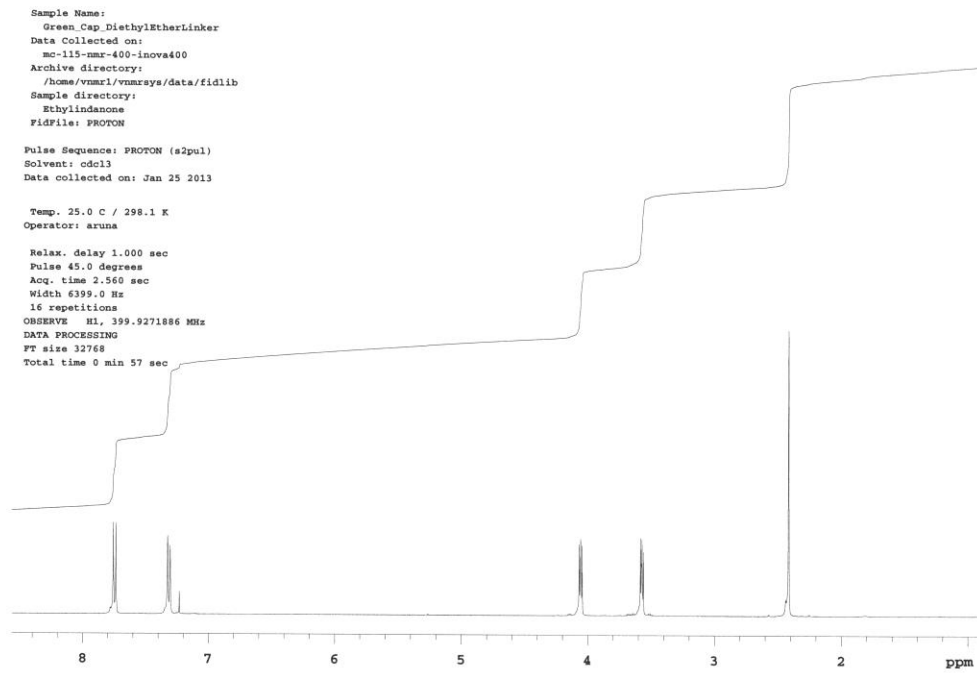


Figure 42.  $^1\text{H}$  NMR (top) and  $^{13}\text{C}$  NMR (bottom) data for compound **21**

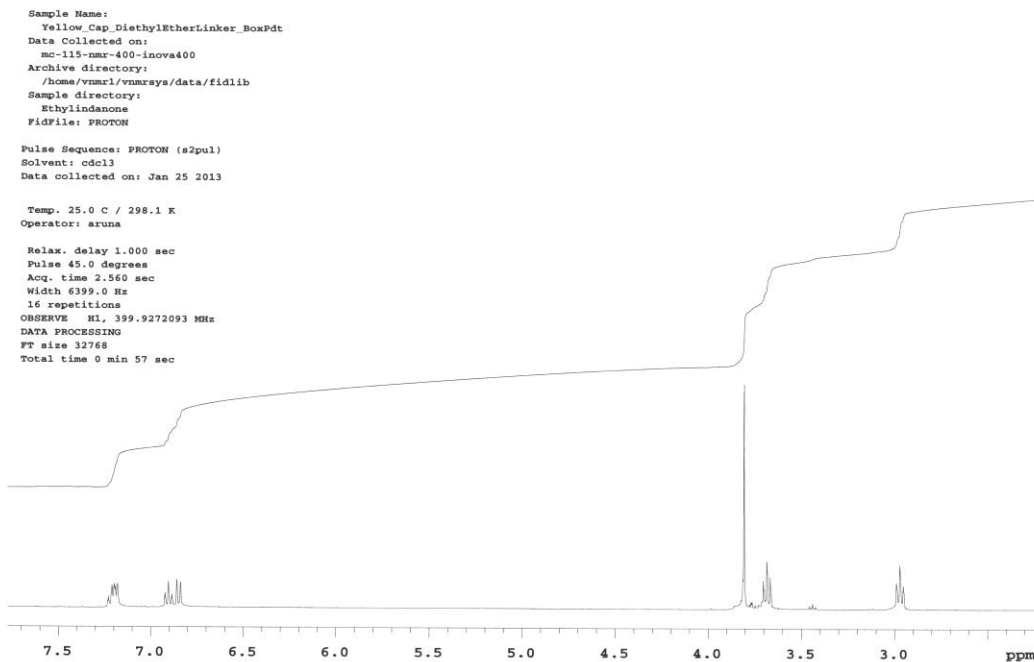


Figure 43.  $^1\text{H}$  NMR data for compound **22**

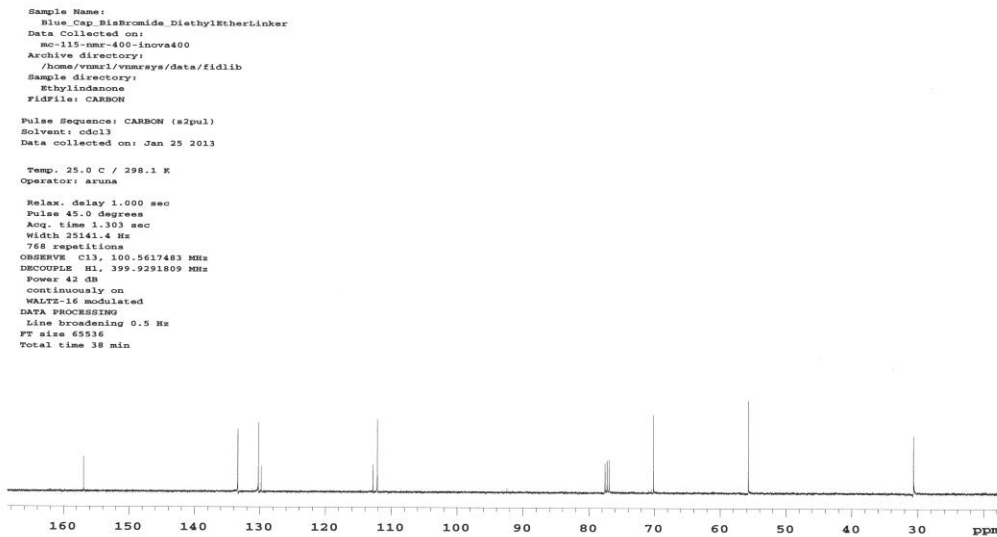
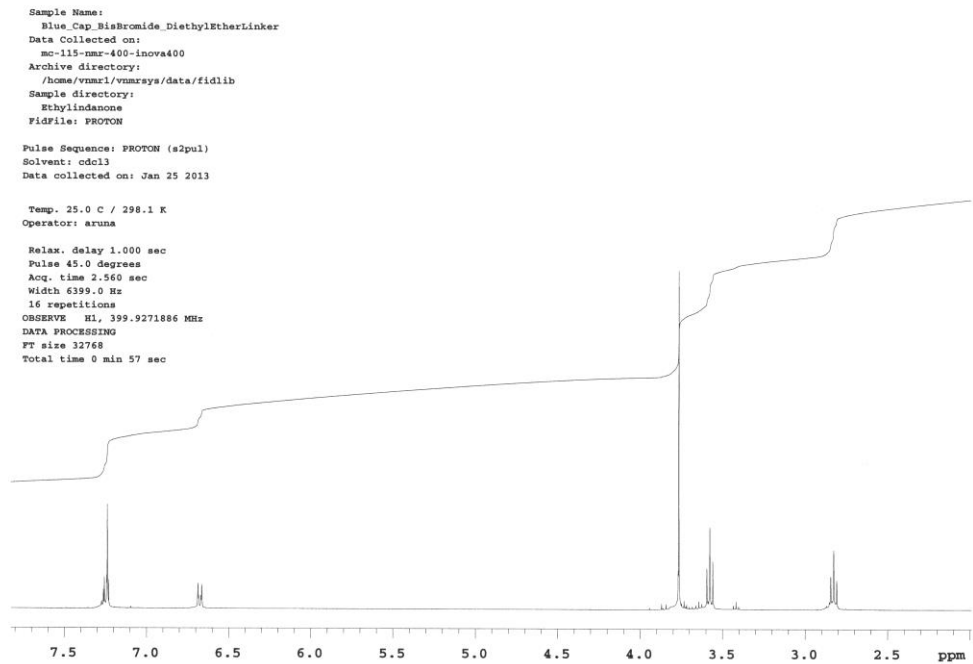
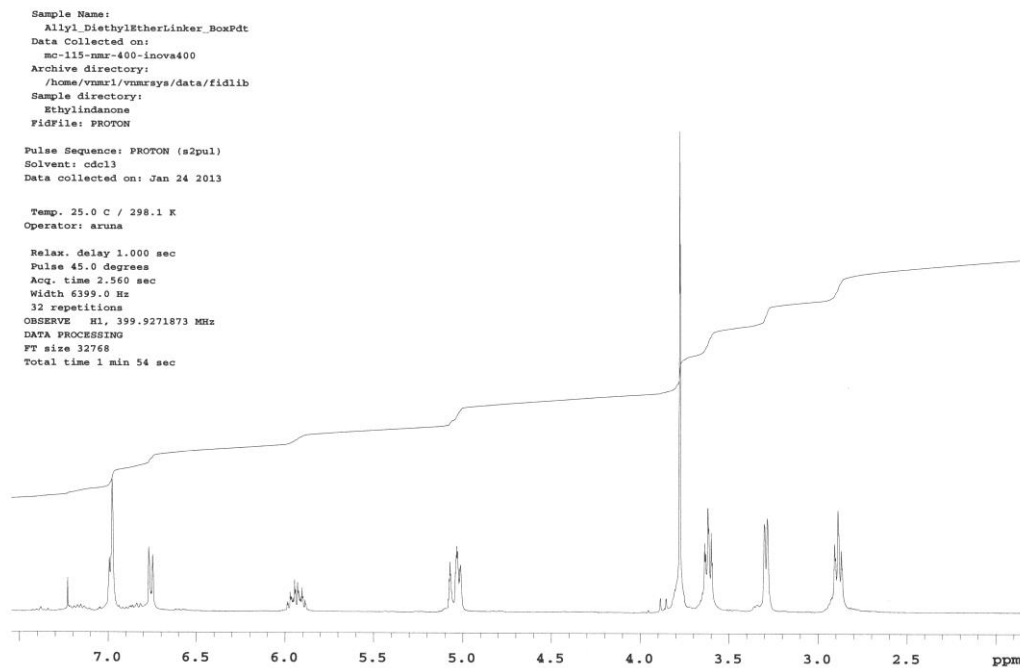


Figure 44.  $^1\text{H}$  NMR (top) and  $^{13}\text{C}$  NMR (bottom) data for compound **23**

blue cap



Sample Name:  
Allyl\_DiethylEtherLinker\_BoxPdt  
Data Collected on:  
mc-115-nmr-400-inova400  
Archive directory:  
/home/vmr1/vnmrsvs/data/fidlib  
Sample directory:  
Ethylindanone  
FidFile: CARBON

Pulse Sequence: CARBON (s2pul)  
Solvent: cdcl3  
Data collected on: Jan 24 2013

Temp. 25.0 C / 298.1 K  
Operator: aruna

Relax. delay 1.000 sec  
Pulse 45.0 degrees  
Acq. time 1.303 sec  
Width 25141.4 Hz  
896 repetitions  
OBSERVE C13, 100.5617499 MHz  
DECOUPLE H1, 399.9291809 MHz  
Power 42 dB  
continuously on  
WALTZ-16 modulated  
DATA PROCESSING  
Line broadening 0.5 Hz  
FT size 65536  
Total time 38 min

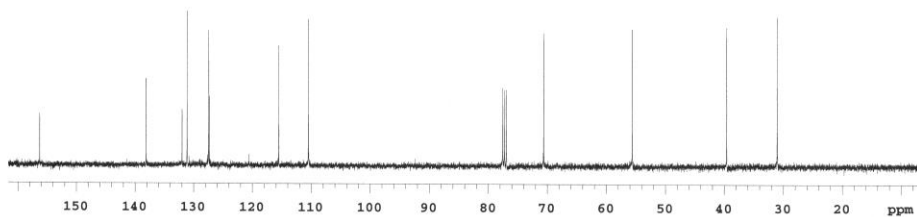


Figure 45.  $^1\text{H}$  NMR (top) and  $^{13}\text{C}$  NMR (bottom) data for compound **24**

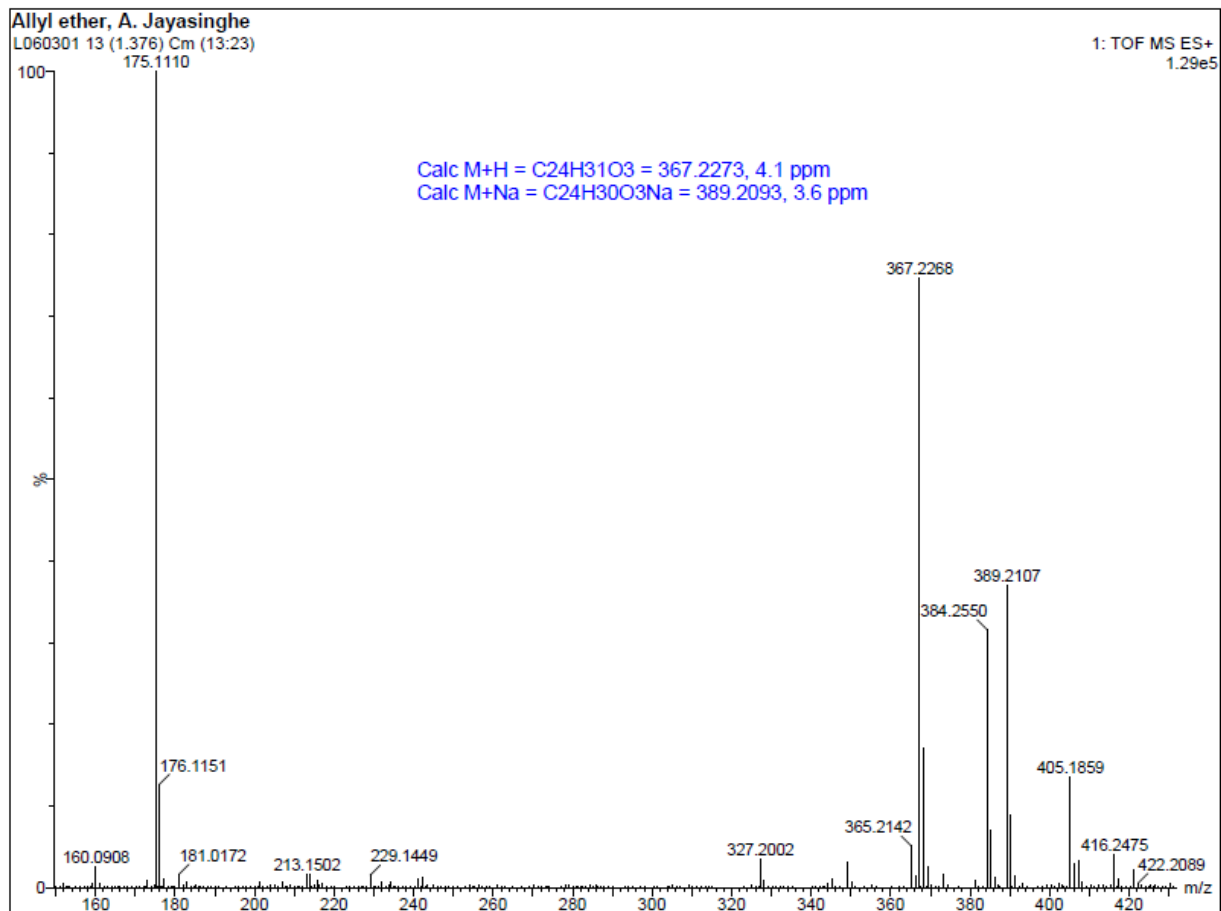


Figure 46. HRMS data for compound **24**

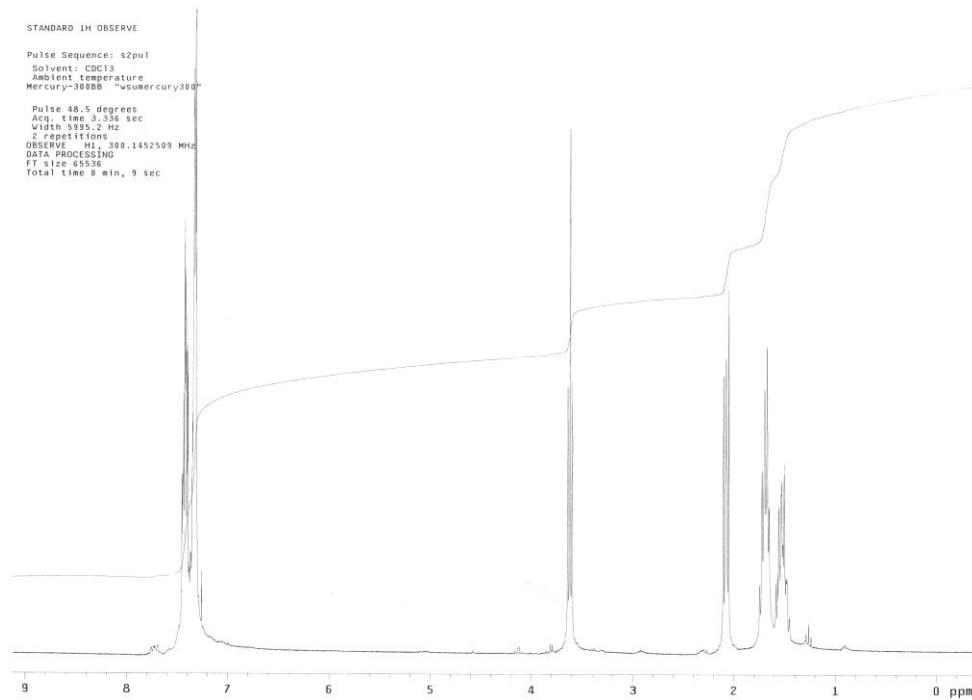


Figure 47.  $^1\text{H}$  NMR data for compound **26**

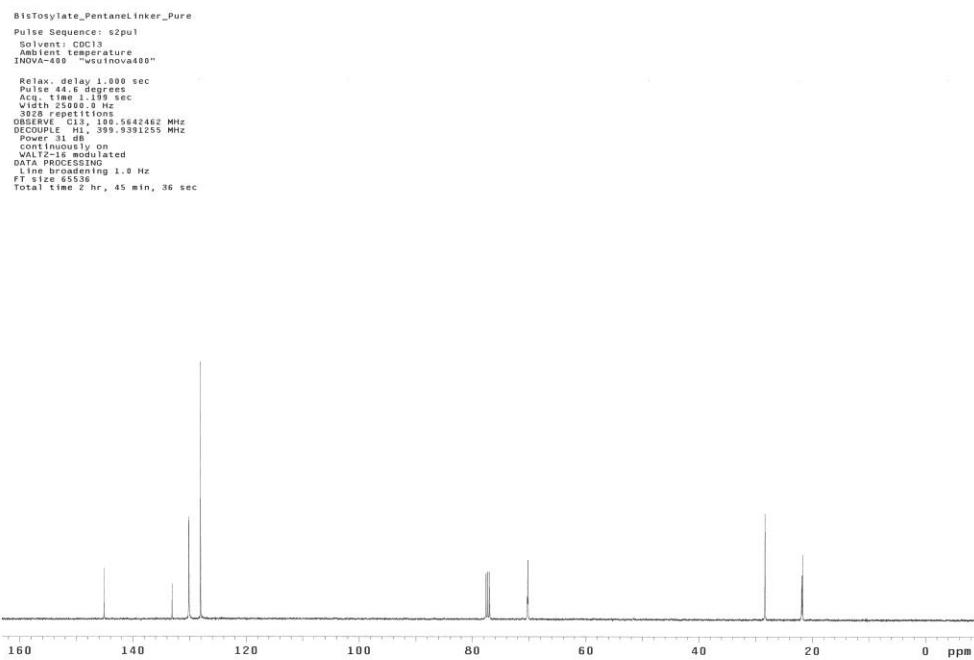
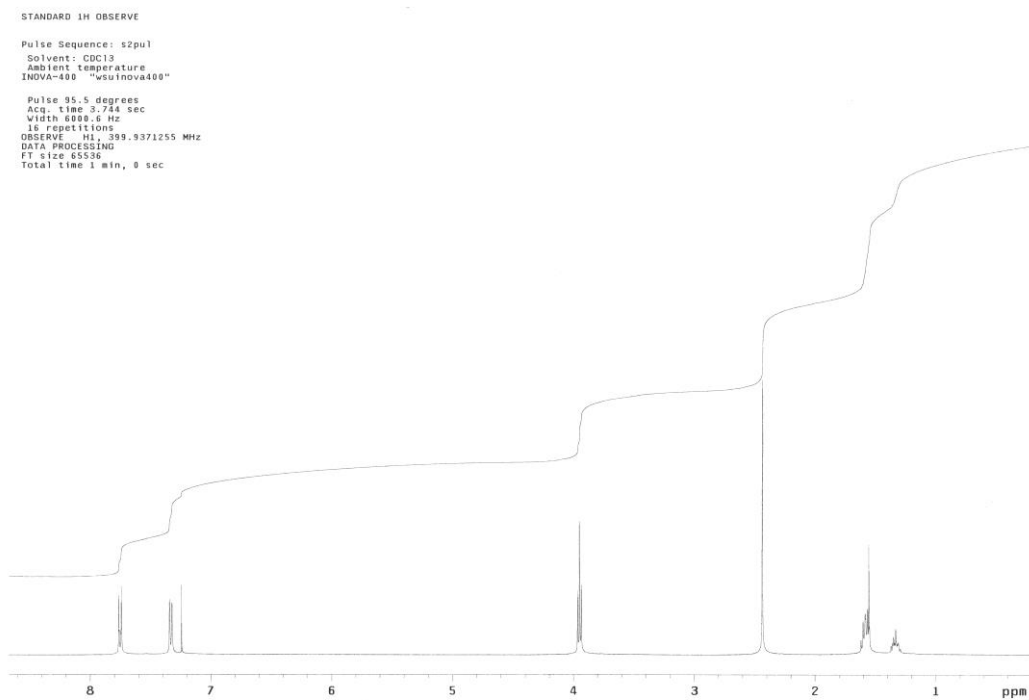


Figure 48.  $^1\text{H}$  NMR (top) and  $^{13}\text{C}$  NMR (bottom) data for compound **27**

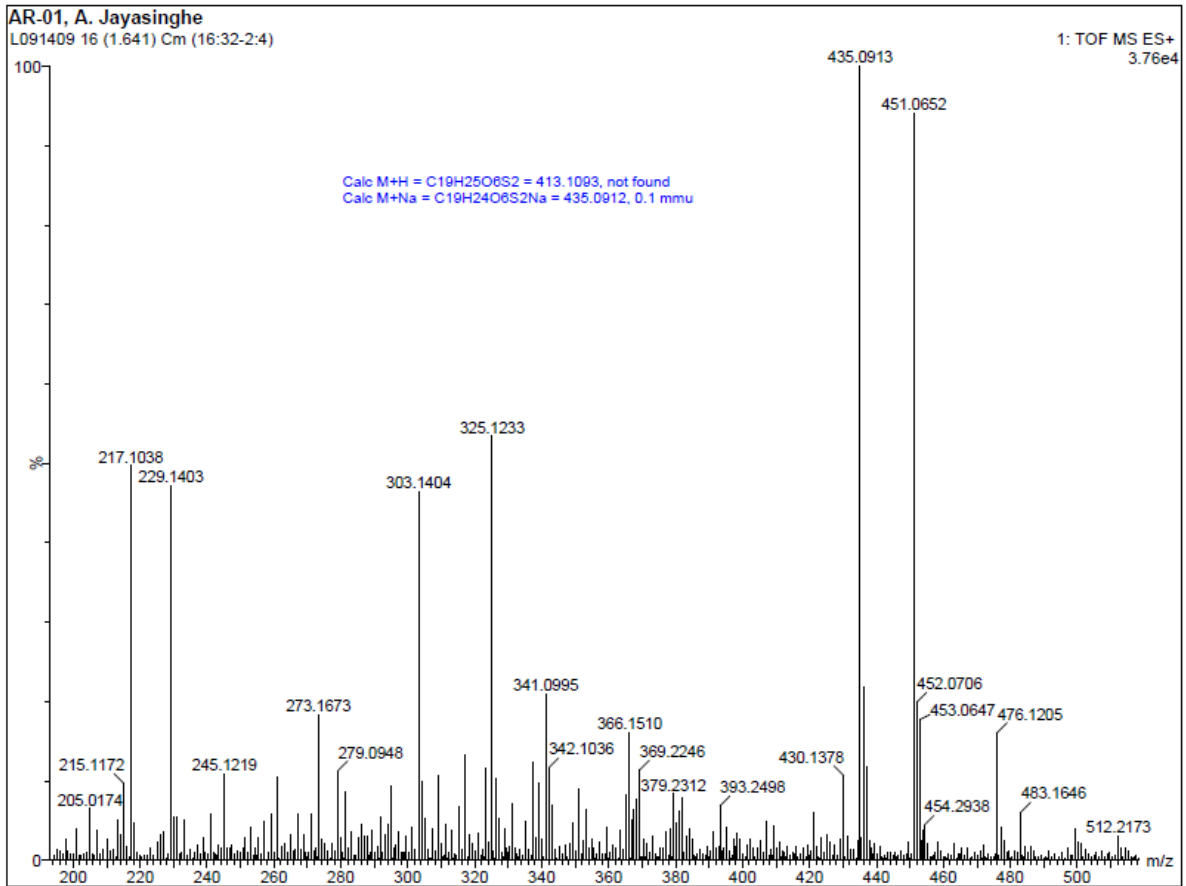


Figure 49. HSMS data for compound **27**

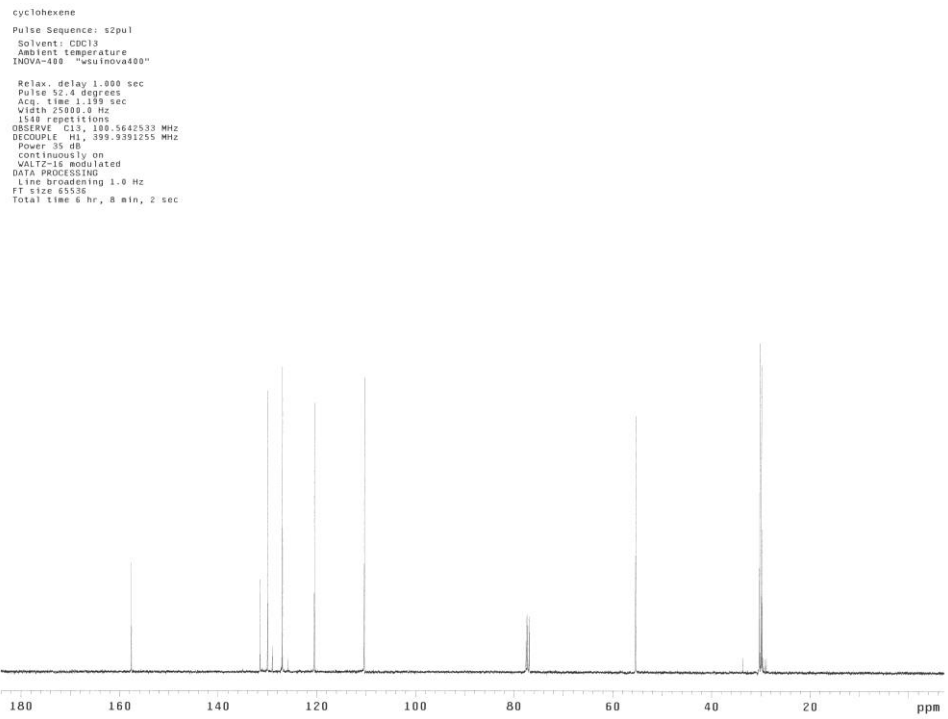
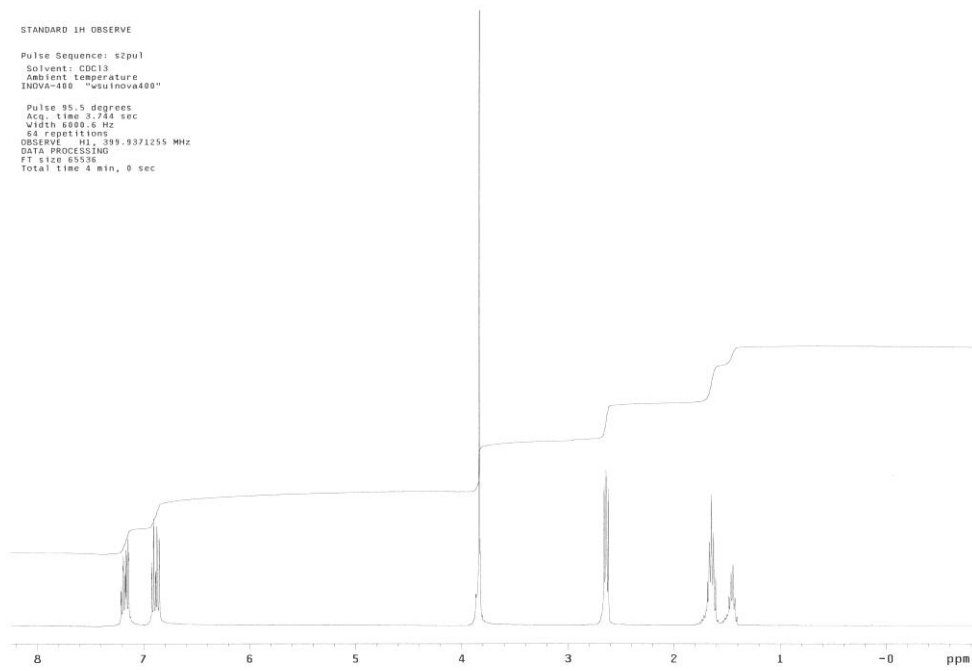
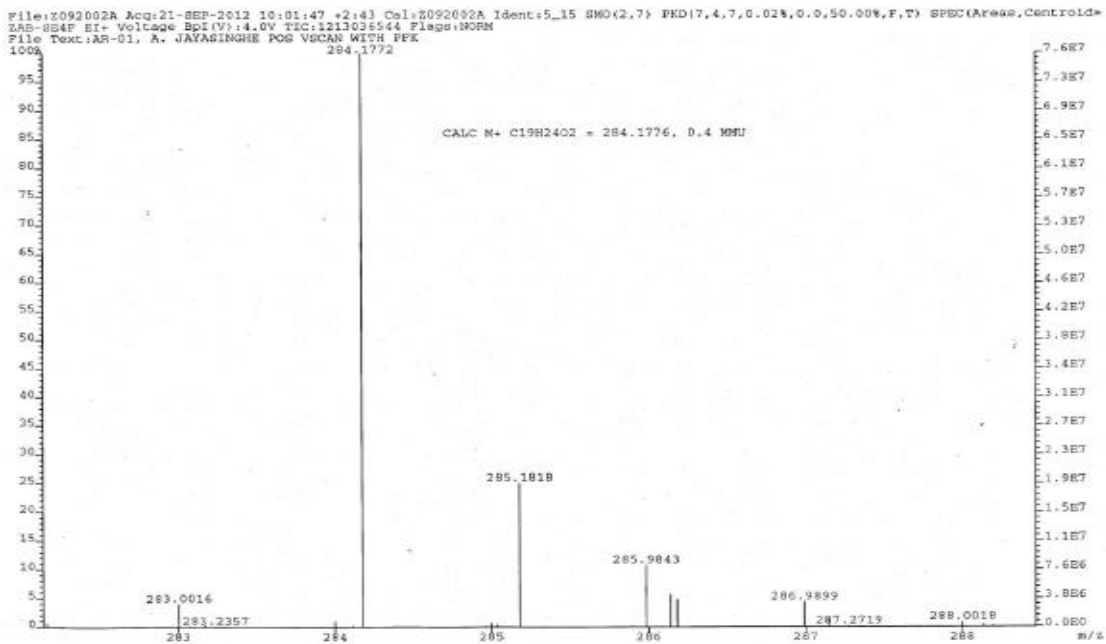


Figure 50. <sup>1</sup>H NMR (top) and <sup>13</sup>C NMR (bottom) data for compound **28**



Print Date: 09 May 2012 17:48:09

Spectrum Plot - 5/9/2012 5:48 PM

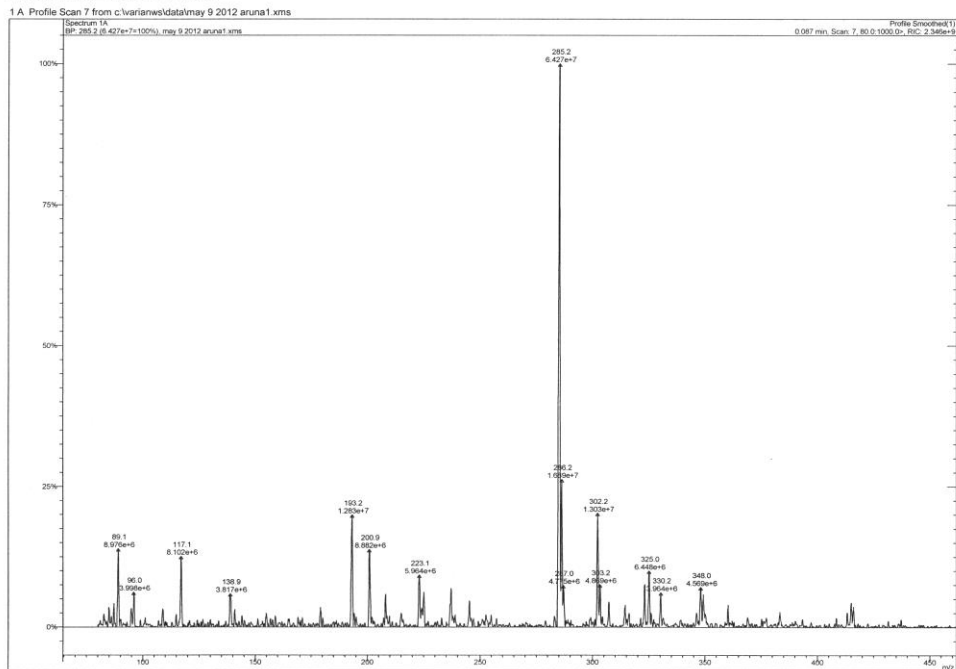


Figure 51. HSMS (top) and ESI-MS (bottom) data for compound **28**

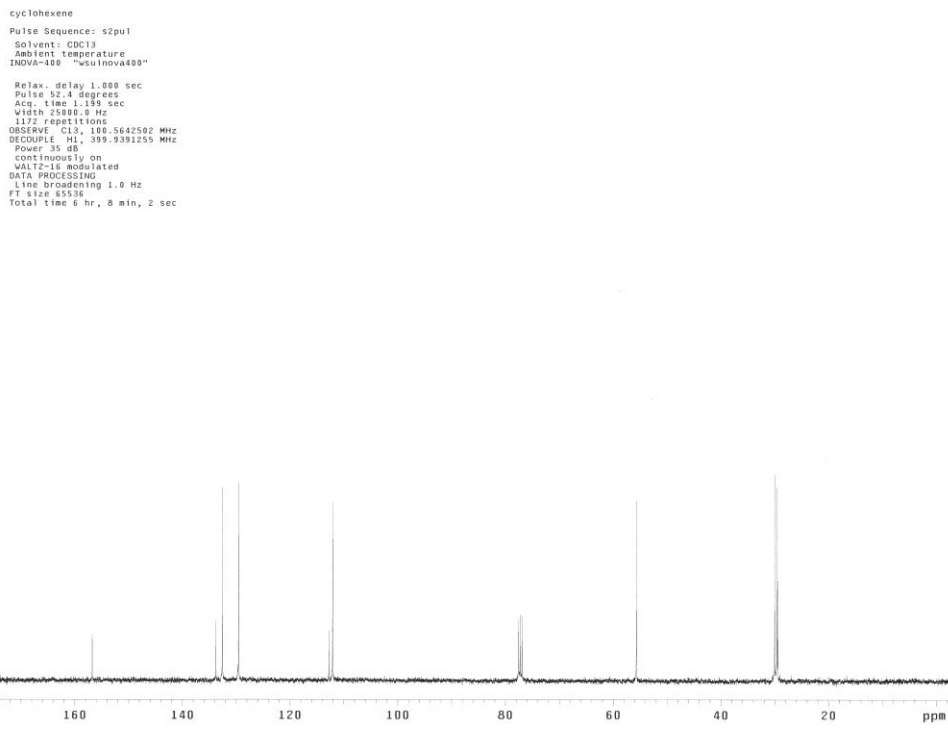
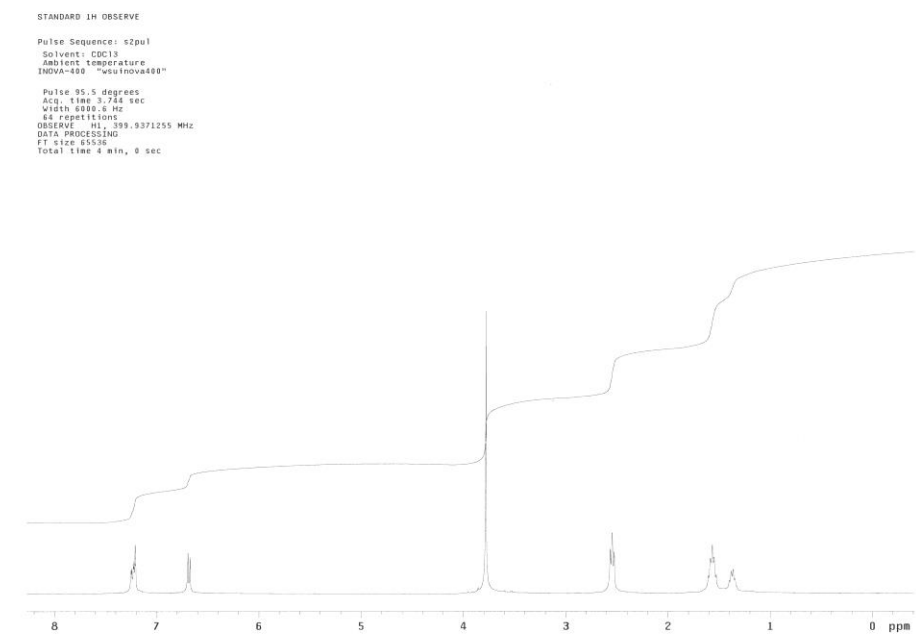


Figure 52.  $^1\text{H}$  NMR (top) and  $^{13}\text{C}$  NMR (bottom) data for compound **29**

File: 2092007 Acq: 21-SEP-2012 10:44:59 \*2:54 Cal: 2092007 Ident: 10\_16 SMO(2,5) PKD(S,3,5,0.02%,0.0,50.00%,P,T) SPEC(Areas, Centroid)\*  
ZAP-SEAP EI+ Voltage Bp(V): 350.0eV TIC: 602087360 Flags: NORM  
File Text: AR-02, A. JAYASINGHE FOB VSCAN WITH PFK

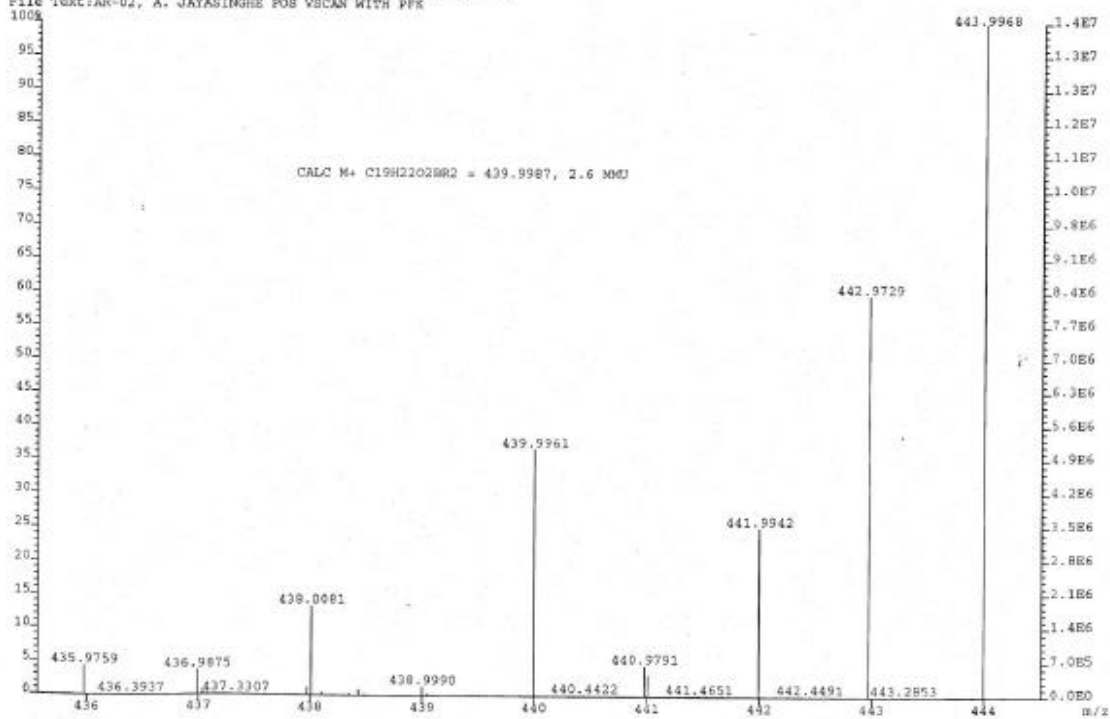
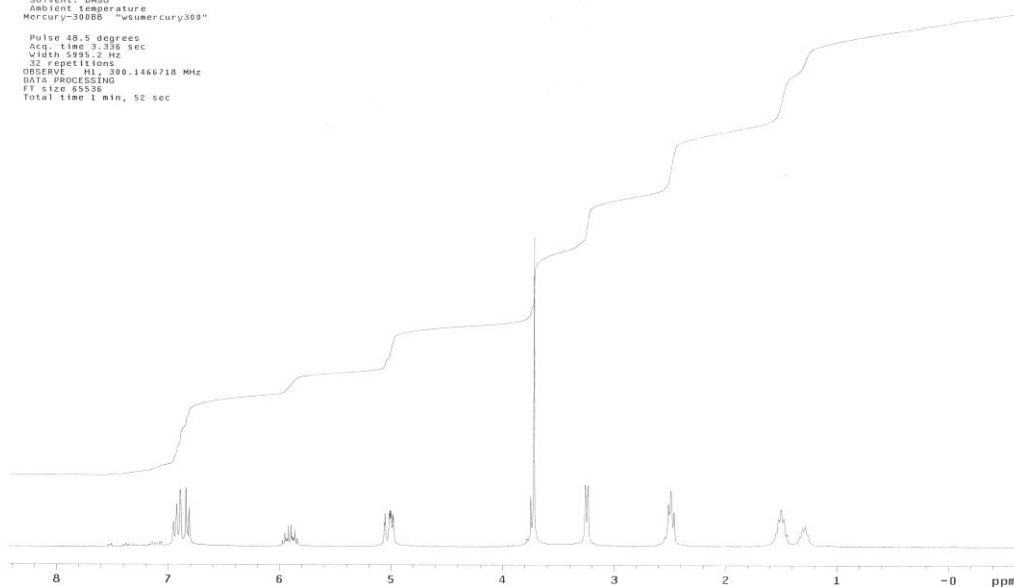


Figure 53. HSMS data for compound 29

STANDARD 1H OBSERVE  
Pulse Sequence: s2pu1  
Solvent: DMSO  
Ambient temperature  
Mercury-300BB "wsmcury300"  
Pulse 48.5 degrees  
Acq. time 2.326 sec  
Width 5995.2 Hz  
32 repetitions  
OBSERVE H1, 300.1466718 MHz  
DATA PROCESSING  
F1 size 65536  
Total time 1 min, 52 sec



cyclohexene  
Pulse Sequence: s2pu1  
Solvent: CDCl3  
Ambient temperature  
INNOVA-400 "wsiInova400"  
Relax. delay 1.000 sec  
Pulse 52.4 degrees  
Acq. time 1.199 sec  
Width 25000.0 Hz  
1280 repetitions  
OBSERVE C13, 100.62699 MHz  
DECOUPLE H1, 399.9391255 MHz  
Power 35 dB  
continuously on  
WALTZ-16 modulated  
DATA PROCESSING  
Line broadening 1.0 Hz  
F1 size 85536  
Total time 6 hr, 8 min, 2 sec

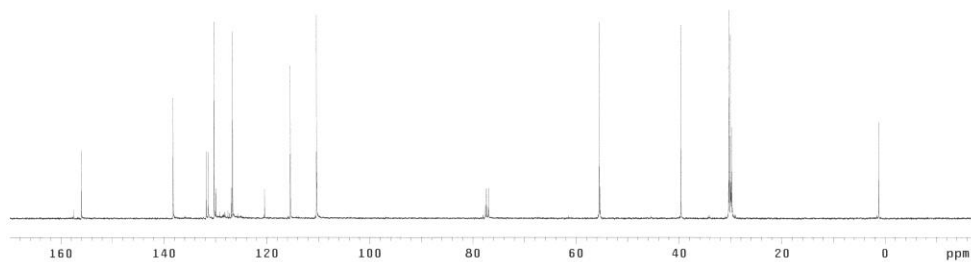


Figure 54.  $^1\text{H}$  NMR (top) and  $^{13}\text{C}$  NMR (bottom) data for compound **30**

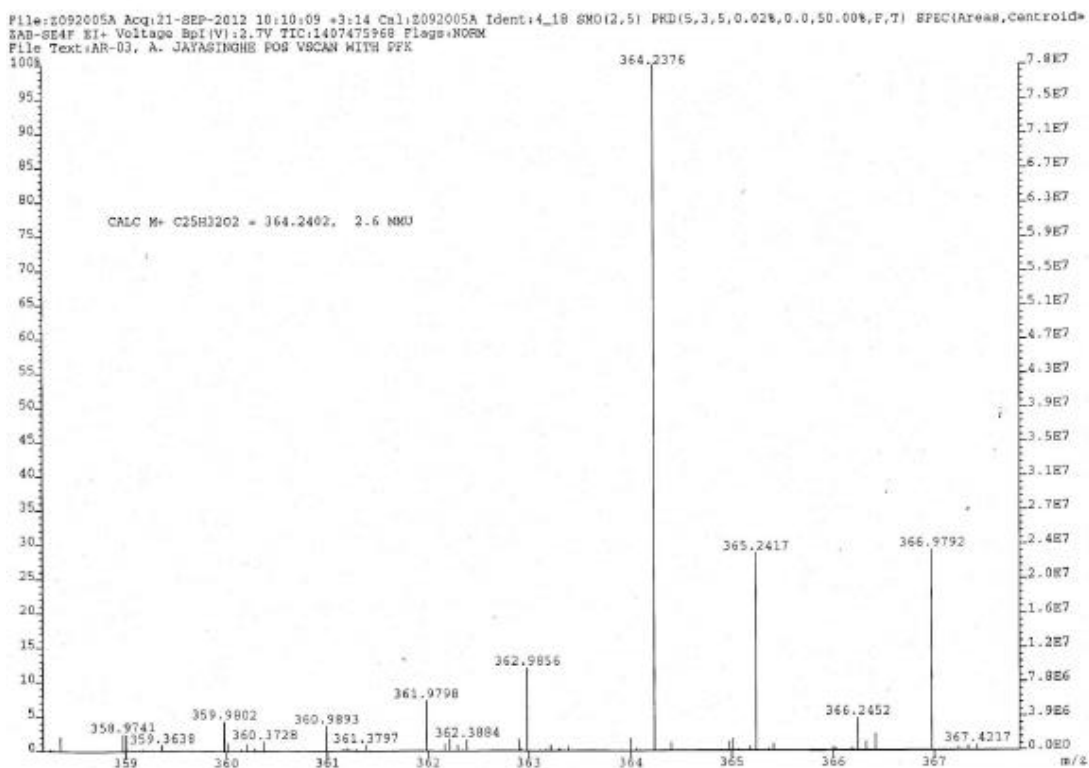
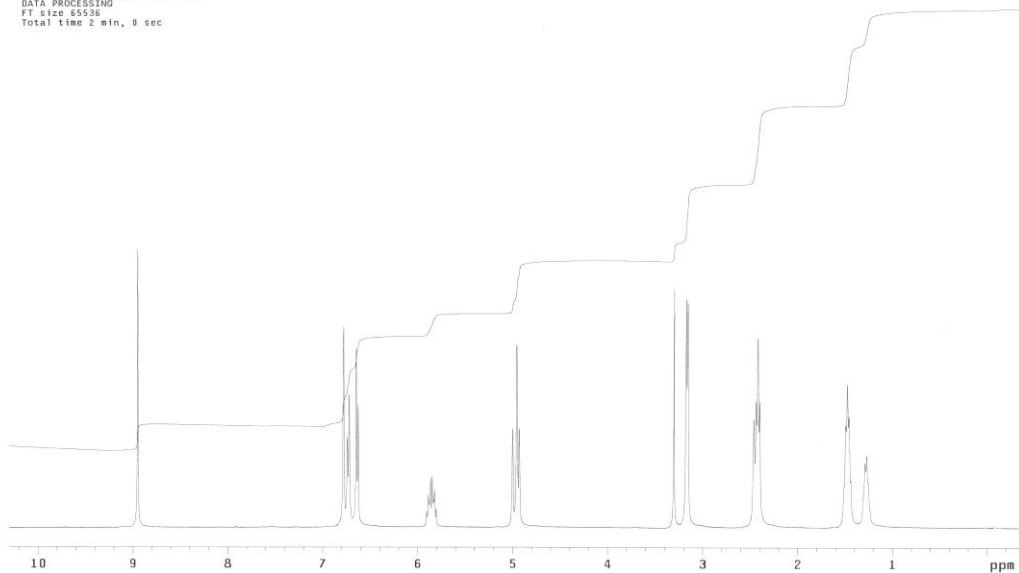


Figure 55. HSMS data for compound **30**

STANDARD 1H OBSERVE

Pulse Sequence: s2pu1  
Solvent: DMSO  
Ambient temperature  
INDVA-400 "gwinova400"  
Pulse 35.5 degrees  
Acq. time 3.714 sec  
Width 6000.6 Hz  
32 repetitions  
OBSERVE H1, 399.9390252 MHz  
DATA PROCESSING  
FT size 65536  
Total time 2 min, 0 sec



cyclohexene  
Pulse Sequence: s2pu1  
Solvent: DMSO  
Ambient temperature  
INDVA-400 "gwinova400"  
Relax. delay 1.000 sec  
Pulse 52.4 degrees  
Acq. time 1.350 sec  
Width 25000.0 Hz  
2616 repetitions  
OBSERVE C13, 100.5647912 MHz  
DECUPLE H1, 399.9390252 MHz  
Power 35 dB  
continuously on  
VALTZ-16 modulated  
DATA PROCESSING  
Line broadening 1.0 Hz  
FT size 65536  
Total time 12 hr, 16 min, 4 sec

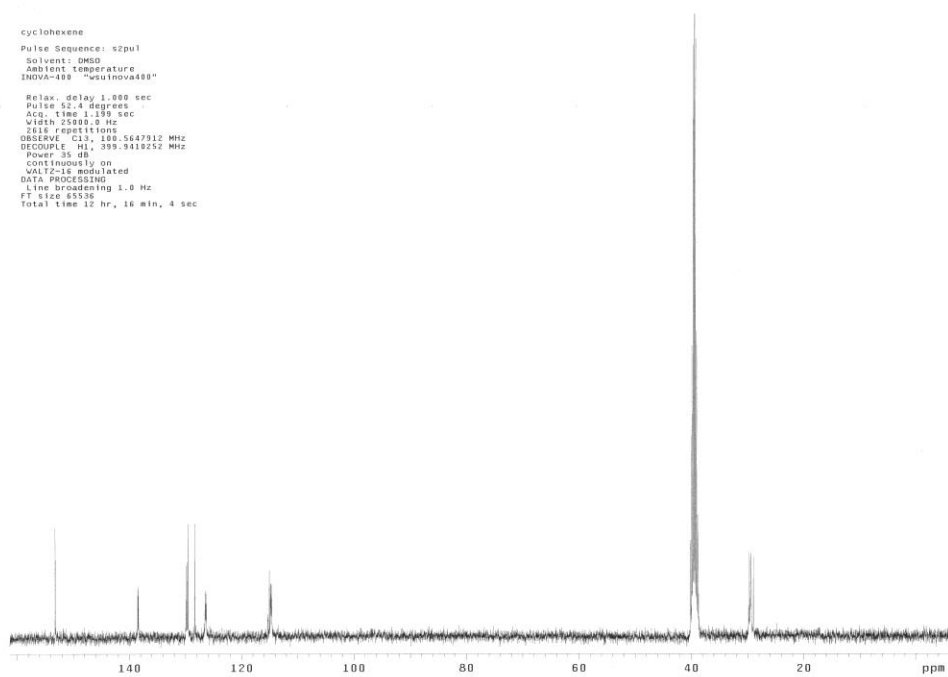
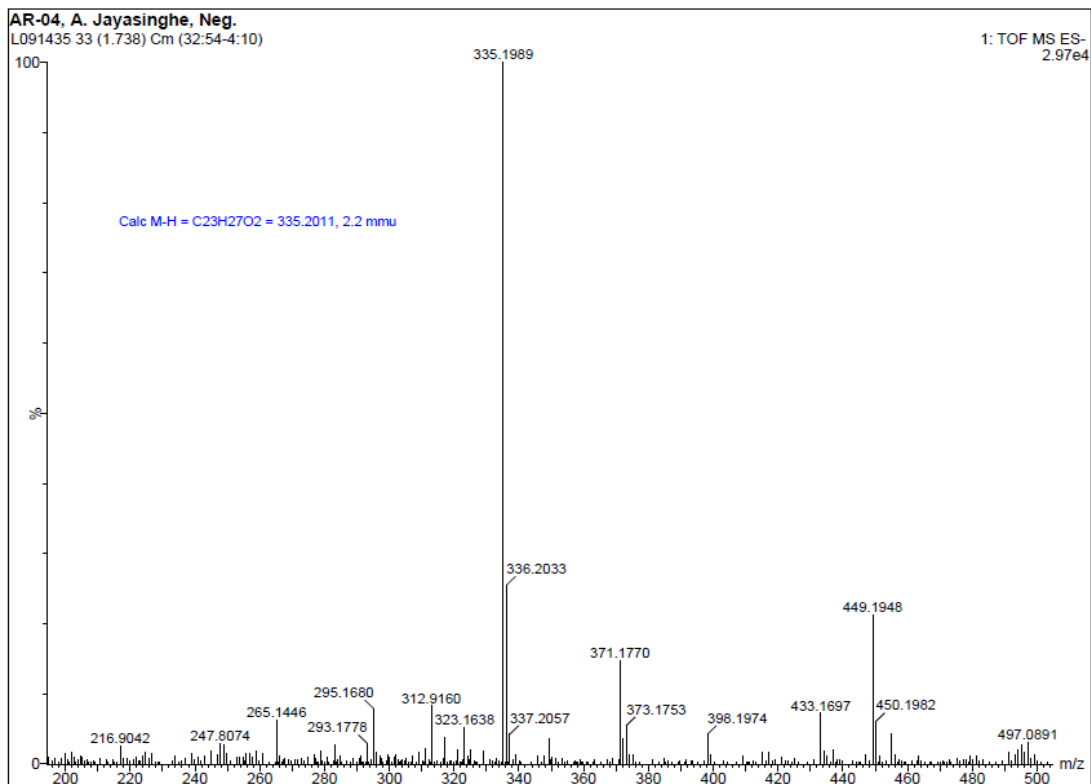


Figure 56.  $^1\text{H}$  NMR (top) and  $^{13}\text{C}$  NMR (bottom) data for compound **31**



Print Date: 09 May 2012 18:05:25

Spectrum Plot - 5/9/2012 6:05 PM

1 A. Profile Scan 35 from c:\varian\data\may 9 2012 aruna2.xms

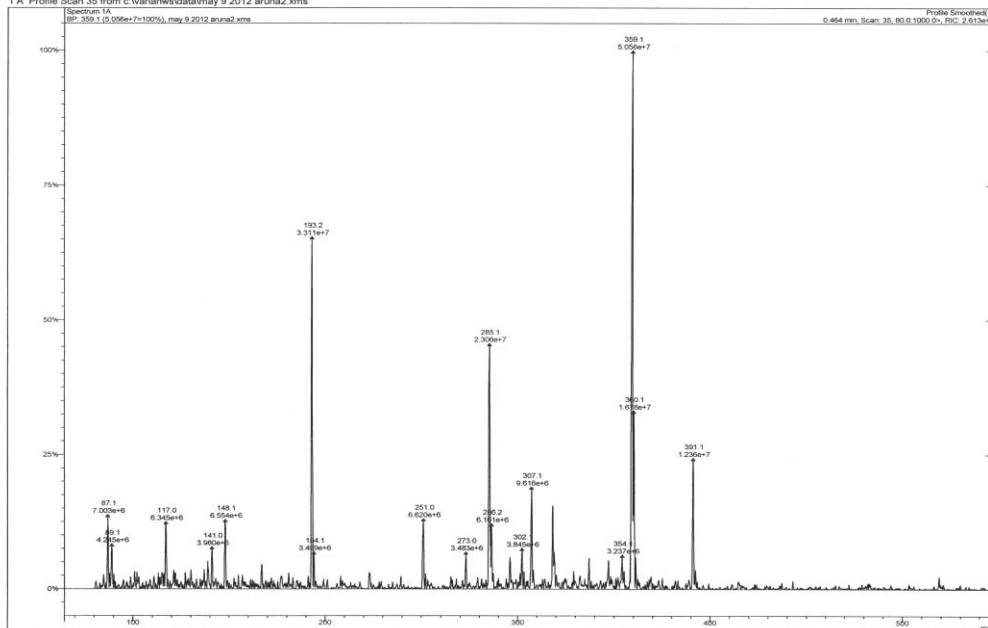


Figure 57. HSMS (top) and ESI-MS (bottom) data for compound **31**

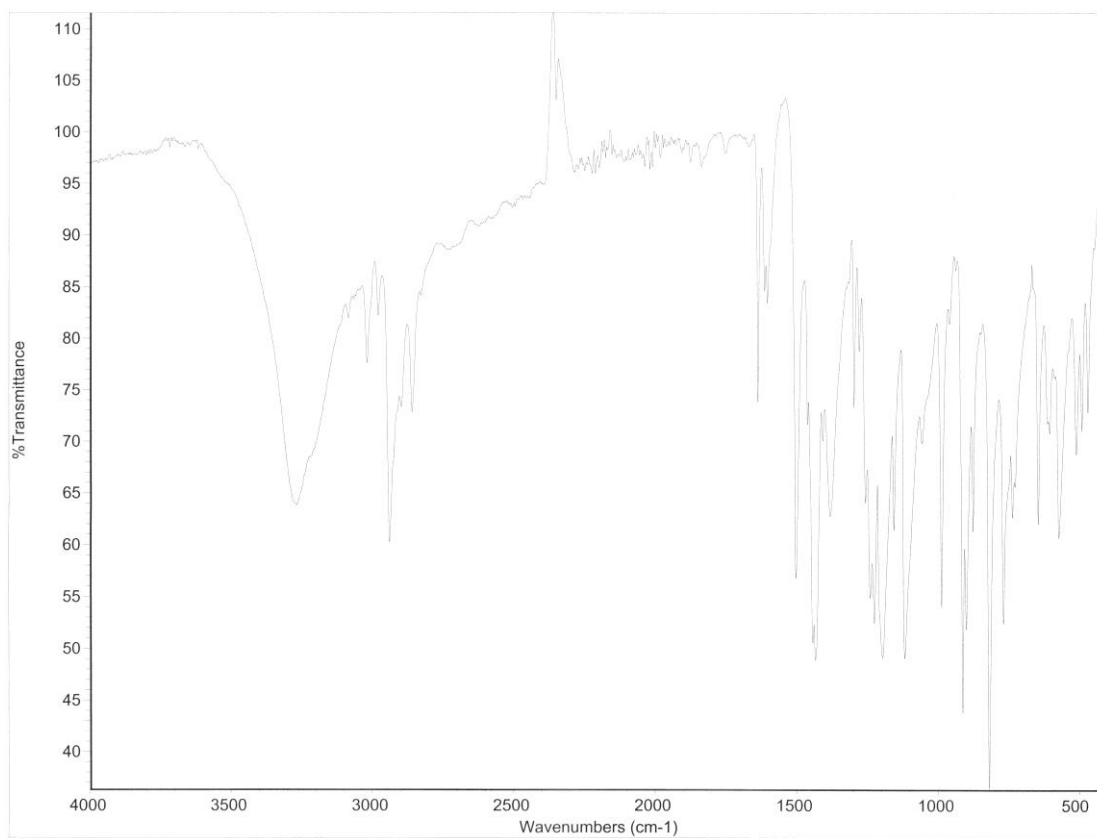


Figure 58. FTIR data for compound **31**

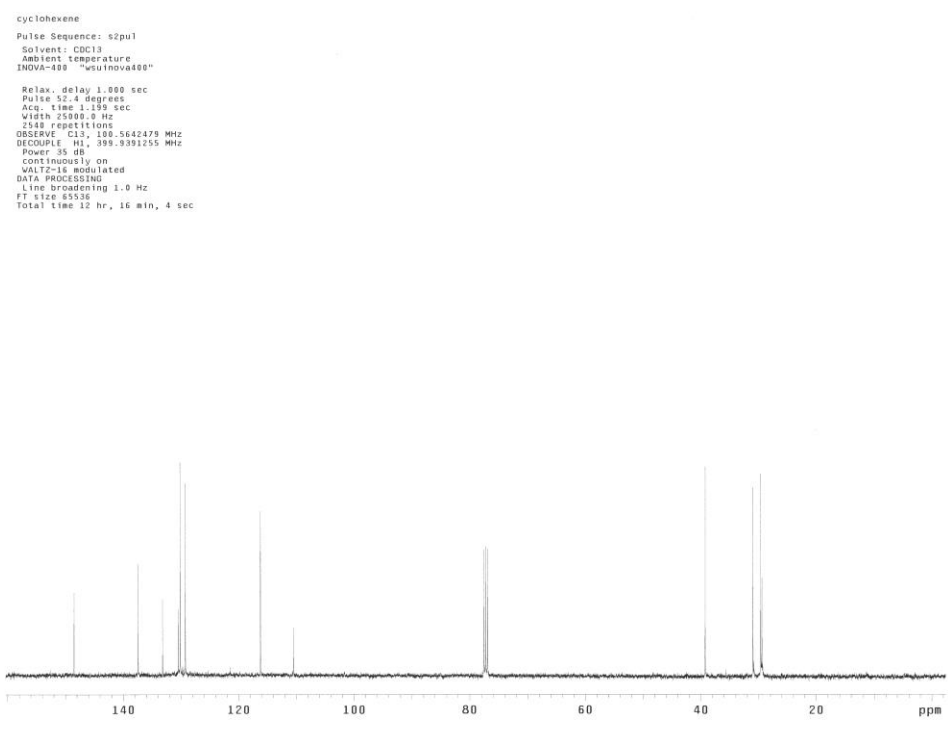
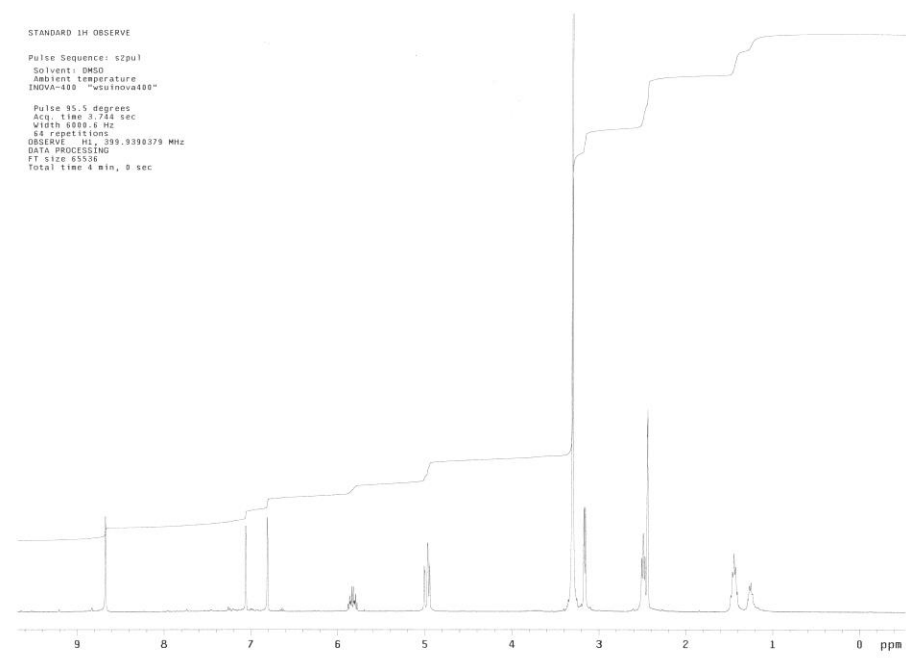
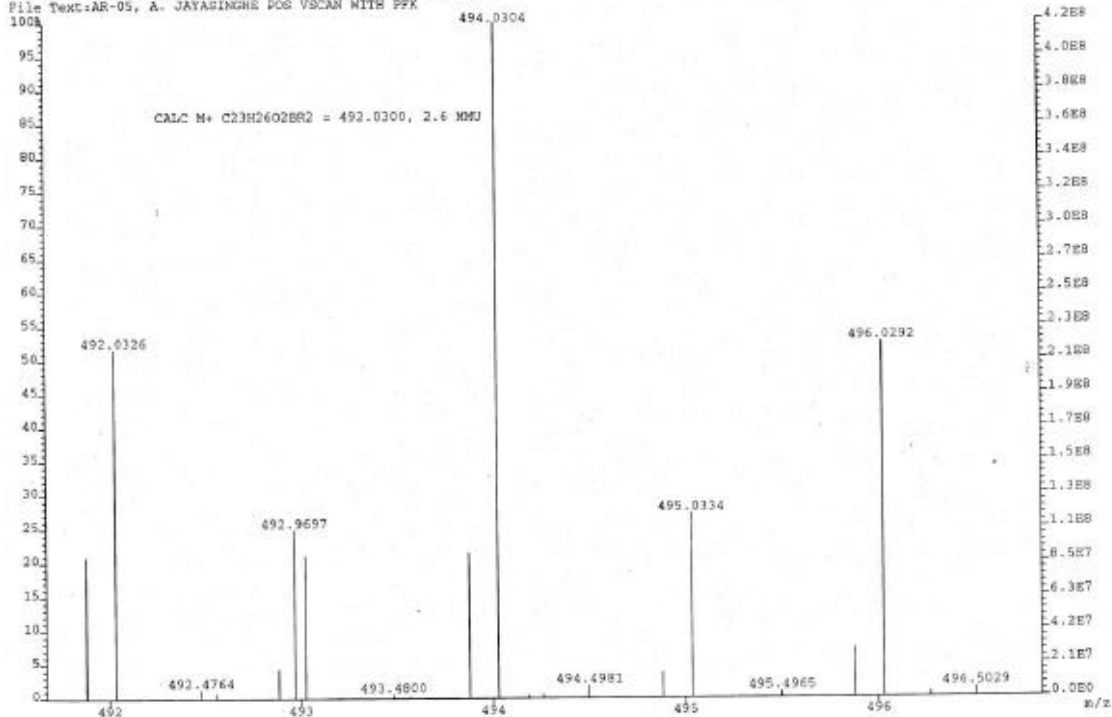


Figure 59. <sup>1</sup>H NMR (top) and <sup>13</sup>C NMR (bottom) data for compound **32**

File:2092003A Acq:21-SEP-2012 10:20:25 +7:29 Cal:2092003A Ident:17\_d3 SMO(2,5) PKD(5,3,5,0.02%,0.0,50.00%,F,T) @PBC(Areas,Center) SA0-SE4F EI+ Voltage Sp(V):6.5V TIC:4911572864 Flags:NONH  
 File Text:AR-05, A- JAYASINGHE POS VSCAN WITH PFK



Print Date: 09 May 2012 18:26:07

Spectrum Plot - 5/9/2012 6:25 PM

1 A Profile Scan 50 from c:\varian\sw\data\may 9 2012\aruna3.xms

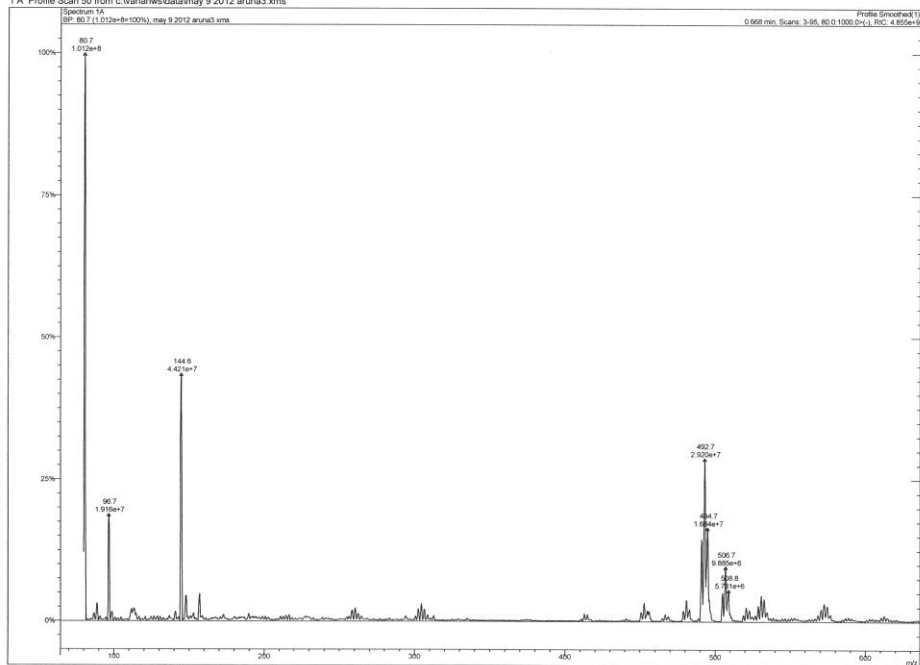


Figure 60. HSMS (top) and ESI-MS (bottom) data for compound 32

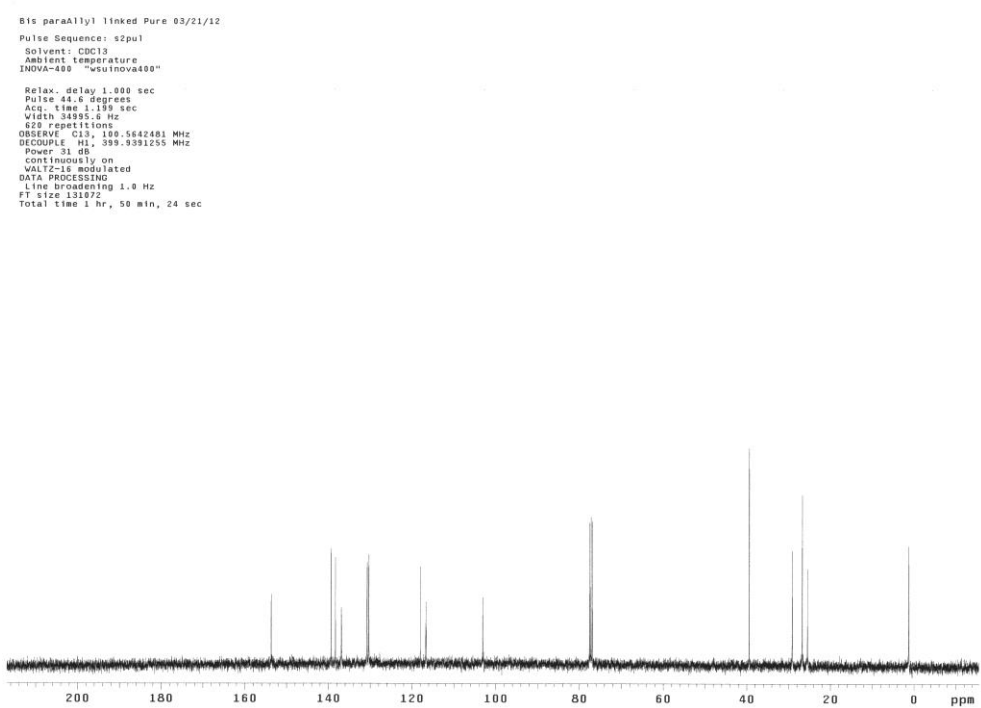
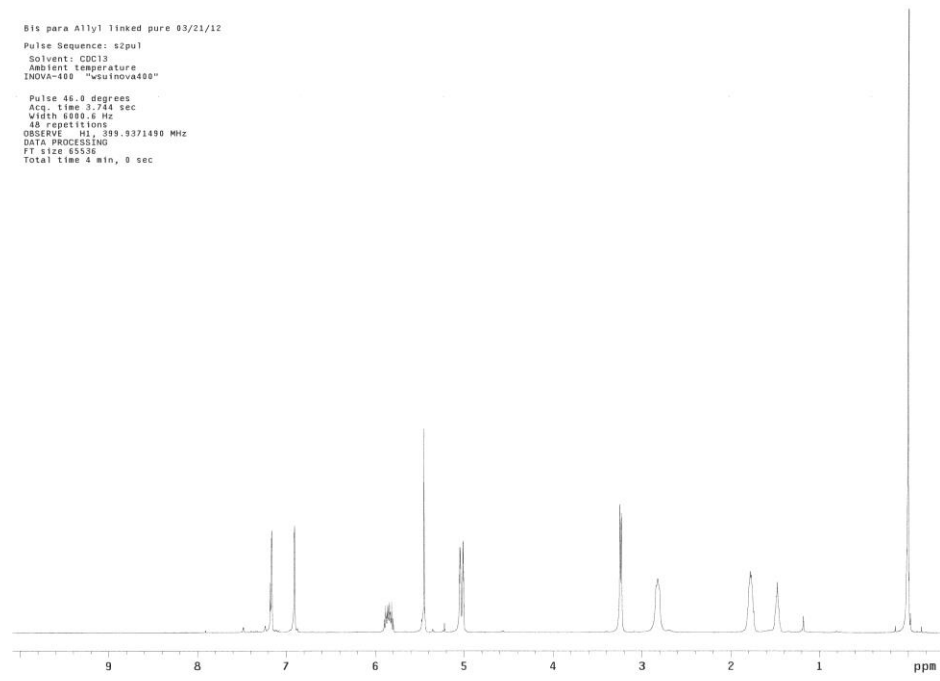


Figure 61. <sup>1</sup>H NMR (top) and <sup>13</sup>C NMR (bottom) data for compound **33**

File:2092004A Acq:21-SEP-2012 10:34:02 +4:15 Cal:2092004A Ident:1B\_24 SMO(2,5) PKD(5,3,5,0.02%,0.),50.00%,P,T) SPBC(Areas,Center) ZAB-SE4F EI+ Voltage BpI(V):406.1mV TIC:626305498 Flags:NDNM  
File Text:AR-06, A. JAYASINGHE POS VSCAN WITH PFK

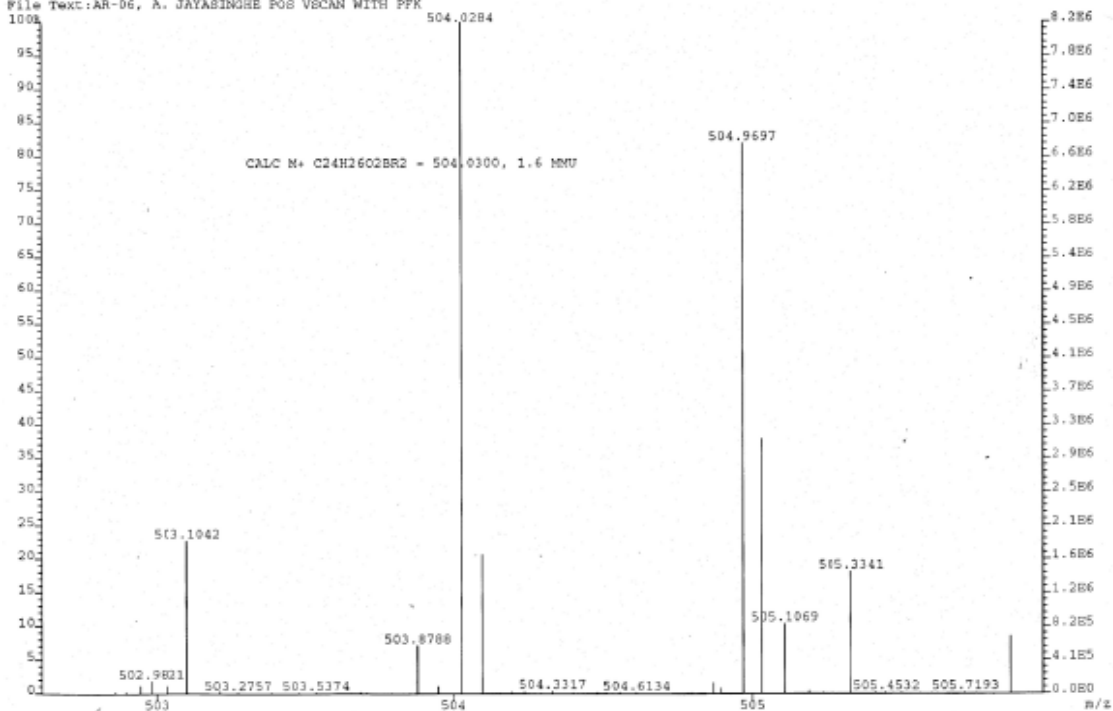
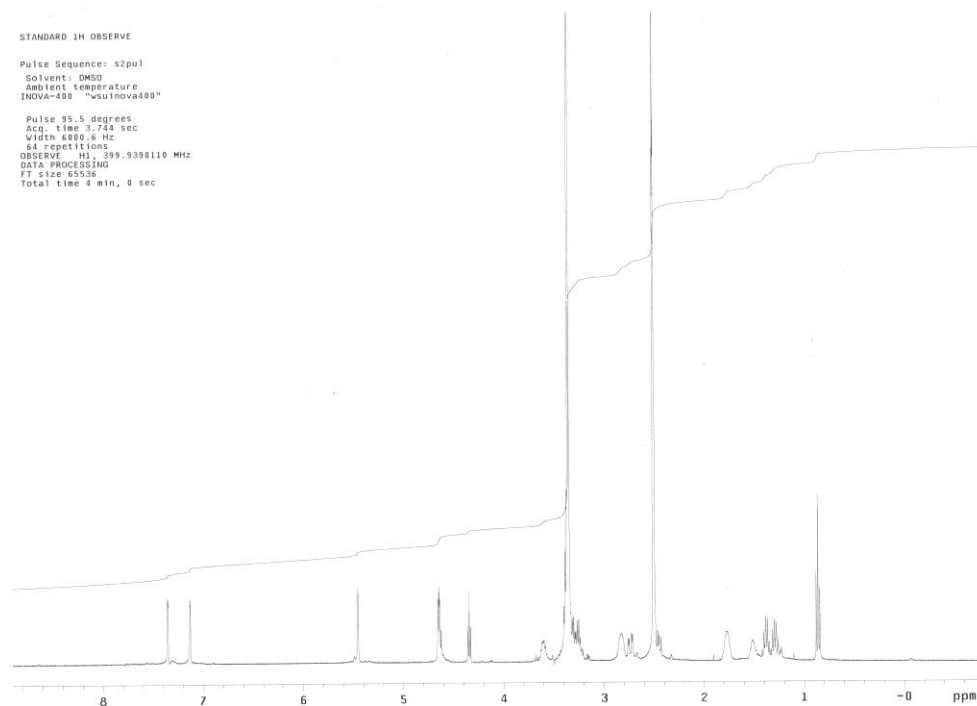


Figure 62. HSMS data for compound 33

STANDARD 1H OBSERVE  
Pulse Sequence: s2pul  
Solvent: DMSO  
Ambient temperature  
INNOVA-400 "jeu1nova400"  
Pulse 35.5 degrees  
Acq. time 3.784 sec  
Width 8500.8 Hz  
64 repetitions  
OBSERVE H1, 399.9399110 MHz  
DATA PROCESSING  
FT size 65536  
Total time 4 min, 0 sec



STANDARD 13C OBSERVE  
Sample Name:  
Data Collected on:  
mc-115-nmr-400-inova400  
Archive directory:  
Sample directory:  
Fidfile: CARBON  
Pulse Sequence: CARBON (s2pul)  
Solvent: CD3OD  
Data collected on: Aug 11 2013  
Temp. 25.0 C / 298.1 K  
Operator: aruna  
Relax. delay 1.000 sec  
Pulse 45.0 degrees  
Acq. time 1.303 sec  
Width 25141.4 Hz  
21149 repetitions  
OBSERVE C13, 100.5620076 MHz  
DECOUPLE H1, 399.9310806 MHz  
Power 42 dB  
continuously on  
WALTZ-16 modulated  
DATA PROCESSING  
Line broadening 0.5 Hz  
FT size 65536  
Total time 642 hr, 16 min

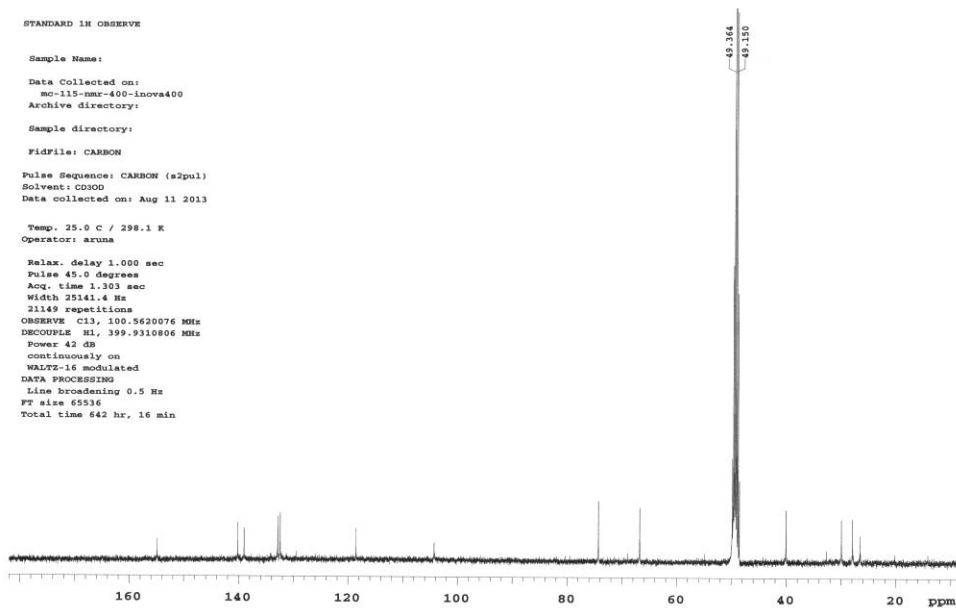


Figure 63.  $^1\text{H}$  NMR (top) and  $^{13}\text{C}$  NMR (bottom) data for compound **34**

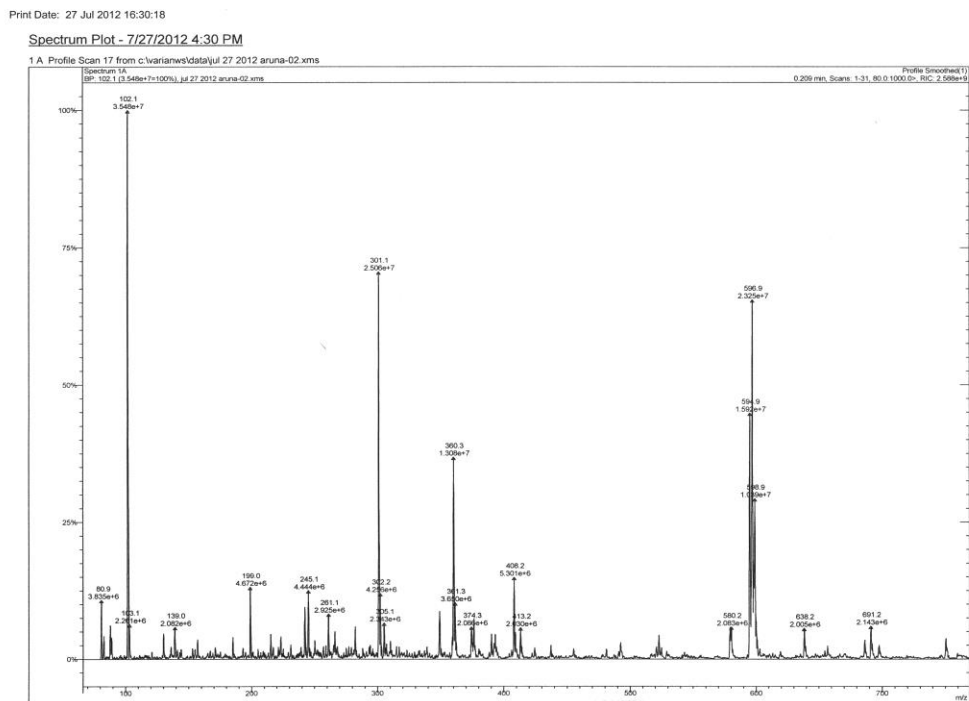
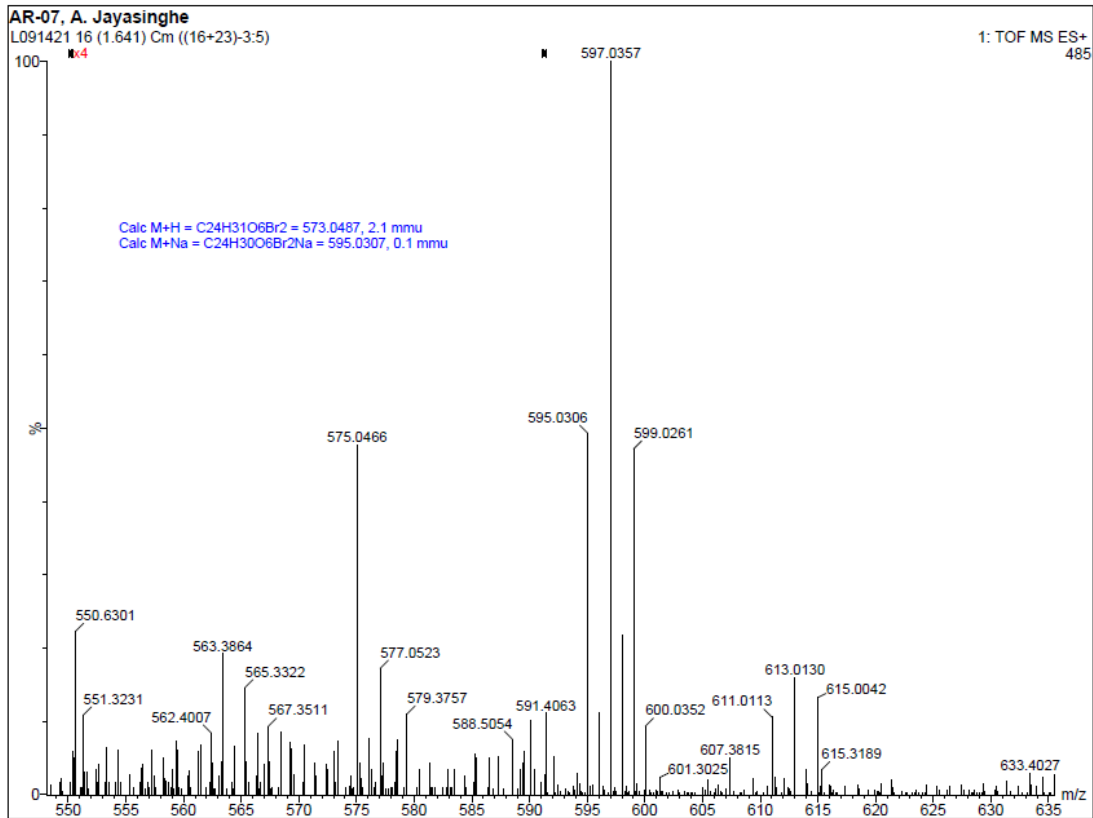


Figure 64. HSMS (top) and ESI-MS (bottom) data for compound **34**

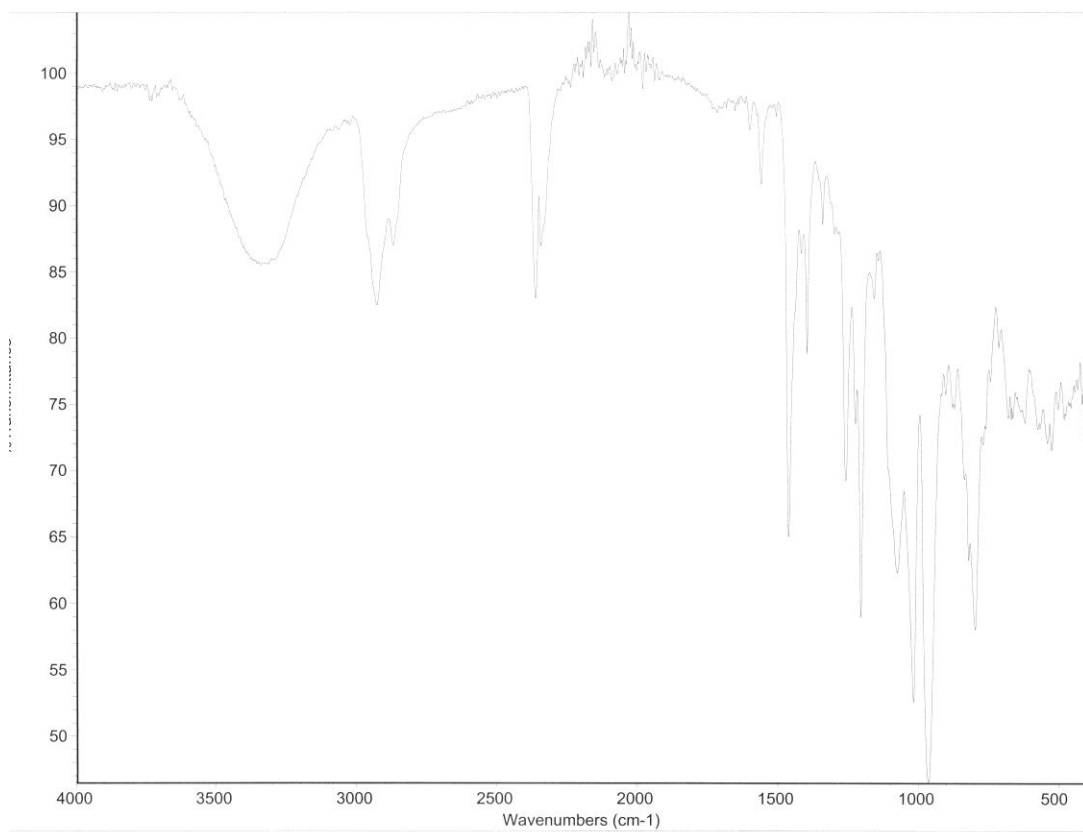
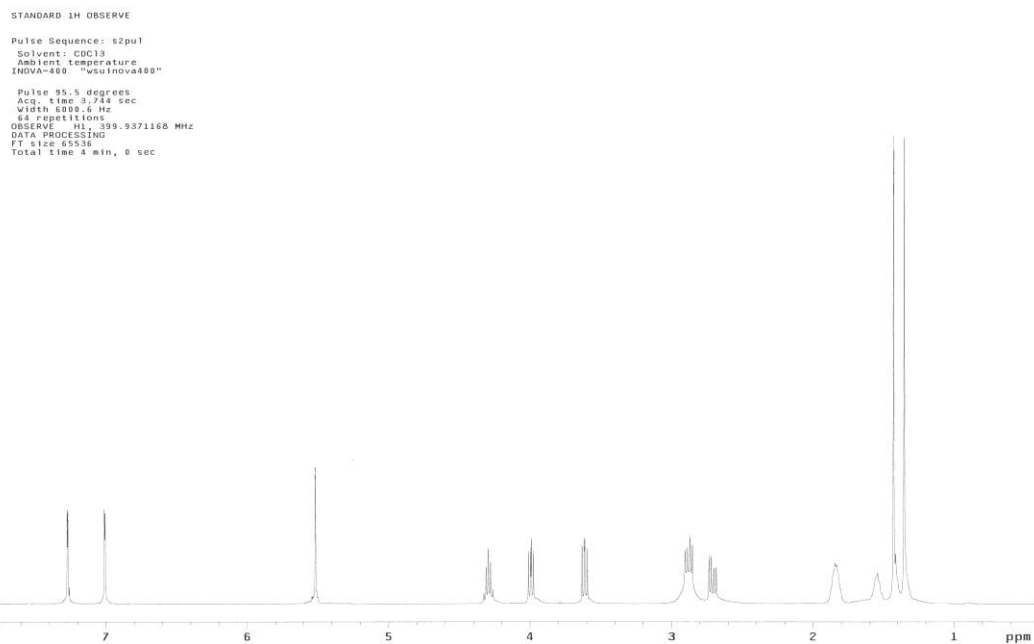


Figure 65. FTIR data for compound **34**



cyclohexene

Pulse Sequence: s2pu1  
 Solvent: CDCl3  
 Ambient temperature  
 INOVA-400 "wstinova400"

Relax. delay 1.000 sec  
 Pulse 32.4 degrees  
 Acq. time 1.199 sec  
 Width 25880.0 Hz  
 1528 repetitions  
 OBSERVE C13, 100.642348 MHz  
 DECOUPLE H1, 399.9391205 MHz  
 Power 35 dB  
 continuously on  
 WALTZ-16 modulated  
 DATA PROCESSING  
 Line broadening 1.0 Hz  
 FT size 55536  
 Total time 12 hr, 16 min, 4 sec

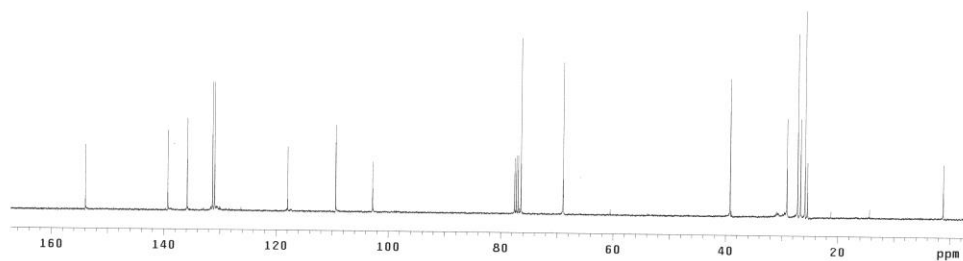
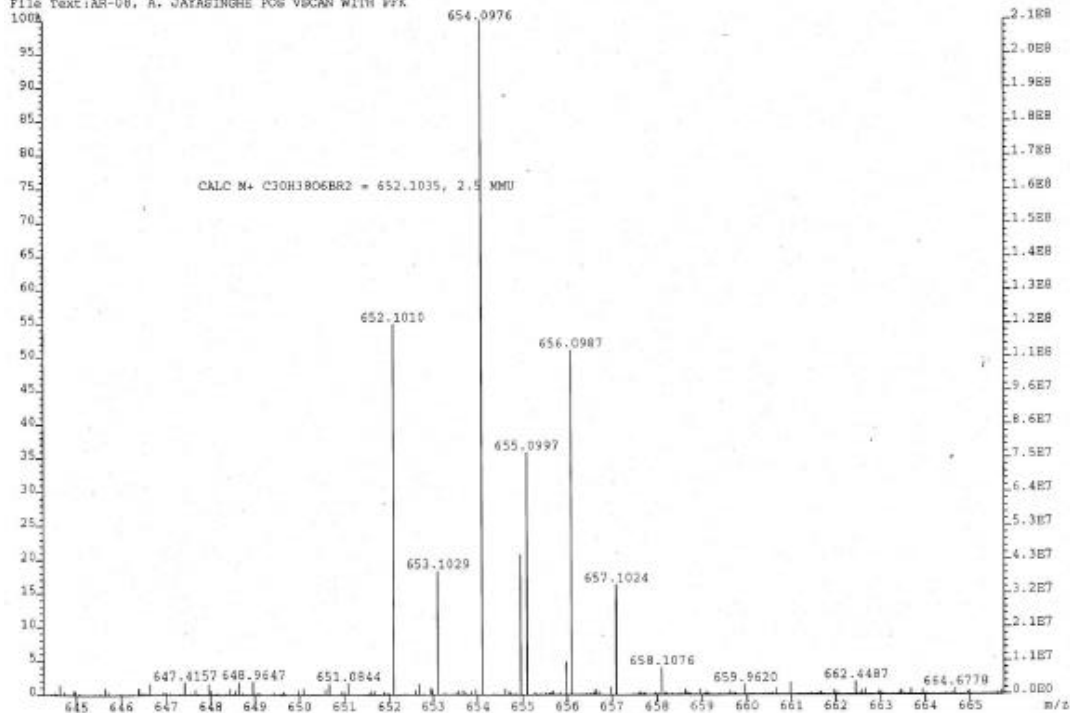


Figure 66.  $^1\text{H}$  NMR (top) and  $^{13}\text{C}$  NMR (bottom) data for compound **35**

File:Z092008 Acq:21-SEP-2012 16:56:03 +8:30 Cal:Z092008 Ident:22\_49 SM012.51 PKD(5.3,5.0,0.01%,0.0,50.00%,F,T) SPBC(Areas,Centroid)\*  
 TAB-854F EI+ Voltage 601(V):13.2V TIC:4131325952 Flags:NCRM  
 File Text:AR-08, A. JAYASINGHE POC VSCAN WITH PPK



Print Date: 27 Jul 2012 16:25:30

Spectrum Plot - 7/27/2012 4:25 PM

1 A Profile Scan 17 from c:\varian\sw\data\jul 27 2012 aruna-01.xms

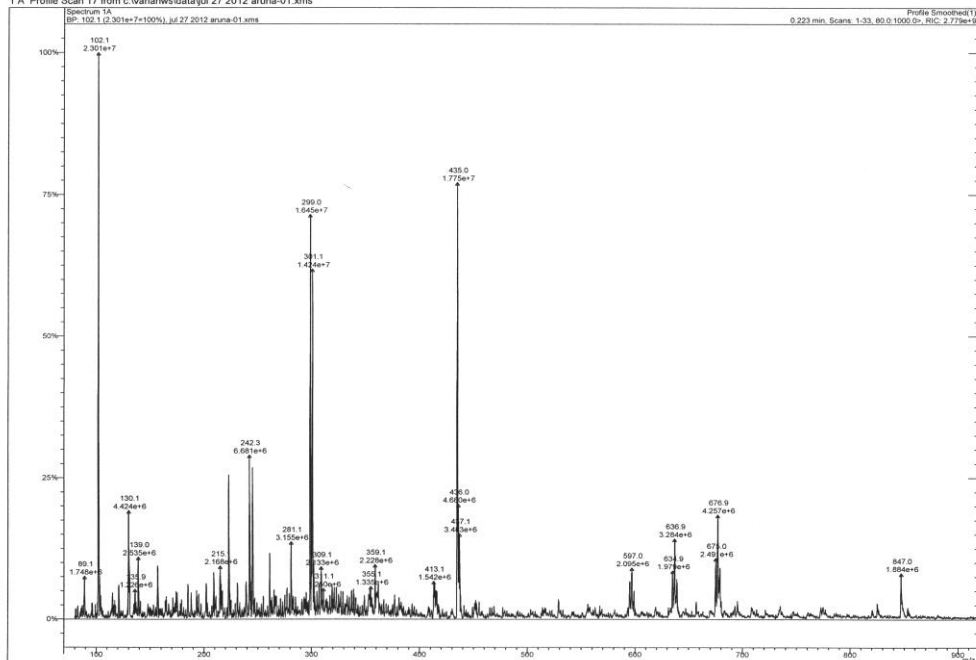


Figure 67. HSMS (top) and ESI-MS (bottom) data for compound 35

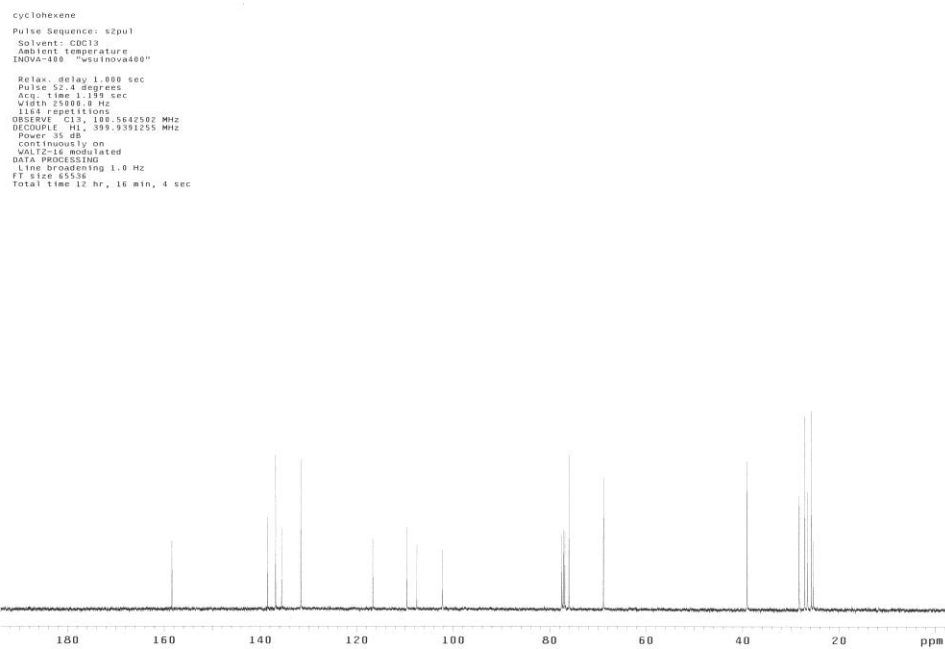
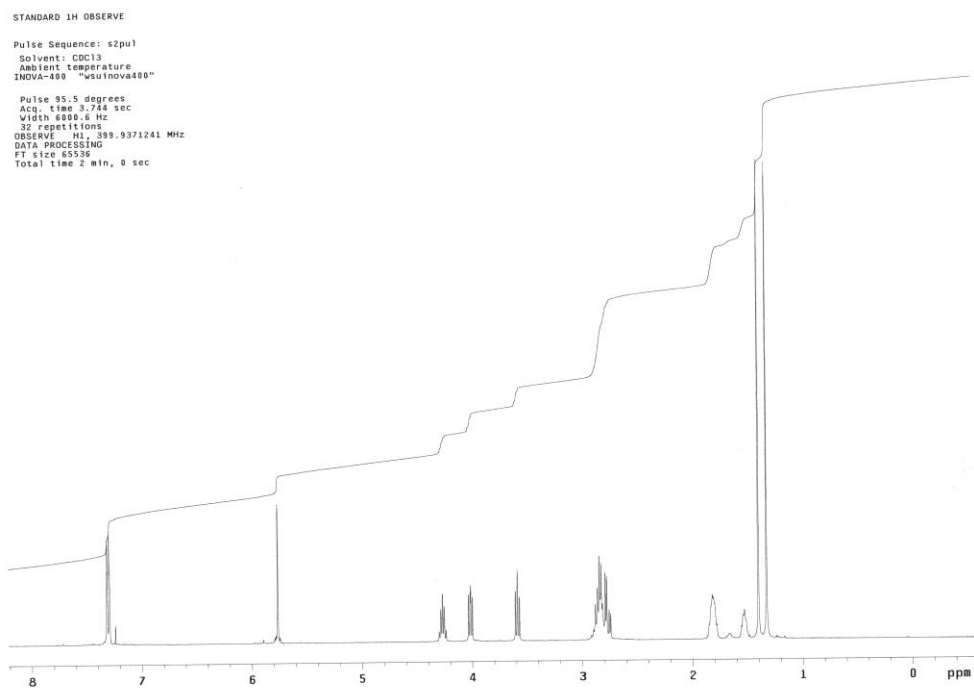
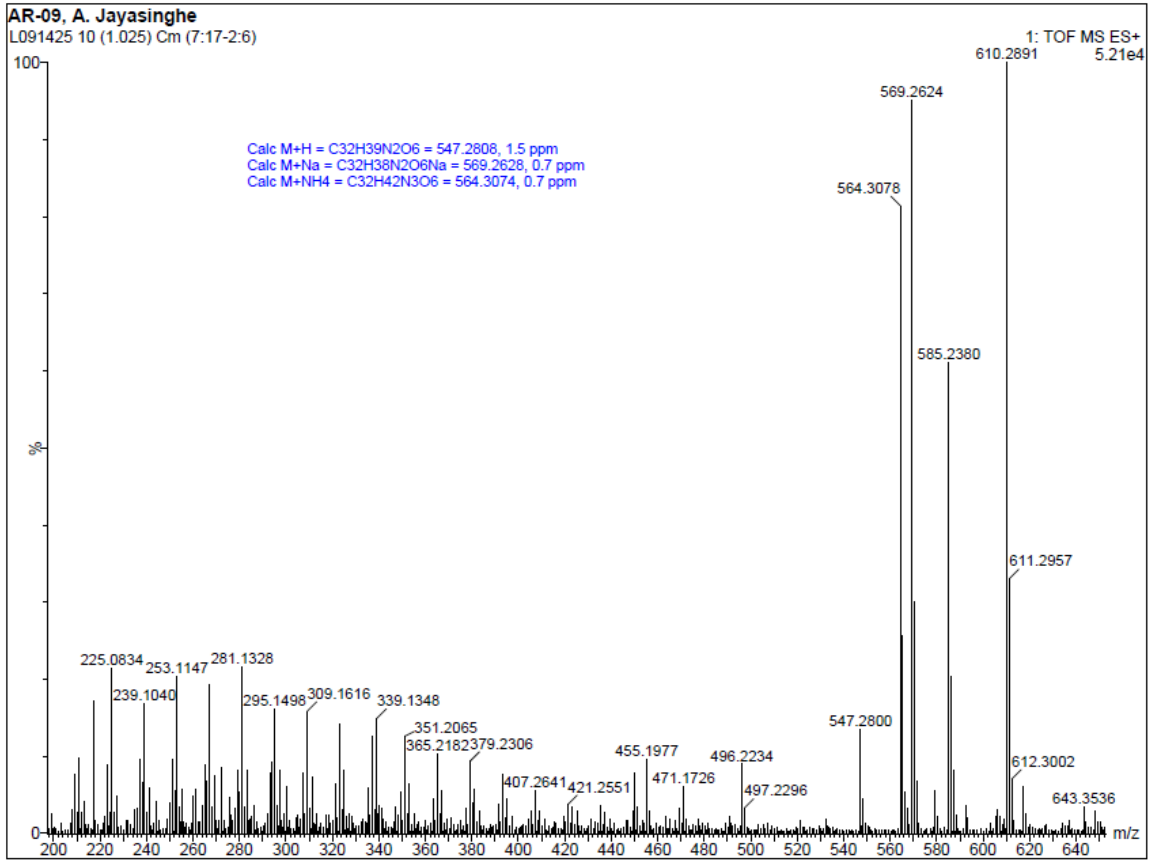


Figure 68.  $^1\text{H}$  NMR (top) and  $^{13}\text{C}$  NMR (bottom) data for compound **36**



Print Date: 31 Oct 2011 14:20:34

Spectrum Plot - 10/31/2011 2:20 PM

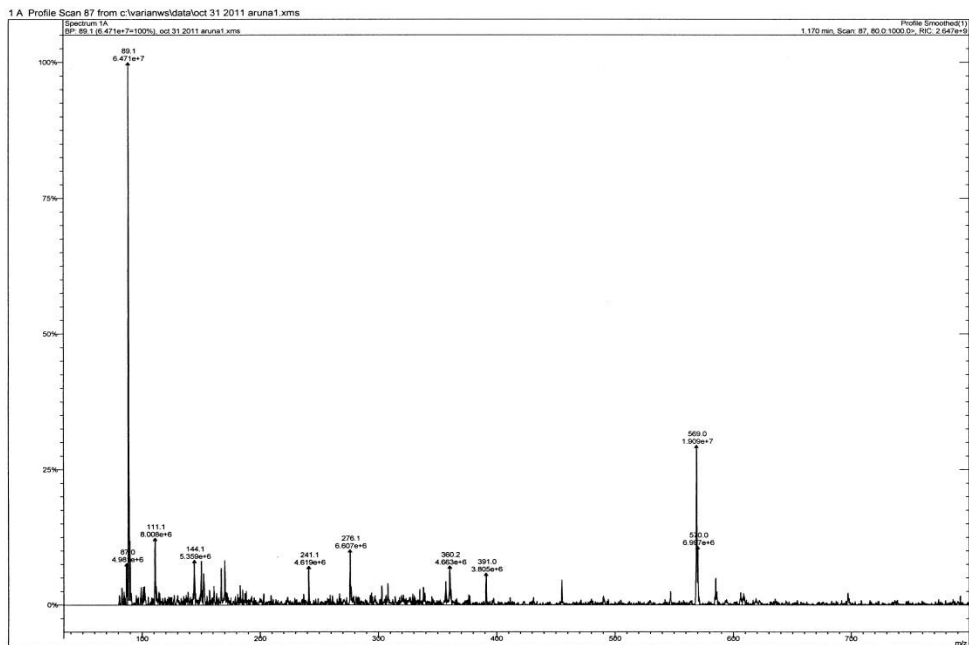


Figure 69. HSMS (top) and ESI-MS (bottom) data for compound **36**

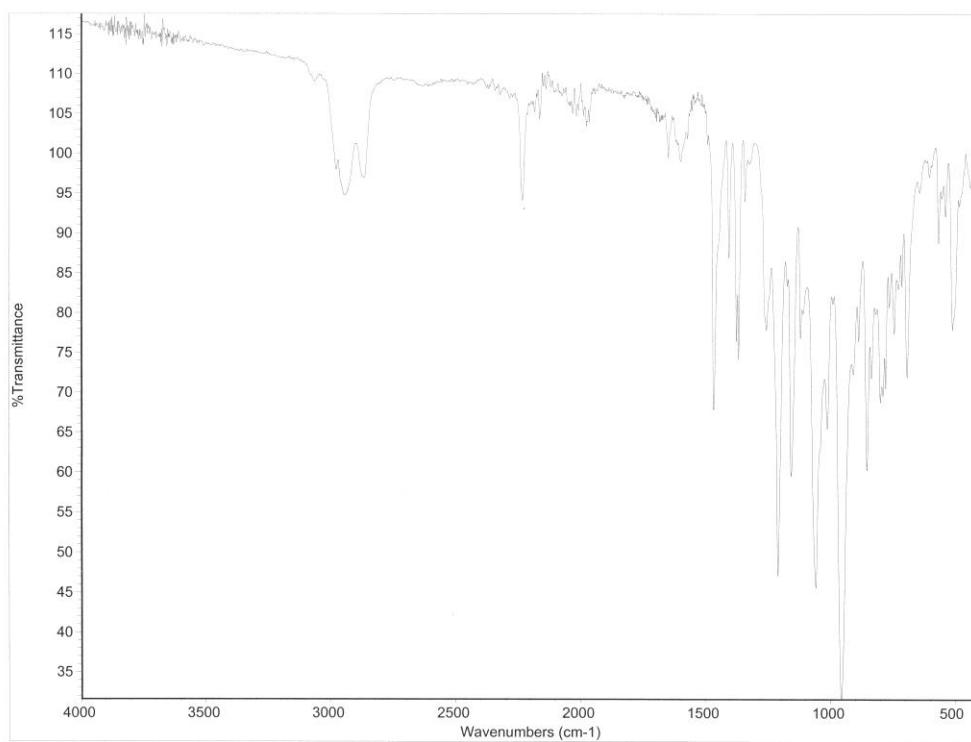


Figure 70. FTIR data for compound **36**

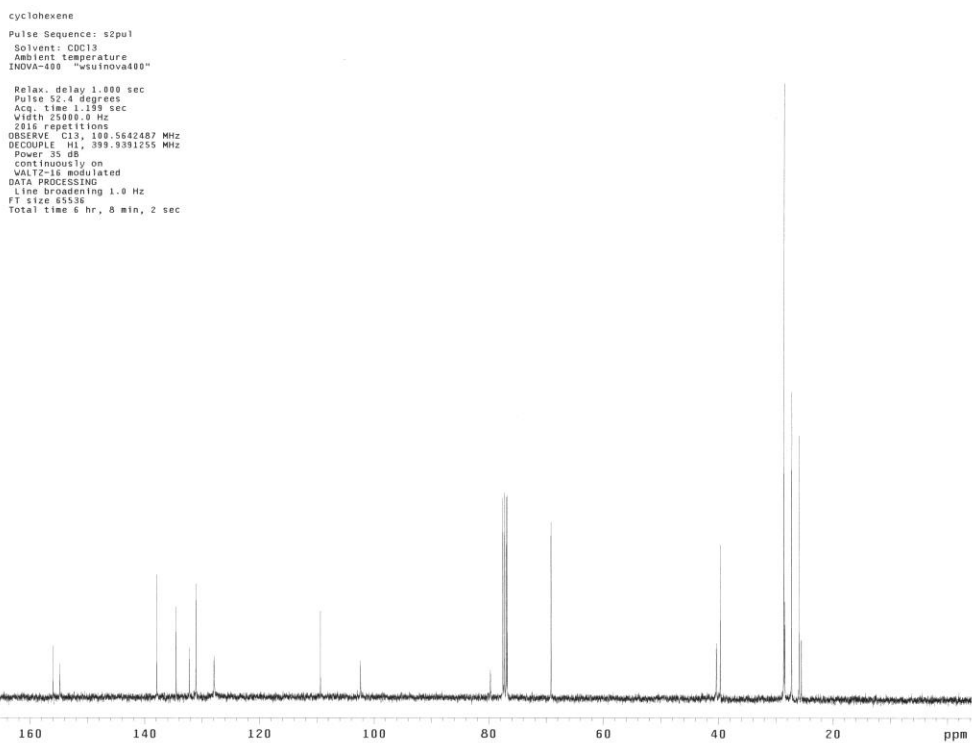
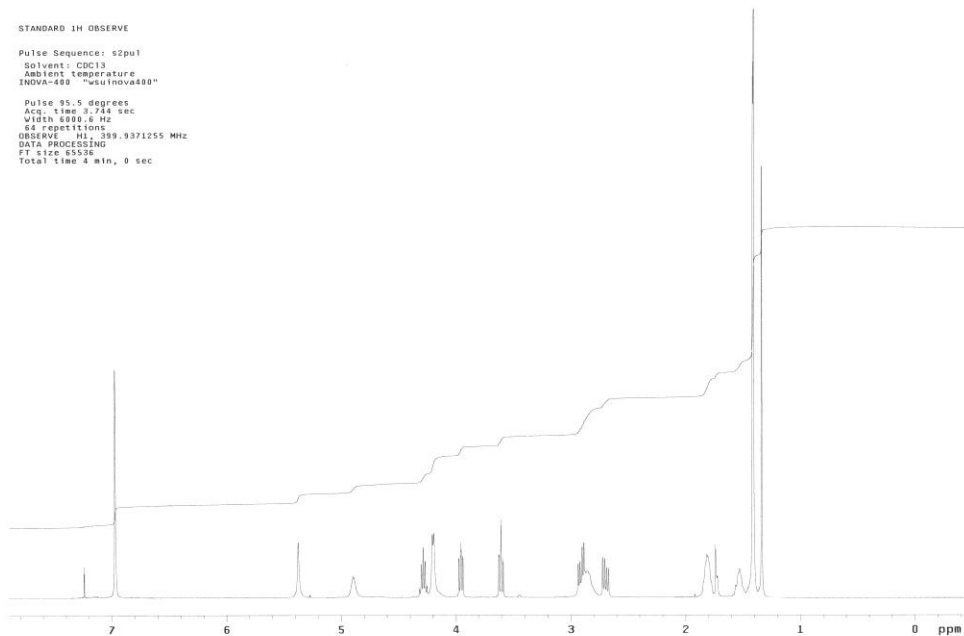
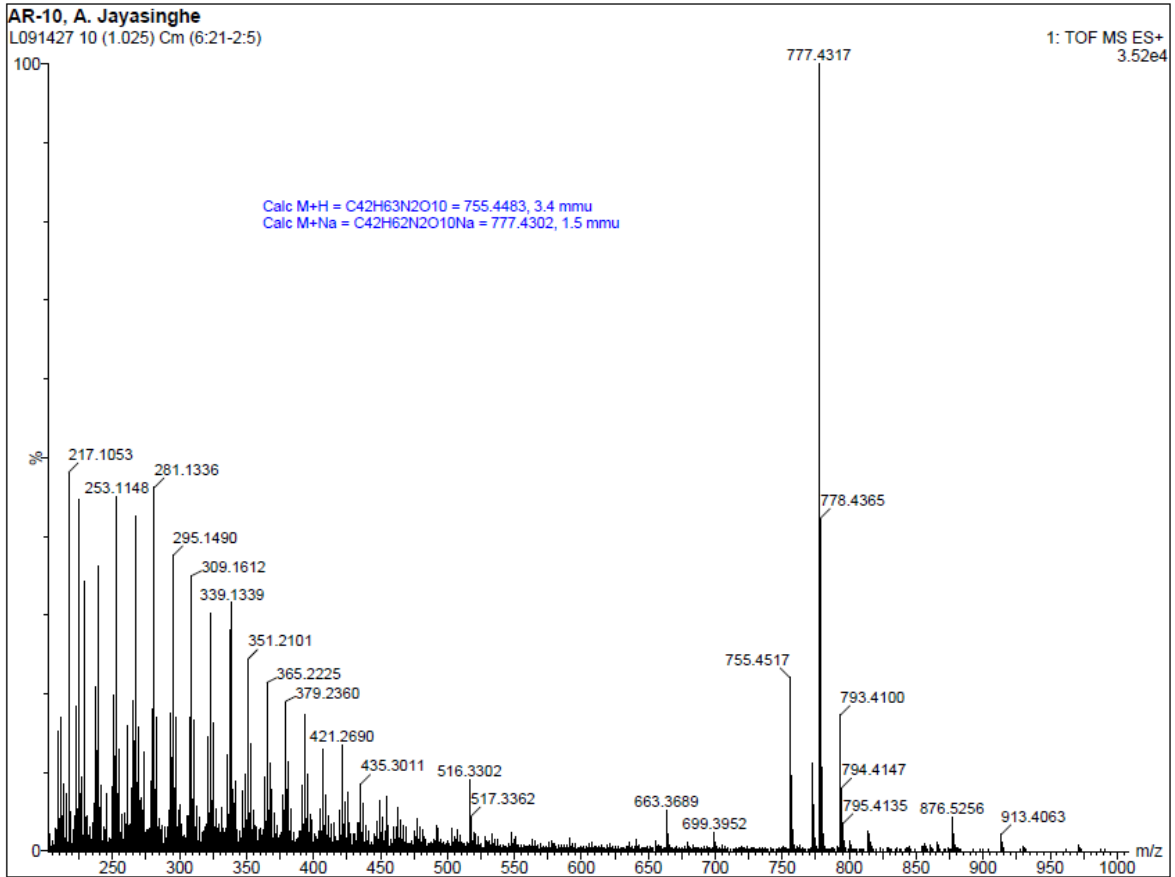


Figure 71.  $^1\text{H}$  NMR (top) and  $^{13}\text{C}$  NMR (bottom) data for compound **38**



Print Date: 06 Jul 2012 14:42:44

Spectrum Plot - 7/6/2012 2:42 PM

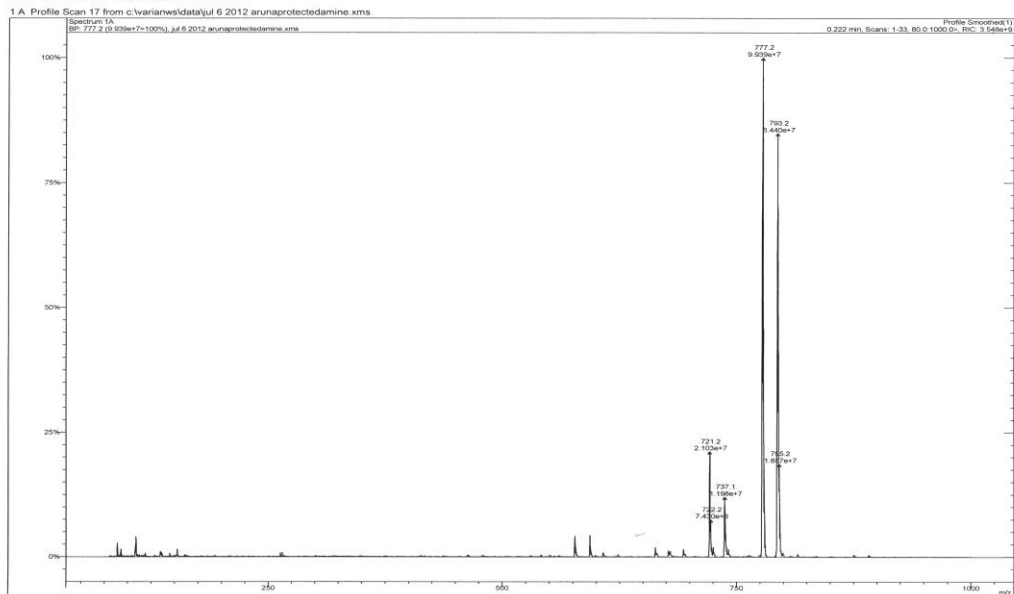


Figure 72. HSMS (top) and ESI-MS (bottom) data for compound **38**

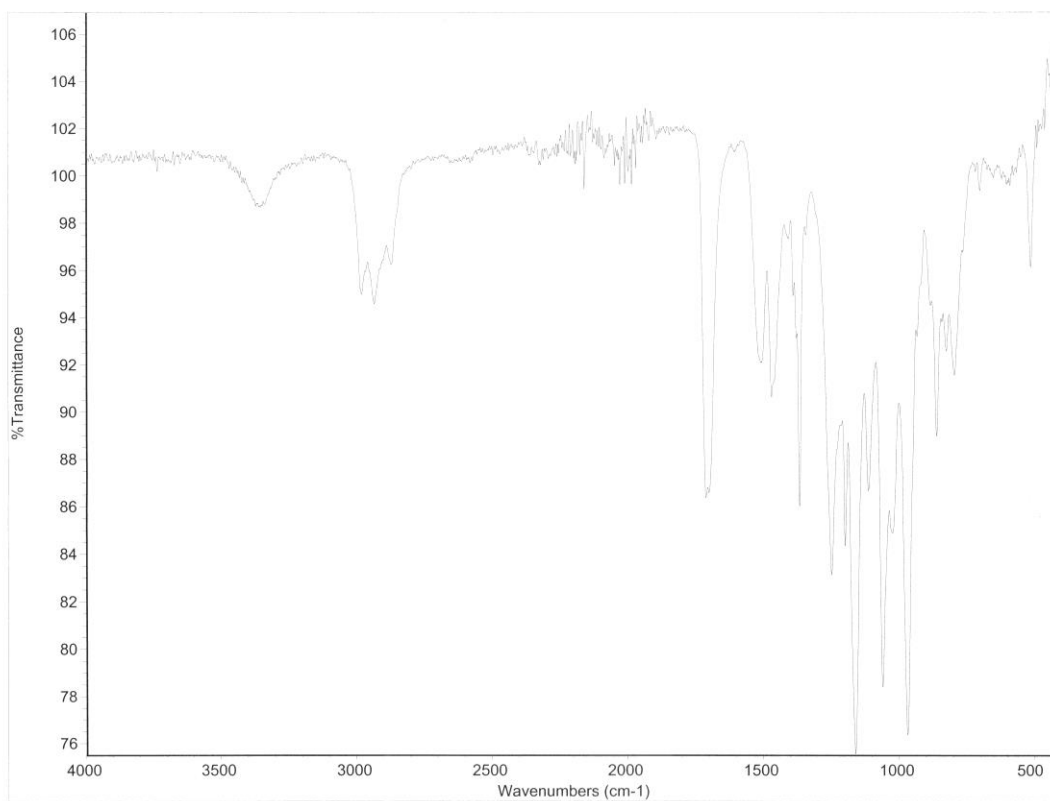


Figure 73. FTIR data for compound **38**

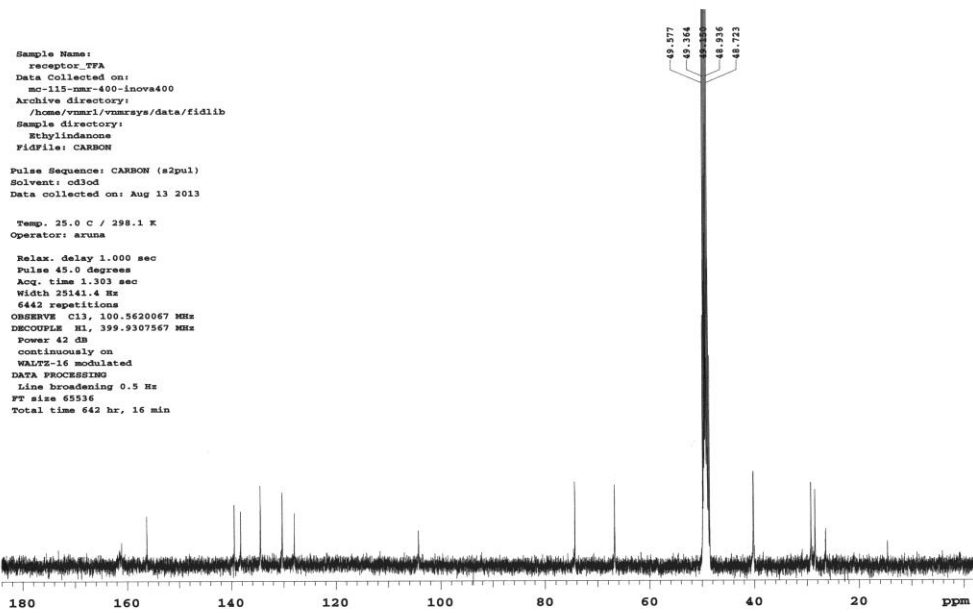
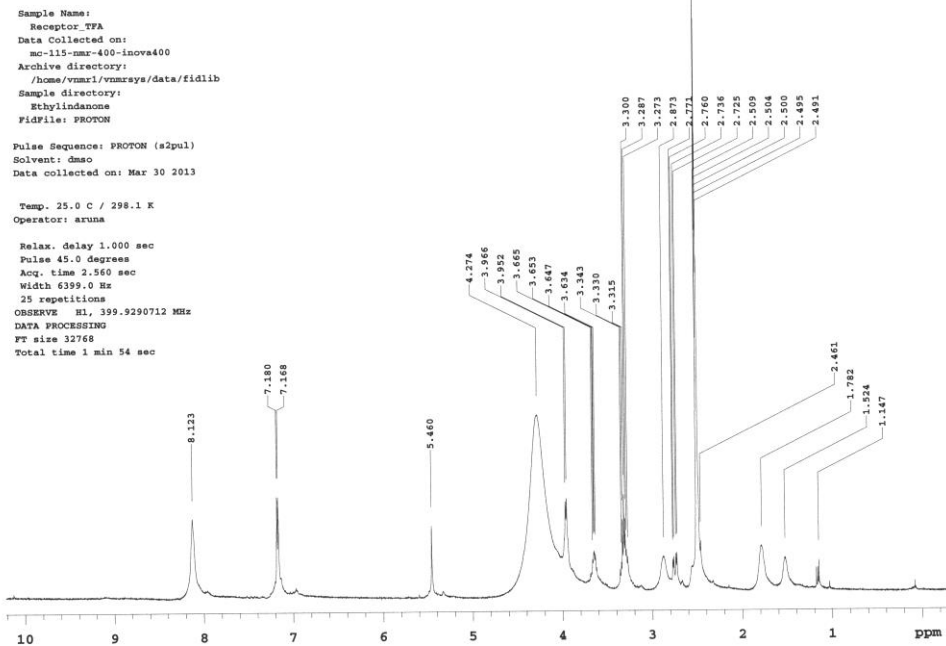


Figure 74.  $^1\text{H}$  NMR (top) and  $^{13}\text{C}$  NMR (bottom) data for compound **39**

Sample Name:  
Receptor\_TFA\_new  
Data Collected on:  
mc-115-nmr-400-inova400  
Archive directory:  
/home/vmmr1/vmmrsys/data/fidlib  
Sample directory:  
Ethylindanone  
Fidfile: FLUORINE  
  
Pulse Sequence: FLUORINE (s2pul)  
Solvent: dmsc  
Data collected on: May 10 2013  
  
Temp. 25.0 C / 298.1 K  
Operator: aruna  
  
Relax. delay 1.000 sec  
Pulse 30.0 degrees  
Acq. time 0.757 sec  
Width 66580.1 Hz  
71 repetitions  
OBSERVE F19, 376.3093134 MHz  
DATA PROCESSING  
FT size 131072  
Total time 490 hr, 30 min

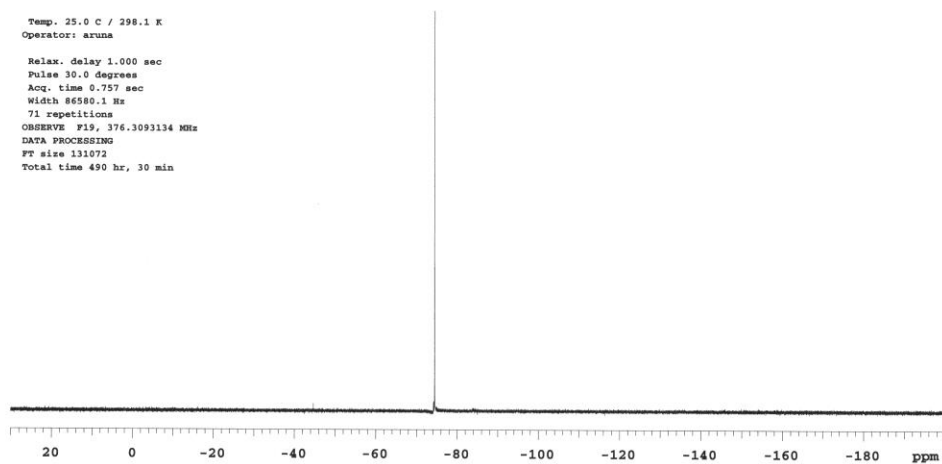


Figure 75.  $^{19}\text{F}$  NMR data for compound **39**

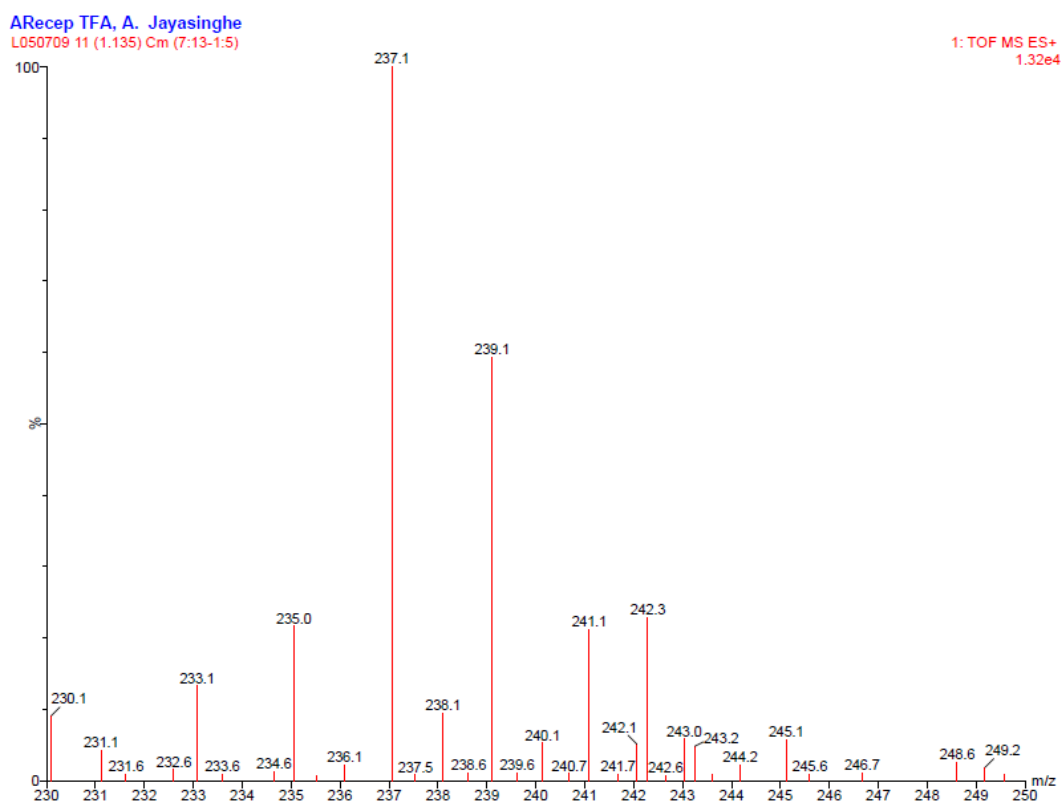
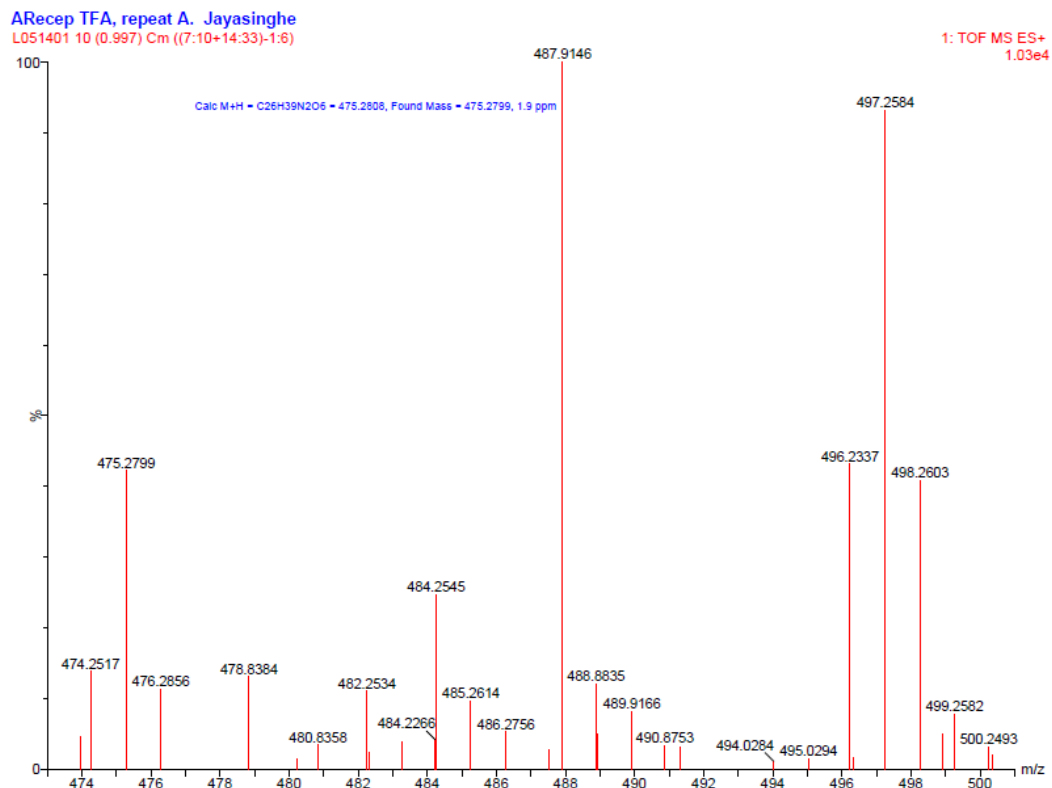


Figure 76. HSMS (top) and ESI-MS (bottom) data for compound **39**

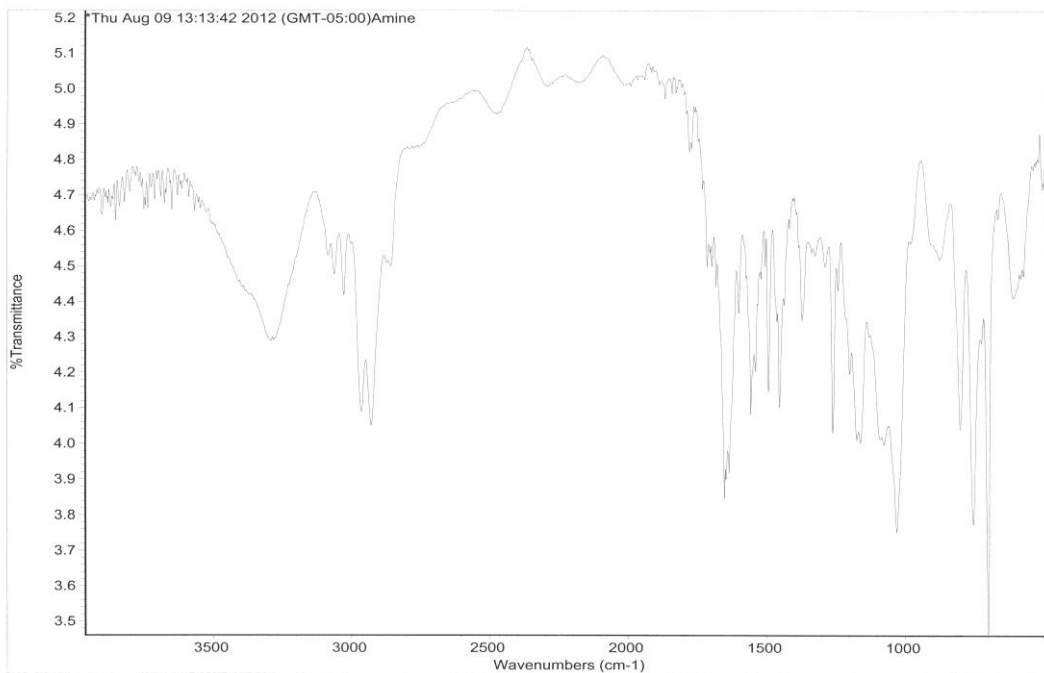
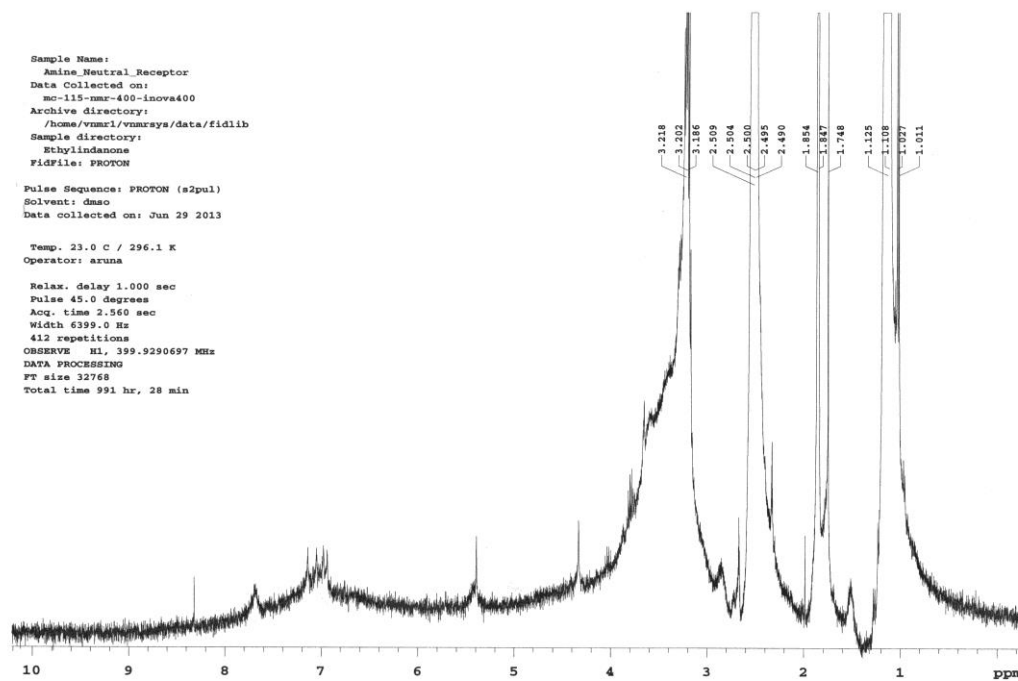


Figure 77.  $^1\text{H}$  NMR (top) and FTIR (bottom) data for compound **40**

Spectrum Plot - 4/17/2013 10:33 PM

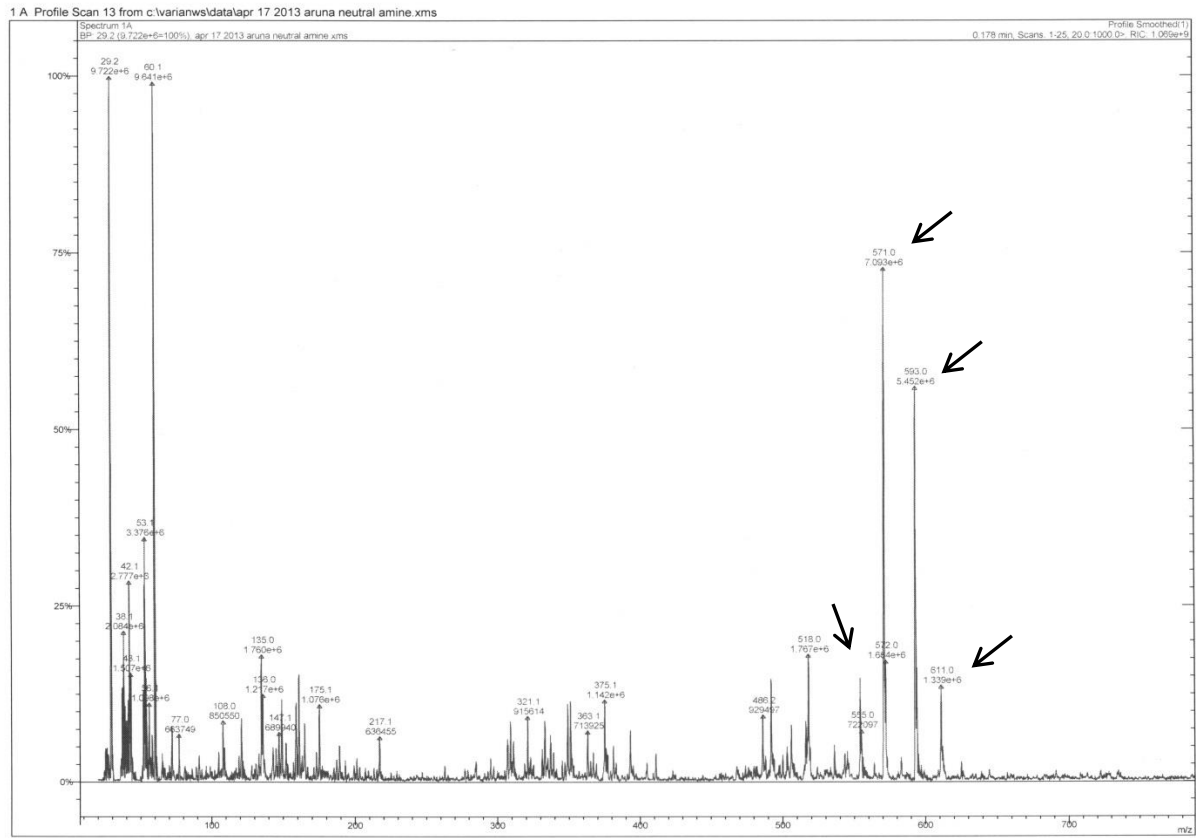


Figure 78. ESI-MS data for compound 40

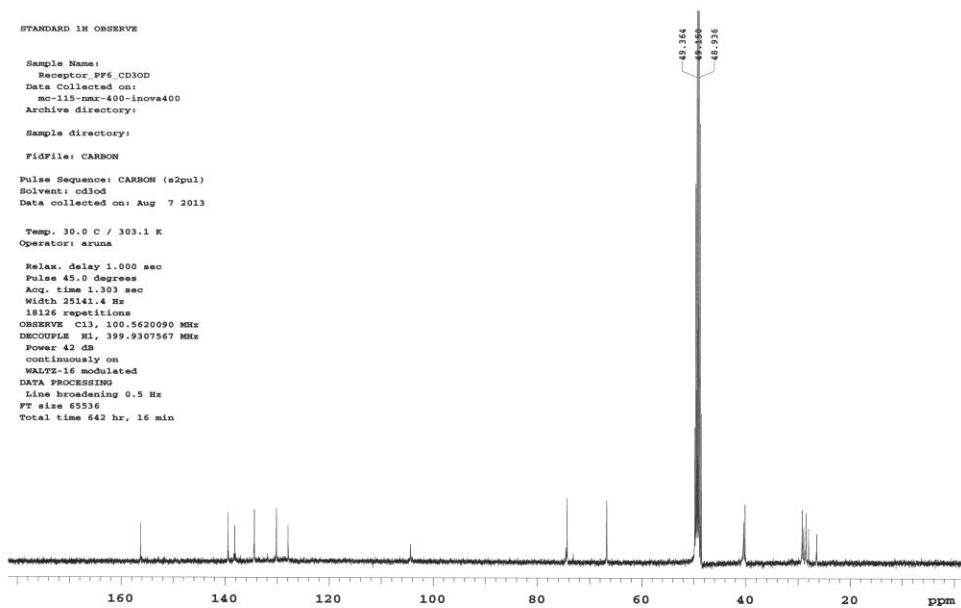
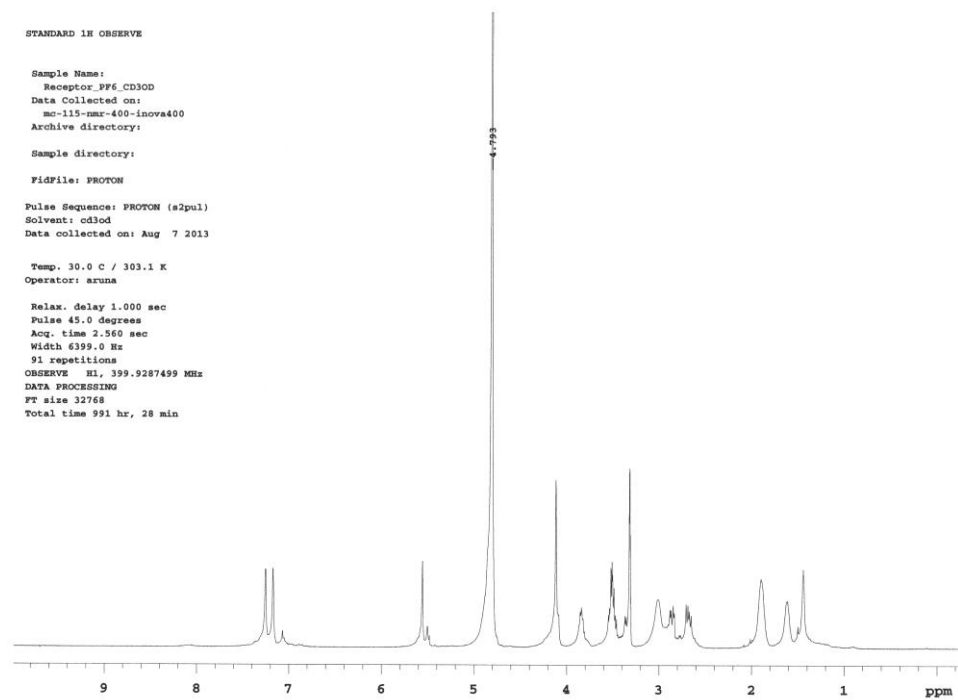


Figure 79.  $^1\text{H}$  NMR (top) and  $^{13}\text{C}$  NMR (bottom) data for compound **5**

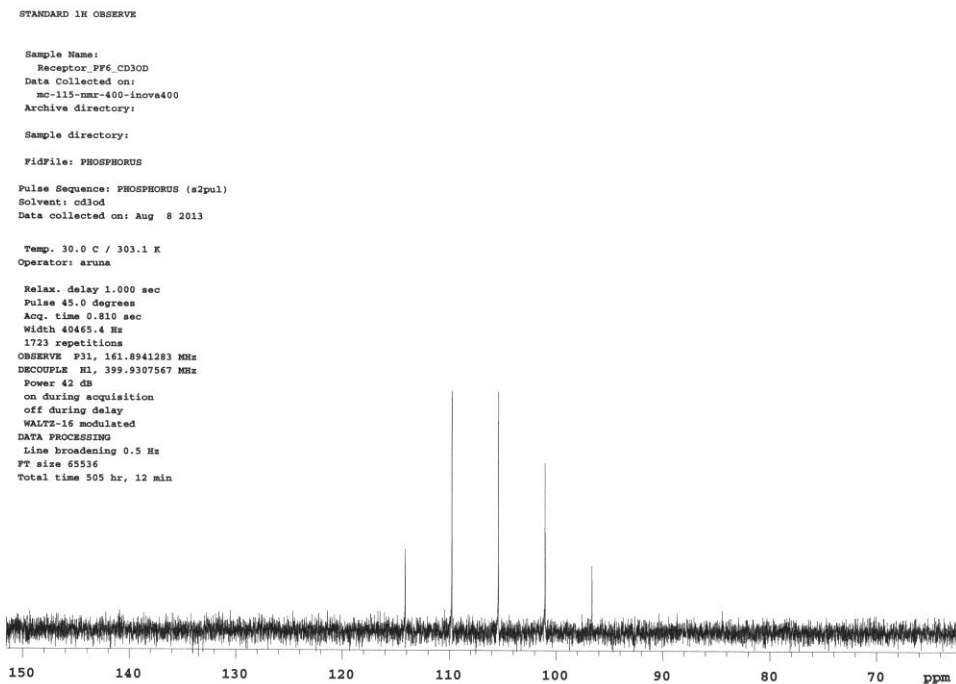
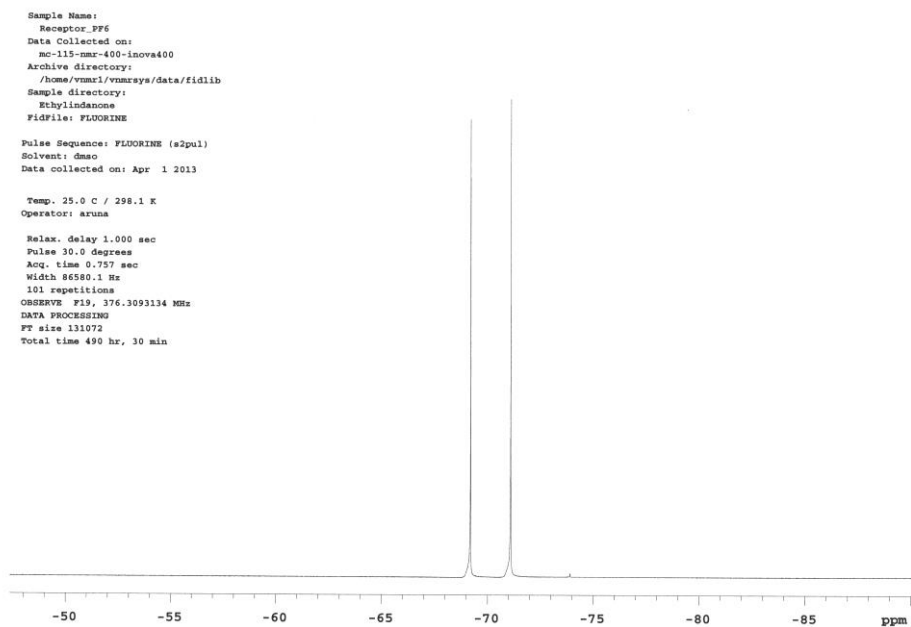


Figure 80.  $^{19}\text{F}$  NMR (top) and  $^{31}\text{P}$  NMR (bottom) data for compound **5**

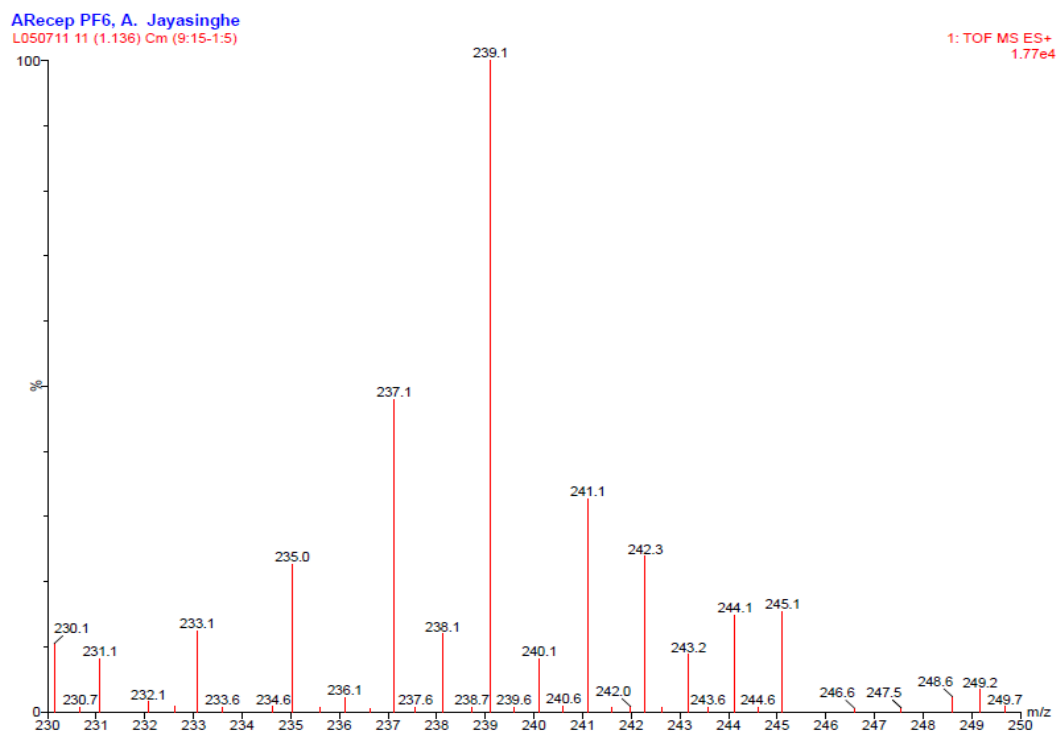
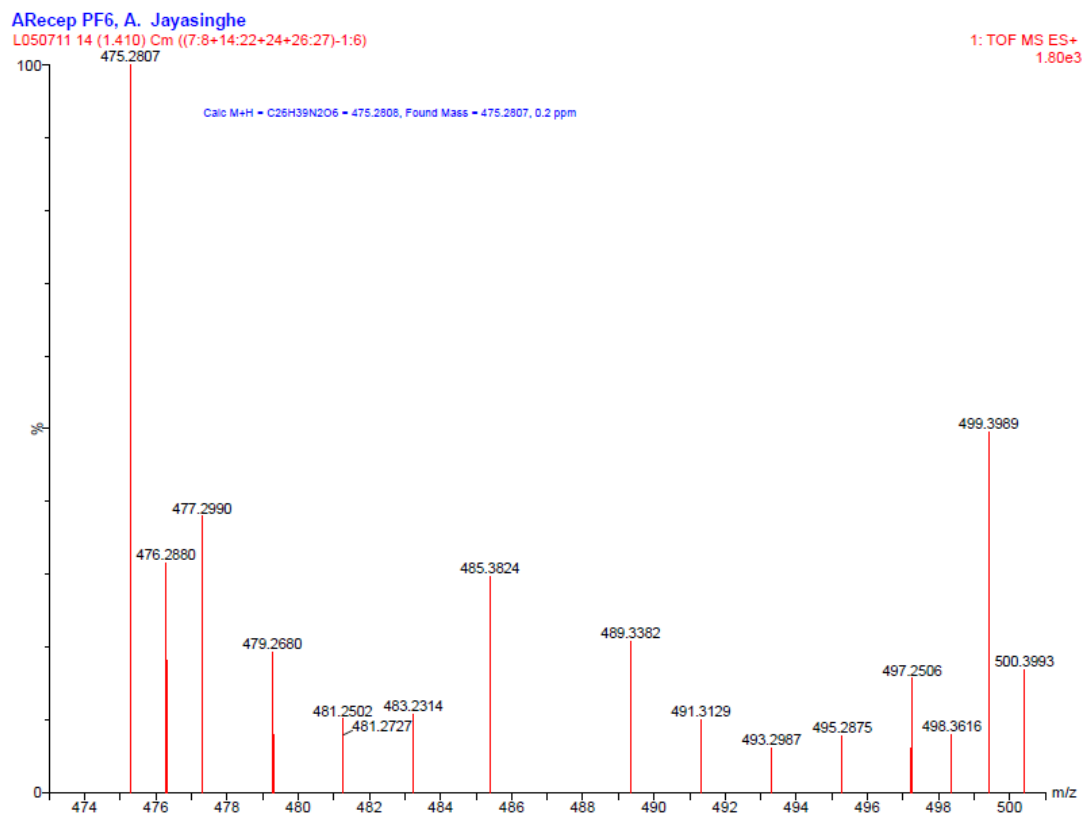
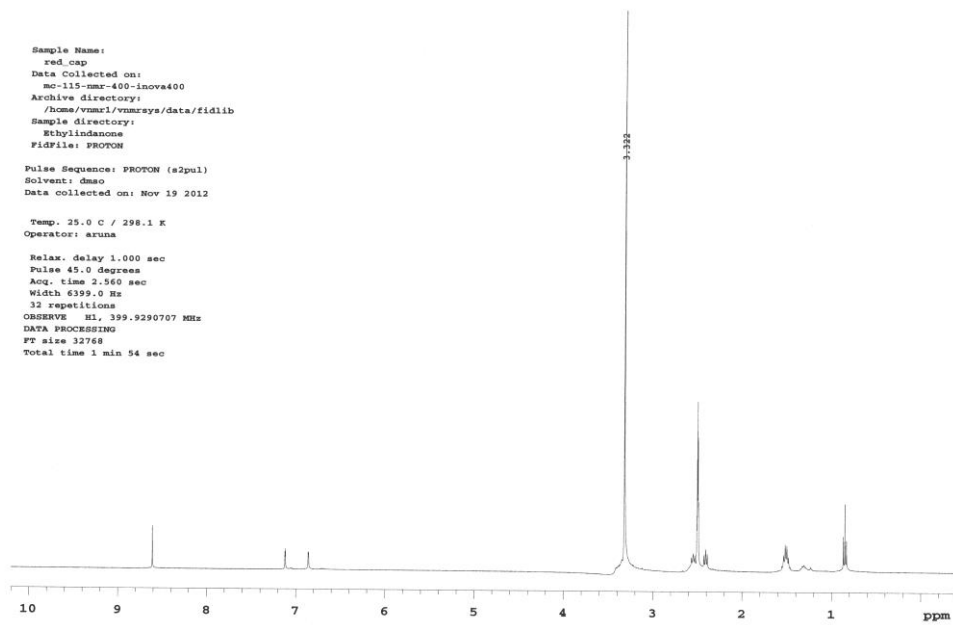


Figure 81. HSMS (top) and ESI-MS (bottom) data for compound 5



cyclohexene  
 Pulse Sequence: s2pul  
 Solvent: CDCl3  
 Ambient temperature  
 INOVA-400  
 Relax. delay 1.000 sec  
 Pulse 52.4 degrees  
 Acq. time 1.199 sec  
 Width 25806.0 Hz  
 256 repetitions  
 OBSERVE F1, 188.564279 MHz  
 DECOUPLE F2, 399.9391255 MHz  
 Power 35 dB  
 Continuously on  
 WALTZ16 Modulated  
 DATA PROCESSING  
 Line broadening 1.0 Hz  
 FT size 85536  
 Total time 12 hr, 16 min, 4 sec

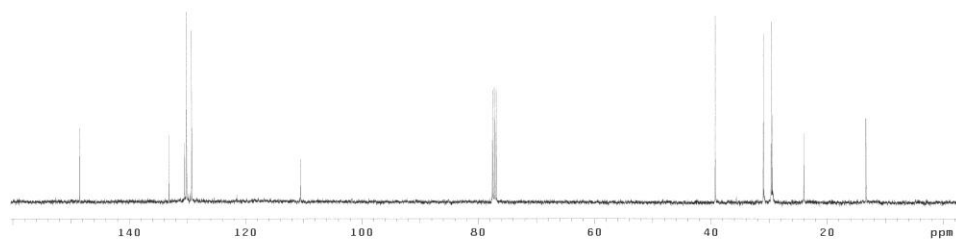


Figure 82.  $^1\text{H}$  NMR (top) and  $^{13}\text{C}$  NMR (bottom) data for compound **41**

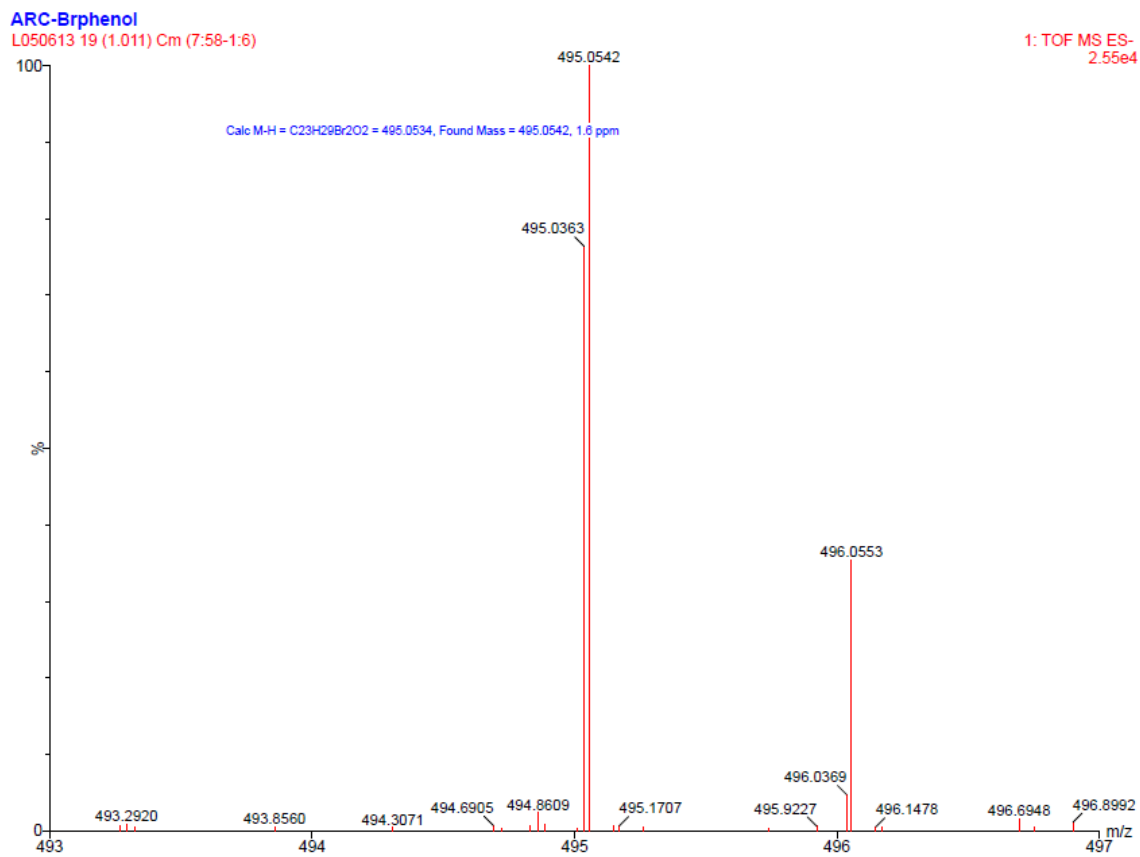
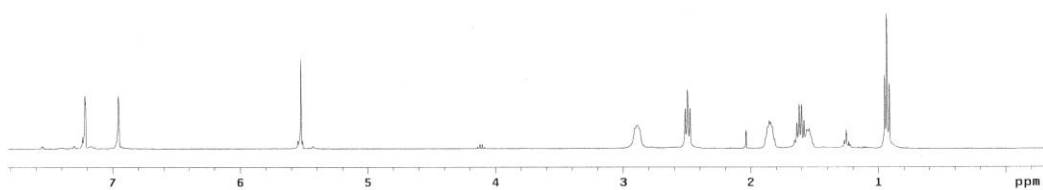


Figure 83. HSMS data for compound **42**

STANDARD 1H OBSERVE  
Pulse Sequence: s2pu1  
Solvent: CDCl3  
Ambient temperature  
INNOVA-400 "wstnnova400"  
Pulse 31.8 degrees  
Acq. time 3.744 sec  
Width 8000.0 Hz  
32 repetitions  
OBSERVE H1 399.9371255 MHz  
DATA PROCESSING  
FT size 65536  
Total time 2 min, 0 sec



cyclohexene  
Pulse Sequence: s2pu1  
Solvent: CDCl3  
Ambient temperature  
INNOVA-400 "wstnnova400"  
Relax. delay 1.000 sec  
Pulse 79.4 degrees  
Acq. time 1.199 sec  
Width 25000.0 Hz  
1232 repetitions  
OBSERVE C13 180.5620462 MHz  
DECOUPLE H1 399.9391255 MHz  
Power 44 dB  
continuously on  
WALTZ-16 modulated  
DATA PROCESSING  
Line broadening 1.0 Hz  
FT size 65536  
Total time 6 hr, 8 min, 2 sec

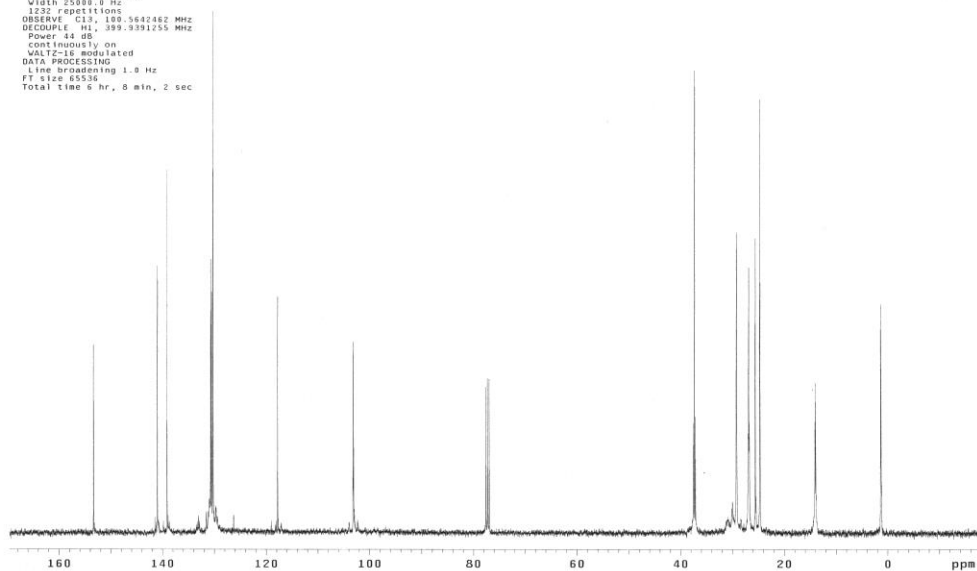


Figure 84. <sup>1</sup>H NMR (top) and <sup>13</sup>C NMR (bottom) data for compound 42

Cont Br Linked, A. Jayasinghe, T-apci

T070301 320 (11.432) AM (Cen,4, 50.00, Ar,5000.0,0.00,0.00); Sm (SG, 2x2.00); Cm (303:340)

TOF MS ES+  
190

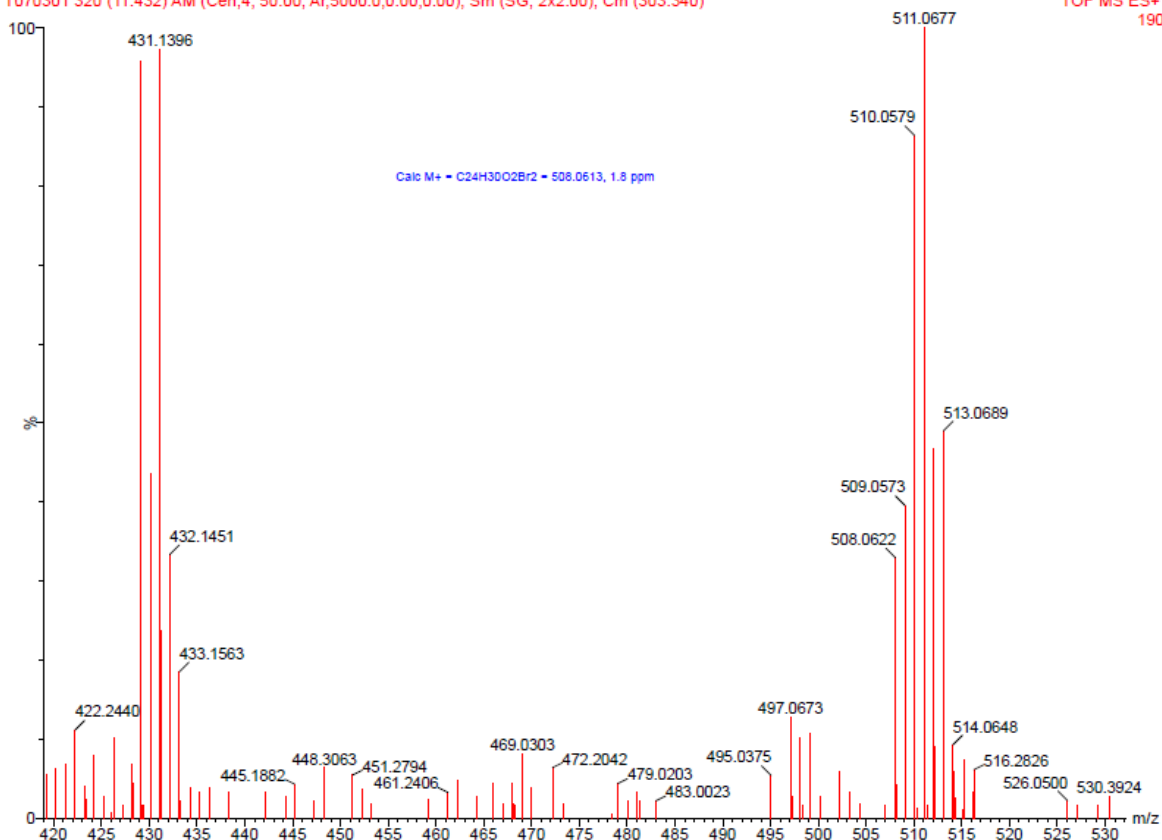


Figure 85. HSMS data for compound **42**

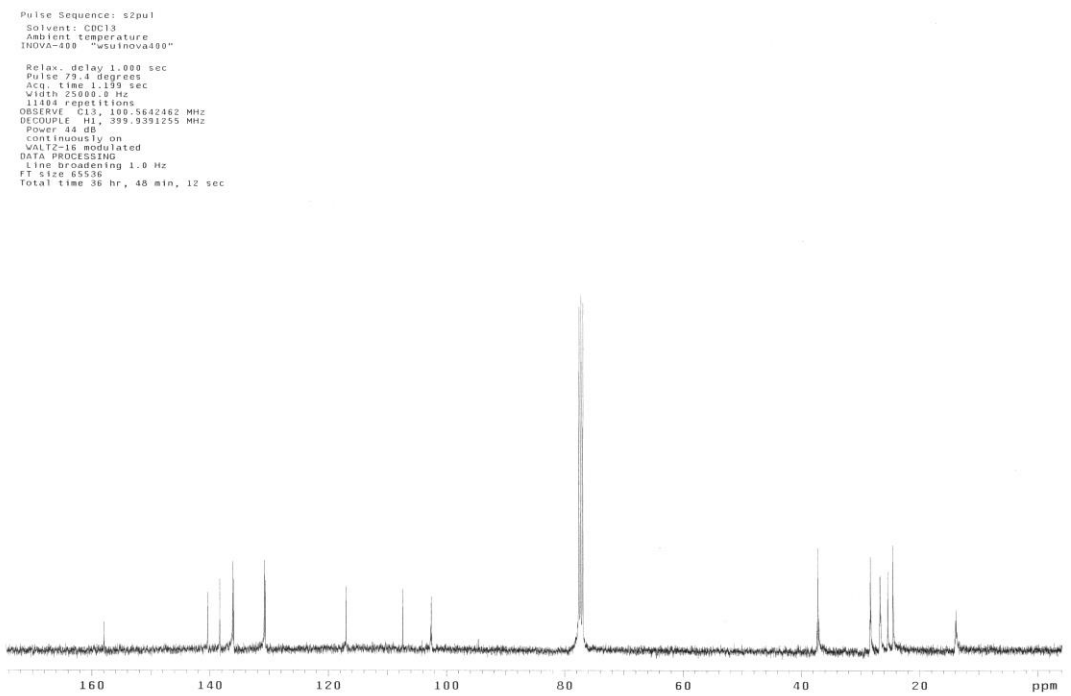
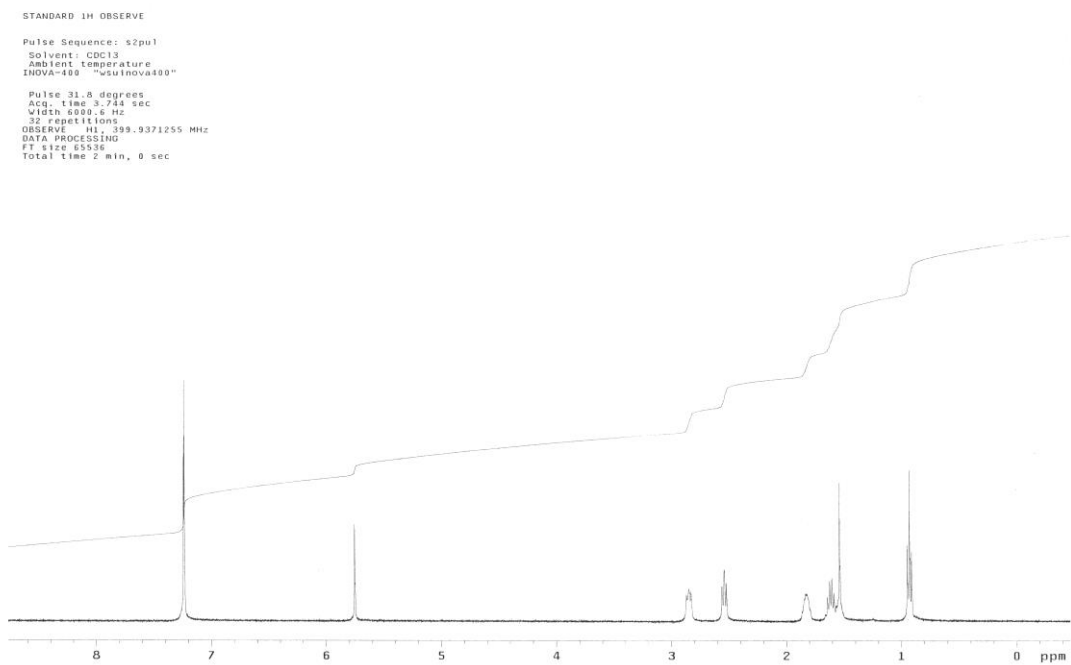


Figure 86.  $^1\text{H}$  NMR (top) and  $^{13}\text{C}$  NMR (bottom) data for compound **43**

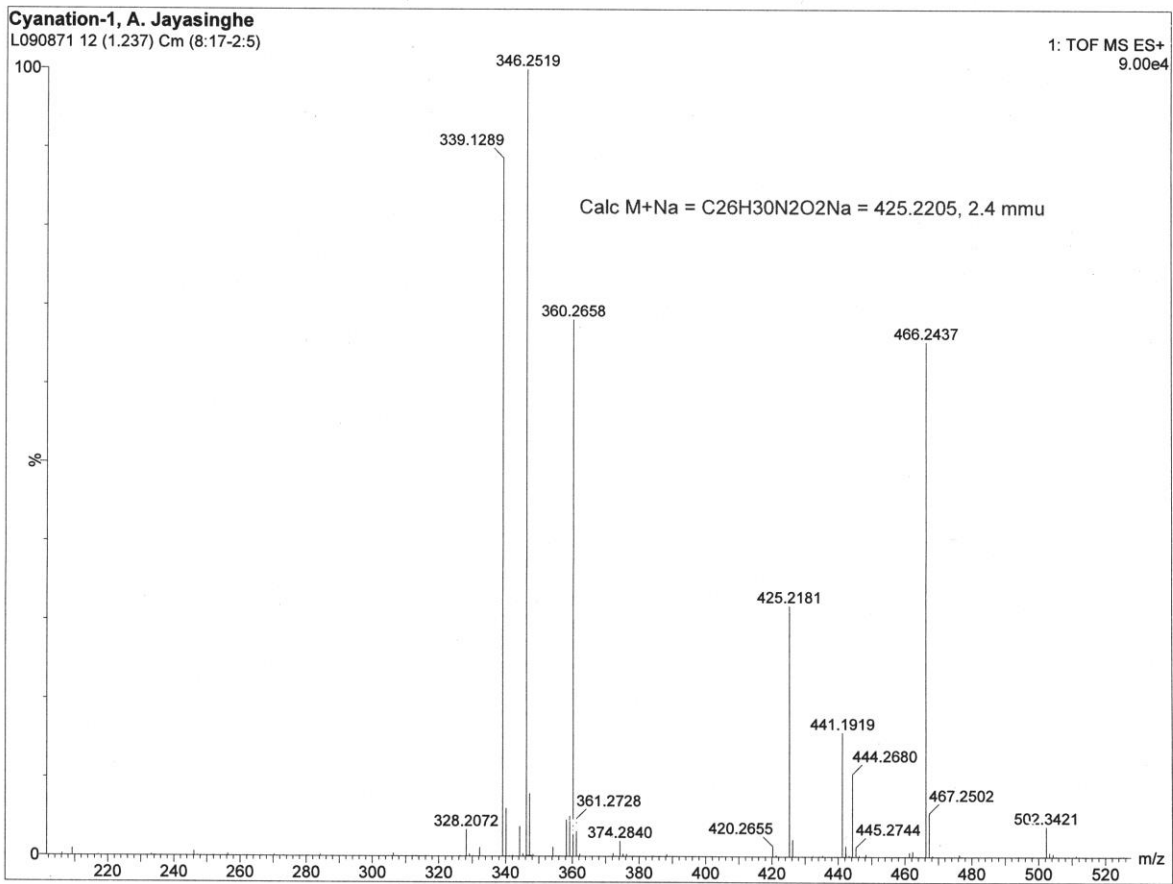


Figure 87. HSMS data for compound **43**

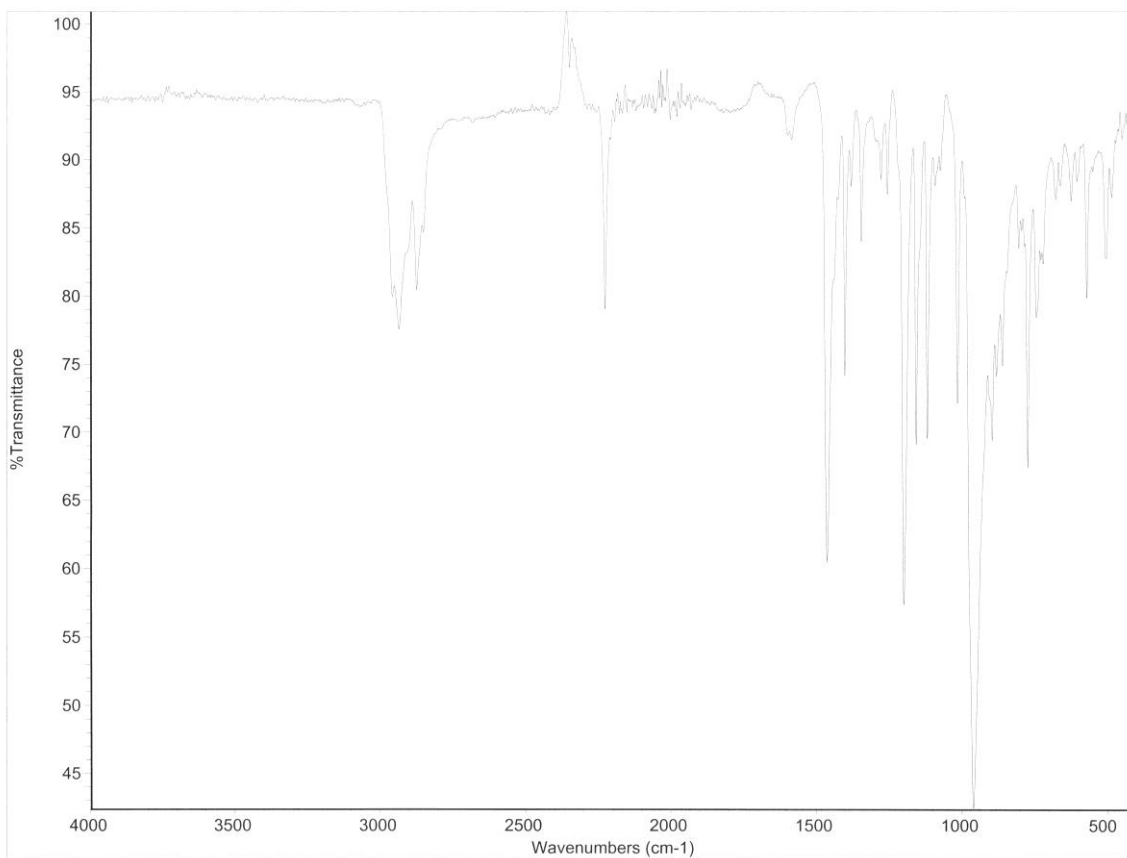


Figure 88. FTIR data for compound **43**

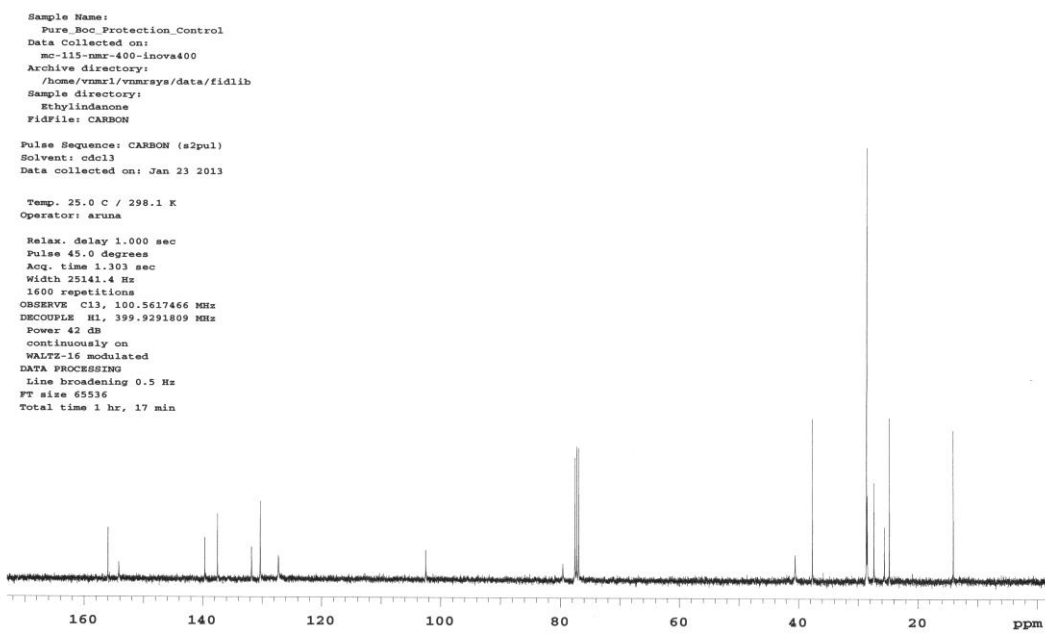
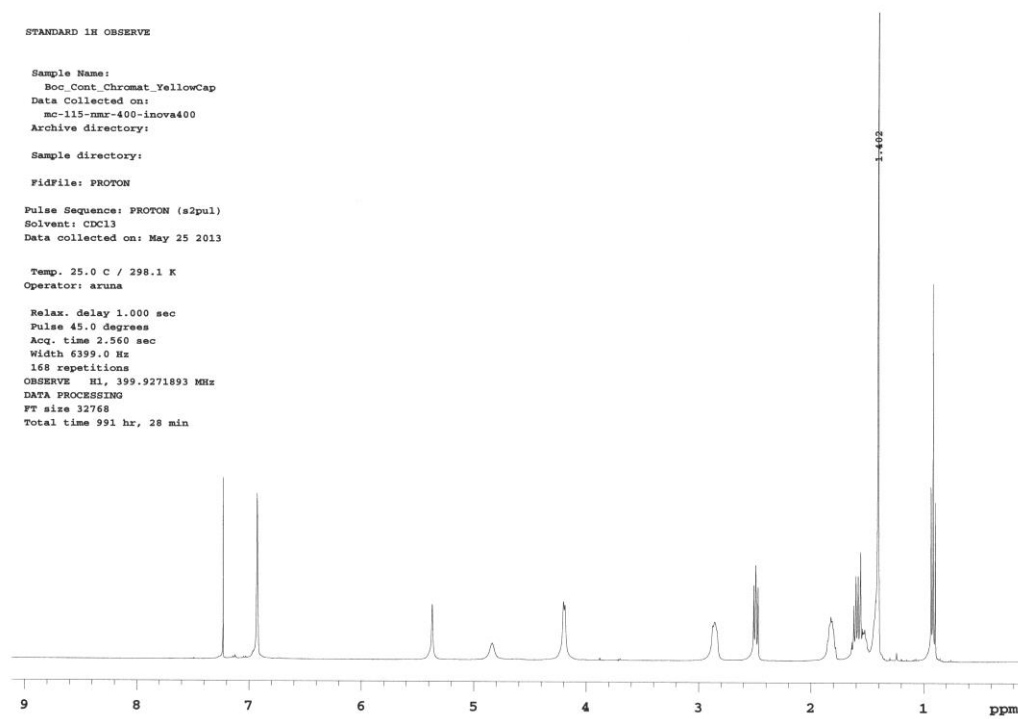


Figure 89.  $^1\text{H}$  NMR (top) and  $^{13}\text{C}$  NMR (bottom) data for compound **44**

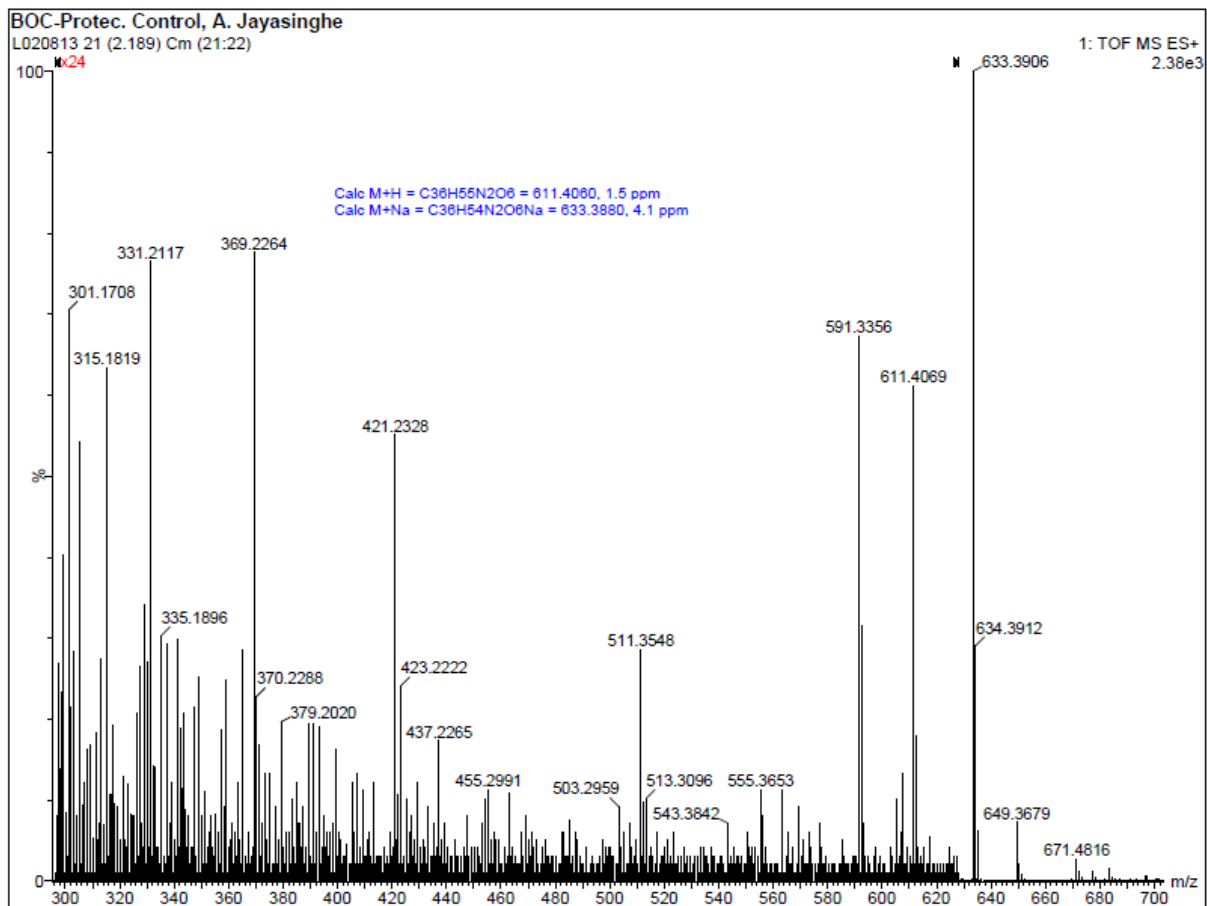


Figure 90. HSMS data for compound **44**

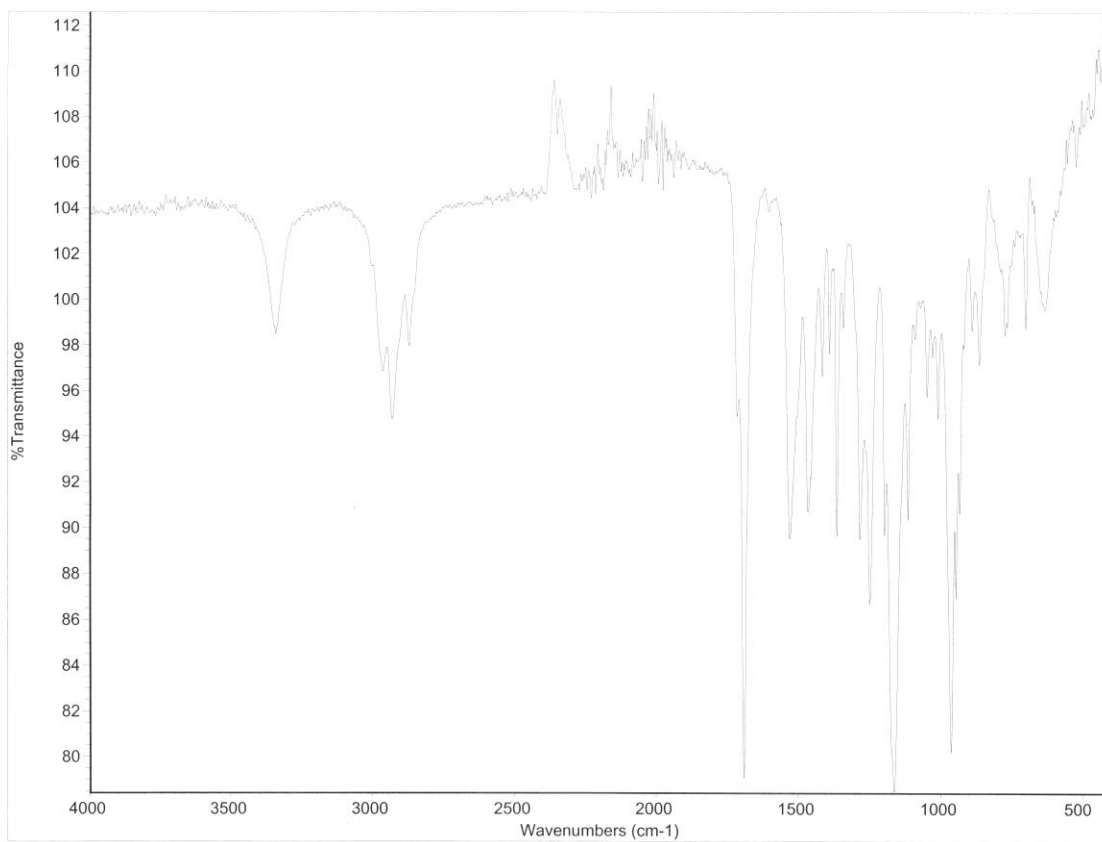
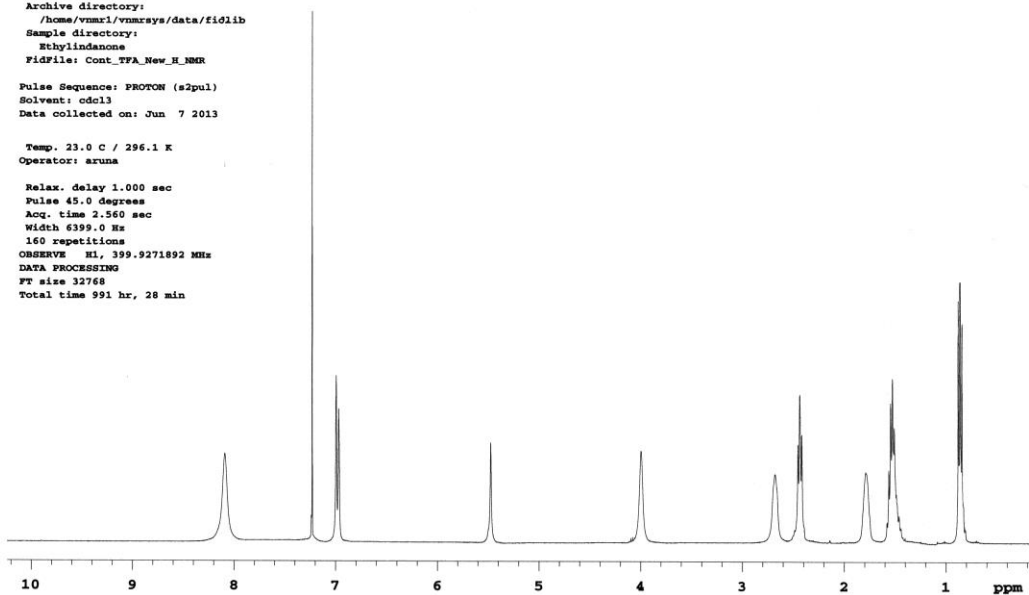


Figure 91. FTIR data for compound **44**

Sample Name:  
Control\_TFA\_2ndRun  
Data Collected on:  
mc-115-nmr-400-inova400  
Archive directory:  
/home/vmr1/vmrsys/data/fidlib  
Sample directory:  
Ethylindanone  
Fidfile: Cont\_TFA\_New\_H\_NMR  
Pulse Sequence: PROTON (s2pul)  
Solvent: cdcl3  
Data collected on: Jun 7 2013  
Temp. 23.0 C / 296.1 K  
Operator: aruna  
Relax. delay 1.000 sec  
Pulse 45.0 degrees  
Acq. time 2.560 sec  
Width 6399.0 Hz  
160 repetitions  
OBSERVE H1, 399.9271892 MHz  
DATA PROCESSING  
FT size 32768  
Total time 991 hr, 28 min



Sample Name:  
Control\_TFA\_reaction  
Data Collected on:  
mc-115-nmr-400-inova400  
Archive directory:  
/home/vmr1/vmrsys/data/fidlib  
Sample directory:  
Ethylindanone  
Fidfile: Control\_TFA\_Carbon\_NMR  
Pulse Sequence: CARBON (s2pul)  
Solvent: cdcl3  
Data collected on: Mar 15 2013  
Temp. 25.0 C / 298.1 K  
Operator: aruna  
Relax. delay 1.000 sec  
Pulse 45.0 degrees  
Acq. time 1.303 sec  
Width 25141.4 Hz  
1827 repetitions  
OBSERVE C13, 100.5617460 MHz  
DECOUPLE H1, 399.9291809 MHz  
Power 42 dB  
continuously on  
WALTZ-16 modulated  
DATA PROCESSING  
Line broadening 0.5 Hz  
FT size 65536  
Total time 642 hr, 16 min

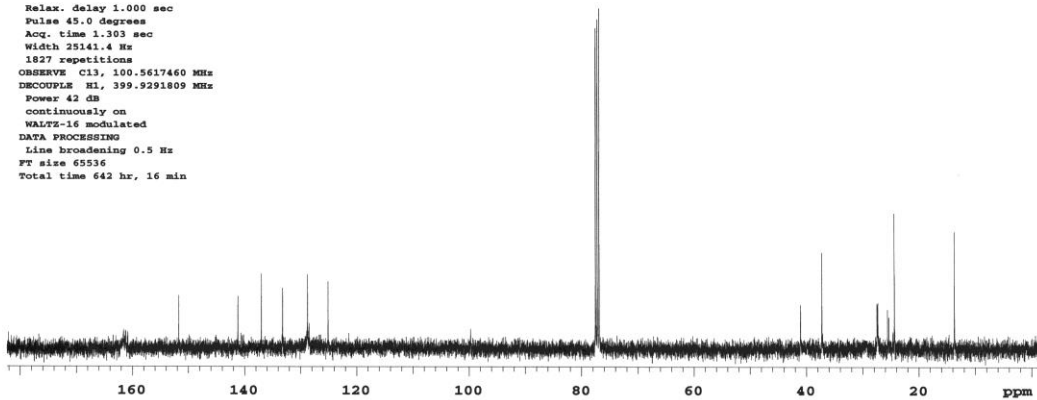


Figure 92.  $^1\text{H}$  NMR (top) and  $^{13}\text{C}$  NMR (bottom) data for compound **45**

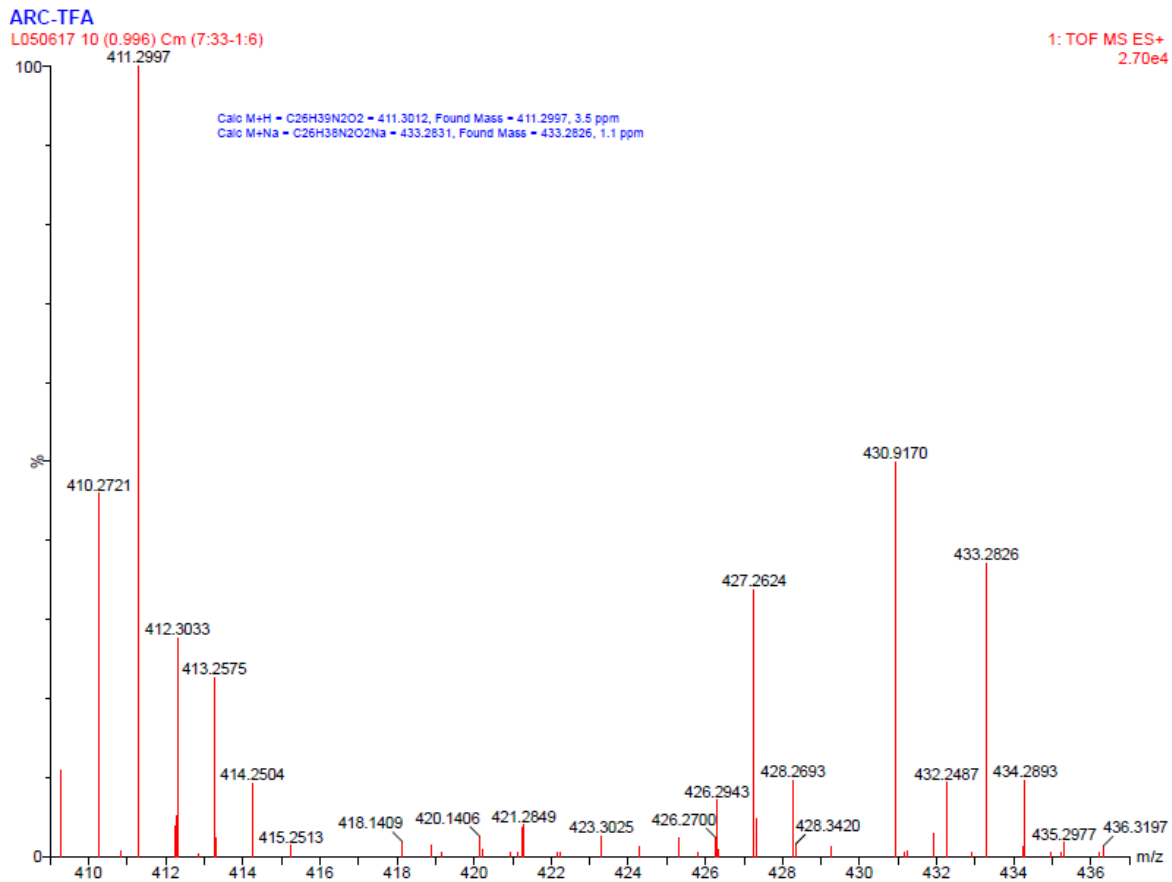


Figure 93. HSMS data for compound **45**

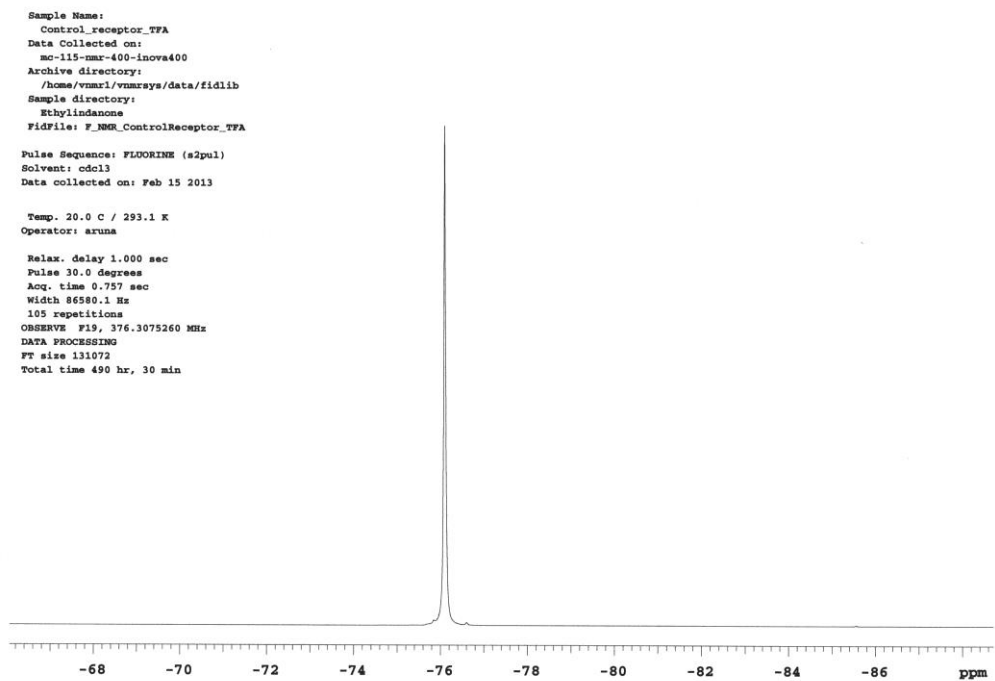
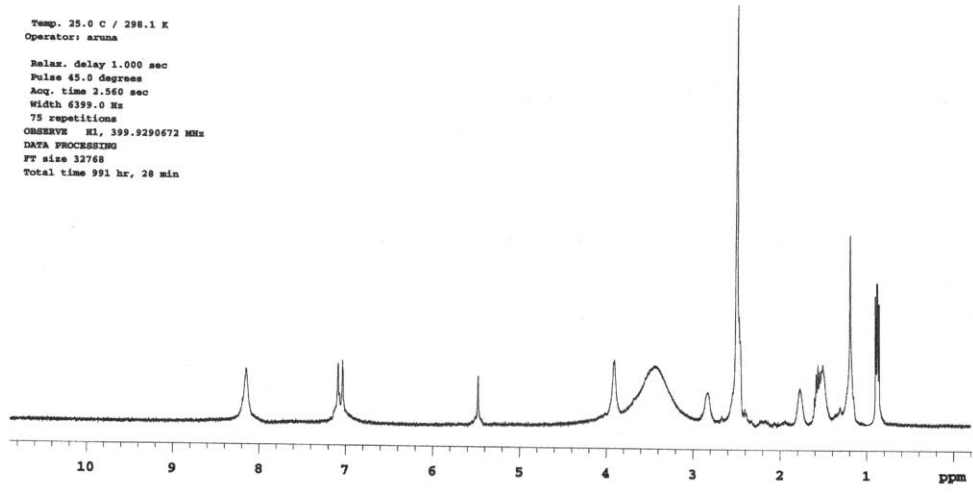


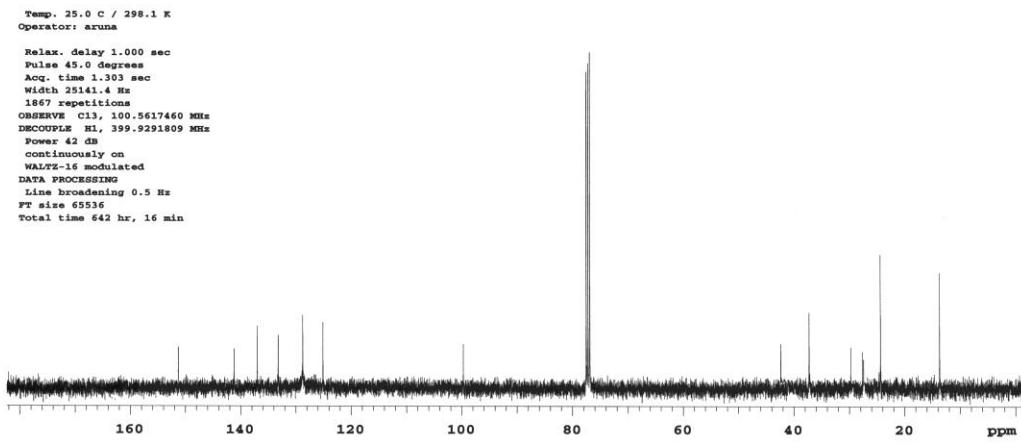
Figure 94. <sup>19</sup>F NMR data for compound **45**

Sample Name:  
Data Collected on:  
mc-115-nmr-400-inova400  
Archive directory:  
/home/vmari/vmrsys/data/fid11b  
Sample directory:  
Ethylindanone  
Fidfile: PROTON  
Pulse Sequence: PROTON (s2pul)  
Solvent: dmsc  
Data collected on: May 1 2013



Temp. 25.0 C / 298.1 K  
Operator: aruna  
Relax. delay 1.000 sec  
Pulse 45.0 degrees  
Acq. time 2.560 sec  
Width 6399.0 Hz  
75 repetitions  
OBSERVE H1, 399.9290672 MHz  
DATA PROCESSING  
FT size 32768  
Total time 991 hr, 28 min

Sample Name:  
Data Collected on:  
mc-115-nmr-400-inova400  
Archive directory:  
/home/vmari/vmrsys/data/fid11b  
Sample directory:  
Ethylindanone  
Fidfile: Carbon\_NMR  
Pulse Sequence: CARBON (s2pul)  
Solvent: cdcl3  
Data collected on: Mar 15 2013



Temp. 25.0 C / 298.1 K  
Operator: aruna  
Relax. delay 1.000 sec  
Pulse 45.0 degrees  
Acq. time 1.303 sec  
Width 25141.4 Hz  
1867 repetitions  
OBSERVE C13, 100.5617460 MHz  
DECOUPLE H1, 399.9291809 MHz  
Power 42 dB  
continuously on  
WALTZ-16 modulated  
DATA PROCESSING  
Line broadening 0.5 Hz  
FT size 65536  
Total time 642 hr, 16 min

Figure 95. <sup>1</sup>H NMR (top) and <sup>13</sup>C NMR (bottom) data for compound 46

ARC-PF6, A. Jayasinghe

L050703 15 (1.550) Cm ((7.8+15:33)-1:6)

1: TOF MS ES+  
4.09e3

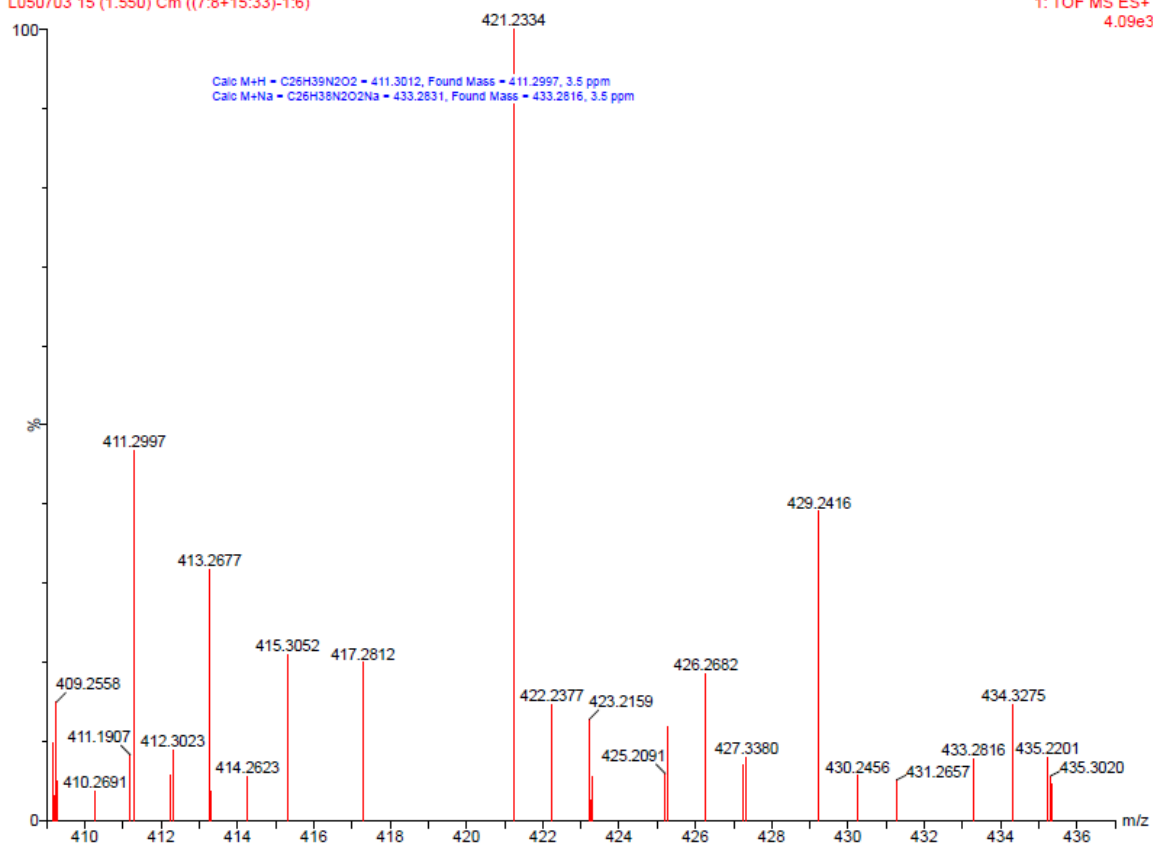
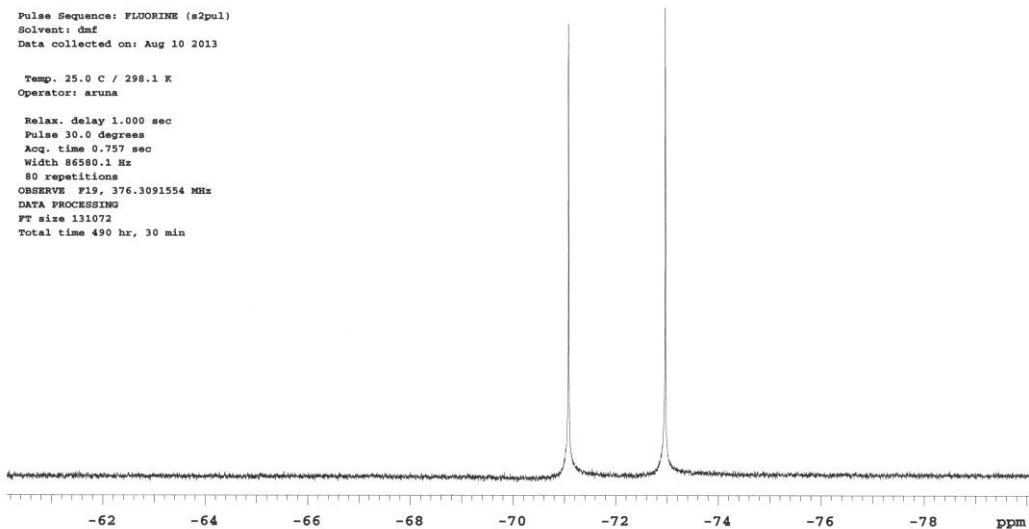


Figure 96. HSMS data for compound 46

STANDARD 1H OBSERVE

Sample Name:  
Control\_FF6  
Data Collected on:  
mc-115-nmr-400-inova400  
Archive directory:  
Sample directory:  
Fidfile: FLOORINE  
Pulse Sequence: FLOORINE (s2pul)  
Solvent: dmf  
Data collected on: Aug 10 2013  
Temp. 25.0 C / 298.1 K  
Operator: aruna  
Relax. delay 1.000 sec  
Pulse 30.0 degrees  
Acq. time 0.757 sec  
Width \$6580.1 Hz  
80 repetitions  
OBSERVE F19, 376.3091554 MHz  
DATA PROCESSING  
FT size 131072  
Total time 490 hr, 30 min



Sample Name:  
Control\_FF6\_Rm  
Data Collected on:  
mc-115-nmr-400-inova400  
Archive directory:  
/home/vnari/vnarsys/data/fidlib  
Sample directory:  
Ethylindanone  
Fidfile: Control\_FF6\_Phosphorus\_NMR  
Pulse Sequence: PHOSPHORUS (s2pul)  
Solvent: cdcl3  
Data collected on: Mar 17 2013  
Temp. 25.0 C / 298.1 K  
Operator: aruna  
Relax. delay 1.000 sec  
Pulse 45.0 degrees  
Acq. time 0.810 sec  
Width 40465.4 Hz  
1390 repetitions  
OBSERVE P31, 161.8934904 MHz  
DECOUPLE H1, 399.9291809 MHz  
Power 42 dB  
on during acquisition  
off during delay  
WALTZ-16 modulated  
DATA PROCESSING  
Line broadening 0.5 Hz  
FT size 65536  
Total time 505 hr, 12 min

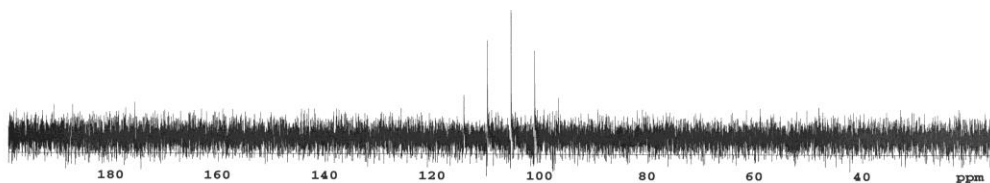


Figure 97.  $^{19}\text{F}$  NMR (top) and  $^{31}\text{P}$  NMR (bottom) data for compound 46

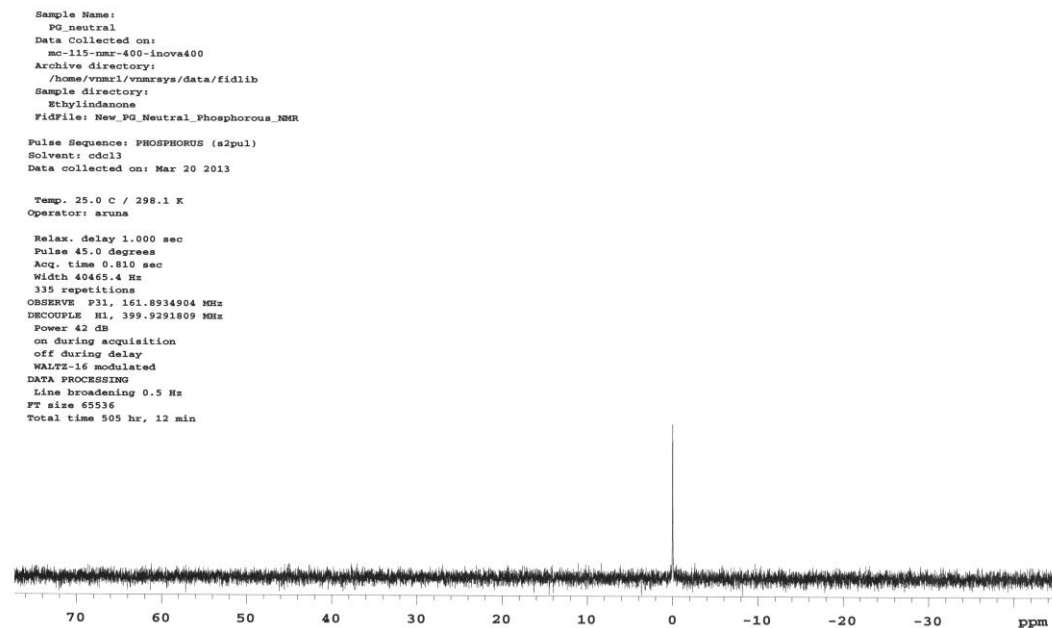
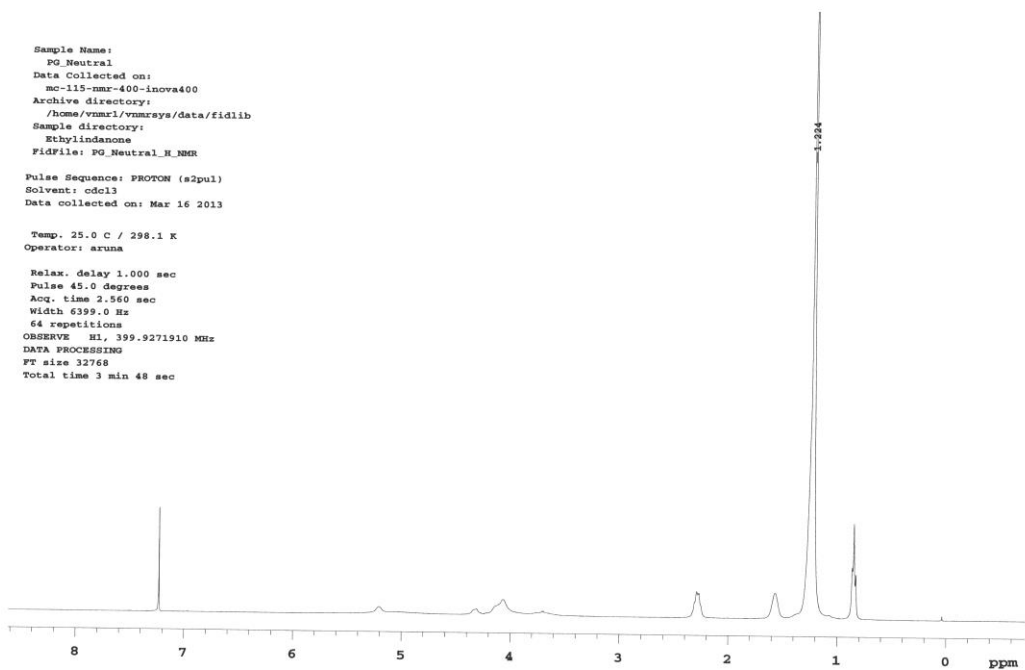


Figure 98  $^1\text{H}$  NMR (top) and  $^{31}\text{P}$  NMR (bottom) data for compound **PG neutral**

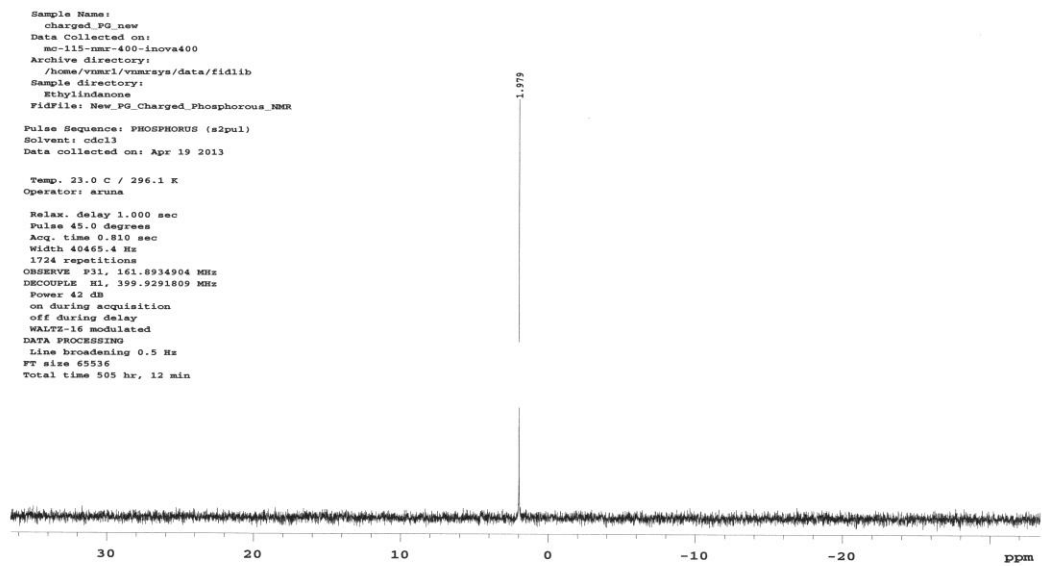
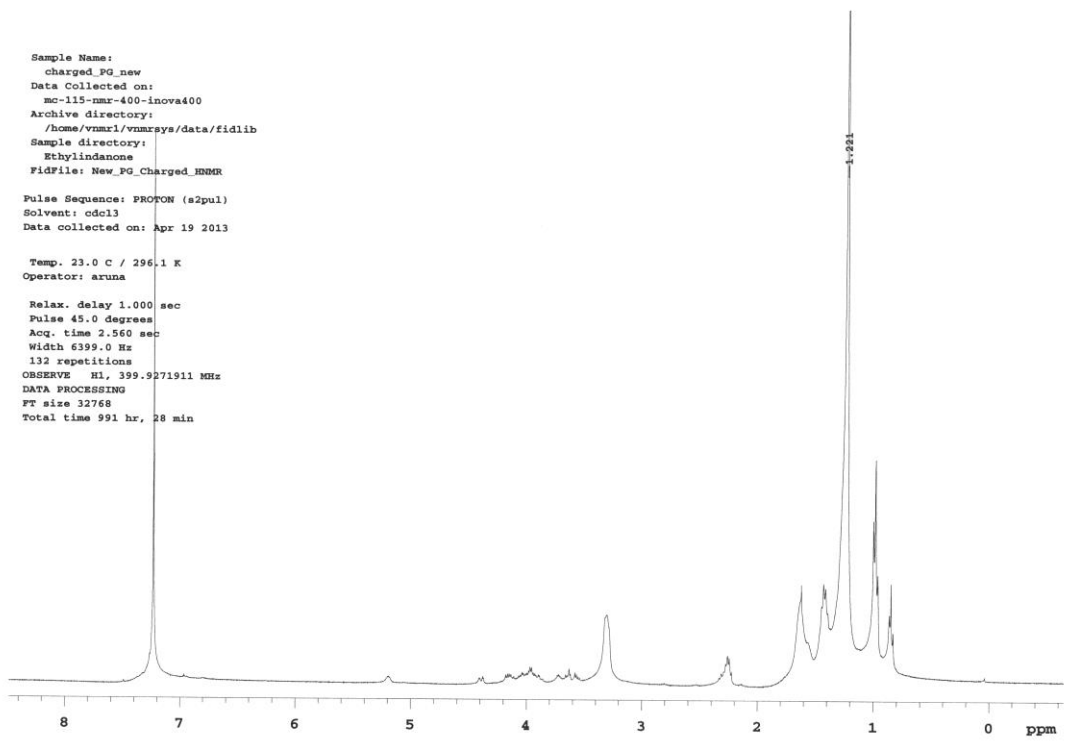


Figure 99.  $^1\text{H}$  NMR (top) and  $^{31}\text{P}$  NMR (bottom) data for compound 3

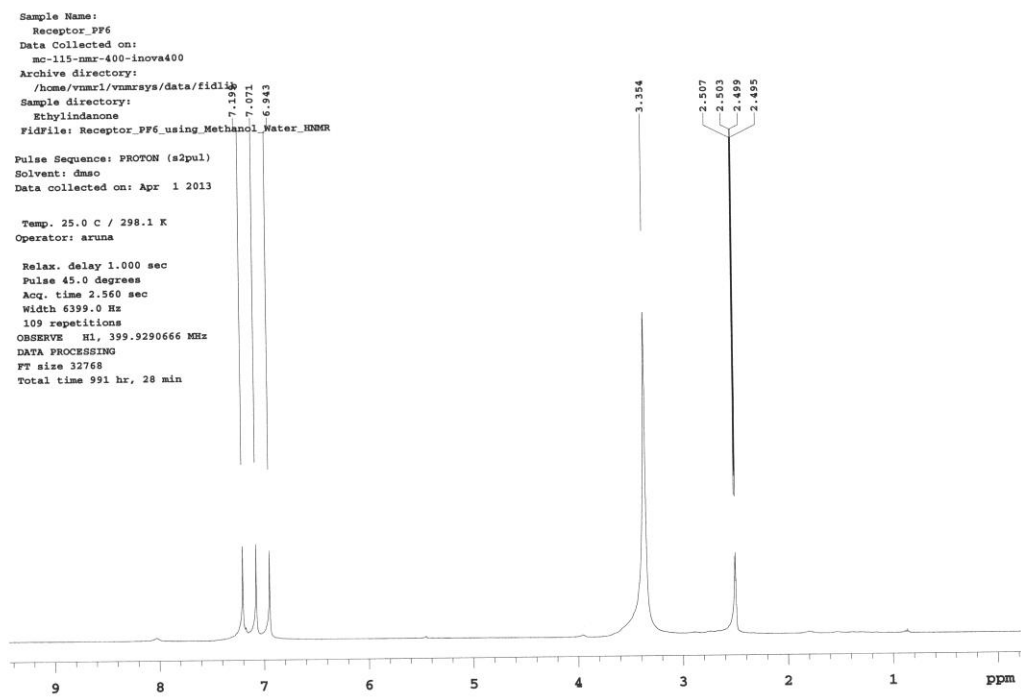


Figure 100  $^1\text{H}$  NMR data for the unknown compound